NOVEL PHOSPHATRIPTYCENE AND NHC SUPPORTED LATE TRANSITION METAL COMPLEXES FOR SMALL MOLECULE TRANSFORMATIONS

A Dissertation
Presented to
The Academic Faculty

by

Yu Cao

In Partial Fulfillment
of the Requirements for the Degree
Doctor of Philosophy in the
School of Chemistry and Biochemistry

Georgia Institute of Technology
December 2018

NOVEL PHOSPHATRIPTYCENE AND NHC SUPPORTED LATE TRANSITION METAL COMPLEXES FOR SMALL MOLECULE TRANSFORMATIONS

Approved by:

Dr. Joseph P. Sadighi, Advisor
School of Chemistry and Biochemistry
Georgia Institute of Technology

Dr. Jake D. Soper
School of Chemistry and Biochemistry
Georgia Institute of Technology

Dr. Z. John Zhang
School of Chemistry and Biochemistry
Georgia Institute of Technology

Dr. Stephen A. France
School of Chemistry and Biochemistry
Georgia Institute of Technology

Dr. Krista S. Walton
School of Chemical and Biomolecular Engineering
Georgia Institute of Technology

Date Approved: October 16, 2018

To my mom and dad,

Aixia Yu and Xulong Cao

ACKNOWLEDGEMENTS

First of all, I would like to thank my parents, Aixia Yu and Xulong Cao, for their endless love and support for the past years. I truly appreciate all they have taught me, from a kid to a grown-up, to guide me to become a nice and useful person. Their smile and happiness always keep me a positive mood no matter what difficulties I come across. They are the best parents and we are the best family. I thank all my families' love and support, and their understanding for my missing important re-unions.

I thank Prof. Joseph P. Sadighi, for the opportunity to work in his research group. I have learned not only academic chemistry knowledge and laboratory techniques from him, but also dedicated spirit to science, critical thinking and creative thoughts. I really appreciate his guidance in my research projects and professional writing development. I also thank his families' treats for several thanksgiving parties and the best tiramisu.

I thank all my committee members past and present: Prof. Jake D. Soper, Prof. Z. John Zhang, Prof. Stephen A. France, Prof. Krista S. Walton and Prof. Pradeep K. Agrawal for their sharing insightful suggestions and comments in my dissertation work, and their kindly allowance in my borrowing research instruments and chemicals from their groups.

I would like to thank all of my fellow group members in Sadighi lab past and present: Mr. Kevin O. Omolo, Mr. Abraham J. Jordan, Dr. Nicholas T. Daugherty, Dr. Jonathan W. Napoline, Dr. Brandon K. Tate, Dr. Chelsea W. Bordley, Mr. Christopher M. Sato, Ms. Sabrine Cypher, Mr. Andrew D. Royappa, Ms. Percie Thompson, Ms. Alyssa Delucia. I would like to especially thank Kevin for his accompany in and outside lab with

humor. I really appreciate his deep-thinking conversations in chemistry or life and support when I need the most. His always funny ideas and surprise have brighten my every day. I thank Abe for being the best glovebox mate and kindly sharing his experience for conducting gas reactions. I thank Nick for his continuous encouragement and his talent in creating songs for me in a positive mood. I thank Wes for his insightful attempt to bring phosphatriptycene into hydroformylation catalysis and helpful discussions in high pressure reaction set-up. I thank Brandon for his knowledgeable advice in spectra analysis and always willing to help answer my questions. I thank Chelsea for her guidance of air-sensitive technique when I started in lab. I thank Chris for his great lab management skill to keep working more efficiently. I thank undergraduate researcher Sabrine for her contributions to develop phosphatriptycene chemistry and I was honored by the opportunity to work with her. I really enjoy the time to work with them all, and I have learned such a lot from every one of them. This is such a good working place where love, happiness and support always exist.

I thank Prof. Charles L. Liotta, Prof. Christopher W. Jones, and Dr. Pamela Pollet for their kindly support and training when I was conducting the hydroformylation project. I thank Dr. John Bacsa for his great collaborative efforts on crystallographic structures to my research. I thank Prof. Emeritus E. Kent Barefield for his suggestions on looking into β-hydride elimination from reactions of NHC supported μ-hydrido dinickel(I) hydride with longer alkyl nitriles, and helpful discussions on safe handling chemicals such $Ni(CO)_4$. I thank Dr. Leslie T. Gelbaum and Dr. Johannes E. Leisen for helping me with NMR experiments. I thank Dr. David Bostwick for his help in performing mass spectrometry experiments. I thank Dr. Robert A. Braga for helping me perform EPR experiments. I thank

Prof. Henry La Pierre for his allowance in my borrowing IR in a glovebox from his group. I thank my teaching supervisors, especially Dr. Carrie Shepler and Dr. Amanda B. Stephens, for the time to work with, that helps me develop teaching, communication and laboratory management skills. I thank all the teachers, professors, and staff who have helped me all over the past years. I thank Dr. Zhao Li for his help in collecting GC-FID data, Mr. Brandon Yik for his help in collecting IR data, Mr. Eric Drew for his discussions in EPR and magnetic susceptibility tests, Mr. Christopher Kuehner and Ms. Jennifer Hill for their help in collecting UV-vis and IR data. I thank Mr. Bhuwan Khatri Chetri, Mr. Ningxin Jiang and Ms. Yifan Zhang for being great organic preparation lab teaching partners. I thank Petroleum Research Funding, the College of Sciences and the School of Chemistry and Biochemistry of Georgia Institute of Technology for financial support.

Finally, I would like to thanks all my friends. I would especially thank Dr. Xiaoling Zang, Dr. Chu Han and Ms. Ying Sha for their friendship and support whenever I need. We have shared our every important moment together during the past five years, and it is really my luck to meet with them, know them well and become a family in which we can reply on each other. I thank Dr. Helen Wei-Ya Chen for her friendship, always kindly sharing her professional experience and being a good listener. I thank Dr. Zhishuai Geng and Dr. Siyuan Zhang's guidance when I first started my life in Atlanta. I really thank all the friends I have met in Atlanta, who have spent great time and shared good memories together. I also thank my old friends no matter where they are, who still keep in touch and encourage each other in new environment. Your friendship has meant a lot to me and I wish all of you the best on the way to pursue your dreams.

TABLE OF CONTENTS

LIST OF TABLES

LIST OF FIGURES

LIST OF SCHEMES

LIST OF SYMBOLS AND ABBREVIATIONS

α	alpha
Å	angstrom
acac	acetylacetonato
atm	atmosphere
ATR	attenuated total reflection
β	beta
b	branched aldehyde
bar	unit of pressure; unit and abbreviation are the same
$BAr^F{}_4$	tetrakis[3,5-bis(trifluoromethyl)phenyl]borate
BF_4	tetrafluoroborate
Bn	benzyl
br	broad or broadened (spectra)
Bu	butyl
i-Bu	isobutyl
t-Bu	*tert*-butyl
C	Celsius
°C	degree(s) Celsius
^{13}C NMR	carbon-13 nuclear magnetic resonance
calcd	calculated
cat.	catalyst
cm	centimeter
cod	1,5-cyclooctadiene

conv %	conversion percent
Cp	cyclopentadienyl
CW	continuous wave
Cy	cyclohexyl
°	degree
δ	delta, chemical shift (relative to tetramethylsilane)
d	day (unit of time)
	doublet (spectra)
d	deuterated
D	deuterium
DCM	dichloromethane
dcpe	1,2-bis(dicyclohexylphosphino)ethane
dd	doublet of doublets (spectra)
ddd	doublet of doublets of doublets (spectra)
dddd	doublet of doublets of doublets of doublets (spectra)
dt	doublet of triplets (spectra)
decomp	decompose
DFT	density functional theory
DI	deionized
dippe	1,2-bis(diisopropylphosphino)ethane
dippm	1,2-bis(diisopropylphosphino)methane
DMG	directed metalation group
dtbpe	1,2-bis(di-*tert*-butylphosphino)ethane
η	eta
e.g.	*exempli gratia* (for example)

EI	electron ionization
equiv	equivalent
ESI	electrospray ionization
Et	ethyl
et al.	and others
etc	*et cetera* (and so forth)
Et_2O	diethyl ether
EtOAc	ethyl acetate
EtOH	ethanol
^{19}F NMR	fluorine-19 nuclear magnetic resonance
FG	functional group
g	gram
GC	gas chromatography
GC-FID	gas chromatography-flame ionization detector
GC-MS	gas chromatography-mass spectrometry
h	hour
^{1}H NMR	proton nuclear magnetic resonance
HOMO	highest occupied molecular orbital
Hz	hertz
LDBB	lithium 4,4'-di-*tert*-butylbiphenylide
IDipp	1,3-bis(2,6-diisopropylphenyl)imidazol-2-ylidene
IR	infrared spectroscopy
K	kelvin
l	linear aldehyde
L	ligand

	liter
LDA	lithium diisopropylamide
LUMO	lowest unoccupied molecular orbital
μ	mu, micro (10^{-6})
μm	micrometer
m	meter
	milli (10^{-3})
	multiplet (spectra)
M	mega (10^{6})
	metal
	molar, or moles per liter
M^+	molecular ion
M_r	relative molecular mass (molecular weight)
m/z	mass-to-charge ratio
Me	methyl
6Mes	1,3-bis(2,4,6-trimethylphenyl)-3,4,5,6-tetrahydropyrimidin-2-ylidene
MHz	megahertz
min	minute
mL	milliliter
mm	millimeter
mmol	millimole
MO	molecular orbital
mol	mole
mol %	mole percent
MS	mass spectrometry

n	nano (10^{-9})
NHC	N-heterocyclic carbene
nm	nanometer
NMR	nuclear magnetic resonance
N. R.	no reaction
NTf_2	bis(trifluoromethanesulfonyl)imide
OAc	acetate
OTf	triflate or trifluoromethanesulfonate
%	percent
π	pi
P	pressure
^{31}P NMR	phosphorus-31 nuclear magnetic resonance
Pent	pentyl
n-Pent	*n*-pentyl
sec-Pent	*sec*-pentyl
PF_6	hexafluophosphate
Ph	phenyl
pin	pinacolate
pp	pages
ppm	parts per million
Pr	propyl
i-Pr	isopropyl
i-PrIm	1,3-bis(2,6-diisopropyl)imidazol-2-ylidene
psi	pounds per square inch
q	quartet (spectra)

quin	quintet (spectra)
rt	room temperature
σ	sigma
s	second
	singlet (spectra)
	strong (spectra)
sec	secondary (as in *sec*-pentyl)
sept	septet (spectra)
sext	sextet (spectra)
Θ	theta, diffraction angle
2	tetrahydrofuran-2-carbaldehyde
	tetrahydro-2*H*-pyran-2-carbaldehyde
3	tetrahydrofuran-3-carbaldehyde
	tetrahydro-2*H*-pyran-3-carbaldehyde
t	triplet (spectra)
t	tertiary (as in *t*-Bu; but *tert*-butyl)
	time
T	temperature (in degrees Celsius)
T	temperature (in kelvins)
tdd	triplet of doublets of doublets (spectra)
temp	temperature
tert	tertiary (as in *tert*-butyl; but *t*-Bu)
THF	tetrahydrofuran
TMEDA	*N,N,N′,N′*-tetramethylethylenediamine
TOF	turnover frequency

tt	triplet of triplets (spectra)
UV-vis	ultraviolet-visible spectroscopy
λ	wavelength
ν	wavenumber
w	weak (spectra)
w/w	weight per weight
wt	weight
wt %	weight percent
1	10-hydroxy-9-phosphatriptycene
2	10-trimethylsiloxy-9-phosphatriptycene
3	10-triethylsiloxy-9-phosphatriptycene
4	10-hydroxy-9-phosphatriptycene oxide
5	10-triethylsiloxy-9-phosphatriptycene oxide
6	10-hydroxy-9-phosphatriptycene 9-phenylimide
7	2,7,14-tri-*tert*-butyl-10-aza-9-phosphatriptycene
8	[(**2**)CuCl]
9	[(**3**)CuCl]$_5$
10	[(**7**)CuCl]$_4$
11	[(**7**)Cu(OAc)]
12	[(**7**)Rh(acac)(CO)]
13[NTf_2]	{[(IDipp)Ni]$_2$(μ-H)}[NTf_2]
13[OTf]	{[(IDipp)Ni]$_2$(μ-H)}[OTf]
14	[(IDipp)Ni$(CN)_2$]$_4$
15[BF_4]	[(IDipp)Ni]$_2$[BF_4]
15[NTf_2]	[(IDipp)Ni]$_2$[NTf_2]

15[OTf] [(IDipp)Ni]$_2$[OTf]

15[PF_6] [(IDipp)Ni]$_2$[PF_6]

16[BF_4] [(IDipp)$_2$Ni][BF_4]

16[NTf_2] [(IDipp)$_2$Ni][NTf_2]

16[OTf] [(IDipp)$_2$Ni][OTf]

16[PF_6] [(IDipp)$_2$Ni][PF_6]

17 [(IDipp)Ni(μ-C_6F_5)]$_2$

SUMMARY

This thesis focuses on the synthesis and characterization of late transition metal complexes supported by novel caged phosphine and NHC ligands, and the study of their reactivity in small molecule transformations.

The first part of the thesis focuses on the design of synthetic routes to, and the coordination chemistry of, novel sterically bulk π-acceptor phosphine molecules based on the class of 9-phosphatriptycene (Chapter 2). While the synthesis of phosphatriptycene bearing functional groups *ortho* to the phosphorus position proved elusive, we have succeeded in the synthesis of several phosphatriptycene derivatives and in the elaboration of an azaphosphatriptycene with *meta* substituents. The new 2,7,14-tri-*tert*-butyl-10-aza-9-phosphatriptycene has been synthesized in high yield, on gram-scale, by a concise route from inexpensive precursors. The solid-state structure of the copper complexes shows that *meta* substitution on the phosphatriptycene framework introduces significant steric bulk around the supported metal centers, with consequences to the aggregation state of the copper chloride complexes. The phosphatriptycene readily dissociates from copper center during attempted transformation reactions, but forms an isolable rhodium complex that can be applied as a highly efficient catalyst precursor in the homogeneous hydroformylation of alkenes (Chapter 3). Infrared spectroscopy of the rhodium(I) carbonyl complex bearing the ligand reflects the strong π-acceptor character of the azaphosphatriptycene, and the solid-state structure reveals its moderate steric demand. Consistent with the expected weak σ-basicity and strong π-acidity of the ligand, the rhodium complex shows remarkable activity

in the hydroformylation of less-reactive internal cyclic alkenes, including heterocyclic alkenes.

The second part of the thesis (Chapter 4) focuses on the design of novel NHC-supported dinuclear nickel complexes. Salts of a mono-cationic, μ-hydrido dinickel(I) complex have been synthesized and the solid-state structure of the cation features a symmetric linear structure with a Ni•••Ni distance of 3.0076(5) Å. The μ-hydrido dinickel(I) monocation complexes activate the C−CN bonds in nitriles to form the corresponding alkane, accompanied by the formation of a nickel(II) cyanide complex in acetonitrile reactions, as well as dinuclear Ni(I)/Ni(0) mixed-valence radical complexes and homoleptic nickel(I) complexes in longer-chain nitriles reactions. The dinuclear Ni(I)/Ni(0) complexes can be synthesized through the comproportionation of Ni(II) and Ni(0), or by the one-electron oxidation of two Ni(0) centers with a mild oxidant. It can also be generated and detected through hydrogen abstraction from the μ-hydrido dinickel(I) monocation complexes using a stable 2,4,6-tri-*tert*-butylphenoxyl radical. The solid-state structure of the dinuclear Ni(I)/Ni(0) mixed-valence cation features a short Ni•••Ni distance of 2.6356(6) Å.

CHAPTER 1. INTRODUCTION

In recent years, studies of low-coordinate late transition metal complexes in synthetic organometallic chemistry has contributed to their unique reactivity in small molecule activation. The properties of a transition metal complex can be probed in a variety of ways, providing information about different aspects of homogeneous organometallic catalyst behavior.[1] Interpretation of ligand effects on experimental observations of the metal centers can provide us with a better understanding of the key that attributes to a desired transformation result, leading to better design criteria.[2]

1.1 Phosphine Ligands in Late Transition Metal Complexes

1.1.1 The nature of metal–phosphine bonding

Phosphines (Figure 1.1a) are one of the most well studied classes of L-type ancillary ligands for transition metals because of their applications in tailoring the reactivity of metals in a wide range of catalytic and stoichiometric chemistry.[3] For monodentate phosphine ligands, electronic properties as well as steric effects strongly influence physical and chemical properties of the catalysts. Numerous efforts have been made to understand the nature of metal–phosphine bonding and the electronic properties of phosphine ligands.[1, 4] The metal–phosphine bond is usually considered to arise from σ-donation from the phosphorus lone pair to empty metal orbital and backbonding from a filled metal d-orbital of π-symmetry to combinations of P−R σ* orbitals (Figure 1.1b).[5]

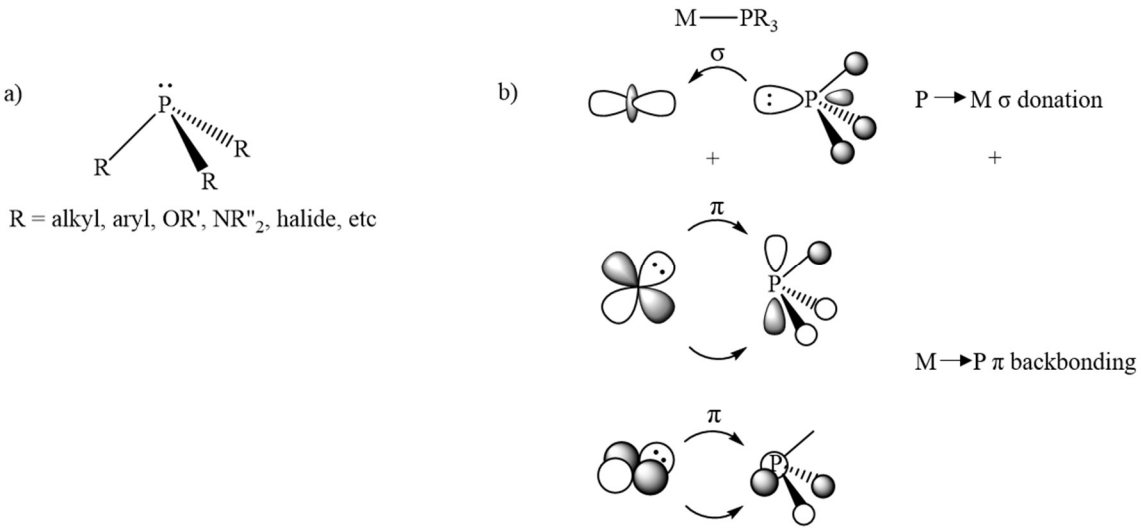

Figure 1.1. General structure of phosphines and metal–phosphine bonding model.

1.1.2 Caged phosphines in literature

Geometrical constraints have been applied to modulate ligand effects. For several decades, many groups have developed phosphorus heterocycle cages.[6] The caged phosphines, organophosphorus compounds in which the phosphorus atom is fixed at the bicyclic bridgehead positions, constitute a unique class of ligands.[6a] Compared with their acyclic analogs, the caged phosphine ligands exhibit interesting electronic features such as increased π-acceptor and decreased σ-donor ability as well as reduced steric demand. These features exert beneficial effects in several transition metal catalyst systems. Notable examples of this ligand class include 1,3,5-triaza-7-phosphaadamantane (Figure 1.2a),[6b, 6c] phosphasemibullvalene derivatives (Figure 1.2b),[6d-f] 4-phenyl-1-phospha-4-silabicyclo[2.2.2]octane (Figure 1.2c),[6g, 6h] bicyclic phosphite esters (Figure 1.2d),[6i-k] proazaphosphatranes (Figure 1.2e),[6l-q] phosphoramidite (Figure 1.2f),[6r] phosphabarrelene derivatives (Figure 1.2g)[6e, 6s-w] and phosphatriptycene derivatives (Figure 1.2h).[6x-ae]

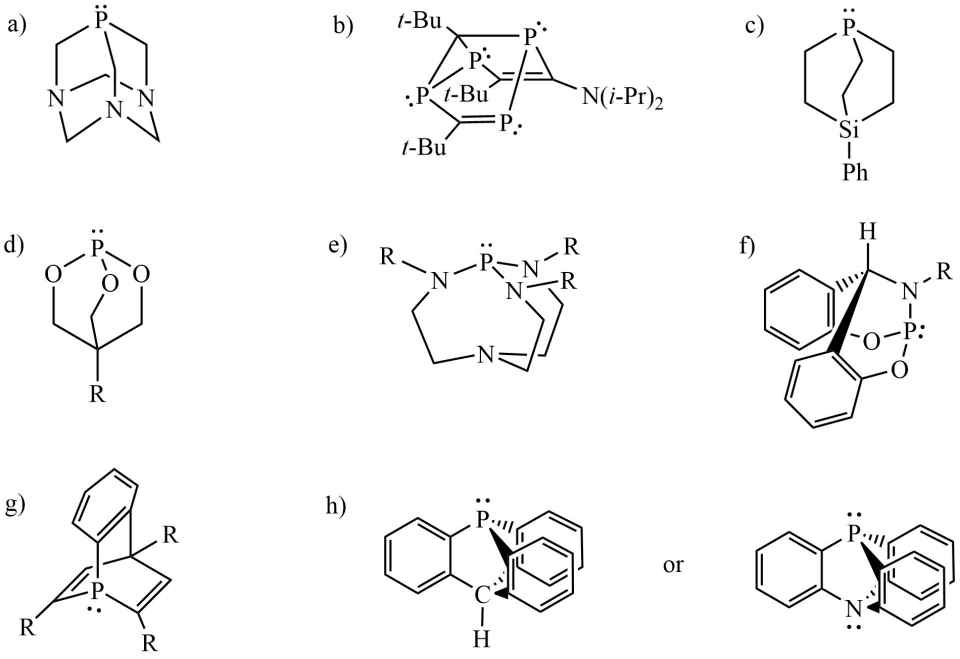

Figure 1.2. Representative bicyclic or caged phosphorus ligands.[6b-ae]

9-Phosphatriptycene[6aa] substitutes a bridgehead carbon of the robust triptycene framework with a phosphorus. Azaphosphatriptycene,[6ad] with a nitrogen atom on the opposite bridgehead position, has also been reported. The unique rigid structures and good π-acceptor characteristics of the class of phosphatriptycene have beneficial effects on several transition-metal-catalyzed reactions, such as palladium-catalyzed Stille coupling[6y] and Suzuki-Miyaura cross-coupling of chloroarenes.[6ae] Effective synthetic routes toward phosphatriptycene and novel derivatives of it could allow its more widespread use in catalysis.

1.1.3 π-Acceptor phosphine ligands in hydroformylation

Theoretical calculations and experiments have shown the importance of π-accepting phosphine ligands in homogeneous catalysis in the past decades.[7] As an

example, the rhodium-catalyzed hydroformylation reaction (Scheme 1.1) is extremely sensitive to ligand effects as well as the specific reaction conditions, so the design of active ligands has moved in the direction of increasing their π-acceptor property. Constrained cage-shaped phosphines such as phosphabarrelenes[6s, 6u] and phosphramidites[6r] with good π-acceptor properties have shown good catalytic reactivity as monodentate phosphorus ligand in the hydroformylation of less reactive alkenes. As far as we know, the phosphatriptycene class has not been introduced into the hydroformylation catalysis as supporting ligands. In light of the special electronic and relatively steric bulky properties of the phosphatriptycene ligand, we wanted to study its application in homogenous hydroformylation catalysis.

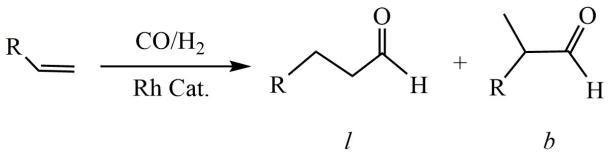

Scheme 1.1. General rhodium-catalyzed hydroformylation reaction.

1.2 NHC Ligands in Late Transition Metal Complexes

1.2.1 The nature of metal–NHC bonding

N-Heterocyclic carbenes (NHCs, Figure 1.3a) serve as electronic-rich and sterically bulky ancillary ligands for a wide variety of metal complexes.[8] The NHC ligand can be viewed as an extreme Fischer-type carbene,[9] in which σ-donation dominates the carbene-metal interaction. The bonding of traditional Fischer-type carbenes includes the σ-donor interaction from the carbene lone pair to a metal-based orbital, and π-backbonding from a filled metal dπ orbital to the carbene p-orbital.[10] Because this p-orbital is raised greatly in

energy through its π-interaction with two nitrogen donors, π-backbonding from the metal to NHC is weak and NHCs act as good σ-donors (Figure 1.2b).[11] In comparison to normal tertiary phosphines, NHCs usually exhibit a lower tendency toward ligand dissociation[12] and degradative cleavage,[13] resulting in more stable metal complexes.

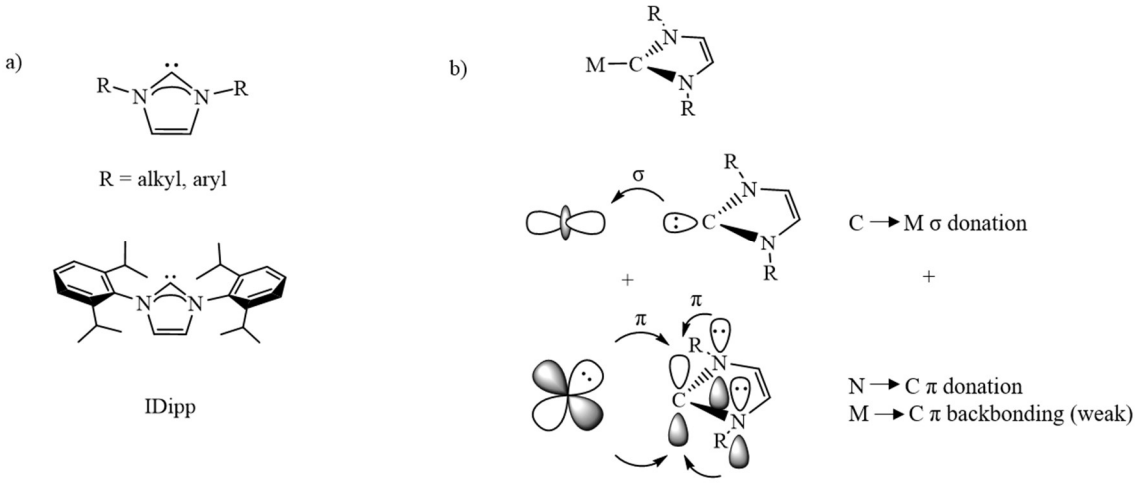

Figure 1.3. a) Examples of five-membered unsaturated NHCs [IDipp = 1,3-bis(2,6-diisopropylphenyl)imidazol-2-ylidene]. b) The metal–NHC bonding model.

1.2.2 NHC-supported transition metal hydride complexes

In recent years, NHC-coordinated metal complexes have shown unprecedented activity in many important catalytic reactions of small molecule transformations, including C−H activation, C−C, C−H, C−O and C−N bond formations.[14] Experimental studies of metal–NHC catalysts has proved that NHC ligands demonstrate their excellence in several specific homogeneous catalytic systems, e.g. palladium-catalyzed Heck-type coupling[14n-q] and ruthenium-catalyzed olefin metathesis,[14r-v] in which metal–NHC catalysts were exploited to have much better catalytic reactivity than the standard metal–phosphine analogs.

NHC ligands have been used in synthesizing a number of unusual coinage metal hydrides (Figure 1.4), which serve as key intermediates in a range of organic molecules transformations, e.g. NHC-supported terminal gold(I) hydrides,[15] a dinuclear gold(I) hydride-bridged cation,[15] a dinuclear silver(I) hydride cation,[16] a dinuclear copper(I) hydride-bridged cation[17] and copper(I) hydride dimers[18] have been reported to perform addition to unsaturated organic substrates, such as alkynes or alkenes, and to react with carbon dioxide as Lewis-base. Short Cu•••Cu distances in copper(I) hydride dimers (Figure 1.4b)[18] were observed, which might be interpreted as resulting from a net bonding interaction between the two d^{10} copper metal centers.[19] This has triggered our initial interest in developing the bonding interaction between two d^9 centers, e.g. two nickel(I) centers, with the possibility of true metal−metal σ-bond formation.

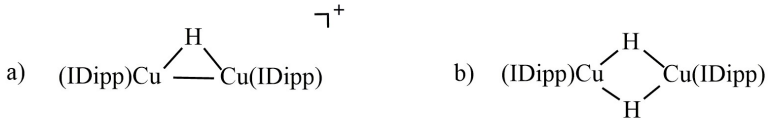

Figure 1.4. Representative NHC–supported copper(I) hydride complexes: a) a dinuclear copper(I) hydride-bridged cation;[17] b) a copper(I) hydride dimer with a Cu•••Cu distance of 2.3059(11) Å.[18a, 20]

1.2.3 Nickel(I) hydride complexes in literature

Nickel(I) is an established oxidation state in nickel chemistry,[21] but studies of nickel(I) hydride complexes are relatively rare.[21b] The reported nickel hydride dimers are mostly supported by various bidentate phosphine ligands.[22] One of the first syntheses was μ-hydrido dinickel(I) $[(dcpe)Ni(\mu\text{-}H)]_2$ (dcpe = 1,2-bis(dicyclohexylphosphino)ethane), Figure 1.5a)[22a] by reduction of $[(dcpe)NiCl_2]$ with sodium hydridotrimethylboronate. Its

molecular structure was determined later to involve two bridging hydrides, with a Ni•••Ni distance of 2.4078(5) Å.[23] μ-Hydrido dinickel(I) [(dtbpe)Ni(μ-H)]$_2$ (dtbpe = 1,2-bis(di-*tert*-butylphosphino)ethane, Figure 1.5b) was synthesized by reduction of [(dtbpe)NiCl$_2$] with activated magnesium under H_2, and it could also be obtained through the reaction of [(dtbpe)Ni^0(benzene)] with H_2.[22b] Another well-studied example is the μ-hydrido dinickel(I) [(dippe)Ni(μ-H)]$_2$ (dippe = 1,2-bis(diisopropylphosphino)ethane, Figure 1.5c),[22e] which easily undergoes H_2 reductive elimination to serve as two Ni(0) centers during reactions, showing reactivity towards several substrates, including C−C bond cleavage in biphenylene,[24] C−S bond cleavage in a variety of thiophenes,[22e, 25] and C−CN bond cleavage in nitriles.[26] Employing NHC ligands in the synthesis of nickel(I) hydride complexes and the study of their reactivity could yield interesting results, due to the compatibility of NHCs with transition metals in a variety of different oxidation states; the strong binding of NHCs to metals, which leads to a lower likelihood of ligand dissociation; and their potential in supporting highly reactive metal catalysts.

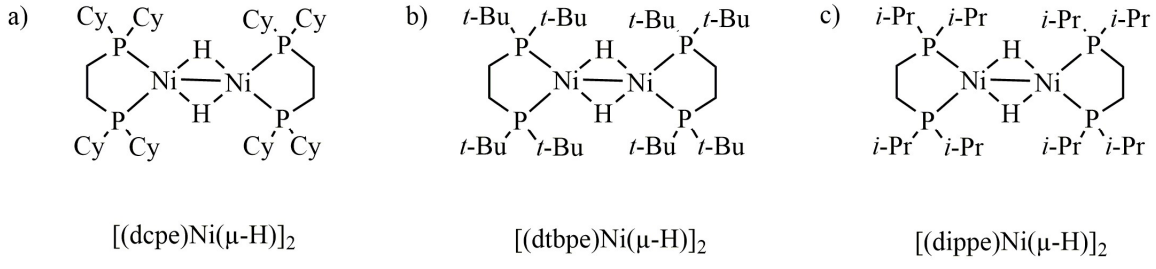

Figure 1.5. Representative nickel(I) hydride complexes.[22a, 22b, 22e, 23]

1.3 Concluding Remarks

This thesis focuses on the synthesis of novel late transition metal complexes for small molecule transformations, and on the exploration of systems on which only limited work has been done. The two avenues of inquire include the design of new caged phosphine ligands with good π-acceptor properties, and the stabilization of unusual metal–element and metal–metal bonds.

1.4 References

[1] a) P. B. Dias, M. E. M. de Piedade, J. A. M. Simões, *Coord. Chem. Rev.* **1994**, *135/136*, 737-807; b) C. A. Tolman, *Chem. Rev.* **1977**, *77*, 313-348.

[2] a) J.-P. Corbet, G. Mignani, *Chem. Rev.* **2006**, *106*, 2651-2710; b) U. Christmann, R. Vilar, *Angew. Chem. Int. Ed.* **2005**, *44*, 366-374; c) B. Schlummer, U. Scholz, *Adv. Synth. Catal.* **2004**, *346*, 1599-1626; d) W. A. Herrmann, K. Öfele, D. v. Preysing, S. K. Schneider, *J. Organomet. Chem.* **2003**, *687*, 229-248; e) P. C. J. Kamer, P. W. N. M. Van Leeuwen, J. N. H. Reek, *Acc. Chem. Res.* **2001**, *34*, 895-904.

[3] a) L. M. Pignolet, *Homogeneous catalysis with metal phosphine complexes*, Springer Science & Business Media, **2013**; b) E. C. Alyea, D. W. Meek, *Catalytic aspects of metal phosphine complexes*, American Chemical Society, **1982**; c) A. Suzuki, *Angew. Chem. Int. Ed.* **2011**, *50*, 6722-6737; d) E. i. Negishi, *Angew. Chem. Int. Ed.* **2011**, *50*, 6738-6764; e) R. H. Grubbs, *Angew. Chem. Int. Ed.* **2006**, *45*, 3760-3765; f) R. Noyori, *Angew. Chem. Int. Ed.* **2002**, *41*, 2008-2022; g) W. S. Knowles, *Angew. Chem. Int. Ed.* **2002**, *41*, 1998-2007.

[4] a) S. Song, E. C. Alyea, *Comments Inorg. Chem.* **1996**, *18*, 145-164; b) E. C. Alyea, S. Song, *Comments Inorg. Chem.* **1996**, *18*, 189-221.

[5] a) A. G. Orpen, N. G. Connelly, *Organometallics* **1990**, *9*, 1206-1210; b) A. G. Orpen, N. G. Connelly, *J. Chem. Soc., Chem. Commun.* **1985**, 1310-1311; c) S.-X. Xiao, W. C. Trogler, D. E. Ellis, Z. Berkovitch-Yellin, *J. Am. Chem. Soc.* **1983**, *105*, 7033-7037.

[6] a) M. Zablocka, A. Hameau, A.-M. Caminade, J.-P. Majoral, *Adv. Synth. Catal.* **2010**, *352*, 2341-2358; b) A. D. Phillips, L. Gonsalvi, A. Romerosa, F. Vizza, M. Peruzzini, *Coord. Chem. Rev.* **2004**, *248*, 955-993; c) M. J. Jacobsen, E. D. Funder, J. R. Cramer, K. V. Gothelf, *Org. Lett.* **2011**, *13*, 3418-3421; d) J. Geier, G. Frison, H. Grützmacher, *Angew. Chem. Int. Ed.* **2003**, *42*, 3955-3957; e) P. Binger, S.

Stutzmann, J. Bruckmann, C. Krüger, J. Grobe, D. Le Van, T. Pohlmeyer, *Eur. J. Inorg. Chem.* **1998**, *1998*, 2071-2074; f) A. Mack, B. Breit, T. Wettling, U. Bergsträsser, S. Leininger, M. Regitz, *Angew. Chem. Int. Ed.* **1997**, *36*, 1337-1340; g) A. Ochida, K. Hara, H. Ito, M. Sawamura, *Org. Lett.* **2003**, *5*, 2671-2674; h) G. Hamasaka, A. Ochida, K. Hara, M. Sawamura, *Angew. Chem. Int. Ed.* **2007**, *46*, 5381-5383; i) R. D. Pike, B. A. Reinecke, M. E. Dellinger, A. B. Wiles, J. D. Harper, J. R. Cole, K. A. Dendramis, B. D. Borne, J. L. Harris, W. T. Pennington, *Organometallics* **2004**, *23*, 1986-1990; j) W. S. Wadsworth, W. D. Emmons, *J. Am. Chem. Soc.* **1962**, *84*, 610-617; k) E. E. Joslin, C. L. McMullin, T. B. Gunnoe, T. R. Cundari, M. Sabat, W. H. Myers, *Inorg. Chem.* **2012**, *51*, 4791-4801; l) Y. Zhou, J. G. Verkade, *Adv. Synth. Catal.* **2010**, *352*, 616-620; m) C. R. Venkat Reddy, S. Urgaonkar, J. G. Verkade, *Org. Lett.* **2005**, *7*, 4427-4430; n) M. V. Nandakumar, J. G. Verkade, *Angew. Chem. Int. Ed.* **2005**, *44*, 3115-3118; o) H. Aneetha, W. Wu, J. G. Verkade, *Organometallics* **2005**, *24*, 2590-2596; p) W. Su, S. Urgaonkar, P. A. McLaughlin, J. G. Verkade, *J. Am. Chem. Soc.* **2004**, *126*, 16433-16439; q) J. You, J. G. Verkade, *Angew. Chem. Int. Ed.* **2003**, *42*, 5051-5053; r) A. Lee, S. Ahn, K. Kang, M.-S. Seo, Y. Kim, W. Y. Kim, H. Kim, *Org. Lett.* **2014**, *16*, 5490-5493; s) B. Breit, E. Fuchs, *Chem. Commun.* **2004**, 694-695; t) G. Märkl, F. Lieb, C. Martin, *Tetrahedron Lett.* **1971**, *12*, 1249-1252; u) E. Fuchs, M. Keller, B. Breit, *Chem. Eur. J.* **2006**, *12*, 6930-6939; v) M. Rigo, J. A. W. Sklorz, N. Hatje, F. Noack, M. Weber, J. Wiecko, C. Müller, *Dalton Trans.* **2016**, *45*, 2218-2226; w) O. Piechaczyk, M. Doux, L. Ricard, P. le Floch, *Organometallics* **2005**, *24*, 1204-1213; x) H. Tsuji, T. Inoue, Y. Kaneta, S. Sase, A. Kawachi, K. Tamao, *Organometallics* **2006**, *25*, 6142-6148; y) T. Agou, J. Kobayashi, T. Kawashima, *Chem. Lett.* **2004**, *33*, 1028-1029; z) H. Ube, Y. Yasuda, H. Sato, M. Shionoya, *Nat. Commun.* **2017**, *8*, 14296; aa) C. Jongsma, J. P. de Kleijn, F. Bickelhaupt, *Tetrahedron* **1974**, *30*, 3465-3469; ab) J. Kobayashi, T. Agou, T. Kawashima, *Chem. Lett.* **2003**, *32*, 1144-1145; ac) T. Agou, J. Kobayashi, T. Kawashim, *Heteroat. Chem* **2004**, *15*, 437-446; ad) D. Hellwinkel, W. Schenk, *Angew. Chem. Int. Ed.* **1969**, *8*, 987-988; ae) T. Iwai, S. Konishi, T. Miyazaki, S. Kawamorita, N. Yokokawa, H. Ohmiya, M. Sawamura, *ACS Catal.* **2015**, *5*, 7254-7264.

[7] A. G. Orpen, N. G. Connelly, *Organometallics* **1990**, *9*, 1206-1210.

[8] a) W. A. Herrmann, C. Köcher, *Angew. Chem. Int. Ed. Engl.* **1997**, *36*, 2162-2187; b) L. Jafarpour, S. P. Nolan, in *Advances in Organometallic Chemistry, Vol. 46*, Academic Press, **2000**, pp. 181-222; c) W. A. Herrmann, T. Weskamp, V. P. W. Böhm, in *Advances in Organometallic Chemistry, Vol. 48*, Academic Press, **2001**, pp. 1-69; d) W. A. Herrmann, *Angew. Chem. Int. Ed.* **2002**, *41*, 1290-1309; e) O. Kühl, *Chem. Soc. Rev.* **2007**, *36*, 592-607; f) D. Bourissou, O. Guerret, F. P. Gabbaï, G. Bertrand, *Chem. Rev.* **2000**, *100*, 39-91.

[9] E. O. Fischer, A. Maasböl, *Angew. Chem.* **1964**, *76*, 645.

[10] T. E. Taylor, M. B. Hall, *J. Am. Chem. Soc.* **1984**, *106*, 1576-1584.

[11] K. L. Fillman, J. A. Przyojski, M. H. Al-Afyouni, Z. J. Tonzetich, M. L. Neidig, *Chem. Sci.* **2015**, *6*, 1178-1188.

[12] a) R. W. Simms, M. J. Drewitt, M. C. Baird, *Organometallics* **2002**, *21*, 2958-2963; b) S. Milosevic, E. Brenner, V. Ritleng, M. J. Chetcuti, *Dalton Trans.* **2008**, 1973-1975.

[13] a) S. H. Hong, A. Chlenov, M. W. Day, R. H. Grubbs, *Angew. Chem.* **2007**, *119*, 5240-5243; b) B. R. Galan, M. Gembicky, P. M. Dominiak, J. B. Keister, S. T. Diver, *J. Am. Chem. Soc.* **2005**, *127*, 15702-15703; c) J. A. Cabeza, I. del Río, D. Miguel, M. G. Sánchez-Vega, *Chem. Commun.* **2005**, 3956-3958; d) R. F. R. Jazzar, S. A. Macgregor, M. F. Mahon, S. P. Richards, M. K. Whittlesey, *J. Am. Chem. Soc.* **2002**, *124*, 4944-4945.

[14] a) A. A. D. Tulloch, A. A. Danopoulos, R. P. Tooze, S. M. Cafferkey, S. Kleinhenz, M. B. Hursthouse, *Chem. Commun.* **2000**, 1247-1248; b) K. L. Tan, R. G. Bergman, J. A. Ellman, *J. Am. Chem. Soc.* **2002**, *124*, 3202-3203; c) M. T. Powell, D.-R. Hou, M. C. Perry, X. Cui, K. Burgess, *J. Am. Chem. Soc.* **2001**, *123*, 8878-8879; d) E. Peris, J. A. Loch, J. Mata, R. H. Crabtree, *Chem. Commun.* **2001**, 201-202; e) D. S. McGuinness, M. J. Green, K. J. Cavell, B. W. Skelton, A. H. White, *J. Organomet. Chem.* **1998**, *565*, 165-178; f) D. S. McGuinness, K. J. Cavell, *Organometallics* **2000**, *19*, 741-748; g) M. F. Lappert, R. K. Maskell, *J. Organomet. Chem.* **1984**, *264*, 217-228; h) M. G. Gardiner, W. A. Herrmann, C.-P. Reisinger, J. Schwarz, M. Spiegler, *J. Organomet. Chem.* **1999**, *572*, 239-247; i) R. H. Crabtree, *Coord. Chem. Rev.* **2007**, *251*, 595-896; j) J. C. C. Chen, I. J. B. Lin, *Organometallics* **2000**, *19*, 5113-5121; k) V. César, S. Bellemin-Laponnaz, L. H. Gade, *Chem. Soc. Rev.* **2004**, *33*, 619-636; l) R. A. Batey, M. Shen, A. J. Lough, *Org. Lett.* **2002**, *4*, 1411-1414; m) M. Albrecht, R. H. Crabtree, J. Mata, E. Peris, *Chem. Commun.* **2002**, 32-33; n) V. P. W. Böhm, C. W. K. Gstöttmayr, T. Weskamp, W. A. Herrmann, *J. Organomet. Chem.* **2000**, *595*, 186-190; o) W. A. Herrmann, J. Schwarz, M. G. Gardiner, M. Spiegler, *J. Organomet. Chem.* **1999**, *575*, 80-86; p) W. A. Herrmann, M. Elison, J. Fischer, C. Köcher, G. R. J. Artus, *Angew. Chem. Int. Ed.* **1995**, *34*, 2371-2374; q) T. Weskamp, V. P. W. Böhm, W. A. Herrmann, *J. Organomet. Chem.* **1999**, *585*, 348-352; r) T. Weskamp, W. C. Schattenmann, M. Spiegler, W. A. Herrmann, *Angew. Chem. Int. Ed.* **1998**, *37*, 2490-2493; s) T. Weskamp, F. J. Kohl, W. Hieringer, D. Gleich, W. A. Herrmann, *Angew. Chem. Int. Ed.* **1999**, *38*, 2416-2419; t) T. Weskamp, F. J. Kohl, W. A. Herrmann, *J. Organomet. Chem.* **1999**, *582*, 362-365; u) U. Frenzel, T. Weskamp, F. J. Kohl, W. C. Schattenmann, O. Nuyken, W. A. Herrmann, *J. Organomet. Chem.* **1999**, *586*, 263-265; v) L. Ackermann, A. Fürstner, T. Weskamp, F. J. Kohl, W. A. Herrmann, *Tetrahedron Lett.* **1999**, *40*, 4787-4790.

[15] E. Y. Tsui, P. Müller, J. P. Sadighi, *Angew. Chem. Int. Ed.* **2008**, *47*, 8937-8940.

[16] B. K. Tate, C. M. Wyss, J. Bacsa, K. Kluge, L. Gelbaum, J. P. Sadighi, *Chem. Sci.* **2013**, *4*, 3068-3074.

[17] C. M. Wyss, B. K. Tate, J. Bacsa, T. G. Gray, J. P. Sadighi, *Angew. Chem. Int. Ed.* **2013**, *52*, 12920-12923.

[18] a) N. P. Mankad, D. S. Laitar, J. P. Sadighi, *Organometallics* **2004**, *23*, 3369-3371; b) A. J. Jordan, C. M. Wyss, J. Bacsa, J. P. Sadighi, *Organometallics* **2016**, *35*, 613-616.

[19] a) C. Kölmel, R. Ahlrichs, *J. Phys. Chem.* **1990**, *94*, 5536-5542; b) K. M. Merz, R. Hoffmann, *Inorg. Chem.* **1988**, *27*, 2120-2127.

[20] The Cu–H and Cu–C bonds are partial.

[21] a) N. A. Eberhardt, H. Guan, *Chem. Rev.* **2016**, *116*, 8373-8426; b) C.-Y. Lin, P. P. Power, *Chem. Soc. Rev.* **2017**, *46*, 5347-5399; c) P. Zimmermann, C. Limberg, *J. Am. Chem. Soc.* **2017**, *139*, 4233-4242.

[22] a) K. Jonas, G. Wilke, *Angew. Chem. Int. Ed.* **1970**, *9*, 312-313; b) I. Bach, R. Goddard, C. Kopiske, K. Seevogel, K.-R. Pörschke, *Organometallics* **1999**, *18*, 10-20; c) M. D. Fryzuk, G. K. B. Clentsmith, D. B. Leznoff, S. J. Rettig, S. J. Geib, *Inorg. Chim. Acta* **1997**, *265*, 169-177; d) B. L. Barnett, C. Krüger, Y.-H. Tsay, R. H. Summerville, R. Hoffmann, *Chem. Ber.* **1977**, *110*, 3900-3909; e) D. A. Vicic, W. D. Jones, *J. Am. Chem. Soc.* **1997**, *119*, 10855-10856.

[23] J. Cornella, E. Gómez-Bengoa, R. Martin, *J. Am. Chem. Soc.* **2013**, *135*, 1997-2009.

[24] a) B. L. Edelbach, D. A. Vicic, R. J. Lachicotte, W. D. Jones, *Organometallics* **1998**, *17*, 4784-4794; b) B. L. Edelbach, R. J. Lachicotte, W. D. Jones, *Organometallics* **1999**, *18*, 4040-4049.

[25] a) D. A. Vicic, W. D. Jones, *Organometallics* **1998**, *17*, 3411-3413; b) J. Torres-Nieto, W. W. Brennessel, W. D. Jones, J. J. García, *J. Am. Chem. Soc.* **2009**, *131*, 4120-4126.

[26] a) T. A. Ateşin, T. Li, S. Lachaize, W. W. Brennessel, J. J. García, W. D. Jones, *J. Am. Chem. Soc.* **2007**, *129*, 7562-7569; b) T. Li, J. J. García, W. W. Brennessel, W. D. Jones, *Organometallics* **2010**, *29*, 2430-2445; c) J. J. García, A. Arévalo, N. M. Brunkan, W. D. Jones, *Organometallics* **2004**, *23*, 3997-4002; d) J. J. Garcia, W. D. Jones, *Organometallics* **2000**, *19*, 5544-5545; e) J. J. Garcia, N. M. Brunkan, W. D. Jones, *J. Am. Chem. Soc.* **2002**, *124*, 9547-9555.

CHAPTER 2. SYNTHESIS, CHARACTERIZATION, COORDINATION CHEMISTRY OF PHOSPHATRIPTYCENE

2.1 Background

Phosphines are well-established supporting ligands applied in homogeneous catalysis for many mid- and late-transition metals.[1] Sterically demanding monodentate phosphines have enabled a number of cross-coupling transformations, including challenging examples of carbon–carbon and carbon–heteroatom bond formation.[2]

Theoretical calculations and experiments have shown the importance of π-back donation to phosphine ligands.[3] As an example, rhodium-catalyzed hydroformylation reactions are extremely sensitive to ligand effects as well as specific reaction conditions, so the designs for active ligands have sought to increase their π-acidity.[4] (These findings will be discussed further in Chapter 3.) The established π-acceptor ligands such as phosphites and phosphonites are susceptible to phosphorus-oxygen bond cleavage, leading to catalyst deactivation.[5] An alternative route to improve the π-acidity of phosphine ligands PR_3 is to constrain the R−P−R angles to form cage-shaped phosphines. Molecular orbital calculations for simple phosphines have shown that when the geometry of phosphine becomes more pyramidal, from the planar symmetry group D_{3h} to the pyramidal symmetry group C_{3v} (constraining to R−P−R angles from 120° toward 90°), the decrease in energy of the LUMO (P−R σ*) would lead to stronger π-back donation from transition metals in metal-phosphine complexes.[3]

New sterically bulky phosphine ligands, with strong π-acidic properties achieved through geometric constraints, could lead to more reactive catalysts in specific systems. Rational design and optimization of synthetic routes for the phosphatriptycene class have triggered our interest due to the unusual electronic properties engendered by their constrained geometries, and intriguing applications in specific reactions. Schenk et al. first synthesized 10-aza-9-phosphatriptycene, noting its very high-field ^{31}P NMR chemical shift and giving evidence for a high degree of s-character in the phosphorus lone pair.[6] Bickelhaupt et al. prepared the parent 9-phosphatriptycene and noted its low Lewis-basicity.[7] Kawashima et al. investigated the strong π-acidity of 9-phosphatriptycene, and employed it as an effective ligand for the palladium-catalyzed Stille reaction.[8] Tsuji, Tamao et al. synthesized a series of 9-phospha-10-silatriptycenes, studying a phosphine selenide and a platinum(II) complex to gain insight into the electronic properties of the ligand.[9] Sawamura et al. modified this synthesis and studied this platform in catalysis, applying a silica-tethered variant in the palladium-catalyzed Suzuki-Miyaura cross-coupling of chloroarenes under mild conditions.[10] Shionoya et al. used 3-methoxy-10-aza-9-phosphatriptycenes, bound to a platinum(II) center, as gears in a study of mechanical switching.[11] Most recently, Sawamura et al.[12] and Peters et al.[13] synthesized salts of the 9-phosphatriptycene-10-phenylborate anion, and studied its coordination to transition metals.

In this chapter we focus on the preparation of phosphatriptycene derivatives and a sterically bulky azaphosphatriptycene. With small atoms such as carbon or nitrogen at the 10-position in the phosphatriptycene framework, the designed molecules are bowl-shaped, and functional groups flanking the bridgehead phosphorus lean outward, leaving space for

the phosphorus atom to bind to a metal (Figure 2.1). Different functionalization routes were attempted.

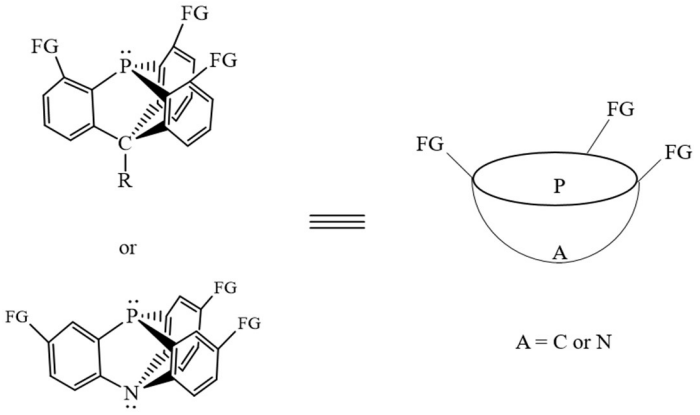

Figure 2.1. Designed phosphatriptycene targets (FG = functional group).

2.2 Results and Discussion

2.2.1 Synthesis of 10-hydroxy-9-phosphatriptycene and derivatives

Until recently, exploration of phosphatriptycenes has been slowed by synthetic challenges. Tris(2-lithiophenyl)phosphine, generated from tris(2-bromophenyl)phosphine by halogen-lithium exchange, served as the key intermediate in the preparation of both 9-phospha-10-silatriptycenes[9-10] and of the 9-phosphatriptycene-10-phenylborate anion.[12-13] The 10-hydroxy-9-phosphatriptycene **1** has been prepared through reaction of tris(2-lithiophenyl)phosphine intermediate with phenyl chloroformate (Scheme 2.1). The ^{31}P NMR spectra of 10-hydroxy-9-phosphatriptycene (δ –72.2 ppm in $CDCl_3$ and δ –73.2 ppm in acetone-d_6) show extremely high-field shifts compared to that of tris(2-bromophenyl)phosphine (δ –3.0 ppm in $CDCl_3$), as the free electron pair on the phosphorus atom in 10-hydroxy-9-phosphatriptycene has higher s-character due to the unusual narrow

C−P−C angles. The phosphorus resonance chemical shift is intermediate between the known 10-hydroxy-9-phospha-10-silatriptycene (δ –54.0 ppm in $CDCl_3$)[10] and 10-aza-9-phosphatriptycene (δ –80.0 ppm in $CDCl_3$),[6a] reflecting the decrease of the C−P−C bond angle due to decreasing sizes of atoms on the 10-position.

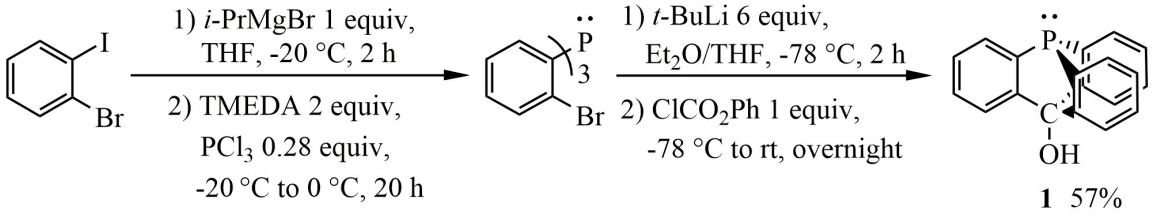

Scheme 2.1. Synthesis of 10-hydroxy-9-phosphatriptycene (**1**).

Silyl groups have been used as effective protective groups for the hydroxyl group at the bridgehead of triptycene, in the presence of *n*-butyllithium.[14] The silylation of **1** proceeded rapidly using the strong homogeneous base sodium bis(trimethylsilyl)amide to deprotonate the hydroxyl, followed by addition of trimethylsilyl or triethylsilyl chloride (Scheme 2.2).

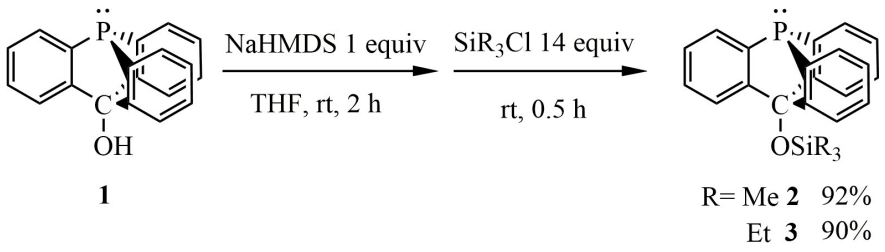

Scheme 2.2. Synthesis of 10-trimethylsiloxy-9-phosphatriptycene (**2**) and 10-triethylsiloxy-9-phosphatriptycene (**3**).

10-Hydroxy-9-phosphatriptycene oxide **4** was prepared by oxidation of **1** with hydrogen peroxide, and the silylated product 10-triethylsiloxy-9-phosphatriptycene 9-oxide **5** was synthesized by reaction of **4** with sodium bis(trimethylsilyl)amide followed by addition of triethylsilyl chloride (Scheme 2.3a). 10-Hydroxy-9-phosphatriptycene 9-phenylimide (**6**) was prepared by reaction of phenyl azide with **1** (Scheme 2.3b).

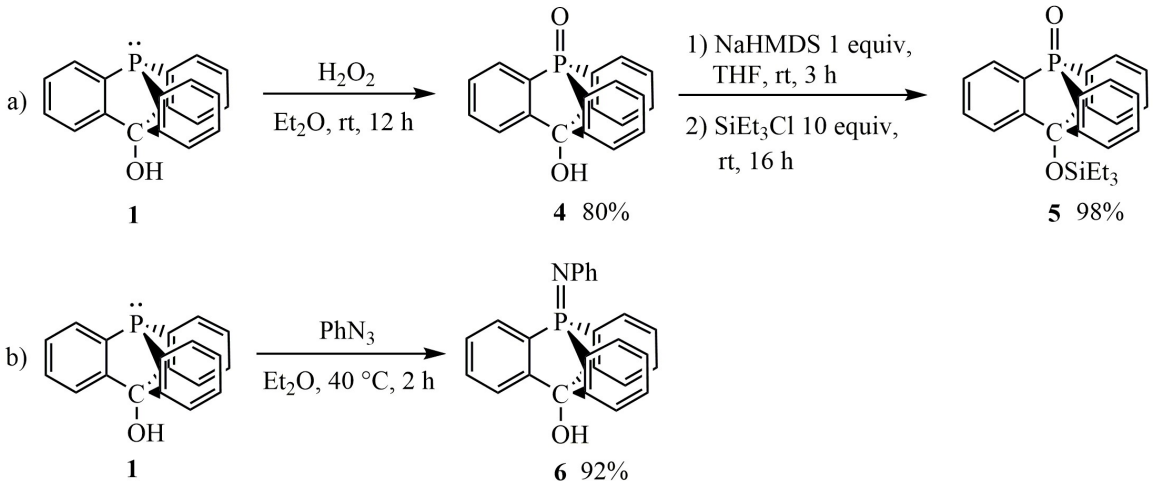

Scheme 2.3. Synthesis of 10-hydroxy-9-phosphatriptycene oxide (**4**), 10-triethylsiloxy-9-phosphatriptycene oxide (**5**), and 10-hydroxy-9-phosphatriptycene 9-phenylimide (**6**).

2.2.2 Attempted routes towards ortho-functionalized 9-phosphatriptycene

2.2.2.1 Directed *ortho* metalation on phosphatriptycene framework

An effective route to control the steric bulk of the 9-phosphatriptycene framework is designed here through directed metalation at the C−H positions adjacent to the phosphorus on the 9-position followed by functionalization. Directed *ortho* metalation[15] comprises the deprotonation of *ortho* position to a heteroatom-containing directed metalation group (DMG) by a metal base, leading to an *ortho*-metallated intermediate

which, upon treatment with electrophilic reagents, yields *ortho*-functionalized product (Scheme 2.4).

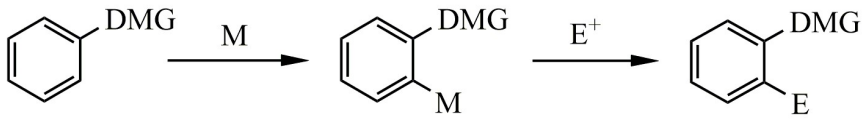

Scheme 2.4. General directed *ortho*-metalation.

Effective directed metalation can be achieved by variations in DMG, base, reaction conditions such as solvent effect, temperature and duration, etc. Phosphine oxide (P=O)[16] and iminophosphorane (P=NPh)[17] groups have been reported in literature as effective DMGs for aryl *ortho* C−H metalation using powerful strong bases such as alkyl- or aryl-lithium reagents. The phosphorus atom might also serve as an effective DMG due to the widespread use of phosphine as ancillary ligand in metal complexes. A number of hindered amide bases such as lithium 2,2,6,6-tetramethylpiperidide,[18] magnesium bromide 2,2,6,6-tetramethylpiperidide,[19] zinc chloride (2,2,6,6-tetramethylpiperidide) lithium chloride,[20] and lithium di-*tert*-butyl-(2,2,6,6-tetramethylpiperidino)zincate[21] have proven to be especially selective metalation reagents under mild conditions. *Ortho*-metallated iminophosphorane complexes have been isolated by reaction of palladium acetate with iminophosphoranes, leading to *ortho*-functionalized phosphine frameworks.[22] Herein, screening of phosphatriptycene substrates with different DMG, metalation reagents and reaction conditions has been conducted to develop possible synthesis routes toward *ortho*-functionalized 9-phosphatriptycene. A brief summary is listed in Table 2.1.

Table 2.1. C−H functionalization of *ortho* H to phosphorus in phosphatriptycene.[a]

Entry	Substrate	Reagent	Ratio[b]	T (°C)	*t* (h)	Result
1	**2**	*t*-BuLi	3	–78	0.3	**1** (25%)
2	**3**	TMPZn(*t*-Bu)$_2$Li	3	25	5	N. R.
3	**5**	*t*-BuLi	3	–78	3	decomp
4	**5**	*t*-BuLi	1	–95	0.5	decomp
5	**5**	TMPLi	3	–78	0.1	**4** (11%), **3** (3%)
6	**5**	TMPMgBr	3	25	13	decomp
7	**5**	TMPZnCl•LiCl	3	25	48	N. R.
8	**6**	PhLi	3	25	6	Scheme 2.5
9	**6**	PhLi	3	40	19	**4** (14%), Scheme 2.5
10	**6**	TMPZn(*t*-Bu)$_2$Li	3	25	17	**4** (17%), decomp
11	**6**	Pd(OAc)$_2$	1	50	21	Scheme 2.6

[a] Metallated intermediates were tested by reaction with deuterium oxide and analysis by ^{1}H NMR and ^{31}P NMR spectroscopy. Entries 1-7 and Entry 10 were conducted in THF, Entries 8-9 were conducted in Et$_2$O and Entry 11 was conducted in DCM. [b] Ratio of metalation reagent to substrate.

Following addition of three equivalents of *tert*-butyllithium to **2,** and quenching with deuterium oxide, there was no decrease in intensity for aromatic hydrogen resonances in the ^{1}H NMR spectrum as expected for deuterium incorporation. In addition, 25 mol % regeneration of desilylated phosphatriptycene **1** was observed (Table 2.1 Entry 1), indicating cleavage of the trimethylsilyl ether by *tert*-butyllithium. Neither *tert*-butyllithium nor the amide base lithium di-*tert*-butyl-(2,2,6,6-tetramethylpiperidino)zincate (Table 2.1 Entry 2) gave rise to deuterium incorporation, indicating that phosphorus did not serve as a directing group for attempted metalation.

Directed *ortho*-metalation of **5** was first attempted by three equivalents of *tert*-butyllithium, and several new ^{31}P resonances were observed after 3 h at –78 °C (Table 2.1 Entry 3), indicating strong competition of P−C cleavage during the process of metalation. Decreasing the reaction temperature to –95 °C, the reaction time to 0.5 h, and the added alkyllithium reagent to one equivalent still gave rise to decomposed phosphine products, albeit to a lesser degree (Table 2.1 Entry 4). Reaction of the sterically hindered metalation reagent lithium 2,2,6,6-tetramethyl-piperidide with **5** generated desilylated product **4** (11 mol %) and deoxygenated product **3** (3 mol %) in 6 min (Table 2.1 Entry 5). As lithium reagents were too harsh for successful metalation of phosphatriptycene oxide, the newly developed softer reagent magnesium bromide 2,2,6,6-tetramethylpiperidide (Table 2.1 Entry 6) was used, leading to several decomposition products. The still-milder reagent zinc chloride (2,2,6,6-tetramethylpiperidide) lithium chloride (Table 2.1 Entry 7) was attempted, but resulted in no reaction.

Directed *ortho*-metalation of **6** was first attempted by reaction with phenyllithium. After six hours at 25 °C and quenching with deuterium oxide, a peak with m/z equal to that

of [**6**+3] was detected in MS/EI. Further study by ^{1}H NMR showed that one *ortho* C−H to P=N on 9-position and one *ortho* C−H to C−OH in 10-postion were metallated (Table 2.1 Entry 8, Scheme 2.5). Increasing reaction temperature to 40 °C and reaction duration did not influence the distribution of metalation percentage, but formed more oxidized product **4** (Table 2.1 Entry 9). The reaction of zincation reagent lithium di-*tert*-butyl-(2,2,6,6-tetramethylpiperidino)zincate with **6** occurred to the formation of hydrolyzed product **4** (17 mol %) and decomposed species (20 mol %) (Table 2.1 Entry 10).

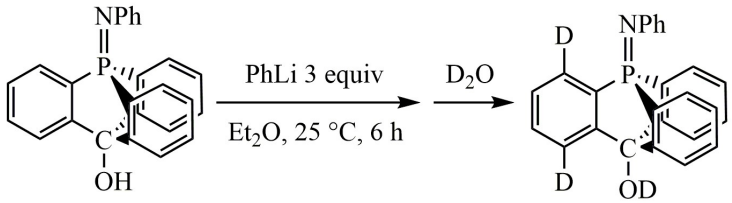

6

Scheme 2.5. Directed *ortho* metalation of **6** using phenyl lithium.

The reaction of **6** with palladium acetate followed by the electrophile *N*-bromosuccinimide did not form the expected *ortho*-metallated iminophosphorane product, while bromination occurred at the *para* and one *ortho* position of the *N*-phenyl group. (Table 2.1 Entry 11, Scheme 2.6)

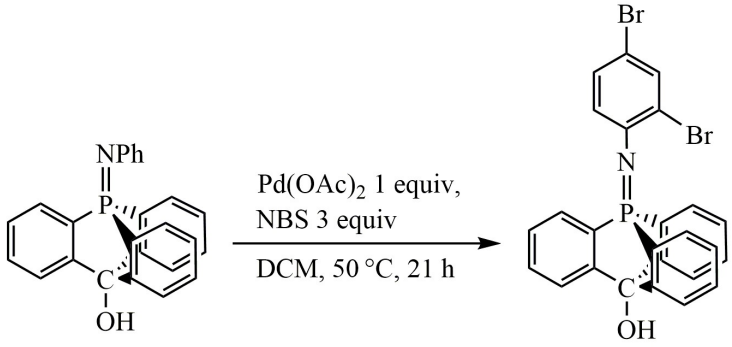

6

Scheme 2.6. Bromination of **6** with palladium acetate.

2.2.2.2 Attempted synthesis starting from pre-functionalized triphenylphosphine

Since directed metalation on parent phosphatriptycene or derivatives did not show promising preliminary results in the synthesis of *ortho*-functionalized phosphatriptycenes, we attempted to follow other routes, starting from elaboration of tris(2-FG-6-metallophenyl)phosphine (FG = functional group) and subsequent reaction with electrophiles to constrain the phosphines.

The first attempt was selective metalation of the known tris(2,6-dichlorophenyl)phosphine[23] to form tris(2-chloro-6-magnesiophenyl)phosphine, followed by reaction with phenyl chloroformate (Scheme 2.7). 1,3-Dichlorobenzene has been reported to react with magnesium in the presence of lithium chloride to give the selectively metallated product 3-chlorophenylmagnesium chloride.[24] Catalytic anthracene in magnesium THF solution generates the magnesium reagent [Mg(anthracene)$(THF)_3$],[25] which could also serve as the metalation reagent. In addition, there is an efficient method for the preparation of aryllithium reagents from aryl chlorides using lithium 4,4'-di-*tert*-butylbiphenylide (LDBB).[26] Thus, we attempted to conduct metalation reactions of our substrate tris(2,6-dichlorophenyl)phosphine under similar reaction conditions then react with phenyl chloroformate to synthesize tris-*ortho*-chloro-substituted phosphatriptycene. A brief summary was listed in Table 2.2. Unfortunately, tris(2,6-dichlorophenyl)phosphine could not be metallated using magnesium and lithium chloride under the same conditions that succeeded for 1,3-dichlorobenzene (Table 2.2 Entry 1). The use of magnesium with added anthracene (Table 2.2 Entry 2), and metalation using LDBB (Table 2.2 Entry 3), formed several unidentified products in ^{31}P NMR, presumably due to reductive cleavage of the C−P bonds.

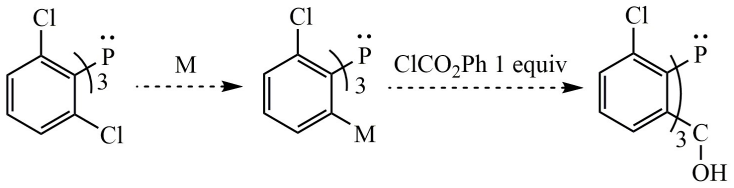

Scheme 2.7. Proposed synthesis for tris-*ortho*-chloro substituted phosphatriptycene.

Table 2.2. Selective metalation on tris(2,6-dichlorophenyl)phosphine.[a]

Entry	Reagent	Additive	T (°C)	*t* (h)	Result
1[b]	Mg	LiCl	25	4.5	no metalation
2[b]	Mg	LiCl, anthracene[c]	25	4.5	mixture
3[d]	LDBB	-	–95	0.5	mixture

[a] Reactions were conducted in THF. [b] Mg 7.5 equiv, pre-activated by 1,2-dibromoethane (2 drops); LiCl 3.75 equiv. [c] Anthracene 0.75 equiv. [d] LDBB 6 equiv.

Another attempt to synthesize tris-*ortho*-FG substituted phosphatriptycene, involved the generation of tris(2-bromo-6-FG-phenyl)phosphine followed by halogen-metal exchange and reaction with phenyl chloroformate (Scheme 2.8a). For synthesis of tris(2-bromo-6-FG-phenyl)phosphine, we started from the similar routes for synthesizing tris(2-bromophenyl)phosphine,[10] by reaction of an *ortho*-metallated bromoarene with a phosphorus electrophile. Two synthetic routes were designed. One used the carbamoyl fragment in 3-bromophenyl *N,N*-diethylcarbamate as the DMG, followed by reaction with a phosphorus source (Scheme 2.8b). A brief summary is listed in Table 2.3.

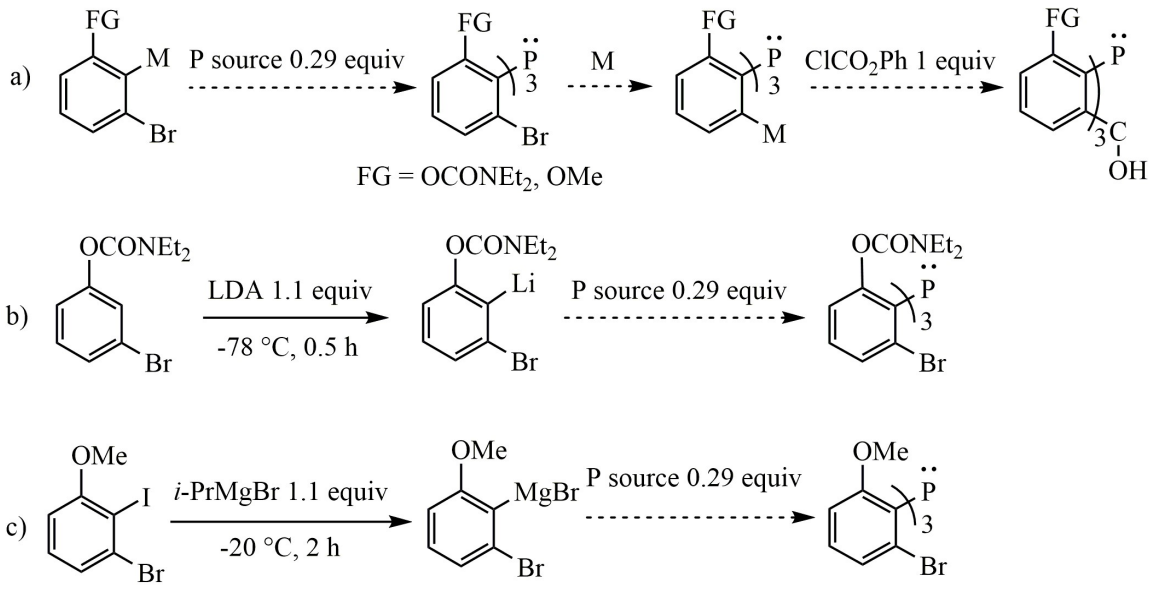

Scheme 2.8. Proposed synthesis for tris-*ortho*-FG substituted phosphatriptycene.

Table 2.3. Attempted synthesis of tris(2-bromo-6-*N,N*-diethylcarbamoylphenyl) phosphine.[a]

Entry	Reagent	Additive	Electrophile	T (°C)	*t* (h)	Result
1	LDA	-	D_2O	–78	0.3	metalation
2	LDA	-	PCl_3	–78	0.5	mixture
3	LDA	$MgCl_2$	PCl_3	25	13	mixture
4	LDA	$ZnCl_2$	PCl_3	40	60	mixture
5	LDA	CuCl	PCl_3	25	72	mixture
6	LDA	-	$P(OPh)_3$	25	20	mixture
7	LDA	-	P(O-2,4-*t*-BuPh)$_3$	25	16	mixture

[a] LDA 1.1 equiv, –78 °C , 0.5 h; additive 1.1 equiv, –78 °C, 1 h; electrophile 0.29 equiv.

Ortho-metalation directed by carbamoyl fragment in 3-bromophenyl *N,N*-diethylcarbamate was conducted smoothly at low temperature by treatment with LDA[27] and quenching with deuterium oxide led to formation of the corresponding deuterated product, indicating complete metalation (Table 2.3 Entry 1). Different phosphorus electrophiles and different transmetalation reagents were selected for screening, however, a mixture of several products formed after each reaction (Table 2.3 Entries 2-7) as judged by ^{31}P NMR spectroscopy.

To rule out the possibility of the carbamoyl fragment reacting with the metalation reagent, a second route towards tris(2-bromo-6-FG-phenyl)phosphine was designed to use the intermediate 3-bromo-2-metalloanisole (Scheme 2.8c). A brief summary is listed in Table 2.4. Metalation of 3-bromo-2-iodoanisole was first tested by reaction with isopropylmagnesium bromide at –20 °C followed by quenching with deionized water. The formation of only 3-bromoanisole indicated the metalation performed smoothly and selectively (Table 2.4 Entry 1). When 3-bromo-2-(bromomagnesio)anisole reacted with 0.29 equivalent of phosphorus trichloride at –20 °C, followed by quenching with water, the major product gives rise to a distinct doublet at δ 8.83 ppm ($^{1}J_{\text{P-H}}$ = 551 Hz) in the ^{1}H NMR spectrum, indicating P−H bond formation in the unexpected molecule bis(2-bromo-6-methoxyphenyl)(oxo)phosphorene (Table 2.4 Entry 3, Scheme 2.9), in analogy to the published bis(2-methoxyphenyl)(oxo)phosphorene.[28] Increasing the temperature for reaction with the electrophile to 0 °C (Table 2.4 Entry 2) and adding transmetalation reagent (Table 2.4 Entry 4) led to formation of several products with phosphorus resonance. We concluded that steric factors inhibited the formation of the desired tris(2-bromo-6-methoxyphenyl)phosphine under our attempted conditions.

Table 2.4. Attempted synthesis of tris(2-bromo-6-methoxyphenyl)phosphine.[a]

Entry	Reagent	Additive	Electrophile	T (°C)	*t* (h)	Result
1	*i*-PrMgBr	none	H_2O	–20	0.3	metalation
2	*i*-PrMgBr	none	PCl_3	0	23	mixture
3	*i*-PrMgBr	none	PCl_3	–20	17	Scheme 2.9
4	*i*-PrMgBr	$ZnCl_2$	PCl_3	70	24	mixture

[a] *i*-PrMgBr 1.1 equiv, –20 °C, 2 h; additive 1.1 equiv, –20 °C, 1 h; electrophile 0.29 equiv.

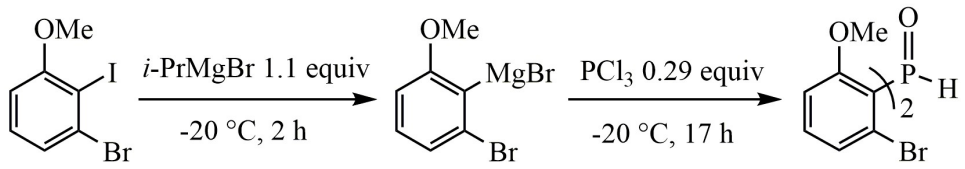

Scheme 2.9. Synthesis of bis(2-bromo-6-methoxyphenyl)(oxo)phosphorene.

2.2.3 Synthesis of 2,7,14-tri-tert-butyl-10-aza-9-phosphatriptycene

Reasoning that the elaboration of selective *ortho*-substituted phosphatriptycene might pose an insolvable challenge, we shifted our focus to the *meta*-substituted phosphatriptycene, which we imagined it could also support low-coordinated metal complexes. The threefold symmetry of 10-aza-9-phosphatriptycene suggests potentially concise routes to a variety of trisubstituted variants. Hellwinkel and coworkers synthesized the *meta*-trisubstituted 2,7,14-trimethyl-10-aza-9-phosphatriptycene from tri-*p*-tolylamine

by a sequence of triple bromination, halogen-metal exchange with *n*-butyllithium, and quenching with triphenyl phosphite. They reported difficulties in reproducing this route,[6b, 29] however, and subsequently analogized the elegant but synthetically demanding route that Bickelhaupt and coworkers used to obtain 9-phosphatriptycene.[7]

We found a triple lithiation procedure effective for the preparation of tris(2-lithiophenyl)amine intermediates from tris(2-bromo-4-*tert*-butylphenyl)amine. The crystalline, air-stable tris(2,4-di-*tert*-butylphenyl)phosphite proved more convenient than triphenyl phosphite as the electrophile, and led to higher yields; we believe that increased steric demand favors closing of the bicyclic framework over intermolecular side-reactions. Scheme 2.10 shows the synthesis of 2,7,14-tri-*tert*-butyl-10-aza-9-phosphatriptycene **7** from readily available, inexpensive precursors. Crystallization of **7** from methanol effectively removes the byproduct 2,4-di-*tert*-butylphenol, and allows isolation of the air-stable product on gram-scale, in 71% yield. The ^{31}P NMR resonance for **7** appears at very high field, δ –77.0 ppm (in $CDCl_3$), similar to that of δ –80 ppm for the parent 10-aza-9-phosphatriptycene.[6a]

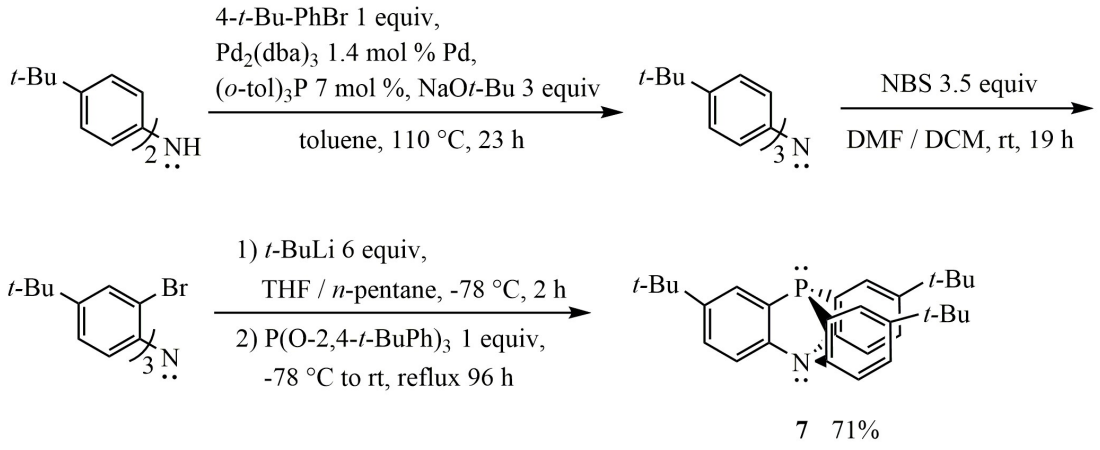

Scheme 2.10. Synthesis of 2,7,14-tri-*tert*-butyl-10-aza-9-phosphatriptycene (**7**).

2.2.4 Coordination chemistry of phosphatriptycene

The first phosphatriptycene-supported copper complexes **8**, **9** and **10** have been prepared by reaction of **2**, **3** and **7** with copper(I) chloride, respectively (Scheme 2.11). The solid-state structures show copper complex **9** crystallizes in an unusual pentameric structure (Figure 2.2) whereas copper complex **10** crystallizes as a tetramer with a heterocubane structure (Figure 2.3), in analog to the acyclic triphenylphosphine copper(I) chloride complex with an M_4X_4 Core.[30] The C−P−C angles are in average of 95.60(4)° in **3** and 95.02(0)° in **7**. With the *meta*-substituents in 7, the cone angle for **7** on complex **10** is about 162.02(0)°, compared to the cone angle for **3** on complex **9** of about 122.76(2)°, reflecting the steric hindrance introduced by the *meta*-substituents.

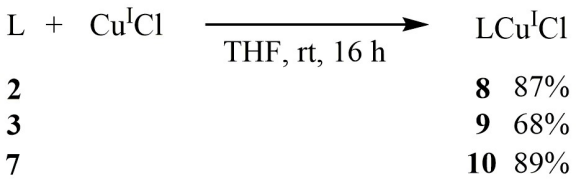

Scheme 2.11. Preparation of phosphatriptycene copper(I) chloride complexes.

Reaction of complex **10** with lithium aluminum hydride led to the dissociation of **7** (Scheme 2.12a). Reaction of ligand **7** with copper(I) acetate led to the formation of copper acetate complex **11.** Upon reaction of this species with triethoxysilane, dissociation of ligand **7** occurred (Scheme 2.12b).

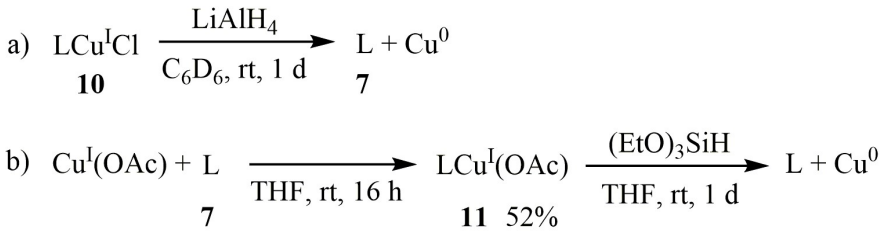

Scheme 2.12. Reactivity of azaphosphatriptycene copper(I) complexes.

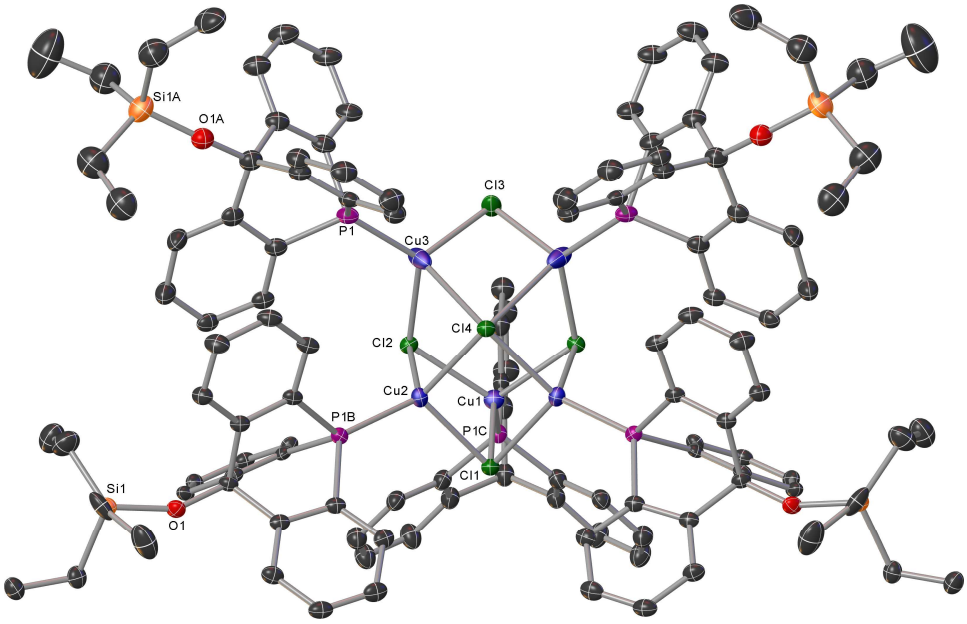

Figure 2.2. Solid-state structure of complex [(**3**)CuCl]$_5$ (**9**), ellipsoids at 50% probability. Calculated hydrogen atoms are omitted for clarity. Selected interatomic distances (Å) and angles (°): Cu1−P1C 2.171(2), Cu1−Cl1 2.417(2), Cu1−Cl2 2.3856(16), Cu2−P1B 2.1938(17), Cu2−Cl1 2.4164(18), Cu2−Cl2 2.4986(16), Cu2−Cl4 2.4004(17), Cu3−P1 2.177(2), Cu3−Cl2 2.3212(17), Cu3−Cl3 2.2632(18), Cu3−Cl4 2.918(2); Cl2−Cu1−Cl1 100.84(5), P1C−Cu1−Cl1 118.19(10), P1C−Cu1−Cl2 113.40(5), Cl1−Cu2−Cl2 97.71(7), Cl4−Cu2−Cl1 97.06(5), Cl4−Cu2−Cl2 93.08(6), P1B−Cu2−Cl1 114.18(7), P1B−Cu2−Cl2 114.66(6), P1B−Cu2−Cl4 133.31(7), Cl2−Cu3−Cl4 84.69(6), Cl3−Cu3−Cl2 109.21(9), Cl3−Cu3−Cl2 100.42(6), P1−Cu3−Cl2 122.21(7), P1−Cu3−Cl3 120.47(9), P1−Cu3−Cl4 111.49(7).

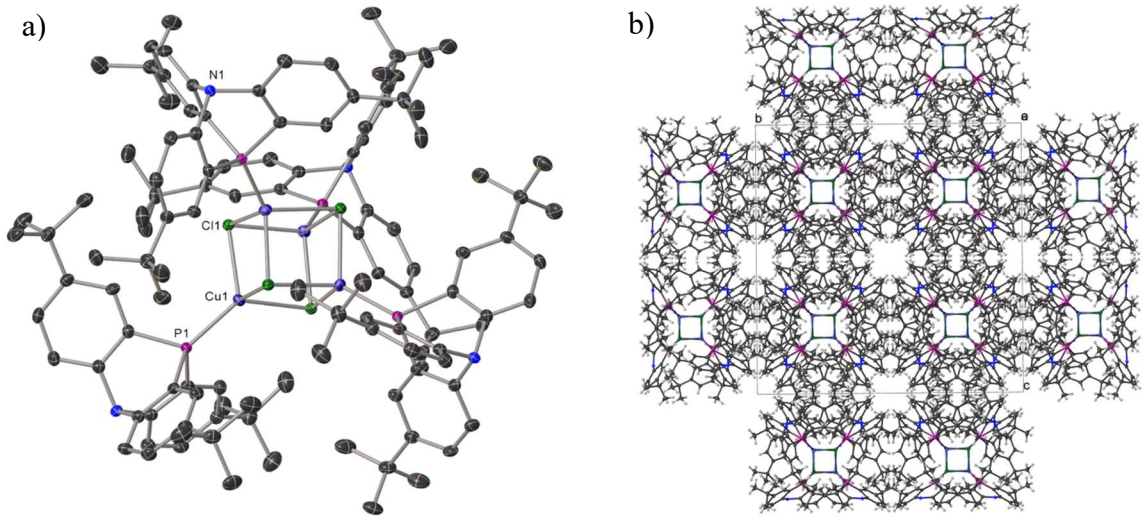

Figure 2.3. Solid-state structures of $[(7)CuCl]_4$ (**10**): a) A single molecule of **10**; b) extended structure. Ellipsoids at 50% probability. Calculated hydrogen atoms are omitted for clarity. Selected interatomic distances (Å) and angles (°): Cu1−P1 2.1668(16), Cu1−Cl1 2.4166(9); P1−Cu1−Cl1 120.97(3).

2.3 Conclusion

The 9-phosphatriptycene framework is a class of ligand with geometric constraints and good π-acceptor properties, and has been studied as a useful ligand in several homogeneous reactions. The synthesis of phosphatriptycenes bearing substituents *ortho* to the bridgehead phosphorus atom proved elusive, but we have succeeded in optimizing routes for synthesizing 10-hydroxy-9-phosphatriptycene derivatives and a new *meta*-trisubstituted azaphosphatriptycene. The phosphatriptycenes examined dissociate readily from copper(I) during attempted substitution reactions. Solid-state structures of the copper complexes show that *meta* substitution on the phosphatriptycene framework introduces significant steric bulk around the supported metal centers, with consequences to the aggregation state of the copper chloride complexes. In light of the special electronic properties and easily controlled steric properties of the azaphosphatriptycene ligand, we proceeded to study its application in homogenous catalysis.

2.4 Experimental

2.4.1 *General considerations*

Unless otherwise indicated, manipulations were carried out in resealable glassware on a Schlenk line under an atmosphere of argon, or in an MBraun glovebox under an atmosphere of nitrogen. Glassware and magnetic stir bars were dried in a ventilated oven at 160 °C and allowed to cool under vacuum.

Tetrahydrofuran (THF, EMD Millipore OmniSolv), toluene (EMD Millipore OmniSolv), diethyl ether (Et_2O, EMD Millipore OmniSolv), hexane (EMD Millipore OmniSolv) and dichloromethane (DCM, EMD Millipore OmniSolv) were sparged with ultra-high purity argon (NexAir) for 45 minutes prior to first use and dried using an MBraun solvent purification system. THF, toluene, Et_2O and hexane were further dried over sodium benzophenone ketyl, degassed by successive freeze-pump-thaw cycles and transferred under vacuum to an oven-dried resealable flasks. DCM was further dried by stirring overnight with calcium hydride (Alfa Aesar, coarse powder), degassed by successive freeze-pump-thaw cycles, and transferred under vacuum into an oven-dried resealable Schlenk flask. Benzene-d_6 (Cambridge Isotope Laboratories) was dried over sodium benzophenone ketyl, degassed by successive freeze-pump-thaw cycles and transferred under vacuum into an oven-dried resealable flask. Dichloromethane-d_2 (Cambridge Isotope Laboratories) was dried by stirring overnight with calcium hydride (Alfa Aesar, coarse powder), degassed by successive freeze-pump-thaw cycles, and transferred under vacuum into oven-dried resealable Schlenk flasks. Triphenyl phosphite (Alfa Aesar), trimethylsilyl chloride (Sigma-Aldrich), triethylsilyl chloride (Oakwood

Chemical) and triethoxysilane (Sigma-Aldrich) were transferred into oven-dried resealable Schlenk flasks and degassed by successive freeze-pump-thaw cycles prior to use. Phosphorus trichloride (Sigma-Aldrich) was distilled into an oven-dried resealable Schlenk flask and degassed by successive freeze-pump-thaw cycles prior to use. Anhydrous pentane (EMD Millipore Drisolv, sealed under a nitrogen atmosphere), copper(I) chloride (Alfa Aesar), copper(I) acetate (Strem Chemicals), sodium bis(trimethylsilyl)amide (Sigma-Aldrich), sodium hydride (Sigma-Aldrich), lithium aluminum hydride (Sigma-Aldrich), palladium acetate (Strem Chemicals) were used as received and stored in a glovebox. Lithium chloride (Sigma-Aldrich), magnesium chloride (Sigma-Aldrich) and zinc chloride (Alfa Aesar) were dried at 140 °C under vacuum overnight and stored in a glovebox. Lithium wire (3.2 mm, diam. Sigma-Aldrich), magnesium turnings (Alfa Aesar) and zinc dust (<10 μm, Sigma-Aldrich) were pre-washed with 1 M hydrochloric acid (EMD), *DI* water and Et_2O, dried under vacuum overnight and stored in a glovebox. Ethyl Acetate (BDH), methanol (BDH), ethanol (200 proof, Koptec), acetone-d_6 (Cambridge Isotope Laboratories), chloroform-*d* (Cambridge Isotope Laboratories), deuterium oxide (Cambridge Isotope Laboratories), *n*-butyllithium (2.5 M in hexanes, Sigma-Aldrich), *tert*-butyllithium (1.7 M in pentane, Sigma-Aldrich), isopropylmagnesium bromide (1.0 M in THF, Sigma-Aldrich), phenyllithium (1.9 M in dibutyl ether, Sigma-Aldrich), ethylmagnesium bromide (1.0 M in THF, Sigma-Aldrich), phosphoric acid (Sigma-Aldrich, 85 wt % in H_2O, ACS grade), hydrochloric acid (EMD), ammonium chloride (Macron Fine Chemicals), sodium chloride (Millipore Sigama), 1-bromo-2-iodobenzene (Oakwood Chemical), *N,N,N′,N′*-tetramethylethylenediamine (TMEDA) (Sigma-Aldrich), phenyl chloroformate (Alfa Aesar), 2,2,6,6-tetramethylpiperidine (Sigma-Aldrich),

sodium nitrite (Sigma-Aldrich), sodium azide (EMD), diisopropylamine (Acros Organics), 3-bromophenol (Oakwood Chemical), 3-bromoanisole (Oakwood Chemical), aniline (Sigma-Aldrich), anthracene (Alfa Aesar), 4,4'-di-*tert*-butylbiphenyl (Alfa Aesar), *N,N*-diethylcarbamoyl choride (Alfa Aesar), tris(2,4-di-*tert*-butylphenyl)phosphite (Strem Chemicals), anhydrous magnesium sulfate (Alfa Aesar, powder), di-(4-*tert*-butylphenyl)amine (TCI America), tris(dibenzylideneacetone)dipalladium(0) (Sigma-Aldrich), tris(*o*-tolyl)phosphine (Sigma-Aldrich), sodium *tert*-butoxide (TCI America), 1-bromo-4-*tert*-butylbenzene (Oakwood Chemicals), *N*-bromosuccinimide (Sigma-Aldrich), hydrogen peroxide solution (30 % w/w in H_2O, J. T. Baker, Avantor), sodium metal (Alfa Aesar), benzophenone (Alfa Aesar), calcium hydride (Alfa Aesar), nitrogen (NexAir) and argon (both industrial and ultra-high purity grades, NexAir) were used as received. Tap water was purified in a Barnstead International automated still prior to use.

Tris(4-*tert*-butylphenyl)amine,[31] tris(2-bromo-4-*tert*-butylphenyl)amine,[32] tris(2-bromophenyl)phosphine,[10] tris(2,6-dichlorophenyl)phosphine,[23] phenyl azide,[33] 3-bromophenyl *N,N*-diethylcarbamate,[27] 3-bromo-2-iodoanisole[21d, 34] were prepared according to the reported procedures and characterized by ^{1}H NMR spectroscopy, and the ^{1}H NMR resonances matched reported values. Lithium 2,2,6,6-tetramethylpiperidide,[35] magnesium bromide 2,2,6,6-tetramethylpiperidide,[19b, 36] zinc chloride (2,2,6,6-tetramethylpiperidide) lithium chloride,[20a] lithium di-*tert*-butyl-(2,2,6,6-tetramethylpiperidino)zincate,[21a] lithium 4,4'-di-*tert*-butylbiphenylide (LDBB)[37] and lithium diisopropylamide (LDA)[27] were prepared according to the reported procedures. An alternative route for synthesizing tris(2-bromophenyl)phosphine is described in Section 2.4.2.1.

^{1}H, ^{13}C and ^{31}P NMR spectra were obtained using a Varian Mercury Vx 300 and Vx 400 spectrometer. ^{1}H and ^{13}C NMR chemical shifts were referenced with respect to solvent signals[38] and reported relative to tetramethylsilane. ^{31}P NMR chemical shifts were reported with 85 wt % aqueous H_3PO_4 as external standard. Chemical shifts δ are reported in ppm. EI-MS and ESI-MS were recorded on MicroMass AutoSpec M at the Georgia Institute of Technology mass spectrometry facility. Elemental analyses were performed by Atlantic Microlab, Inc. in Norcross, GA.

2.4.2 Synthetic procedures

2.4.2.1 Tris(2-bromophenyl)phosphine

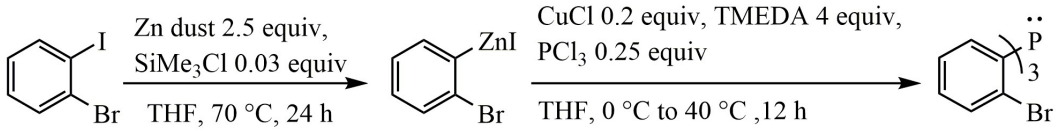

Scheme 2.13. An alternative synthesis of tris(2-bromophenyl)phosphine.

Tris(2-bromophenyl)phosphine was also prepared by an alternative method (Scheme 2.13). 1-Bromo-2-iodobenzene (4.41 g, 2.00 mL, 15.6 mmol), zinc dust (2.6 g, 40 mmol) and trimethylsilyl chloride (0.05 g, 0.06 mL, 0.5 mmol) were added in a 100-mL Schlenk flask with THF (10 mL), the solution was stirred at 70 °C for 24 h. The solution was cooled to room temperature and filtered, added dropwise to another 100-mL Schlenk flask with copper(I) chloride (0.309 g, 3.12 mmol), TMEDA (7.24 g, 9.33 mL, 62.3 mmol) and phosphorus trichloride (0.54 g, 0.34 mL, 3.90 mmol) and THF (5 mL) at 0 °C. The solution was stirred at 40 °C for another 12 h. The solution was cooled to room temperature, quenched with distilled water, and then extracted with Et_2O (3 portions, 30 mL each). The

combined organic portions were washed with distilled water and dried over $MgSO_4$. The resulting mixture was filtered, then concentrated in vacuo. The crude product was recrystallized from toluene/EtOH to afford tris(2-bromophenyl)phosphine as a white solid, 0.272 g (14%). ^{1}H and ^{31}P NMR spectra were consistent with the reported data.[10] ^{1}H NMR (400 MHz, $CDCl_3$): δ (ppm) 7.66-7.63 (m, 3H), 7.29-7.22 (m, 6H), 6.76-6.74 (m, 3H); ^{31}P NMR (162 MHz, $CDCl_3$): δ (ppm) –3.00 (s).

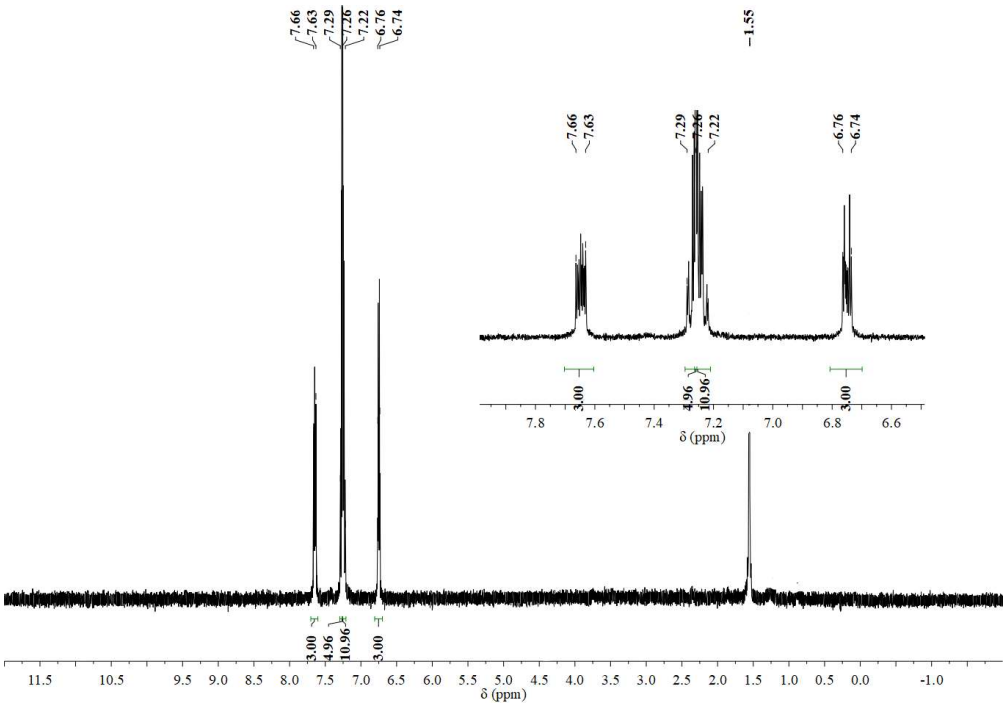

Figure 2.4. ^{1}H NMR (400 MHz, $CDCl_3$) spectrum of tris(2-bromophenyl)phosphine.

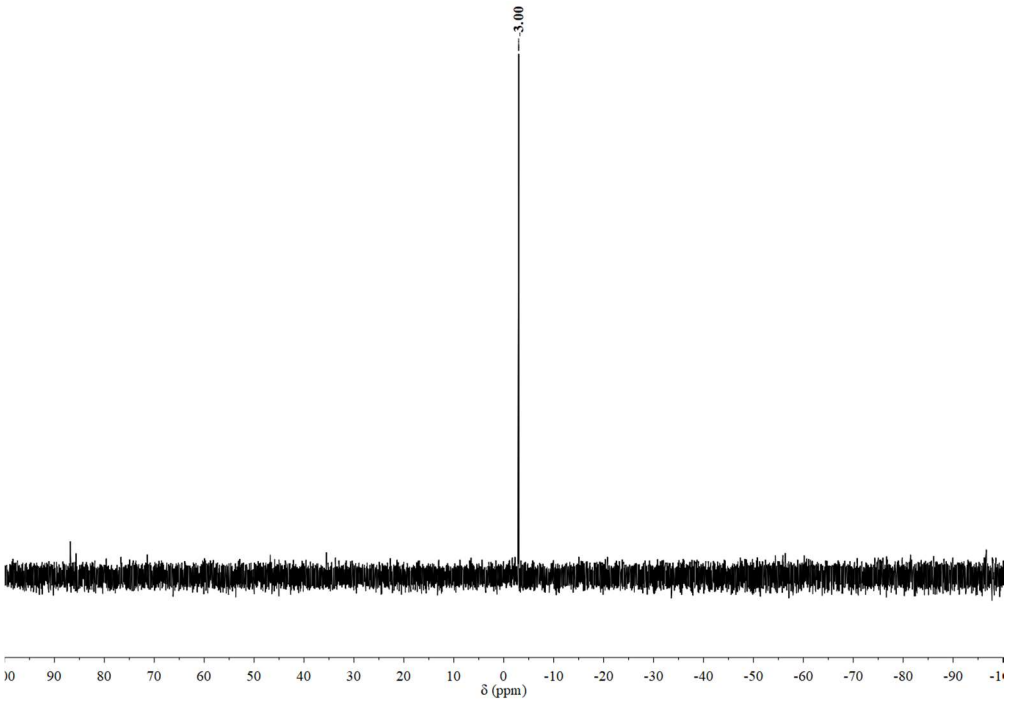

Figure 2.5. $^{31}P\{^{1}H\}$ NMR (162 MHz, $CDCl_3$) spectrum of tris(2-bromophenyl)phosphine.

2.4.2.2 10-Hydroxy-9-phosphatriptycene (**1**)

Tris(2-bromophenyl)phosphine (1 g, 2 mmol) was dissolved in THF (5 mL)/Et_2O (25 mL) mixture in a 100-mL Schlenk flask and the solution was cooled to –78 °C. *tert*-Butyllithium (1.7 M in pentane, 7.10 mL, 12 mmol) was added dropwise and the resulting solution was stirred at –78 °C for 2 h. Phenyl chloroformate (0.31 g, 0.25 mL, 2.0 mmol) was added dropwise to the reaction mixture, which was allowed to warm slowly to ambient temperature overnight. The solution was quenched with concentrated NH_4Cl aqueous solution at 0 °C, then extracted with ethyl acetate (3 x 20 mL). The combined organic portions were washed with brine (3 x 50 mL) and dried over $MgSO_4$. The resulting mixture was filtered, then concentrated in vacuo. The crude product was cleaned by washing with Et_2O (3 x 2 mL) and collected by filtration to afford **1** as a white solid, 0.331 g (57%). ^{1}H NMR (400 MHz, acetone-d_6): δ (ppm) 7.88 (ddd, $J_{H\text{-}H,\ ortho}$= 7.6 Hz, $J_{H\text{-}H,\ meta}$= 1.1 Hz, $J_{H\text{-}$

$_{H,\ para}$= 0.5 Hz, 3H), 7.75 (dddd, $^{3}J_{H\text{-}P}$= 9.1 Hz, $J_{H\text{-}H,\ ortho}$= 7.2 Hz, $J_{H\text{-}H,\ meta}$= 1.2 Hz, $J_{H\text{-}H,\ para}$= 0.5 Hz, 3H), 7.28 (tt, $J_{H\text{-}H,\ ortho}$= 7.6 Hz, $J_{H\text{-}H,\ meta}$= 1.1 Hz, $^{5}J_{H\text{-}P}$= 1.1 Hz, 3H), 7.11 (tdd, $J_{H\text{-}H,\ ortho}$= 7.3 Hz, $^{4}J_{H\text{-}P}$= 2.1 Hz, $J_{H\text{-}H,\ meta}$= 1.2 Hz, 3H), 6.50 (s, O*H*, integration decreased due to exchange of the hydroxyl proton with acetone-d_6); $^{13}C\{^{1}H\}$ NMR (101 MHz, $CDCl_3$): δ (ppm) 149.99 (d, $J_{C\text{-}P}$= 4.1 Hz), 139.63 (d, $J_{C\text{-}P}$= 10.4 Hz), 132.41 (d, $^{2}J_{C\text{-}P}$= 48.7 Hz), 128.48 (d, $J_{C\text{-}P}$= 2.0 Hz), 125.66 (d, $J_{C\text{-}P}$= 16.7 Hz), 120.97 (d, $J_{C\text{-}P}$= 1.0 Hz), 81.91 (d, $J_{C\text{-}P}$= 1.9 Hz, *C*-OH); $^{31}P\{^{1}H\}$ NMR (162 MHz, acetone-d_6): δ (ppm) –73.2 (s); $^{31}P\{^{1}H\}$ NMR (162 MHz, $CDCl_3$): δ (ppm) –72.2 (s); MS(EI): calcd m/z 288.07, found m/z 288.1 (M^{+}).

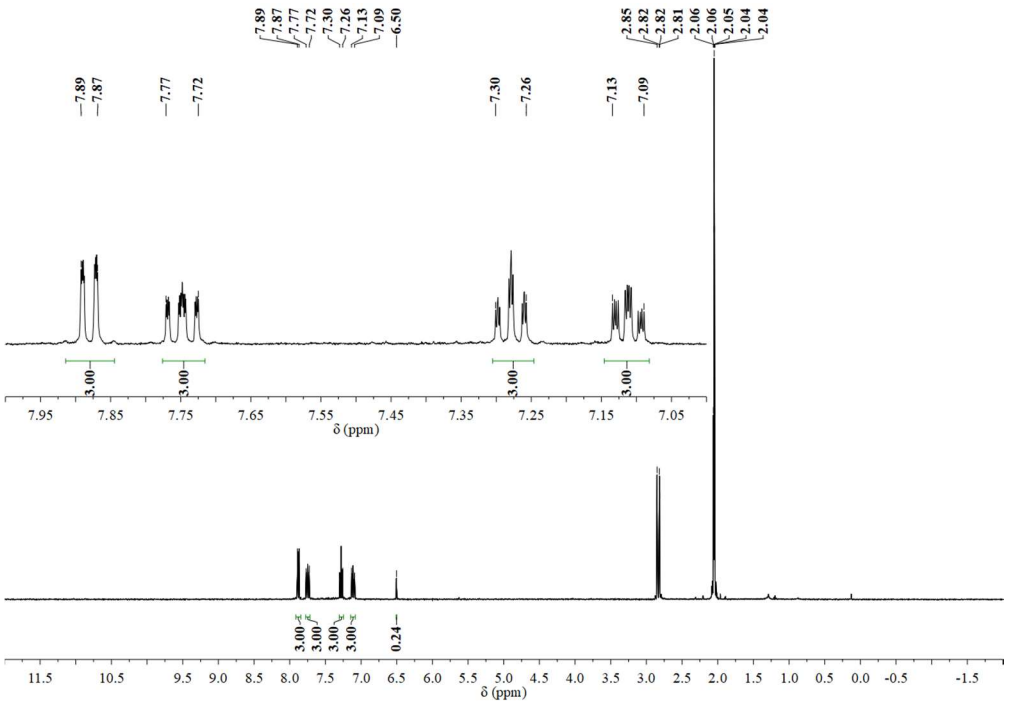

Figure 2.6. ^{1}H NMR (400 MHz, acetone-d_6) spectrum of **1**. Signals for H_2O (δ 2.85 ppm, s) and HDO (δ 2.81 ppm, t, $^{2}J_{H\text{-}D}$ = 1.0 Hz) were observed in $(CD_3)_2CO$.[38]

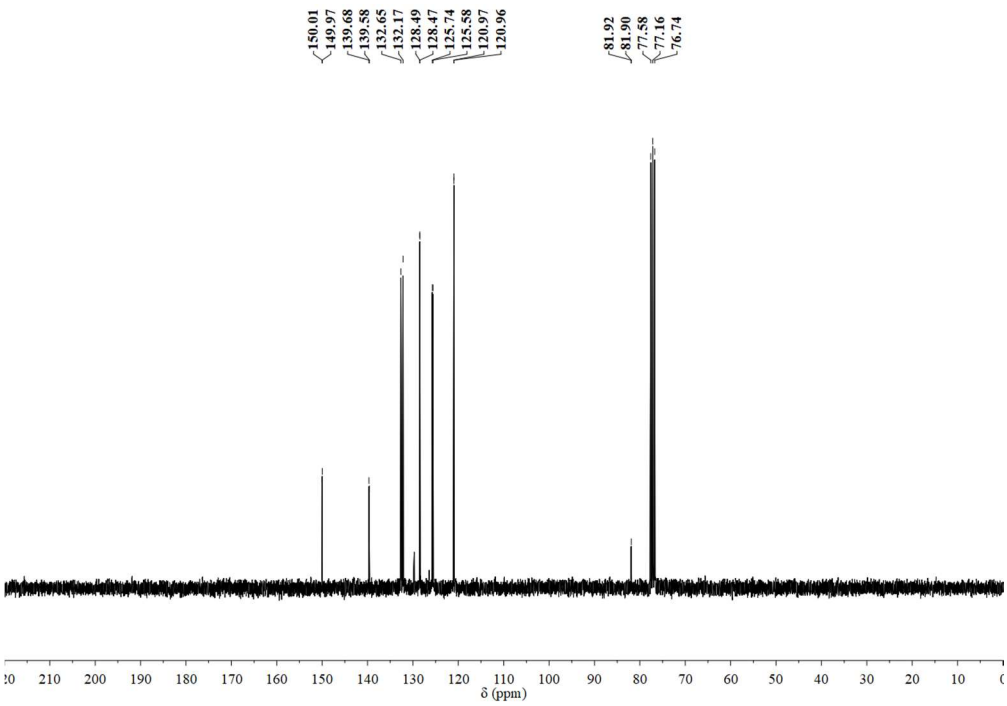

Figure 2.7. $^{13}C\{^{1}H\}$ NMR (101 MHz, $CDCl_3$) spectrum of **1**.

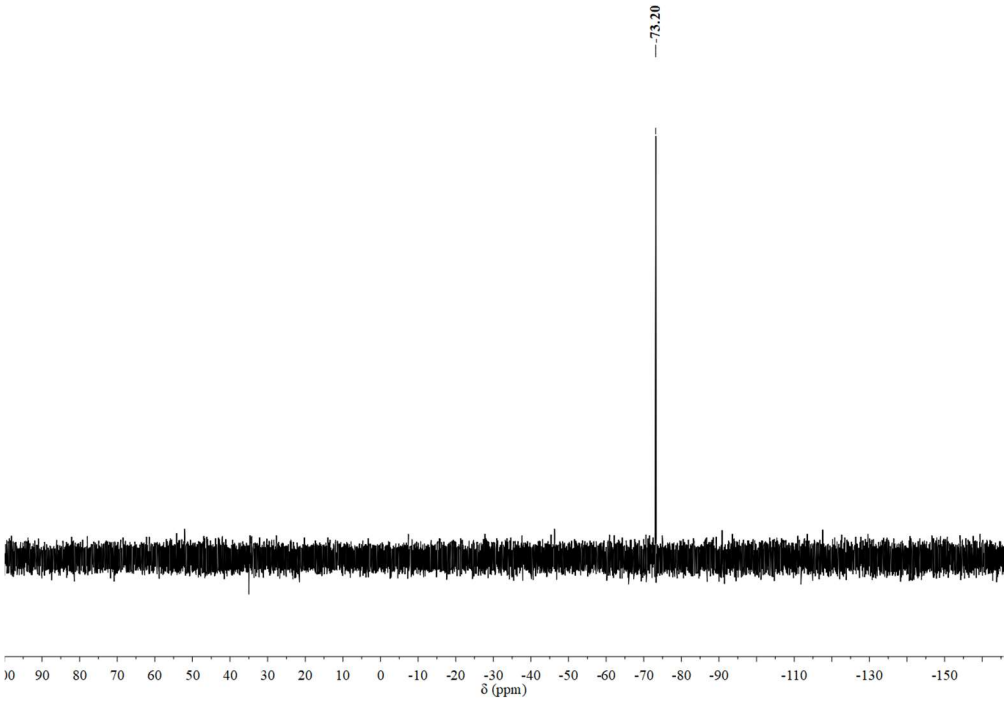

Figure 2.8. $^{31}P\{^{1}H\}$ NMR (162 MHz, acetone-d_6) spectrum of **1**.

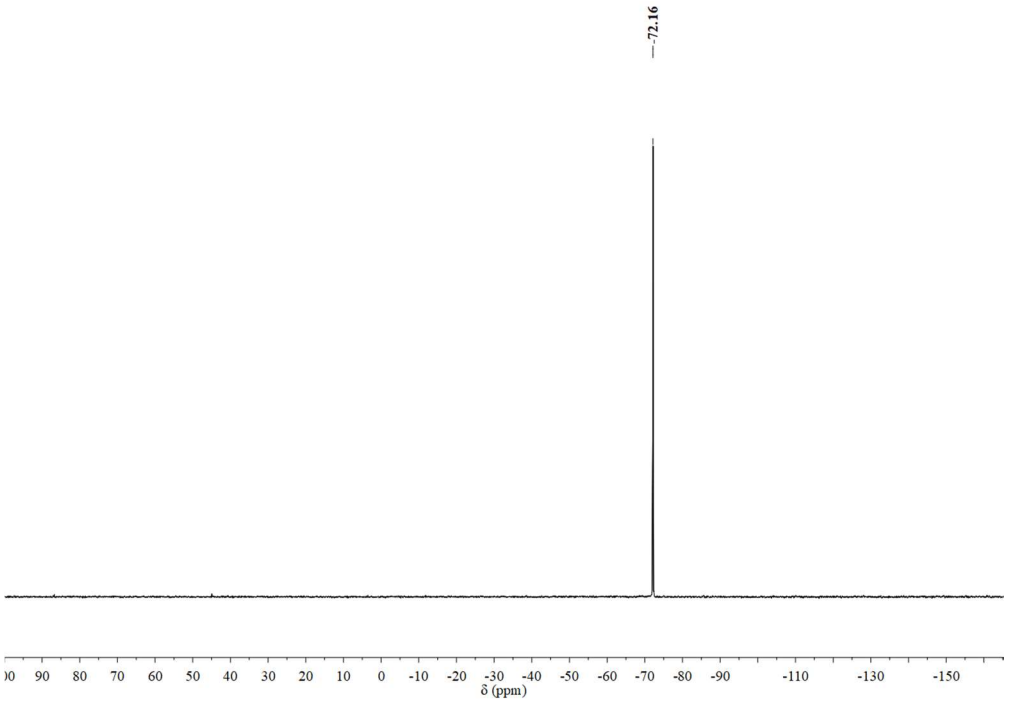

Figure 2.9. $^{31}P\{^{1}H\}$ NMR (162 MHz, $CDCl_3$) spectrum of **1**.

2.4.2.3 10-Trimethylsiloxy-9-phosphatriptycene (**2**)

1 (0.030 g, 0.10 mmol) was dissolved in THF (3 mL) in a 25-mL Schlenk flask and sodium bis(trimethylsilyl)amide (19.0 mg, 0.104 mmol) was added, then the solution was stirred at room temperature for 2 h. Trimethylsilyl chloride (0.16 g, 0.18 mL, 1.5 mmol) was added dropwise at room temperature to the solution mixture and the solution was stirred for another 0.5 h. The solution was evaporated in vacuo until white solid appeared. The crude product was passing through a short silica gel column with hexanes/EtOAc 50:1 as the eluant and concentrated to afford **2** as a white solid, 0.034 g (92%). ^{1}H NMR (300 MHz, acetone-d_6): δ (ppm) 7.85 (ddd, $J_{H\text{-}H,\ ortho}$= 7.8 Hz, $J_{H\text{-}H,\ meta}$= 1.2 Hz, $J_{H\text{-}H,\ para}$= 0.6 Hz, 3H), 7.77 (dddd, $^{3}J_{H\text{-}P}$= 9.9 Hz, $J_{H\text{-}H,\ ortho}$= 7.2 Hz, $J_{H\text{-}H,\ meta}$= 1.2 Hz, $J_{H\text{-}H,\ para}$= 0.6 Hz, 3H), 7.35 (tdd, $J_{H\text{-}H,\ ortho}$= 7.8 Hz, $^{5}J_{H\text{-}P}$= 1.5 Hz, $J_{H\text{-}H,\ meta}$= 1.2 Hz, 3H), 7.14 (dddd, $J_{H\text{-}H,}$

$_{ortho}$= 7.5 Hz, $J_{H\text{-}H,\ ortho}$= 7.2 Hz, $^{4}J_{H\text{-}P}$= 2.1 Hz, $J_{H\text{-}H,\ meta}$= 1.2 Hz, 3H), 0.64 (s, 9H, CH_3); $^{31}P\{^{1}H\}$ NMR (162 MHz, acetone-d_6): δ (ppm) –73.2 (s).

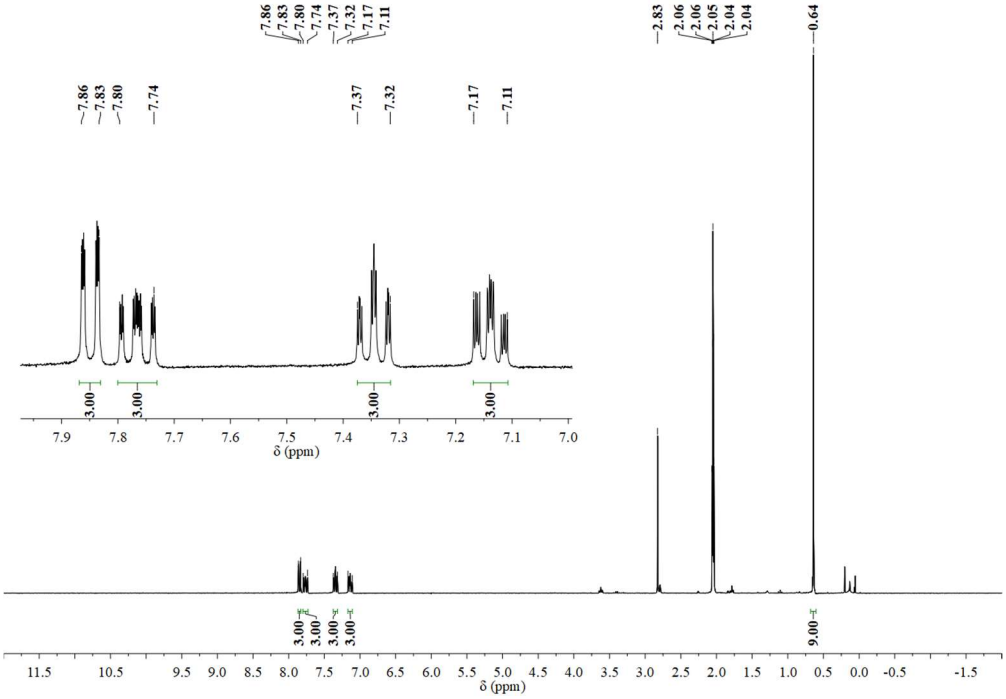

Figure 2.10. ^{1}H NMR (300 MHz, acetone-d_6) spectrum of **2**.

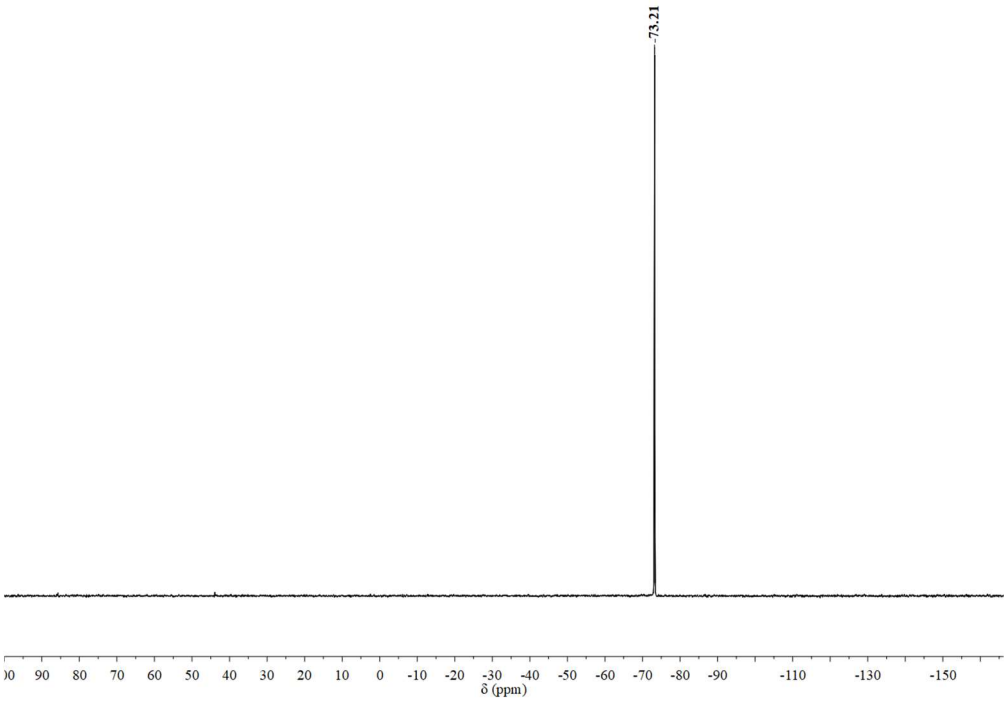

Figure 2.11. $^{31}P\{^{1}H\}$ NMR (162 MHz, acetone-d_6) spectrum of **2**.

2.4.2.4 10-Triethylsiloxy-9-phosphatriptycene (**3**)

1 (0.030 g, 0.10 mmol) was dissolved in THF (3 mL) in a 25-mL Schlenk flask and sodium bis(trimethylsilyl)amide (19.0 mg, 0.104 mmol) was added, then the solution was stirred at room temperature for 2 h. Triethylsilyl chloride (0.22 g, 0.24 mL, 1.5 mmol) was added dropwise at room temperature to the solution mixture and the solution was stirred for another 0.5 h. The solution was evaporated in vacuo until white solid appeared. The crude product was passing through a short silica gel column with hexane/EtOAc 50:1 as the eluant and concentrated to afford **3** as a white solid, 0.038 g (90%). ^{1}H NMR (300 MHz, acetone-d_6): δ (ppm) 7.84 (ddd, $J_{\text{H-H, }ortho}$= 7.7 Hz, $J_{\text{H-H, }meta}$= 1.2 Hz, $J_{\text{H-H, }para}$= 0.6 Hz, 3H), 7.77 (dddd, $^{3}J_{\text{H-P}}$= 9.7 Hz, $J_{\text{H-H, }ortho}$= 7.2 Hz, $J_{\text{H-H, }meta}$= 1.2 Hz, $J_{\text{H-H, }para}$= 0.6 Hz, 3H), 7.35 (tdd, $J_{\text{H-H, }ortho}$= 7.6 Hz, $^{5}J_{\text{H-P}}$= 1.3 Hz, $J_{\text{H-H, }meta}$= 1.0 Hz, 3H), 7.14 (dddd, $J_{\text{H-H, }ortho}$= 7.5 Hz, $J_{\text{H-H, }ortho}$= 7.2 Hz, $^{4}J_{\text{H-P}}$= 2.1 Hz, $J_{\text{H-H, }meta}$= 1.2 Hz, 3H), 1.26-1.11 (m, 15H, CH_2CH_3); ^{31}P{^{1}H} NMR (162 MHz, acetone-d_6): δ (ppm) –73.2 (s).

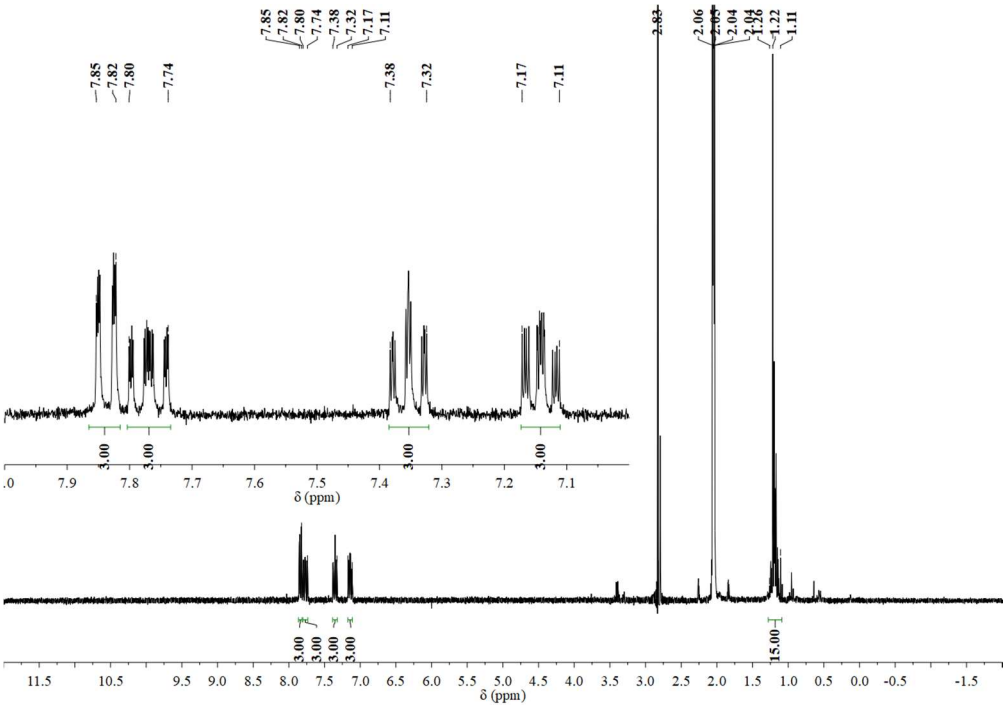

Figure 2.12. ^{1}H NMR (300 MHz, acetone-d_6) spectrum of **3**.

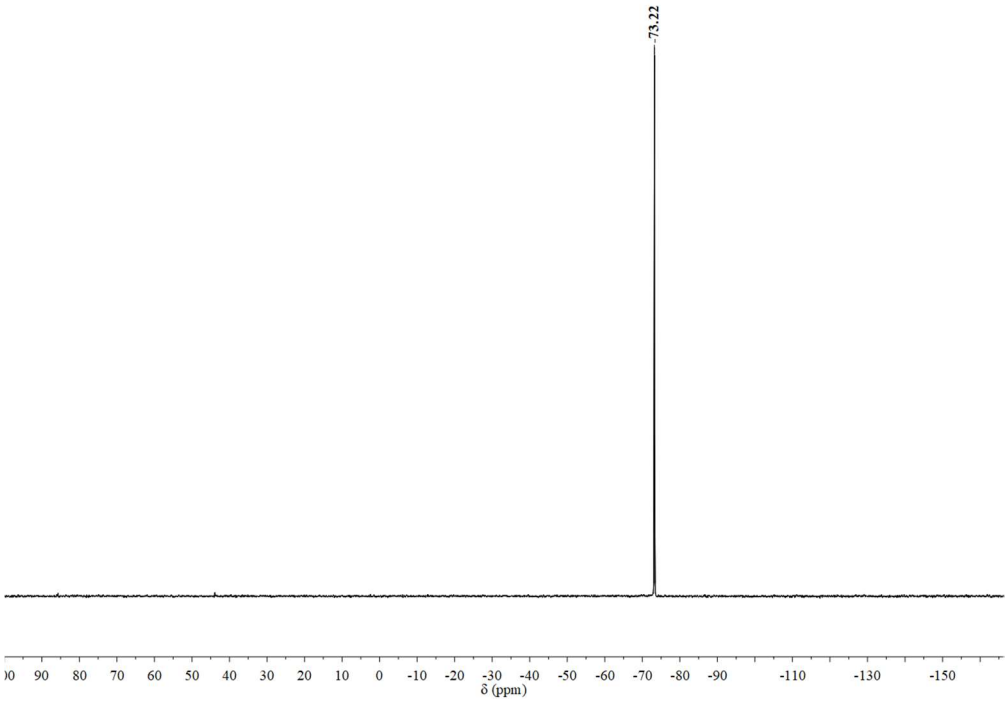

Figure 2.13. $^{31}P\{^{1}H\}$ NMR (162 MHz, acetone-d_6) spectrum of **3**.

2.4.2.5 10-Hydroxy-9-phosphatriptycene oxide (**4**)

1 (0.107 g, 0.373 mmol) was dissolved in Et_2O (5 mL) in a 2-mL scintillation vial and hydrogen peroxide solution (2 mL, 30 % w/w in H_2O) was added, then the solution was stirred at room temperature for 12 h until it became white and cloudy in appearance. The solution was filtered and the white solid was collected. The solid was dissolved in THF and evaporated in vacuo to afford **4** as a white solid, 0.091 g (80%) ^{1}H NMR (400 MHz, acetone-d_6): δ (ppm) 7.91 (m, 6H), 7.42 (tdd, $J_{H\text{-}H,\ ortho}$= 7.6 Hz, $^{5}J_{H\text{-}P}$= 1.6 Hz, $J_{H\text{-}H,\ meta}$= 1.2 Hz, 3H), 7.33 (tdd, $J_{H\text{-}H,\ ortho}$= 7.6 Hz, $^{4}J_{H\text{-}P}$= 2.8 Hz, $J_{H\text{-}H,\ meta}$= 0.8 Hz, 3H), 6.76 (s, 1H, O*H*); $^{31}P\{^{1}H\}$ NMR (162 MHz, acetone-d_6): δ (ppm) 0.88 (s) (Note: solubility of **4** in acetone-d_6 is low); MS(EI): calcd m/z 304.07, found m/z 304.1 (M^+).

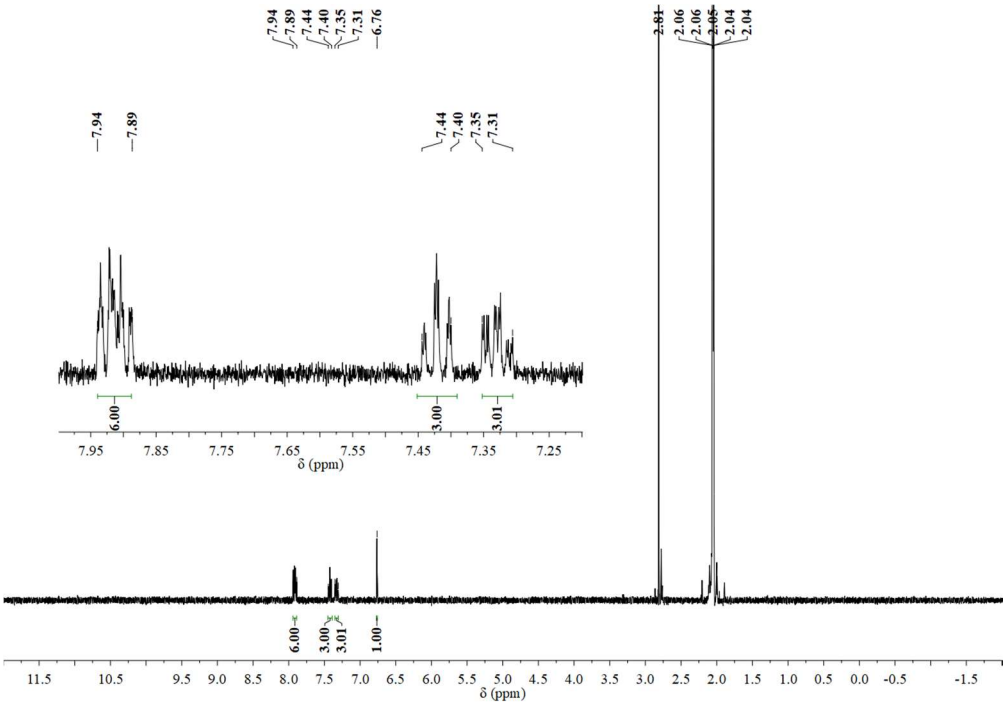

Figure 2.14. ^{1}H NMR (400 MHz, acetone-d_6) spectrum **4**.

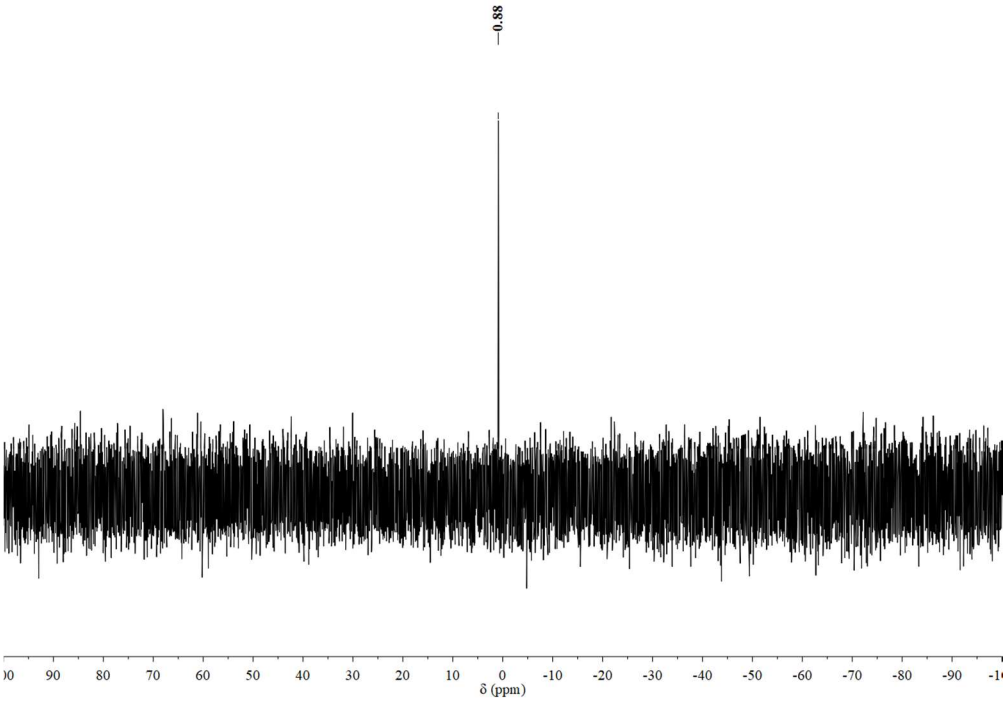

Figure 2.15. ^{31}P{^{1}H} NMR (162 MHz, acetone-d_6) spectrum of **4**.

2.4.2.6 10-Triethylsiloxy-9-phosphatriptycene oxide (**5**)

4 (0.086 g, 0.28 mmol) was dissolved in THF (10 mL) in a 25-mL Schlenk flask and sodium bis(trimethylsilyl)amide (0.052 g, 0.28 mmol) was added, then the solution was stirred at room temperature for 3 h. Triethylsilyl chloride (0.45 g, 0.50 mL, 3.0 mmol) was added dropwise at room temperature to the solution mixture and the solution was stirred for another 12h. The solution was evaporated in vacuo to afford **5** as a white solid, 0.116 g (98%). ^{1}H NMR (400 MHz, acetone-d_6): δ (ppm) 7.94 (dddd, $^{3}J_{H\text{-}P}$= 12.4 Hz, $J_{H\text{-}H,\ ortho}$= 7.2 Hz, $J_{H\text{-}H,\ meta}$= 1.2 Hz, $J_{H\text{-}H,\ para}$= 0.4 Hz, 3H), 7.88 (dddd, $J_{H\text{-}H,\ ortho}$= 7.6 Hz, $^{4}J_{H\text{-}P}$= 4.8 Hz, $J_{H\text{-}H,\ meta}$= 0.8 Hz, $J_{H\text{-}H,\ para}$= 0.4 Hz, 3H), 7.50 (tdd, $J_{H\text{-}H,\ ortho}$= 7.6 Hz, $^{5}J_{H\text{-}P}$= 1.2 Hz, $J_{H\text{-}H,\ meta}$= 0.8 Hz, 3H), 7.36 (tdd, $J_{H\text{-}H,\ ortho}$= 7.6 Hz, $^{4}J_{H\text{-}P}$= 2.8 Hz, $J_{H\text{-}H,\ meta}$= 1.2 Hz, 3H), 1.24-1.13 (m, 15H, CH_2CH_3); ^{31}P{^{1}H} NMR (162 MHz, acetone-d_6): δ (ppm) –0.19 (s).

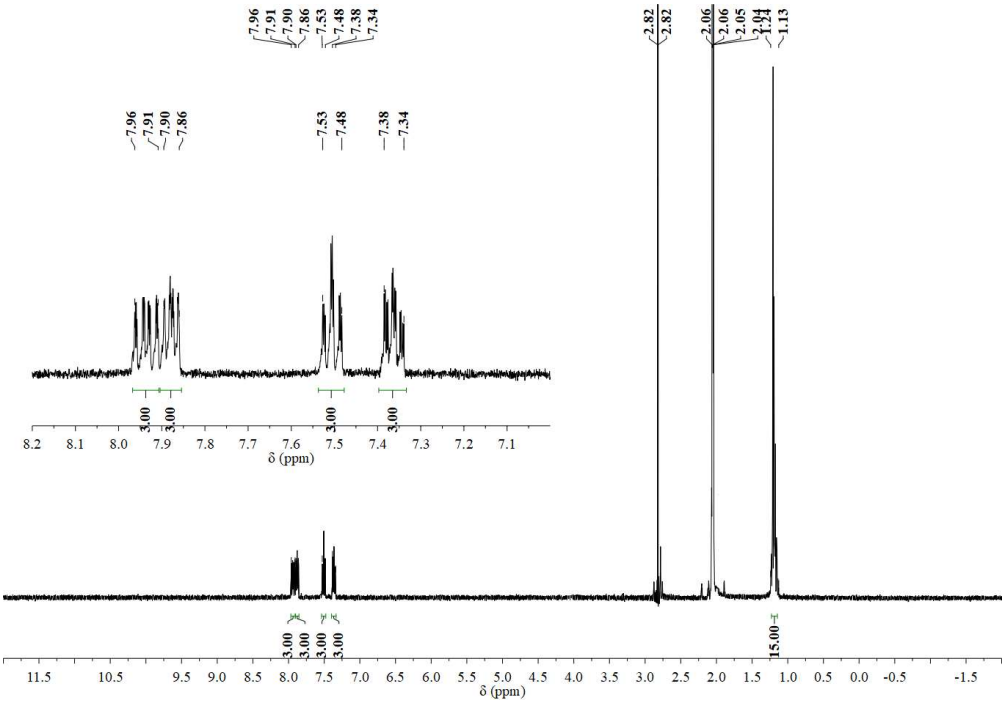

Figure 2.16. ^{1}H NMR (400 MHz, acetone-d_6) spectrum of **5**.

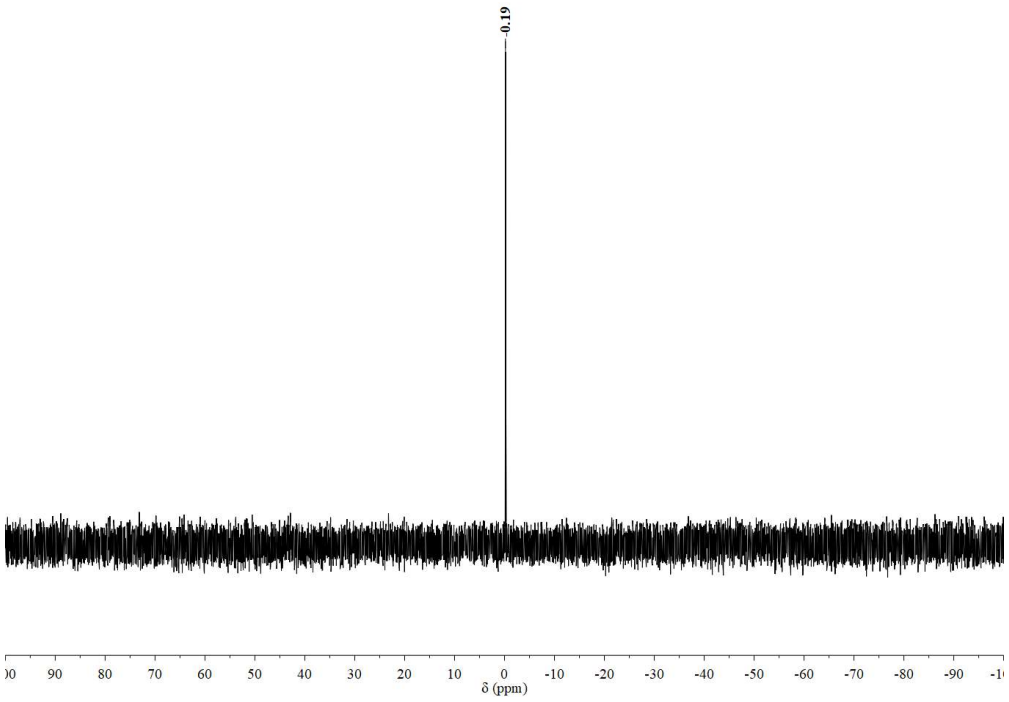

Figure 2.17. $^{31}P\{^{1}H\}$ NMR (162 MHz, acetone-d_6) spectrum of **5**.

2.4.2.7 10-Hydroxy-9-phosphatriptycene 9-phenylimide (**6**)

1 (0.019 g, 0.066 mmol) was dissolved in Et_2O (3 mL) in a 20-mL scintillation vial and phenyl azide (0.031 g, 0.025 mL, 0.26 mmol) was added, then the solution was stirred at 40 °C for 2 h. The solution was evaporated in vacuo and the residue was washed with EtOH (0.5 mL, 2 portions). The mixture was filtered to afford **6** as an off-white solid, 0.023 g (92%). ^{1}H NMR (400 MHz, CD_2Cl_2): δ (ppm) 7.94 (dddd, $^{3}J_{H\text{-}P}$= 12.4 Hz, $J_{H\text{-}H,\ ortho}$= 7.6 Hz, $J_{H\text{-}H,\ meta}$= 1.2 Hz, $J_{H\text{-}H,\ para}$= 0.4 Hz, 3H), 7.82 (dddd, $J_{H\text{-}H,\ ortho}$= 7.6 Hz, $^{4}J_{H\text{-}P}$= 4.4 Hz, $J_{H\text{-}H,\ meta}$= 0.8 Hz, $J_{H\text{-}H,\ para}$= 0.4 Hz, 3H), 7.37 (tt, $J_{H\text{-}H,\ ortho}$= 7.6 Hz, $^{5}J_{H\text{-}P}$= 1.2 Hz, $J_{H\text{-}H,\ meta}$= 1.2 Hz, 3H), 7.23 (tdd, $J_{H\text{-}H,\ ortho}$= 7.6 Hz, $^{4}J_{H\text{-}P}$= 2.8 Hz, $J_{H\text{-}H,\ meta}$= 0.8 Hz, 3H), 7.18 (m, 4H, *ortho* and *meta H* in NPh), 6.83 (m, 1H, *para H* in NPh); $^{31}P\{^{1}H\}$ NMR (162 MHz, CD_2Cl_2): δ (ppm) –26.41 (s); MS(EI): calcd m/z 379.1, found m/z 379 (M^+).

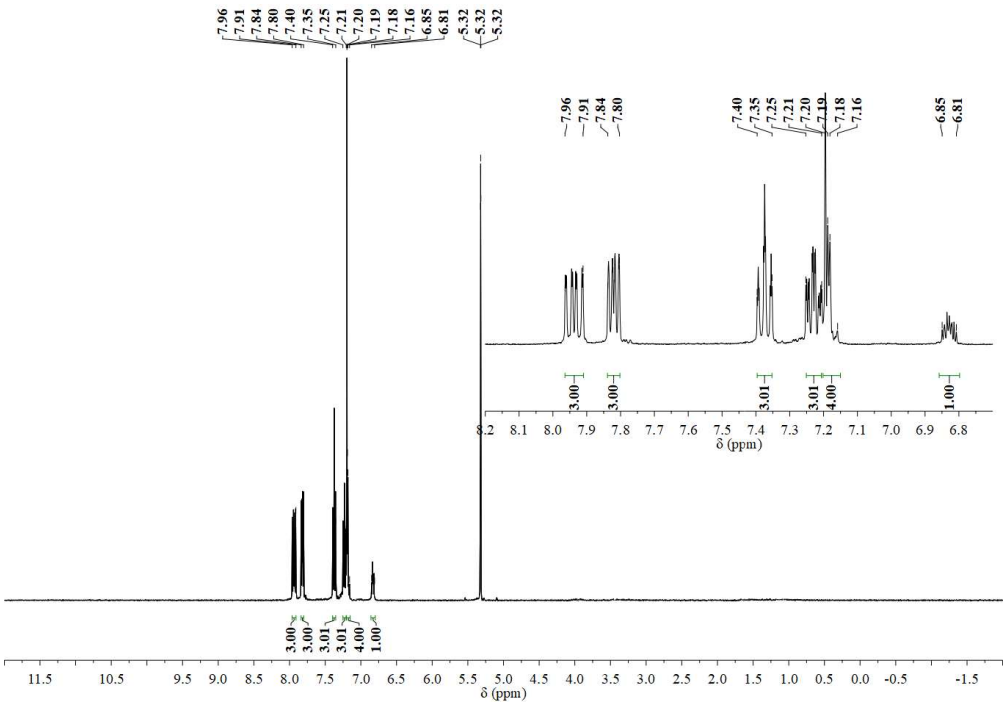

Figure 2.18. ^{1}H NMR (400 MHz, CD_2Cl_2) spectrum of **6**.

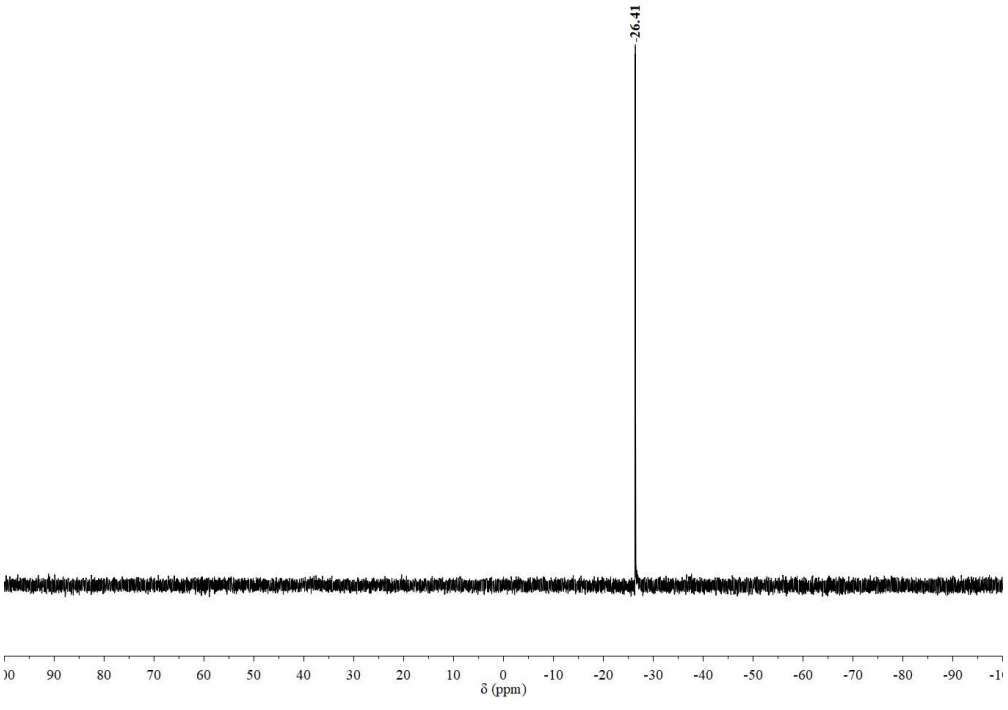

Figure 2.19. $^{31}P\{^{1}H\}$ NMR (162 MHz, CD_2Cl_2) spectrum of **6**.

2.4.2.8 2,7,14-Tri-*tert*-butyl-10-aza-9-phosphatriptycene (**7**)

Tris(2-bromo-4-*tert*-butylphenyl)amine (4.056 g, 6.237 mmol) was dissolved in THF (150 mL) in a 500-mL Schlenk flask and the solution was cooled to –78 °C. *tert*-Butyllithium (1.7 M in pentane, 22.0 mL, 37.4 mmol) was added dropwise at –78 °C and the resulting solution was stirred at –78 °C for 2 h. A solution of tris(2,4-di-*tert*-butylphenyl)phosphite (4.035 g, 6.237 mmol) in THF (20 mL) was added dropwise to the reaction mixture, which was allowed to warm slowly to ambient temperature, then refluxed for 96 h. The solution was cooled to room temperature, quenched with distilled water, and then extracted with ethyl acetate (3 x 50 mL). The combined organic portions were washed with distilled water and dried over $MgSO_4$. The resulting mixture was filtered, then concentrated in vacuo. Addition of methanol (50 mL) to the residue caused a microcrystalline solid to form. The off-white precipitate was collected by filtration and recrystallized from CH_2Cl_2/EtOH to afford **7** as a white solid, 1.945 g (71%). ^{1}H NMR (400 MHz, $CDCl_3$): δ (ppm) 7.80 (dd, $^3J_{H\text{-}P}$= 8.8 Hz, $J_{H\text{-}H,\ meta}$= 2.2 Hz, 3H), 7.53 (d, $J_{H\text{-}H,\ ortho}$= 8.0 Hz, 3H), 7.23 (dd, $J_{H\text{-}H,\ ortho}$= 8.0 Hz, $J_{H\text{-}H,\ meta}$= 2.0 Hz, 3H), 1.28 (s, 27H, C(CH_3)$_3$); ^{13}C{^{1}H} NMR (101 MHz, $CDCl_3$): δ (ppm) 155.47 (d, $^2J_{C\text{-}P}$= 1.2 Hz), 148.01 (d, $^1J_{C\text{-}P}$= 10.8 Hz), 144.69 (d, $^3J_{C\text{-}P}$= 7.5 Hz), 129.88 (d, $^2J_{C\text{-}P}$= 34.4 Hz), 126.30 (d, $^3J_{C\text{-}P}$= 1.4 Hz), 125.62 (s), 34.73 (s, *C*(CH$_3$)$_3$), 31.57 (s, *C*H$_3$); ^{31}P{^{1}H} NMR (162 MHz, $CDCl_3$): δ (ppm) –77.0 (s); Elemental analysis calcd (%) for $C_{30}H_{36}NP$ (441.60): C 81.60 H 8.22 N 3.17, found C 81.72, H 8.27, N 3.19; MS(EI): calcd m/z 441.26, found m/z 441.3 (M^+).

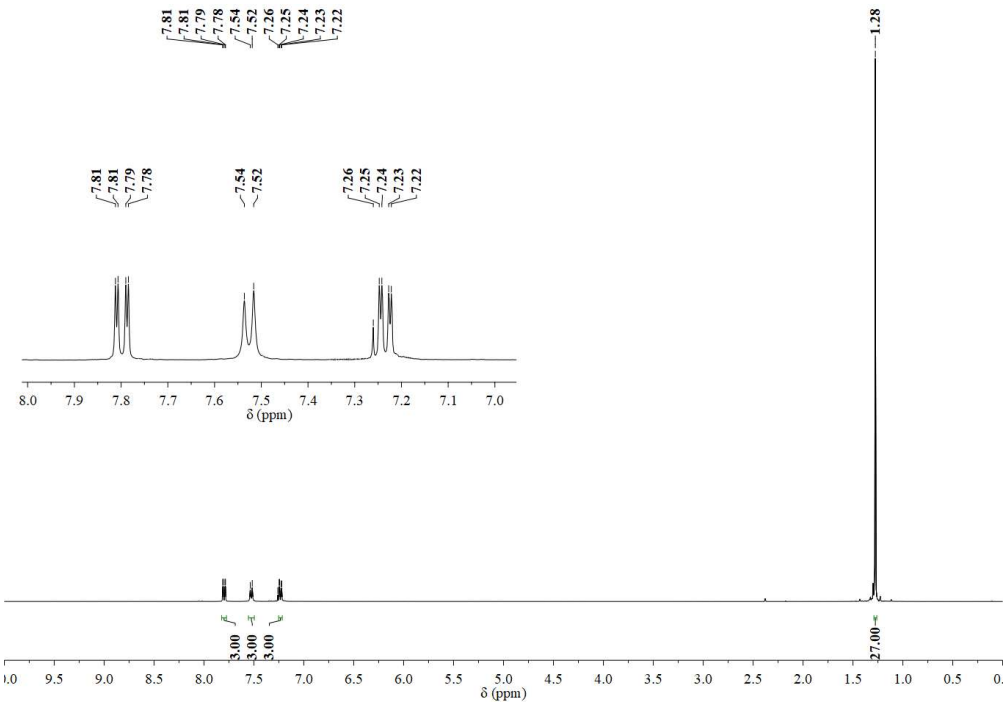

Figure 2.20. ^{1}H NMR (400 MHz, $CDCl_3$) spectrum of **7**.

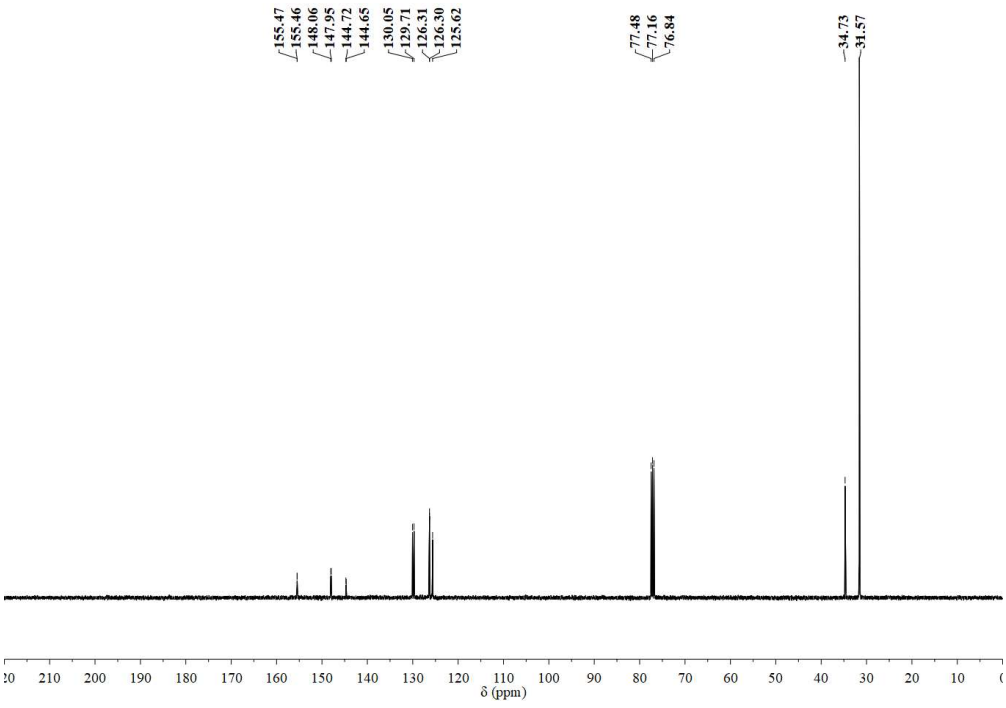

Figure 2.21. $^{13}C\{^{1}H\}$ NMR (101 MHz, $CDCl_3$) spectrum of **7**.

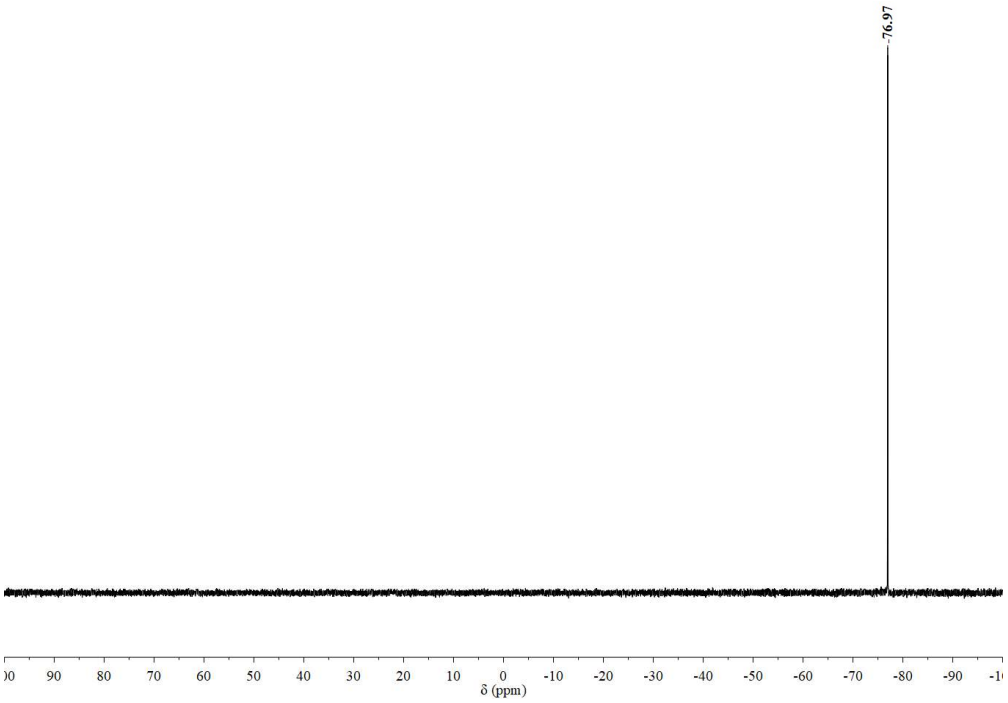

Figure 2.22. $^{31}P\{^{1}H\}$ NMR (162 MHz, $CDCl_3$) spectrum of **7**.

2.4.2.9 (10-Trimethylsiloxy-9-phosphatriptycene)copper(I) chloride (**8**)

2 (0.037 g, 0.10 mmol) was dissolved in THF (5 mL) in a 25-mL Schlenk flask and copper(I) chloride (0.034 g, 0.34 mmol) was added, then the solution was stirred at room temperature for 2 d. The solution was filtered through Celite and concentrated, dissolved in DCM and filtered through Celite twice, concentrated to get crude product. The crude product was recrystallized from CH_2Cl_2/pentane to afford **8** as a white solid, 0.041 g (87%). ^{1}H NMR (400 MHz, $CDCl_3$): δ (ppm) 8.47 (d, $^{3}J_{H\text{-}P}$= 12.8 Hz, $J_{H\text{-}H,\ ortho}$= 7.2 Hz, 3H), 7.78 (d, , $J_{H\text{-}H,\ ortho}$= 7.6 Hz, 3H), 7.26 (t, $J_{H\text{-}H,\ ortho}$= 7.4 Hz, 3H), 7.03 (t, $J_{H\text{-}H,\ ortho}$= 7.4 Hz, 3H), 0.63 (s, 9H, CH_3); $^{31}P\{^{1}H\}$ NMR (162 MHz, $CDCl_3$): δ (ppm) –57.50 (br); MS(ESI): calcd m/z 458, found m/z 464.3, 505.3 (MeCN adducts with the loss of Cl, ESI solvent: MeCN:DCM = 50:50).

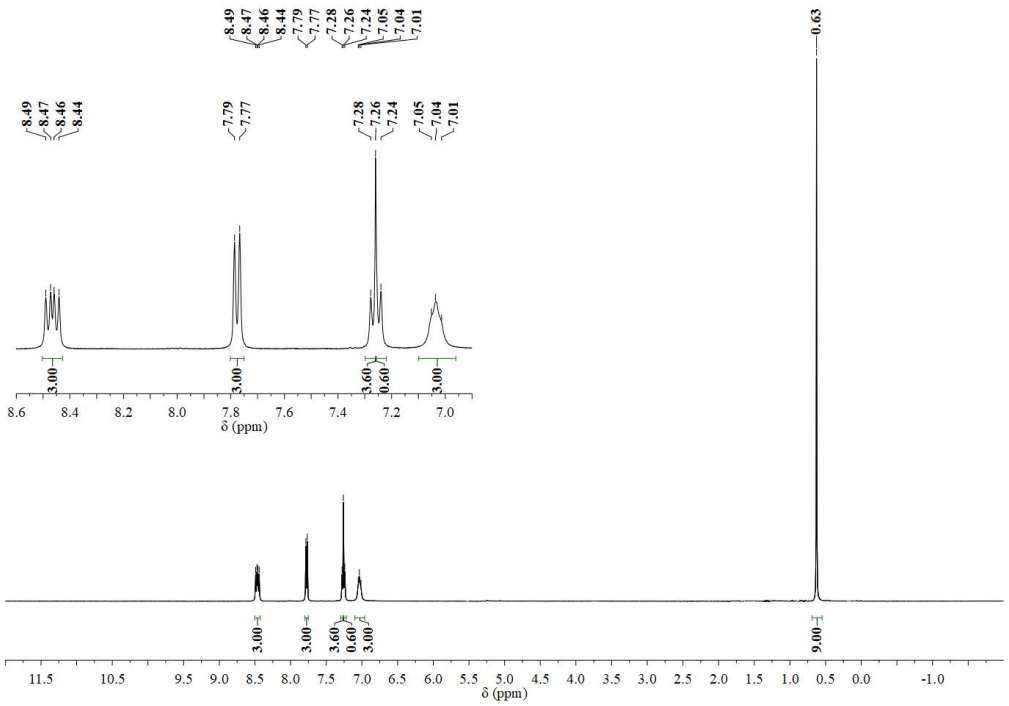

Figure 2.23. ^{1}H NMR (400 MHz, $CDCl_3$) spectrum of **8**.

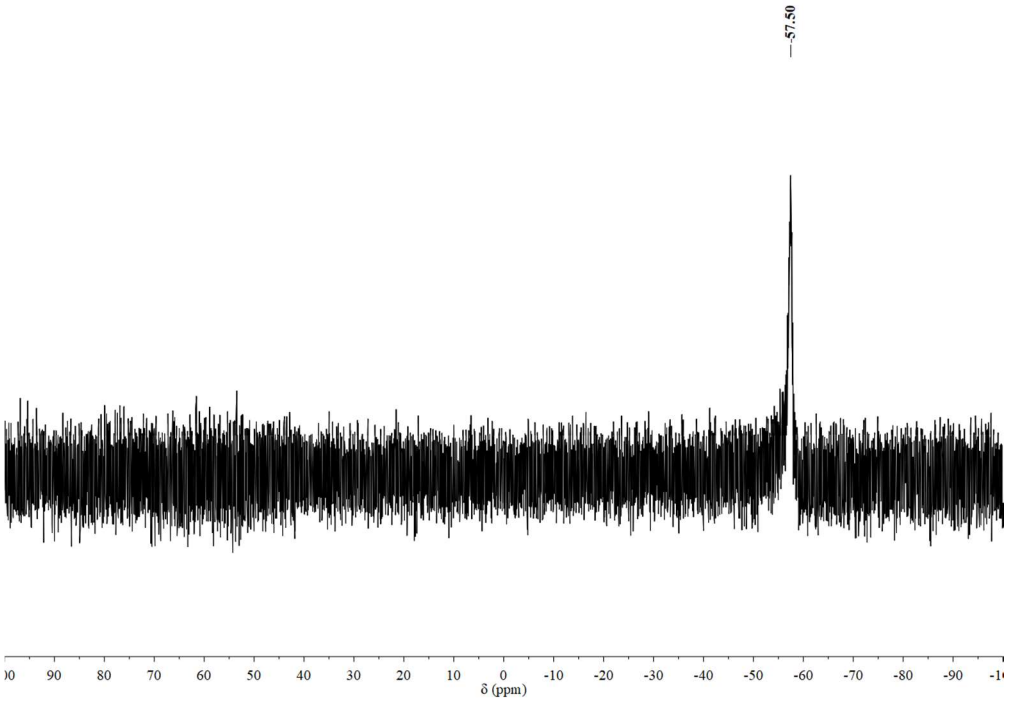

Figure 2.24. $^{31}P\{^{1}H\}$ NMR (162 MHz, $CDCl_3$) spectrum of **8**.

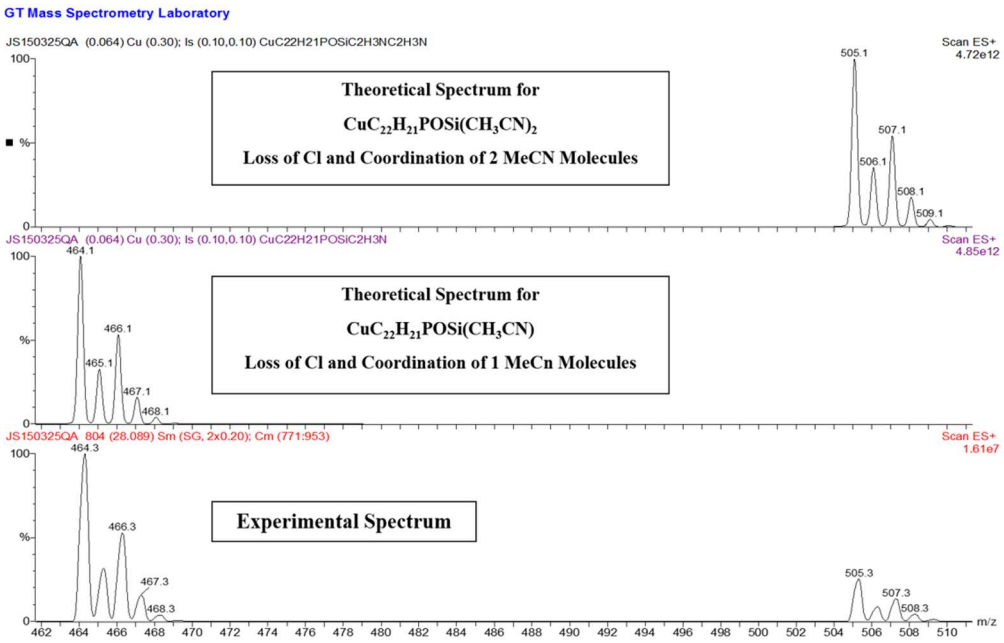

Figure 2.25. MS(ESI) spectrum of **8**. Solvent: MeCN:DCM=50:50.

2.4.2.10 (10-Triethylsiloxy-9-phosphatriptycene)copper(I) chloride (**9**)

3 (0.040 g, 0.099 mmol) was dissolved in THF (5 mL) in a 25-mL Schlenk flask and copper(I) chloride (0.030 g, 0.30 mmol) was added, then the solution was stirred at room temperature for 16 h. The solution was filtered through Celite and concentrated, then dissolved in DCM, filtered through Celite twice, and concentrated again. The crude product was recrystallized from CH_2Cl_2/pentane to afford **9** as a white solid, 0.034 g (68%). ^{1}H NMR (400 MHz, acetone-d_6): δ (ppm) 8.50 (ddd, $^3J_{H\text{-}P}$= 12.4 Hz, $J_{H\text{-}H,\ ortho}$= 7.2 Hz, $J_{H\text{-}H,\ meta}$= 0.8 Hz, 3H), 7.91 (dt, $J_{H\text{-}H,\ ortho}$= 7.6 Hz, $J_{H\text{-}H,\ meta}$= 0.8 Hz, 3H), 7.41 (tt, $J_{H\text{-}H,\ ortho}$= 7.6 Hz, $^4J_{H\text{-}P}$= 0.8 Hz, $J_{H\text{-}H,\ meta}$= 0.8 Hz, 3H), 7.06 (t, $J_{H\text{-}H,\ ortho}$= 7.6 Hz, 3H), 1.29-1.14 (m, 15H, CH_2CH_3); ^{31}P{^{1}H} NMR (162 MHz, acetone-d_6): δ (ppm) –57.39 (br).

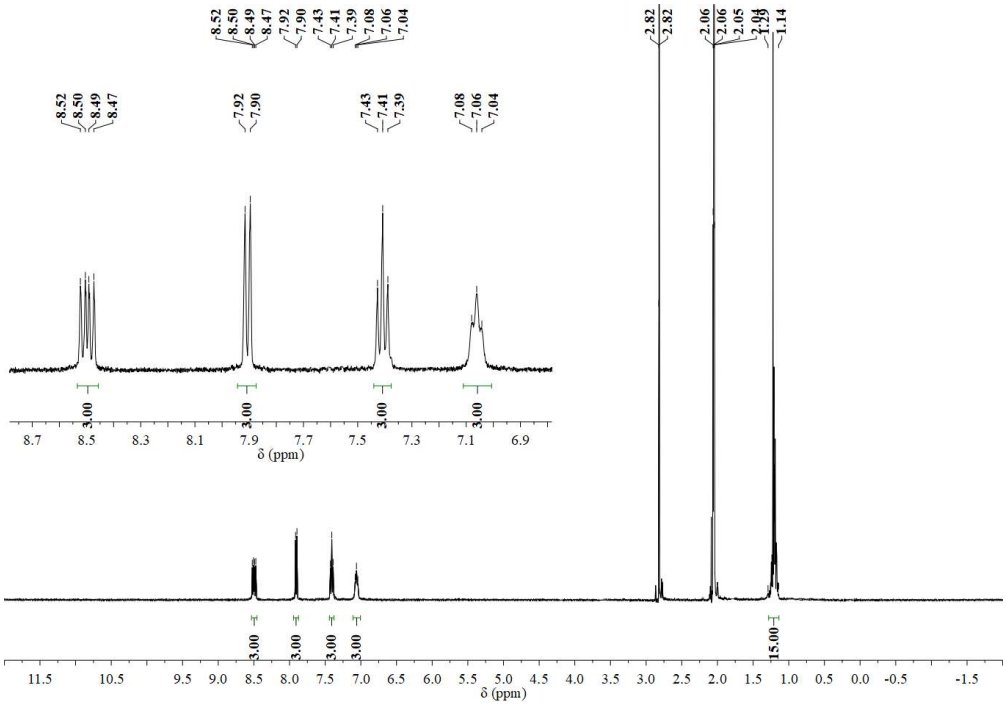

Figure 2.26. ^{1}H NMR (400 MHz, acetone-d_6) spectrum of **9**.

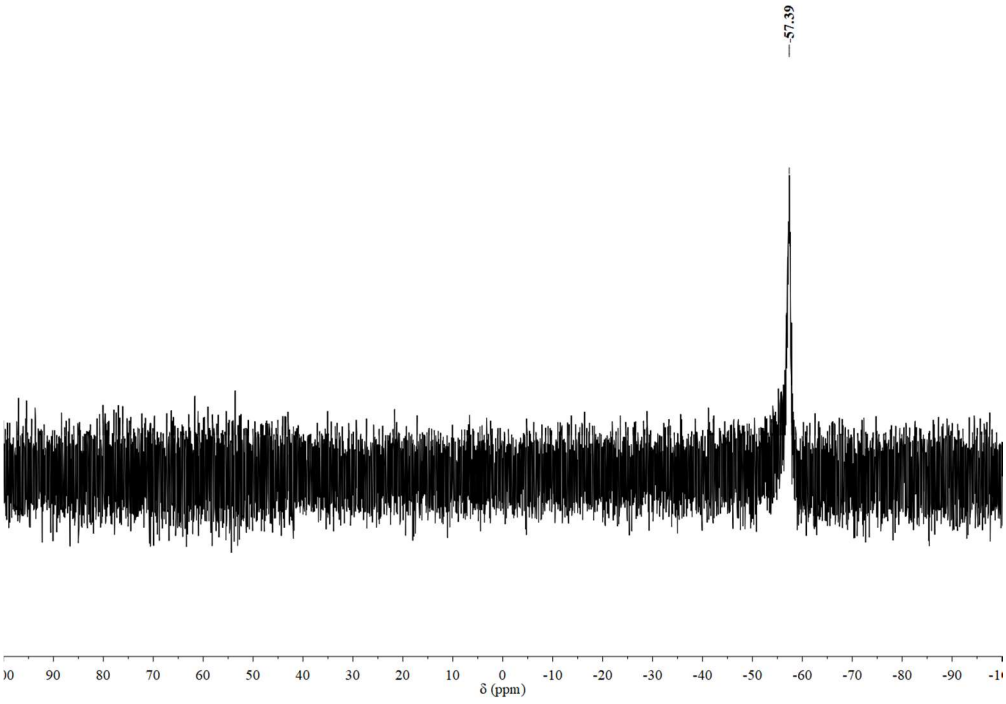

Figure 2.27. ^{31}P{^{1}H} NMR (162 MHz, acetone-d_6) spectrum of **9**.

2.4.2.11 (2,7,14-Tri-*tert*-butyl-10-aza-9-phosphatriptycene)copper(I) chloride (**10**)

8 (0.046 g, 0.10 mmol) was dissolved in THF (5 mL) in a 25-mL Schlenk flask and copper(I) chloride (0.034 g, 0.34 mmol) was added, then the solution was stirred at room temperature for 1 d. The solution was filtered through Celite and concentrated, then redissolved in DCM, filtered through Celite twice, and concentrated. The crude product was recrystallized from CH_2Cl_2/pentane to afford **11** as a white solid, 0.050 g (89%). ^{1}H NMR (400 MHz, $CDCl_3$): δ (ppm) 8.41 (dd, $^3J_{H\text{-}P}$= 12.0 Hz, $J_{H\text{-}H,\ meta}$= 2.0 Hz, 3H), 7.47 (d, $J_{H\text{-}H,\ ortho}$= 8.0 Hz, 3H), 7.16 (dd, $J_{H\text{-}H,\ ortho}$= 8.0 Hz, $J_{H\text{-}H,\ meta}$= 2.0 Hz, 3H), 0.94 (s, 27H, $C(CH_3)_3$); $^{31}P\{^1H\}$ NMR (162 MHz, $CDCl_3$): δ (ppm) –60.67 (br).

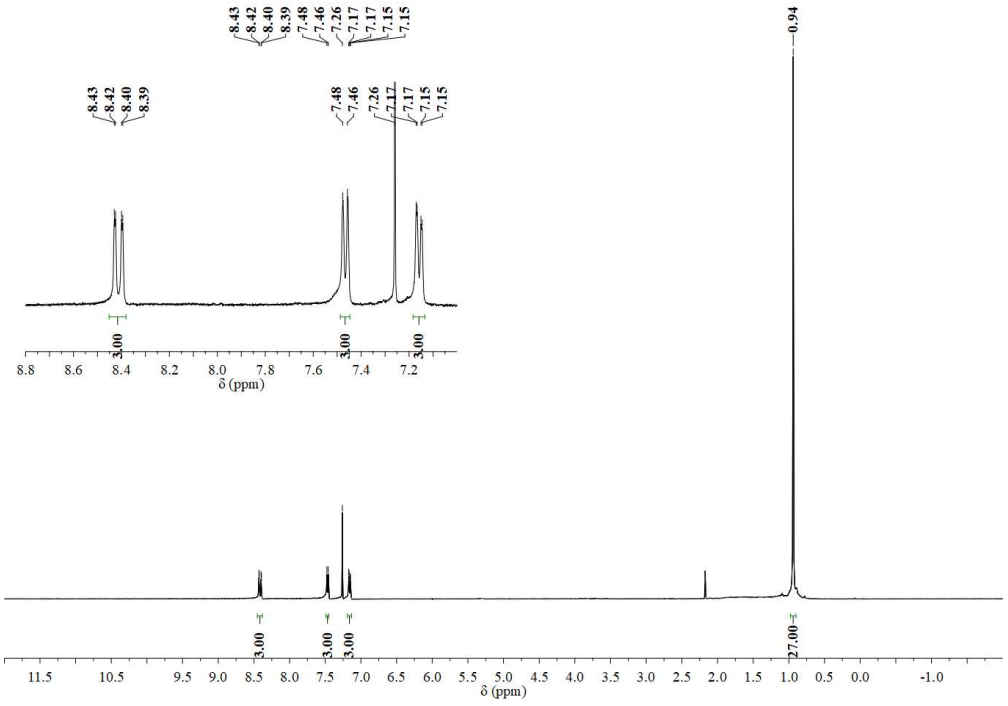

Figure 2.28. ^{1}H NMR (400 MHz, $CDCl_3$) spectrum of **10**.

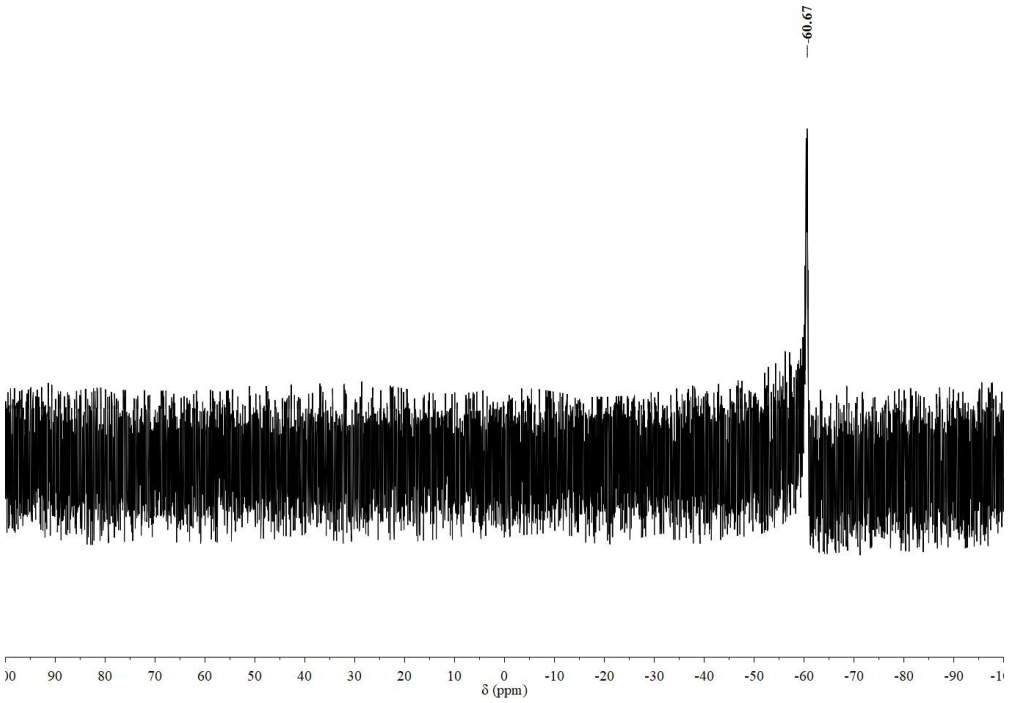

Figure 2.29. $^{31}P\{^{1}H\}$ NMR (162 MHz, $CDCl_3$) spectrum of **10**.

2.4.2.12 (2,7,14-Tri-*tert*-butyl-10-aza-9-phosphatriptycene)copper(I) acetate (**11**)

8 (0.015 g, 0.034 mmol) was dissolved in THF (5 mL) in 20-mL scintillation vial and copper(I) acetate (0.005 g, 0.04 mmol) was added, then the solution was stirred at room temperature for 4 h. The solution was filtered through Celite and concentrated to afford **11** as a yellow solid, 0.010 g (52%). ^{1}H NMR (300 MHz, C_6D_6): δ (ppm) 8.51 (br, 3H), 7.72 (d, $J_{H\text{-}H,\ ortho}$= 7.8 Hz, 3H), 7.04 (dd, $J_{H\text{-}H,\ ortho}$= 7.8 Hz, 3H), 2.25 (br, 3H, O(CO)CH_3), 1.00 (s, 27H, C(CH_3)$_3$); $^{31}P\{^{1}H\}$ NMR (162 MHz, C_6D_6): δ (ppm) –61.60 (br).

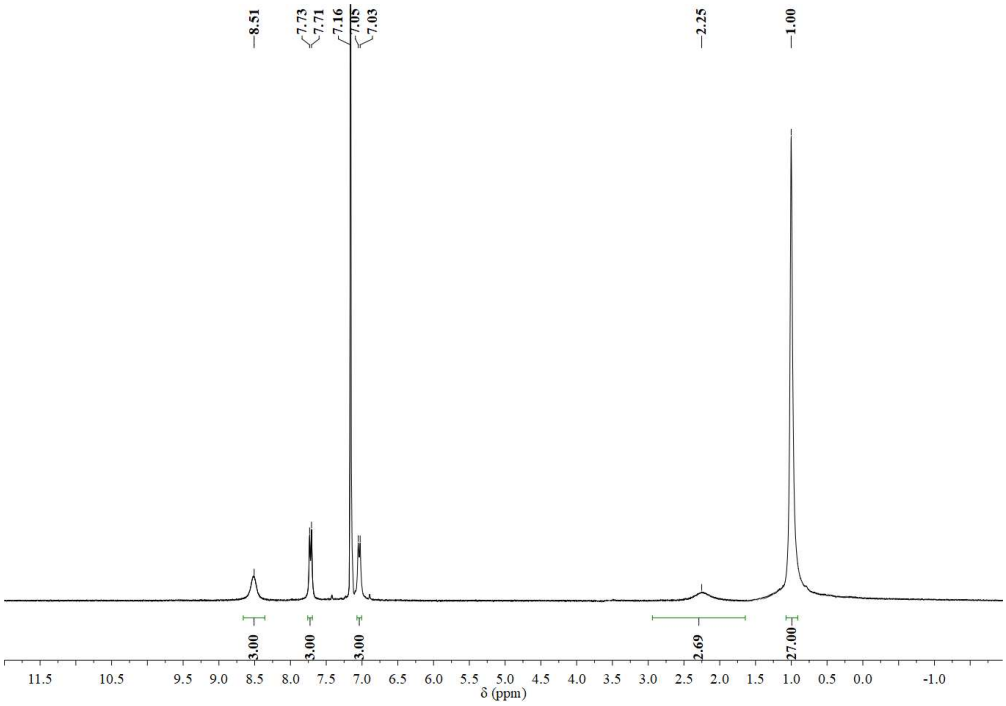

Figure 2.30. ^{1}H NMR (300 MHz, C_6D_6) spectrum of **11**.

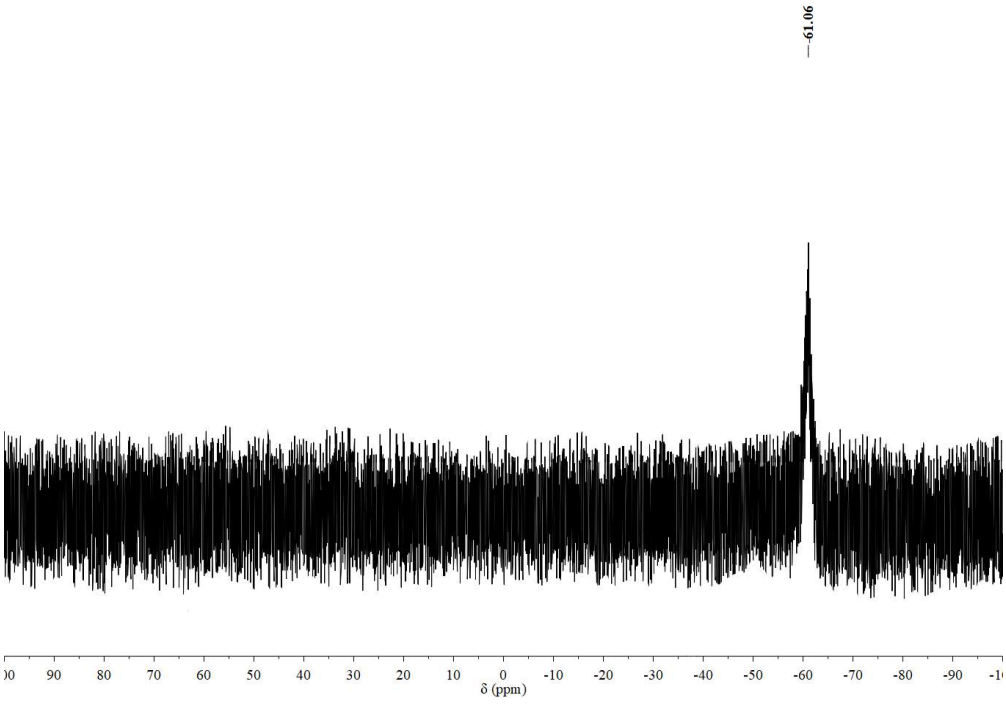

Figure 2.31. $^{31}P\{^{1}H\}$ NMR (162 MHz, C_6D_6) spectrum of **11**.

2.4.3 Reactivity studies

2.4.3.1 General procedures of directed *ortho* metalation on phosphatriptycene

Unless otherwise indicated, substrates **2**, **3** and **5** (0.030 mmol) were dissolved in THF (2 mL) — substrate **6** was dissolved in Et_2O (2 mL) — in a 10-mL Schlenk flask and the solution was brought to the desired temperature, metalation reagent was added dropwise, and the reaction was conducted for the desired duration. The solution was quenched with excess deuterium oxide (0.11 g, 0.10 mL, 5.5 mmol) at the reaction temperature and stirred for 15 min, then allowed to warm to room temperature. Ethyl acetate (2 mL) was added, and the organic layer was collected and dried over $MgSO_4$. The solution was filtered through Celite and evaporated in vacuo to afford product.

2.4.3.2 Bromination of **6**

6 (0.006 g, 0.02 mmol), palladium acetate (0.004 g, 0.02 mmol) and *N*-bromosuccinimide (0.009 g, 0.05 mmol) was dissolved in DCM (2 mL) in a 20-mL scintillation vial, then the solution was stirred at 50 °C for 21 h. The solution was cooled to room temperature and quenched with deuterium oxide (0.11 g, 0.10 mL, 5.5 mmol). The organic layer was collected and dried over $MgSO_4$. The solution was filtered through Celite and evaporated in vacuo to afford the product. ^{1}H NMR (400 MHz, $CDCl_3$): δ (ppm) 7.96 (ddd, $^3J_{H\text{-}P}$= 12.4 Hz, $J_{H\text{-}H,\ ortho}$= 7.2 Hz, $J_{H\text{-}H,\ meta}$= 0.8 Hz, 3H), 7.81 (dd, $J_{H\text{-}H,\ ortho}$= 7.6 Hz, $^4J_{H\text{-}P}$= 4.8 Hz, 3H), 7.76 (t, $J_{H\text{-}H,\ meta}$= 2.4 Hz, $^5J_{H\text{-}P}$= 2.4 Hz, 1H, *meta H* on NPh), 7.35 (tt, $J_{H\text{-}H,\ ortho}$= 7.6 Hz, $^5J_{H\text{-}P}$= 1.2 Hz, $J_{H\text{-}H,\ meta}$= 1.2 Hz, 3H), 7.22 (tdd, $J_{H\text{-}H,\ ortho}$= 7.2 Hz, $^4J_{H\text{-}P}$= 2.8 Hz, $J_{H\text{-}H,\ meta}$= 0.8 Hz, 3H), 7.15 (dd, $J_{H\text{-}H,\ ortho}$= 8.4 Hz, $J_{H\text{-}H,\ meta}$= 2.4 Hz, 1H, *meta*

H on NPh), 7.07 (dd, $J_{\text{H-H, ortho}}$= 8.4 Hz, $^{4}J_{\text{H-P}}$= 1.6 Hz, 1H, *ortho H* on NPh); $^{31}P\{^{1}H\}$ NMR (162 MHz, $CDCl_3$): δ (ppm) –24.37 (s); MS(EI): calcd m/z 536.93, found m/z 536.9 (M^+).

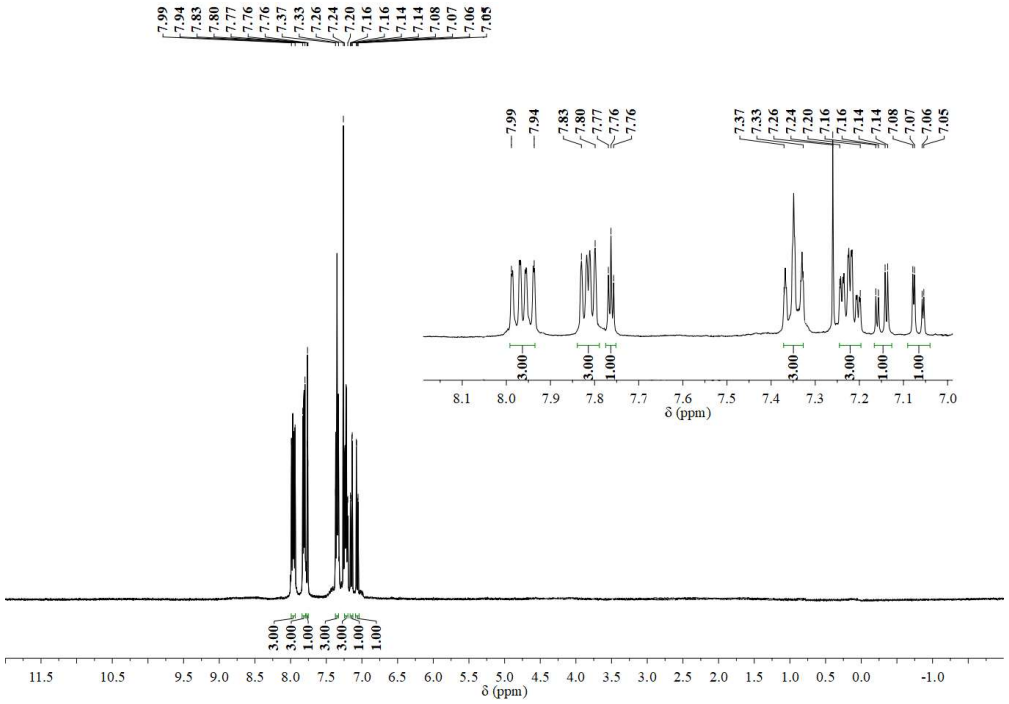

Figure 2.32. ^{1}H NMR (400 MHz, $CDCl_3$) spectrum of the bromination product of **6**.

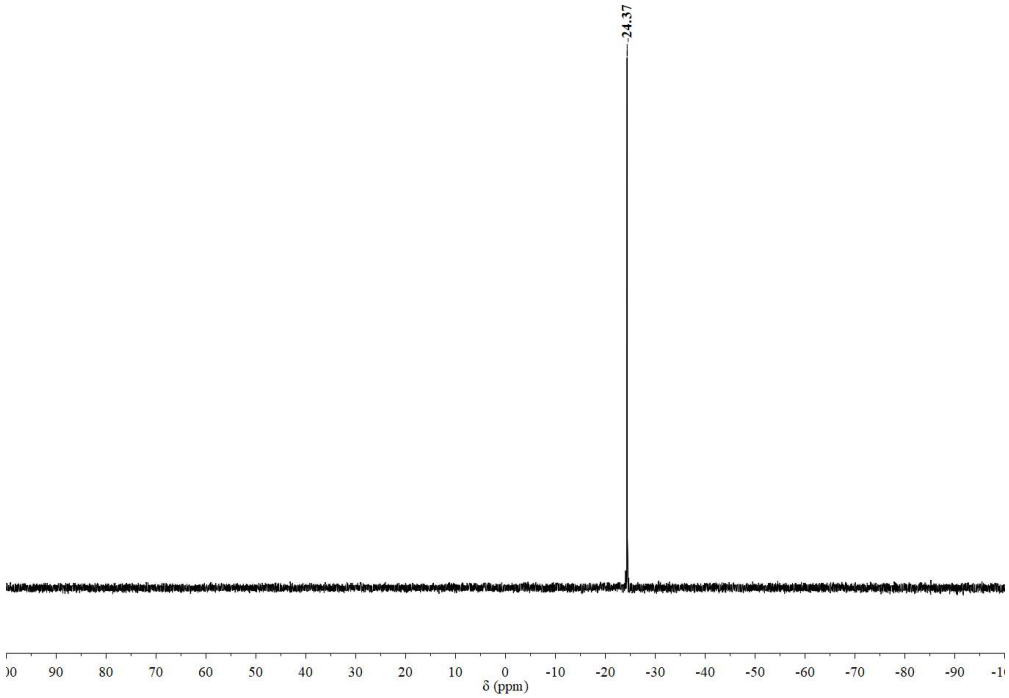

Figure 2.33. $^{31}P\{^{1}H\}$ NMR (162 MHz, $CDCl_3$) spectrum of the bromination product of **6**.

2.4.3.3 Selective metalation on tris(2,6-dichlorophenyl)phosphine

Unless otherwise indicated, tris(2,6-dichlorophenyl)phosphine (0.023 g, 0.049 mmol) and additive were dissolved in THF (2 mL) in a 10-mL Schlenk flask and the solution was kept cooled when metalation reagent was added dropwise, and the reaction was conducted for the desired duration. The solution was quenched with *DI* water (1 mL) at the reaction temperature and stirred for 15 min, then allowed to warm to room temperature. Ethyl acetate (2 mL) was added to extract, and the organic layer was collected and dried over $MgSO_4$. The solution was filtered through Celite and evaporated in vacuo to afford the product.

2.4.3.4 Directed metalation on 3-bromophenyl *N,N*-diethylcarbamate

Unless otherwise indicated, LDA was synthesized in situ for metalation. Diisopropylamine (0.22 g, 0.31 mL, 2.2 mmol) was dissolved in THF (5 mL) in a 25-mL Schlenk flask and the solution was cooled down to 0 °C. *n*-Butyllithium (2.5 M in hexanes, 0.88 mL, 2.2 mmol) was added dropwise and the solution was stirred at 0 °C for 0.5 h. The solution was cooled to –78 °C and 3-bromophenyl *N, N*-diethylcarbamate (0.54 g, 0.40 mL, 2.0 mmol) was added dropwise and the solution was stirred for another 0.5 h. Where applicable, additive (2.2 mmol) was introduced, and the resulting mixture stirred at –78 °C for 1 h, then brought to the desired temperature. The solution was then treated with excess deuterium oxide (0.11 g, 0.10 mL, 5.5 mmol) or phosphorus electrophile (0.58 mmol) at the reaction temperature, and stirred for the desired duration. The solution was brought to room temperature. *DI* water (2 mL) was added to quench, and ethyl acetate (2 mL) was

added to extract. The organic layer was collected and dried over $MgSO_4$. The solution was filtered through Celite and evaporated in vacuo to afford product.

2.4.3.5 Halogen-metal exchange on 3-bromo-2-iodoanisole

Unless otherwise indicated, 3-bromo-2-iodoanisole (0.10 g, 0.32 mmol) was dissolved in THF (3 mL) in a 10-mL Schlenk flask and the solution was cooled to –20 °C. Isopropylmagnesium bromide (1.0 M in THF, 0.33 mL, 0.33 mmol) was added dropwise and the solution was stirred at –20 °C for 2 h, followed by adding additive (0.33 mmol) and stirred at –20 °C for 1 h before adjusting to the desired temperature. The solution was reacted with excess deuterium oxide (0.11 g, 0.10 mL, 5.53 mmol) / phosphorus trichloride (0.01 g, 0.008 mL, 0.09 mmol) at the reaction temperature and stirred for the desired duration. The solution was brought to room temperature. *DI* water (2 mL) was added to quench, and ethyl acetate (2 mL) was added to extract. The organic layer was collected and dried over $MgSO_4$. The solution was filtered through Celite and evaporated in vacuo to afford product.

2.4.3.6 Synthesis of bis(2-bromo-6-methoxyphenyl)(oxo)phosphorene

^{1}H NMR (400 MHz, $CDCl_3$): δ (ppm) 8.83 (d, $^1J_{H\text{-}P}$= 550.8 Hz, 1H, P-*H*), 7.08 (d, $J_{H\text{-}H,\ ortho}$= 8.0 Hz, 2H, *meta H*), 7.00 (t, $J_{H\text{-}H,\ ortho}$= 8.0 Hz, 2H, para *H*), 6.66 (d, $J_{H\text{-}H,\ ortho}$= 8.0 Hz, 2H, *meta H*), 3.52 (s, 6H, OCH_3); ^{31}P{^{1}H} NMR (162 MHz, $CDCl_3$): δ (ppm) 9.31 (s); MS(EI): calcd m/z 419.89, found m/z 419.7 (M^+).

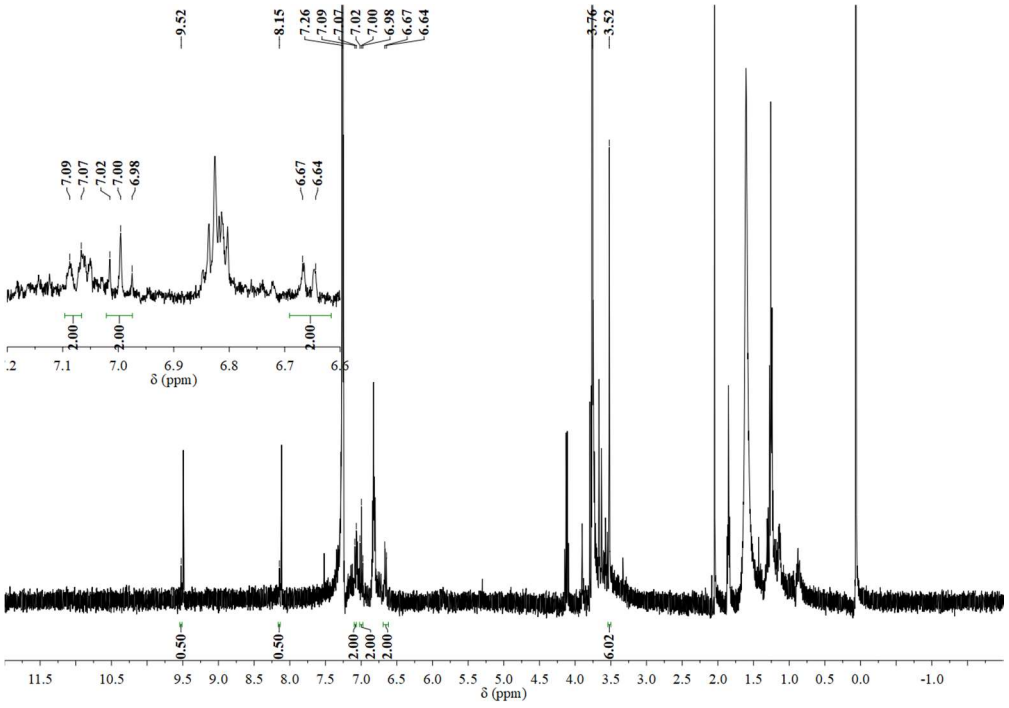

Figure 2.34. ^{1}H NMR (400 MHz, $CDCl_3$) spectrum of bis(2-bromo-6-methoxyphenyl)(oxo)phosphorene.

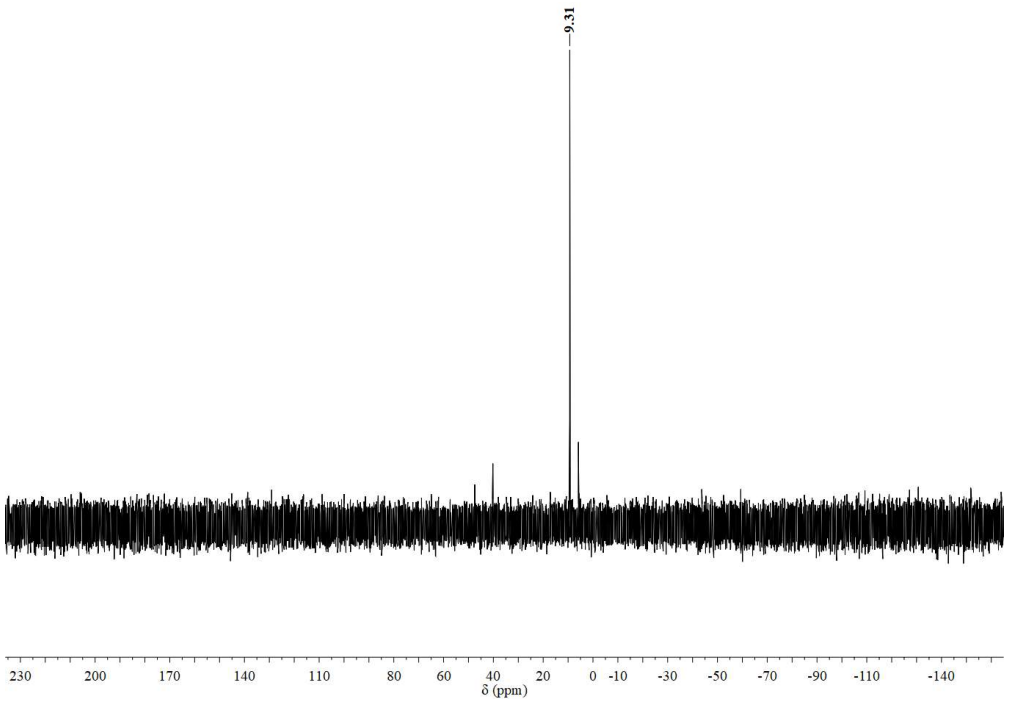

Figure 2.35. $^{31}P\{^{1}H\}$ NMR (162 MHz, $CDCl_3$) spectrum of bis(2-bromo-6-methoxyphenyl)(oxo)phosphorene.

2.4.3.7 Reaction of **10** with $LiAlH_4$

10 (0.005 g, 0.009 mmol) and lithium aluminum hydride (0.003 g, 0.08 mmol) was stirred in C_6D_6 (0.5 mL) at room temperature for 1 d. The solution became black in color. ^1H NMR and $^{31}P\{^1H\}$ NMR indicated the dissociation of ligand **7**.

2.4.3.8 Reaction of **11** with $(EtO)_3SiH$

11 (0.015 g, 0.027 mmol) was dissolved in THF (3 mL) in a 20-mL scintillation vial and triethoxysilane (0.044 g, 0.050 mL, 0.27 mmol) was added, then the solution was stirred at room temperature for 1 d. The solution became black in color when triethoxysilane was added. ^1H NMR and $^{31}P\{^1H\}$ NMR indicated the dissociation of ligand **7**.

2.4.4 X-ray diffraction studies

2.4.4.1 (10-Triethylsiloxy-9-phosphatriptycene)copper(I) chloride complex (**9**)

Diffraction-quality crystals were grown by the diffusion of pentane vapor into a solution of **9** in THF at room temperature. Single colorless plate-shaped crystal with dimensions 0.99 mm x 0.75 mm x 0.11 mm was mounted on a loop with Paratone oil. Data were collected by a Bruker APEX II CCD diffractometer equipped with an Oxford Cryosystems low-temperature device operating at $T = 100(2)$ K.

Data were measured using ω and ϕ scans of 1.0° per frame for 60.0 s using MoK_α radiation. The total number of runs and images was based on the strategy calculation from the program APEX2.[39] The maximum resolution that was achieved was $\Theta = 25.681°$. The

diffraction pattern was indexed using APEX2[39] and the unit cell was refined using CrysAlisPro[40] on 13604 reflections, 29% of the observed reflections. Data reduction, scaling and absorption corrections were performed using CrysAlisPro.[40] The final completeness is 99.70% out to 25.681° in Θ. A multi-scan absorption correction was performed using CrysAlisPro[40] Empirical absorption correction using spherical harmonics, implemented in SCALE3 ABSPACK scaling algorithm. The absorption coefficient μ of this material is 1.038 mm^{-1} at this wavelength (λ = 0.71073 Å) and the minimum and maximum transmissions are 0.56716 and 1.00.

The structure was solved and the space group was determined by the ShelXT[41] structure solution program using Intrinsic Phasing and refined by Least Squares using version 2018/3 of ShelXL-2014.[42] All non-hydrogen atoms were refined anisotropically. Hydrogen atom positions were calculated geometrically and refined using the riding model. The value of Z' is 0.5, meaning only half of the formula unit is present in the asymmetric unit, with the other half consisting of symmetry equivalent atoms. The Cu3 atom shows dynamic Jahn-Teller distortion as evidenced by the thermal ellipsoids.

Crystal Data for $C_{125}H_{135}Cl_5Cu_5O_5P_5Si_5$ (M_r = 2442.06 g/mol): monoclinic, space group $P2_1/m$ (no. 11), a = 11.646(5) Å, b = 27.726(11) Å, c = 20.644(8) Å, β = 97.801(7)°, V = 6604(5) $Å^3$, Z = 2, T = 100(2) K, $\mu(MoK_\alpha)$ = 1.046 mm^{-1}, D_{calc} = 1.228 g/cm^3, 60100 reflections measured (1.992° ≤ 2Θ ≤ 56.606°), 16179 unique (R_{int} = 0.1011, R_{sigma} = 0.1105) which were used in all calculations. The final R_1 was 0.1129 (I > 2σ(I)) and wR_2 was 0.2814 (all data).

2.4.4.2 (2,7,14-Tri-*tert*-butyl-10-aza-9-phosphatriptycene)copper(I) chloride (**10**)

Diffraction-quality crystals were grown by the diffusion of pentane vapor into a solution of **10** in THF at room temperature. A suitable crystal was selected and mounted on a Bruker D8 diffractometer with APEX2 detector diffractometer. The crystal was kept at 100(2) K during data collection. Using Olex2,[43] the structure was solved with the ShelXL[41] structure solution program using Intrinsic Phasing and refined with the ShelXL[42] refinement package using Least Squares minimization.

Crystal Data for $C_{120}H_{144}Cl_4Cu_4N_4P_4$ (M_r = 2162.22 g/mol): cubic, space group *F*-43*c* (no. 219), a = 28.8550(11) Å, V = 24025(3) Å^3, Z = 8, T = 100(2) K, μ(MoK$_\alpha$) = 0.886 mm^{-1}, D_{calc} = 1.196 g/cm^3, 10414 reflections measured (6.918° ≤ 2Θ ≤ 60.954°), 2831 unique (R_{int} = 0.0355, R_{sigma} = 0.0459) which were used in all calculations. The final R_1 was 0.0397 (I > 2σ(I)) and wR_2 was 0.1008 (all data).

2.5 References

[1] a) W. S. Knowles, *Angew. Chem. Int. Ed.* **2002**, *41*, 1998-2007; b) R. H. Grubbs, *Angew. Chem. Int. Ed.* **2006**, *45*, 3760-3765; c) R. Noyori, *Angew. Chem. Int. Ed.* **2002**, *41*, 2008-2022; d) A. Suzuki, *Angew. Chem. Int. Ed.* **2011**, *50*, 6722-6737; e) E.-i. Negishi, *Angew. Chem. Int. Ed.* **2011**, *50*, 6738-6764.

[2] a) D. S. Surry, S. L. Buchwald, *Angew. Chem. Int. Ed.* **2008**, *47*, 6338-6361; b) Q. Shen, T. Ogata, J. F. Hartwig, *J. Am. Chem. Soc.* **2008**, *130*, 6586-6596; c) C. V. Reddy, J. V. Kingston, J. G. Verkade, *J. Org. Chem.* **2008**, *73*, 3047-3062; d) F. Rataboul, A. Zapf, R. Jackstell, S. Harkal, T. Riermeier, A. Monsees, U. Dingerdissen, M. Beller, *Chem. Eur. J.* **2004**, *10*, 2983-2990.

[3] A. G. Orpen, N. G. Connelly, *Organometallics* **1990**, *9*, 1206-1210.

[4] a) A. van Rooy, E. N. Orij, P. C. J. Kamer, P. W. N. M. van Leeuwen, *Organometallics* **1995**, *14*, 34-43; b) A. van Rooy, E. N. Orij, P. C. J. Kamer, F. van den Aardweg, P. W. N. M. van Leeuwen, *J. Chem. Soc., Chem. Commun.* **1991**, 1096-1097; c) P. W. N. M. van Leeuwen, C. F. Roobeek, *J. Organomet. Chem.*

1983, *258*, 343-350; d) R. L. Pruett, J. A. Smith, *J. Org. Chem.* **1969**, *34*, 327-330; e) A. Polo, J. Real, C. Claver, S. Castillón, J. C. Bayón, *J. Chem. Soc., Chem. Commun.* **1990**, 600-601; f) T. Jongsma, G. Challa, P. W. N. M. van Leeuwen, *J. Organomet. Chem.* **1991**, *421*, 121-128; g) E. Fernández, A. Ruiz, C. Claver, S. Castillón, A. Polo, J. F. Piniella, A. Alvarez-Larena, *Organometallics* **1998**, *17*, 2857-2864.

[5] A. M. Trzeciak, J. J. Ziółkowski, *Coord. Chem. Rev.* **1999**, *190-192*, 883-900.

[6] a) D. Hellwinkel, W. Schenk, *Angew. Chem. Int. Ed.* **1969**, *8*, 987-988; b) D. Hellwinkel, W. Schenk, W. Blaicher, *Chem. Ber.* **1978**, *111*, 1798-1814.

[7] C. Jongsma, J. P. de Kleijn, F. Bickelhaupt, *Tetrahedron* **1974**, *30*, 3465-3469.

[8] T. Agou, J. Kobayashi, T. Kawashima, *Chem. Lett.* **2004**, *33*, 1028-1029.

[9] H. Tsuji, T. Inoue, Y. Kaneta, S. Sase, A. Kawachi, K. Tamao, *Organometallics* **2006**, *25*, 6142-6148.

[10] T. Iwai, S. Konishi, T. Miyazaki, S. Kawamorita, N. Yokokawa, H. Ohmiya, M. Sawamura, *ACS Catal.* **2015**, *5*, 7254-7264.

[11] H. Ube, Y. Yasuda, H. Sato, M. Shionoya, *Nat. Commun.* **2017**, *8*, 14296.

[12] S. Konishi, T. Iwai, M. Sawamura, *Organometallics* **2018**, *37*, 1876-1883.

[13] M. W. Drover, K. Nagata, J. C. Peters, *Chem. Commun.* **2018**, *54*, 7916-7919.

[14] D. Bézier, M. Brookhart, *ACS Catal.* **2014**, *4*, 3411-3420.

[15] V. Snieckus, *Chem. Rev.* **1990**, *90*, 879-933.

[16] a) L. Green, B. Chauder, V. Snieckus, *J. Heterocyclic Chem.* **1999**, *36*, 1453-1468; b) H. Tsuji, S. Komatsu, Y. Kanda, T. Umehara, T. Saeki, K. Tamao, *Chem. lett.* **2006**, *35*, 758-759.

[17] C. G. Stuckwisch, *J. Org. Chem.* **1976**, *41*, 1173-1176.

[18] M. W. Rathke, R. Kow, *J. Am. Chem. Soc.* **1972**, *94*, 6854-6856.

[19] a) M. Widhalm, K. Mereiter, *Bull. Chem. Soc. Jpn.* **2003**, *76*, 1233-1244; b) P. E. Eaton, C.-H. Lee, Y. Xiong, *J. Am. Chem. Soc.* **1989**, *111*, 8016-8018.

[20] a) M. Mosrin, P. Knochel, *Org. Lett.* **2009**, *11*, 1837-1840; b) T. Bresser, M. Mosrin, G. Monzon, P. Knochel, *J. Org. Chem.* **2010**, *75*, 4686-4695; c) G. Monzon, P. Knochel, *Synlett* **2010**, *2*, 304-308; d) T. Bresser, G. Monzon, M. Mosrin, P. Knochel, *Org. Process Res. Dev.* **2010**, *14*, 1299-1303; e) S. Duez, S. Bernhardt, J. Heppekausen, F. F. Fleming, P. Knochel, *Org. Lett.* **2011**, *13*, 1690-1693.

[21] a) Y. Kondo, M. Shilai, M. Uchiyama, T. Sakamoto, *J. Am. Chem. Soc.* **1999**, *121*, 3539-3540; b) M. Uchiyama, T. Miyoshi, Y. Kajihara, T. Sakamoto, Y. Otani, T. Ohwada, Y. Kondo, *J. Am. Chem. Soc.* **2002**, *124*, 8514-8515; c) M. Uchiyama, Y. Matsumoto, D. Nobuto, T. Furuyama, K. Yamaguchi, K. Morokuma, *J. Am. Chem. Soc.* **2006**, *128*, 8748-8750; d) M. Uchiyama, Y. Kobayashi, T. Furuyama, S. Nakamura, Y. Kajihara, T. Miyoshi, T. Sakamoto, Y. Kondo, K. Morokuma, *J. Am. Chem. Soc.* **2008**, *130*, 472-480.

[22] a) J. Vicente, J.-A. Abad, R. Clemente, J. López-Serrano, M. C. Ramírez de Arellano, P. G. Jones, D. Bautista, *Organometallics* **2003**, *22*, 4248-4259; b) R. Bielsa, A. Larrea, R. Navarro, T. Soler, E. P. Urriolabeitia, *Eur. J. Inorg. Chem.* **2005**, *2005*, 1724-1736.

[23] C. Palau, Y. Berchadsky, F. Chalier, J.-P. Finet, G. Gronchi, P. Tordo, *J. Phys. Chem.* **1995**, *99*, 158-163.

[24] C. Dunst, P. Knochel, *Synlett* **2011**, *22*, 2064-2068.

[25] L. M. Engelhardt, S. Harvey, C. L. Raston, A. H. White, *J. Organomet. Chem.* **1988**, *341*, 39-51.

[26] Z.-L. Shen, K. Sommer, P. Knochel, *Synthesis* **2015**, *47*, 2617-2630.

[27] R. Sanz, M. P. Castroviejo, Y. Fernández, F. J. Fañanás, *J. Org. Chem.* **2005**, *70*, 6548-6551.

[28] G. Baccolini, M. Bazzocchi, C. Boga, *Eur. J. Org. Chem.* **2001**, 2229-2233.

[29] C.-F. Chen, Y.-X. Ma, *Iptycenes Chemistry: From Synthesis to Applications*, Springer-Verlag, Berlin, **2013**.

[30] M. R. Churchill, K. L. Kalra, *Inorg. Chem.* **1974**, *13*, 1065-1071.

[31] T. Michinobu, E. Tsuchida, H. Nishide, *Bull. Chem. Soc. Jpn.* **2000**, *73*, 1021-1027.

[32] M. R. Talipov, M. M. Hossain, A. Boddeda, K. Thakur, R. Rathore, *Org. Biomol. Chem.* **2016**, *14*, 2961-2968.

[33] a) S. W. Kwok, J. R. Fotsing, R. J. Fraser, V. O. Rodionov, V. V. Fokin, *Org. Lett.* **2010**, *12*, 4217-4219; b) R. O. Lindsay, C. F. H. Allen, *Org. Synth.* **1942**, *22*, 96.

[34] R. Sanz, M. P. Castroviejo, V. Guilarte, A. Pérez, F. J. Fañanás, *J. Org. Chem.* **2007**, *72*, 5113-5118.

[35] A. Frischmuth, M. Fernández, N. M. Barl, F. Achrainer, H. Zipse, G. Berionni, H. Mayr, K. Karaghiosoff, P. Knochel, *Angew. Chem. Int. Ed.* **2014**, *53*, 7928-7932.

[36] J. J. Eisch, Z.-R. Liu, X. Ma, G.-X. Zheng, *J. Org. Chem.* **1992**, *57*, 5140-5144.

[37] a) K. Deng, A. Bensari, T. Cohen, *J. Am. Chem. Soc.* **2002**, *124*, 12106-12107; b) B. Mudryk, T. Cohen, *Org. Synth.* **1995**, *72*, 173.

[38] G. R. Fulmer, A. J. M. Miller, N. H. Sherden, H. E. Gottlieb, A. Nudelman, B. M. Stoltz, J. E. Bercaw, K. I. Goldberg, *Organometallics* **2010**, *29*, 2176-2179.

[39] *Bruker Advanced X-Ray Solutions APEX2 User Manual - Version 2, Vol. 5-1*, **2016**.

[40] *CrysAlisPro Software System, Rigaku Oxford Diffraction*, **2018**.

[41] G. M. Sheldrick, *Acta Cryst.* **2015**, *A71*, 3-8.

[42] G. Sheldrick, *Acta Cryst.* **2015**, *C71*, 3-8.

[43] O. V. Dolomanov, L. J. Bourhis, R. J. Gildea, J. A. K. Howard, H. Puschmann, *J. Appl. Cryst.* **2009**, *42*, 339-341.

CHAPTER 3. AZAPHOSPHATRIPTYCENE IN RHODIUM-CATALYZED HYDROFORMYLATION

3.1 Background

Hydroformylation of olefins to make aldehydes has developed into an important industrial process since its discovery by Roelen in 1938, and synthetic aldehydes have applications in plasticizers, pharmaceutical and fine chemical synthesis.[1] During the 1960s, the discovery of (phosphine)rhodium complexes as chemo-selective catalysts for the homogeneous hydroformylation of terminal alkenes by Wilkinson represented a breakthrough.[2] Since then, one of the most active areas in hydroformylation research has been the design and synthesis of new ligands to optimize catalyst activity and selectivity.[1e, 3] Since the 1980s, bulky phosphite[4] and phosphonite[5] donors, combining strong π-acidity with high steric demand, have proven remarkably effective ligands in the hydroformylation of terminal alkenes, and led to enhanced catalyst activity toward less reactive internal olefins, including cycloalkenes. The strong π-accepting electronic properties of these donors increase the Lewis acidity of the rhodium center and thus facilitate alkene coordination to the rhodium center. In addition, high steric demand facilitates CO dissociation from the rhodium center during catalytic cycles, contributing to higher reaction rate.[3b] However, the degradation of these ligands through hydrolysis or alcoholysis represents a weakness of this framework, and has spurred the search for alternatives that retain their steric and electronic properties.[1f]

In recent years, subsequent efforts have sought to expand the range of design possibilities, and improve the resistance of the ligand toward degradation via P–O bond cleavage.[1f] Several new strong π-acceptor ligands have shown beneficial effects in rhodium-catalyzed hydroformylation. Van Leeuwen et al.[6] studied *N*-pyrrolyl substituted phosphines as ligands supporting very active catalysts for the hydroformylation of terminal alkenes. Beller et al.[7] investigated pyrrolyl-, indolyl-, and carbazolylphosphanes as ligands for the rhodium-catalyzed hydroformylation of internal alkenes, and obtained higher regio-selectivities than those obtained using triphenylphosphine. Breit et al. developed bulky phosphabenzene[8] and phosphabarrelene[8d, 9] ligands, which enabled highly active and regio-selective rhodium catalysts for the hydroformylation of terminal and internal alkenes under mild conditions.

We have reported the preparation of a good π-acceptor azaphosphatriptycene ligand **7** in Chapter 2, bearing *tert*-butyl substituents *meta* to the phosphorus to increase overall steric demand on the rigid heterotriptycene backbone without directly crowding the metal center. This ligand could be isolated in good overall yield through a straightforward sequence. Studies on synthesis of its rhodium precursor and its first application in rhodium-catalyzed hydroformylation of terminal and internal cyclic alkenes are described in this chapter.

3.2 Results and Discussion

3.2.1 Synthesis of (acetylacetonato)carbonyl(2,7,14-tri-tert-butyl-9-phospha-10-aza-triptycene)rhodium(I) complex

To obtain the rhodium precursor applied in the hydroformylation, (acetylacetonato)carbonyl(2,7,14-tri-*tert*-butyl-9-phospha-10-aza-triptycene)rhodium(I) complex **12** was prepared by treatment of one equivalent of azaphosphatriptycene **7** with (acetylacetonato)dicarbonylrhodium(I) [Rh(acac)(CO)$_2$] in toluene (Scheme 3.1). The ^{31}P NMR spectrum of **12** displays a doublet resonance at δ –1.3 ppm with $^{1}J_{P\text{-}Rh}$= 189 Hz. The infrared stretching frequency of metal-bound carbonyls (ν_{CO}) reflects the degree of π-backbonding from the metal center, which is affected by the σ-donor and π-acceptor character of supporting ligands. A higher CO stretching frequency reflects less π-backbonding from the metal center, reflecting weaker σ-donor and stronger π-acceptor character at the other supporting ligands.[10] For complex **12**, ν_{CO} is 1985 cm^{-1}, intermediate between the values of 1975 cm^{-1} for the corresponding triphenylphosphine complex, and 2006 cm^{-1} for the triphenyl phosphite complex.[11]

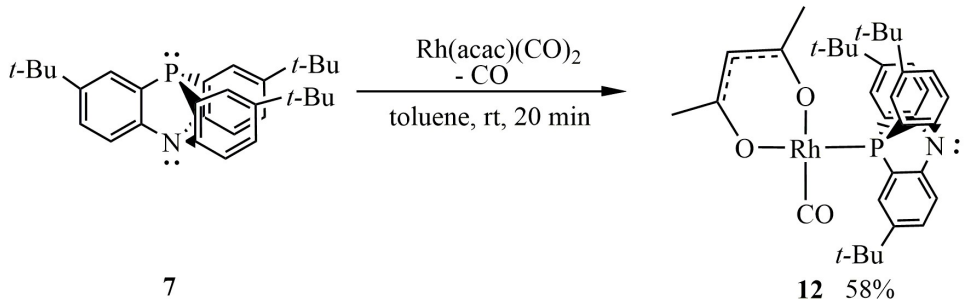

7 **12** 58%

Scheme 3.1. Synthesis of rhodium precursor [(**7**)Rh(acac)(CO)] (**12**).

The molecular structure of **12** was determined by single crystal X-ray diffraction (Figure 3.1). Complex **12** is planar with a Rh−P bond distance of 2.2080(8) Å. The Rh−O bond distances are 2.067(2) Å (*trans* to ligand **7**) and 2.044(2) Å (*trans* to CO), as comparison with [Rh(acac)(CO)(PPh$_3$)] which has 2.087(4) Å for Rh−O bond distance

(*trans* to PPh_3) and 2.029(5)Å (*trans* to CO).[12] The cone angle for **7** on complex **12** is about 151°, somewhat larger than that of 145° for triphenylphosphine.[13] Within the bound phosphatriptycene the C−P−C angles are only 95.00(13)° to 95.14(13)°, whereas the C−N−C angles about the other bridgehead are more nearly tetrahedral, ranging from 107.5(2)°-108.9(2)°. Constraining the phenyl groups from triphenylphosphine to a triptycene framework results in a much smaller ligand, but the *tert*-butyl substituents restore some steric demand.

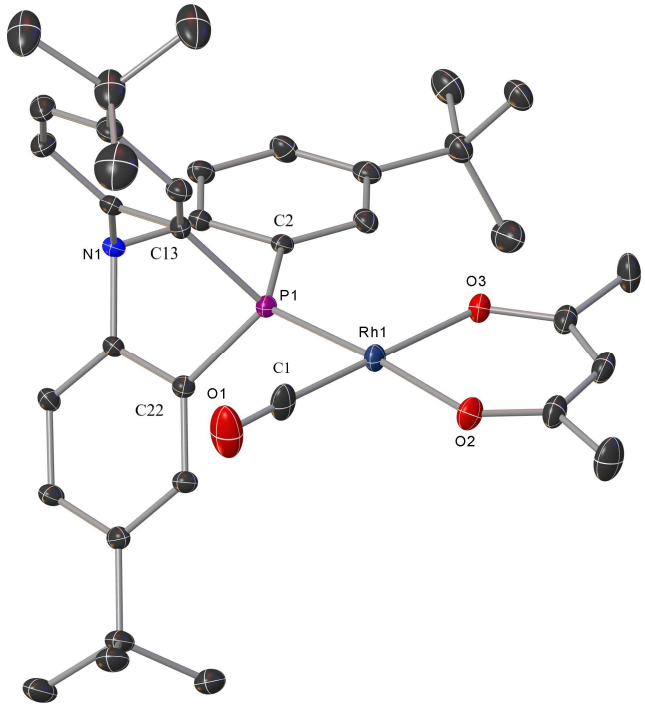

Figure 3.1. Solid-state structure of [(**7**)Rh(acac)(CO)] (**12**), ellipsoids at 50% probability. Calculated hydrogen atoms are omitted for clarity. Selected interatomic distances (Å) and angles (°): Rh1−P1 2.2080(8), Rh1−C1 1.821(3), Rh1−O2 2.067(2), Rh1−O3 2.044(2), C1−O1 1.142(4); P1−Rh1−C1 86.43(10), C2−P1−C13 95.00(13), C2−P1−C22 95.14(13), C13−P1−C22 95.13(13).[14]

3.2.2 Hydroformylation studies

3.2.2.1 Azaphosphatriptycene in the hydroformylation of 1-octene

Hydroformylation catalysts are usually assessed by their activity, as well as chemo- and regio-selectivity.[3] To compare **7** as a supporting ligand in rhodium-catalyzed hydroformylation with the well-studied triphenylphosphine, combinations with the precatalyst [Rh(acac)$(CO)_2$] were first examined in the hydroformylation of 1-octene (Scheme 3.2).

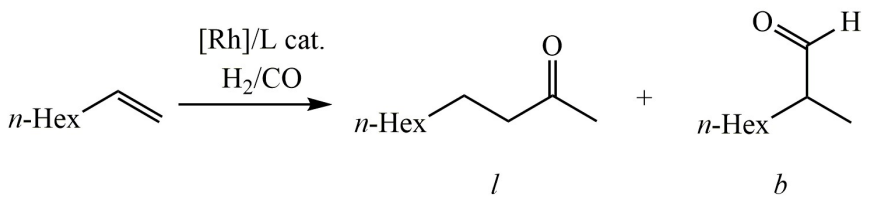

Scheme 3.2. Hydroformylation of 1-octene.

The results are summarized in Table 3.1. In previous studies using triphenylphosphine PPh_3, the use of excess ligand leads to lower reaction rates, but improves selectivity for the preferred linear aldehyde. As a result, phosphine to rhodium ratios of 20:1 may be preferred. In contrast, the use of such a high ratio of **7**/[Rh] nearly suppresses catalysis altogether (Table 3.1 Entry 3). A decrease in the **7**/[Rh] ratio to 4:1 (Table 3.1 Entry 4) or even 2:1 (Table 3.1 Entry 5) greatly enhanced the conversion of 1-octene and the yield of aldehyde. No alkane or alcohol byproducts were detected and the balance of olefin conversion represents a mixture of internal octenes.

Table 3.1. Hydroformylation of 1-octene.[a]

Entry	L	L/M	Alkene Conv (%)	Aldehyde (%)	*l* : *b*	Aldehyde TOF (h^{-1})
1	PPh_3	20	42	42	2.8	2100[15]
2	PPh_3	20	76	28	2.8	1390
3	**7**	20	1	0.3	-[b]	15
4	**7**	4	80	56	3.1	2780
5[c]	**7**	2	99	53	1.5	5300
6[c,d]	**7**	2	20	13	3.2	1270

[a] $[Rh(acac)(CO)_2]$, 0.020 mol %; $[1\text{-octene}]_{initial}$ = 0.84 M in toluene; H_2/CO (1:1) 20 bar. Unless noted otherwise, 80 °C, 1 h. [b] Only *n*-aldehyde detected. [c] Reaction time 0.5 h. [d] Reaction temp 60 °C.

The effects of π-acidic ligands on the formation and reactivity of key catalytic intermediates in hydroformylation, and on the rates of carbonylation versus alkene formation from rhodium alkyls, has been studied in details in literature.[4b, 4d, 4f, 8c] The isomerization reaction for terminal alkenes has a higher free activation energy than

hydroformylation reaction,[4f] thus a lower reaction temperature could decrease the proportion of isomerization products in all products (Table 3.1 Entry 6). The linear/branched aldehyde ratio decreased at lower ligand/metal ratios and higher temperatures. Although selectivity for the linear aldehyde was modest, the high activity of the system under mild reaction conditions was encouraging.

3.2.2.2 Azaphosphatriptycene in the hydroformylation of cyclic alkenes

Disubstituted alkenes undergo hydroformylation much more slowly than terminal alkenes. The Ph_3P/[Rh] catalyst system exhibits low activity in the hydroformylation of cyclic alkenes under mild conditions.[2b] In contrast, π-acidic bulky phosphite ligands[4b] have enabled very high reactivity toward these substrates. Cyclohexene was chosen first as an internal alkene substrate for hydroformylation (Scheme 3.3), because its isomerization leaves the substrate unchanged. No alcohol or alkane byproducts were detected using this system, so alkene conversion and the yield of aldehyde are identical.

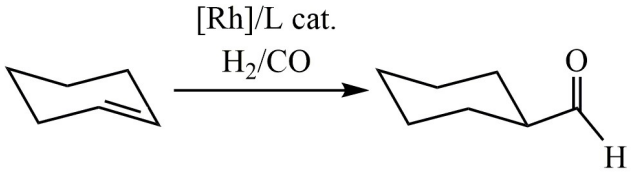

Scheme 3.3. Hydroformylation of cyclohexene.

The **7**/[Rh] catalyst system displayed much higher activity toward cyclohexene than the PPh_3/[Rh] catalyst system, as shown in Table 3.2. The addition of cyclohexene to the rhodium precursor represents the rate-limiting step in cyclohexene hydroformylation[4f] and with the π-acidic ligands, the rhodium center is more Lewis-acidic toward the

cyclohexene substrate. The turnover frequency (TOF) for cyclohexanecarbaldehye formation could be influenced by initial cyclohexene concentration (Table 3.1 Entry 5), reaction temperature (Table 3.1 Entry 7) and syngas pressure (Table 3.1 Entry 8). Increasing initial cyclohexene concentration, temperature and pressure had positive influence on the reaction rates. Quantitative conversion was observed using 0.020 mol % [Rh] precatalyst and 0.040 mol % **7** (Table 3.2 Entry 9), after 4 h at 100 °C under 20 bar of syngas.

Table 3.2. Hydroformylation of cyclohexene.[a]

Entry	L	*t* (h)	T (°C)	P (bar)	Aldehyde (%)	Aldehyde TOF (h^{-1})
1[b]	PPh_3	2	90	15	2	20[4b]
2[c]	PPh_3	2	90	15	7	70
3[d]	**7**	2	90	15	65	650
4	**7**	2	100	20	85	2130
5[e]	**7**	2	100	20	73	1830
6[f]	**7**	2	100	20	5	120
7	**7**	2	80	20	49	1230
8	**7**	2	100	15	64	1610
9	**7**	4	100	20	100	1250

[a] Unless noted otherwise, $[Rh(acac)(CO)_2]$ 0.020 mol %; Ligand **7** 0.040 mol %; $[Cyclohexene]_{initial}$ = 0.86 M. [b] [Rh(acac)(cod)] 0.050 mol %; PPh_3 1.00 mol %;

$[Cyclohexene]_{initial}$ = 0.91 M. [c] $[Rh(acac)(CO)_2]$ 0.050 mol %; PPh_3 1.00 mol %; $[Cyclohexene]_{initial}$ = 0.91 M. [d] $[Rh(acac)(CO)_2]$ 0.050 mol %; Ligand **7** 0.10 mol %; $[Cyclohexene]_{initial}$ = 0.91 M. [e] $[Cyclohexene]_{initial}$ = 0.56 M. [f] Ligand **7** 0.080 mol %.

3.2.2.3 Hydroformyation of heteroatom-substituted cyclic alkenes

Formyl furan and formyl pyran derivatives, for example, are relevant to natural product synthesis.[4c] We therefore examined the hydroformylation of 2,3-dihydrofuran and 3,4-dihydro-2*H*-pyran (Scheme 3.4).

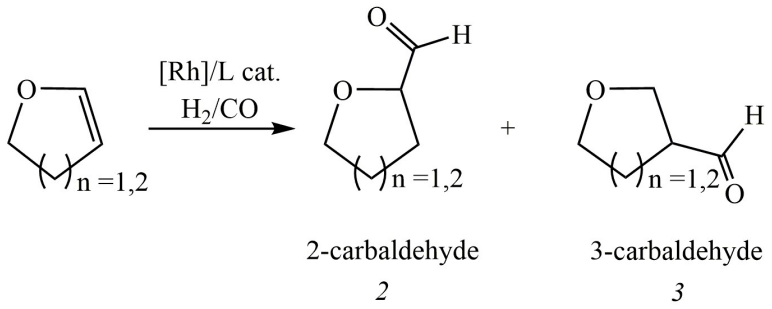

Scheme 3.4. Hydroformyation of heteroatom-substituted cyclic alkenes.

Conversion of 2,3-dihydrofuran to a mixture of the 2- and 3-formyl derivatives proceeded under mild conditions. The selectivity for 2-formyltetrahydrofuran (Table 3.3 Entry 3), while moderate, was higher than that of the Ph_3P/[Rh] system under comparable conditions.[4c] The hydroformylation of 3,4-dihydro-*2H*-pyran proceeded to lower conversion than that of 2,3-dihydrofuran even under higher temperature and pressure (Table 3.3 Entry 6), perhaps due to greater hindrance about the C=C bond, and the absence of ring strain compared to the five-membered substrate.[16]

Table 3.3. Hydroformyation of heteroatom-substituted alkenes.[a]

Entry	n	L	*t* (h)	T (°C)	P (bar)	Conv (%)	*2:3*	Aldehyde TOF (h^{-1})
1[b]	1	PPh_3	20	80	5	95	1.4	10[4c]
2[c]	1	PPh_3	20	80	5	94	1.7	20
3	1	**7**	20	80	5	91	3.2	230
4[d]	1	**7**	20	80	5	99	2.7	100
5[e]	2	PPh_3	8	120	75	3	1.6	1[16]
6	2	**7**	20	120	20	62	0.9	160

[a] $[2, 3\text{-dihydrofuran}]_{initial}$ = 1.2 M; $[3,4\text{-dihydro-2}H\text{-pyran}]_{initial}$ = 1.2 M. Unless noted otherwise, $[Rh(acac)(CO)_2]$ 0.02 mol %; Ligand **7** 0.04 mol %. [b] $[Rh_2\{\mu\text{-}S(CH_2)_3NMe_2\}_2(cod)_2]$ 0.25 mol %; PPh_3 0.5 mol %. [c] $[Rh(acac)(CO)_2]$ 0.25 mol %; PPh_3 0.5 mol %. [d] $[Rh(acac)(CO)_2]$ 0.050 mol %; Ligand **7** 0.10 mol %. [e] CO/H_2 = 0.5; $[Rh_2\{\mu\text{-}S(CH_2)_3NMe_2\}_2(cod)_2]$ 0.25 mol %; PPh_3 2.50 mol %.

3.3 Conclusion

The rhodium complex of a new azaphosphatriptycene with *meta* substituents serves as an active precursor in the hydroformylation of terminal alkene, with unfortunately high activity for competing isomerization. This rhodium precatalyst has exhibited remarkable activity in the hydroformylation of internal cyclic alkenes, including heterocyclic alkenes. The strong π-accepting electronic properties and relatively steric demand of the new azaphosphatriptycene ligands have proved to facilitate the hydroformylation reactions.

3.4 Experimental

3.4.1 *General considerations*

Unless otherwise indicated, manipulations were carried out in resealable glassware on a Schlenk line under an atmosphere of argon, or in an MBraun glovebox under an atmosphere of nitrogen. Glassware and magnetic stir bars were dried in a ventilated oven at 160 °C and allowed to cool under vacuum.

Tetrahydrofuran (THF, EMD Millipore OmniSolv), toluene (EMD Millipore OmniSolv) and dichloromethane (DCM, EMD Millipore OmniSolv) were sparged with ultra-high purity argon (NexAir) for 45 minutes prior to first use and dried using an MBraun solvent purification system. THF and toluene were further dried over sodium benzophenone ketyl, degassed by successive freeze-pump-thaw cycles and transferred under vacuum to an oven-dried resealable flasks. DCM was further dried by stirring overnight with calcium hydride (Alfa Aesar, coarse powder), degassed by successive freeze-pump-thaw cycles, and transferred under vacuum into oven-dried resealable Schlenk flask. Benzene-d_6 (Cambridge Isotope Laboratories) was dried over sodium benzophenone ketyl, degassed by successive freeze-pump-thaw cycles and transferred under vacuum into oven-dried resealable flask. 1-Octene (Acros Organics), cyclohexene (Alfa Aesar), 2,3-dihydrofuran (Alfa Aesar) and 3,4-dihydro-2*H*-pyran (Sigma-Aldrich) were dried by stirring overnight with calcium hydride (Alfa Aesar, coarse powder), degassed by successive freeze-pump-thaw cycles, and transferred under vacuum into oven-dried resealable Schlenk flasks. Anhydrous pentane (EMD Millipore Drisolv, sealed under a nitrogen atmosphere) and (acetylacetonato)dicarbonylrhodium(I) (Sigma-Aldrich) were

used as received and stored in a glovebox. Ethyl Acetate (BDH), methanol (BDH), ethanol (200 proof, Koptec), chloroform-*d* (Cambridge Isotope Laboratories), *tert*-butyllithium (1.7 M in pentane, Aldrich), nitric acid (BDH, 68-70 %, ACS grade), tris(2,4-di-*tert*-butylphenyl)phosphite (Strem Chemicals), anhydrous $MgSO_4$ (Alfa Aesar, powder), sodium hydroxide (EMD Millipore), nonanal (Sigma-Aldrich, analytical standard), cyclohexanecarboxaldehyde (Sigma-Aldrich), di-(4-*tert*-butylphenyl)amine (TCI America), tris(dibenzylideneacetone)dipalladium(0) (Aldrich), tris(*o*-tolyl)phosphine (Aldrich), sodium *tert*-butoxide (TCI America), 1-bromo-4-*tert*-butylbenzene (Oakwood Chemicals), *N*-bromosuccinimide (Aldrich), sodium metal (Alfa Aesar), benzophenone (Alfa Aesar), calcium hydride (Alfa Aesar), nitrogen (NexAir), syngas (CO/H_2= 1, NexAir) and argon (both industrial and ultra-high purity grades, NexAir) were used as received. Tap water was purified in a Barnstead International automated still prior to use. Tris(4-*tert*-butylphenyl)amine[17] and tris(2-bromo-4-*tert*-butylphenyl)amine[18] were prepared according to reported procedures, and characterized by ^{1}H NMR and ^{13}C NMR spectroscopy.

^{1}H, ^{13}C and ^{31}P NMR spectra were obtained using a Varian Mercury Vx 400 spectrometer. ^{1}H and ^{13}C NMR chemical shifts were referenced with respect to solvent signals and reported relative to tetramethylsilane. ^{31}P NMR chemical shifts were reported with phosphoric acid (85 wt % in H_2O) as external standard. Chemical shifts δ are reported in ppm. Fourier Transform Infrared spectra were collected using microcrystalline samples on a Shimadzu IRAffinity-1S fourier transform infrared spectrophotometer. Samples were exposed to air as briefly as possible prior to data collection. Only characteristic peaks were reported in cm^{-1}. EI-MS and GC-MS were recorded on MicroMass AutoSpec M by Georgia

Institute of Technology mass spec facility. Elemental analyses were performed by Atlantic Microlab, Inc. in Norcross, GA.

Hydroformylation reactions were performed in a 300-mL stainless steel stirred Parr reactor (Parr Instrument Company, model 452HC, maximum allowable working pressure: 2000 psi (137.9 bar) at 350 °C). The 300-mL stainless steel stirred Parr reactor was thoroughly washed with nitric acid (1 M, 3 x 300 mL), neutralized with 1 M NaOH solution, followed by several rinse cycles with *DI* water and acetone. The reactor was dried in pieces in a ventilated oven at 160 °C for 12 h, then reconstructed and purged with 7 bar nitrogen 10 times when heating to 140 °C. The reactor was cooled to room temperature under N_2 (7 bar) before each experiment. Syngas was added to the vessel via high pressure stainless steel tubing, using a Matheson Tri-Gas control system (PAN-5500 Series Analytical Grade Panel) and 500D Syringe Pump (Teledyne Isco). GC-FID analyses were performed using a Shimadzu GC-2010 Plus gas chromatograph fitted with a Supelco PTA-5 (30 m x 0.25 mm x 0.50 μm, length x inside diameter x film thickness) capillary GC column. Calibration curves for 1-octene, nonanal, cyclohexene, cyclohexanecarboxaldehyde, 2,3-dihydrofuran and 3,4-dihydro-2*H*-pyran were recorded on the GC-FID.

3.4.2 Synthetic procedures

3.4.2.1 [(**7**)Rh(acac)(CO)] (**12**)

In a glovebox, ligand **7** (0.017 g, 0.039 mmol) and (acetylacetonato)dicarbonyl rhodium(I) [Rh(acac)$(CO)_2$] (0.010 g, 0.039 mmol) were dissolved in toluene (0.5 mL); bubbles were observed immediately. The solution was layered with pentane (5 mL) and

stored at –35 °C for 3 d. The solution was filtered and a yellow crystalline solid was collected. The solid was dried under vacuum for 12 h to afford the complex **12**, 0.015 g (58%). ^{1}H NMR (400 MHz, C_6D_6): δ (ppm) 8.70 (dd, $^{3}J_{H\text{-}P}$= 12.4 Hz, $J_{H\text{-}H,\ meta}$= 2.0 Hz, 3H), 7.69 (dd, $J_{H\text{-}H,\ ortho}$= 8.0 Hz, $^{4}J_{H\text{-}P}$ = 2.4 Hz, 3H), 7.03 (dd, $J_{H\text{-}H,\ ortho}$= 8.0 Hz, $J_{H\text{-}H,\ meta}$= 2.4 Hz, 3H), 5.43 (s, 1H, C*H*, acac), 2.00 (s, 3H, CH_3, acac), 1.86 (s, 3H, CH_3, acac), 1.08 (s, 27H, C(CH_3)$_3$); ^{13}C{^{1}H} NMR (101 MHz, C_6D_6): δ (ppm) 189.17 (dd, $^{1}J_{C\text{-}Rh}$= 72.3 Hz, $^{2}J_{C\text{-}P}$= 29.5 Hz, *C*O), 188.34 (s, *C*O, acac), 185.00 (s, *C*O, acac), 154.78 (d, $^{2}J_{C\text{-}P}$= 1.9 Hz), 148.91 (d, $^{1}J_{C\text{-}P}$= 11.2 Hz), 141.49 (d, $^{2}J_{C\text{-}P}$= 45.3 Hz), 131.37 (d, $^{3}J_{C\text{-}P}$= 16.6 Hz), 127.44 (d, $^{4}J_{C\text{-}P}$= 1.4 Hz), 125.90 (d, $^{3}J_{C\text{-}P}$= 3.7 Hz), 101.53 (d, $^{3}J_{C\text{-}Rh}$= 1.7 Hz, *C*H, acac), 34.78 (s, *C*(CH$_3$)$_3$), 31.40 (s, *C*H$_3$), 27.57 (s, *C*H$_3$, acac); ^{31}P{^{1}H} NMR (162 MHz, C_6D_6): δ (ppm) –1.28 (d, $^{1}J_{P\text{-}Rh}$ = 189.0 Hz); Elemental analysis calcd (%) for $C_{36}H_{43}NO_3PRh$ (671.62): C 64.38 H 6.45 N 2.09, found C 64.37, H 7.04, N 1.90; IR: ν (cm^{-1}): 2961 (s), 1985 (s, CO), 1584(s), 1524(s), 1474(s), 1391(s), 1051 (s), 729(s).

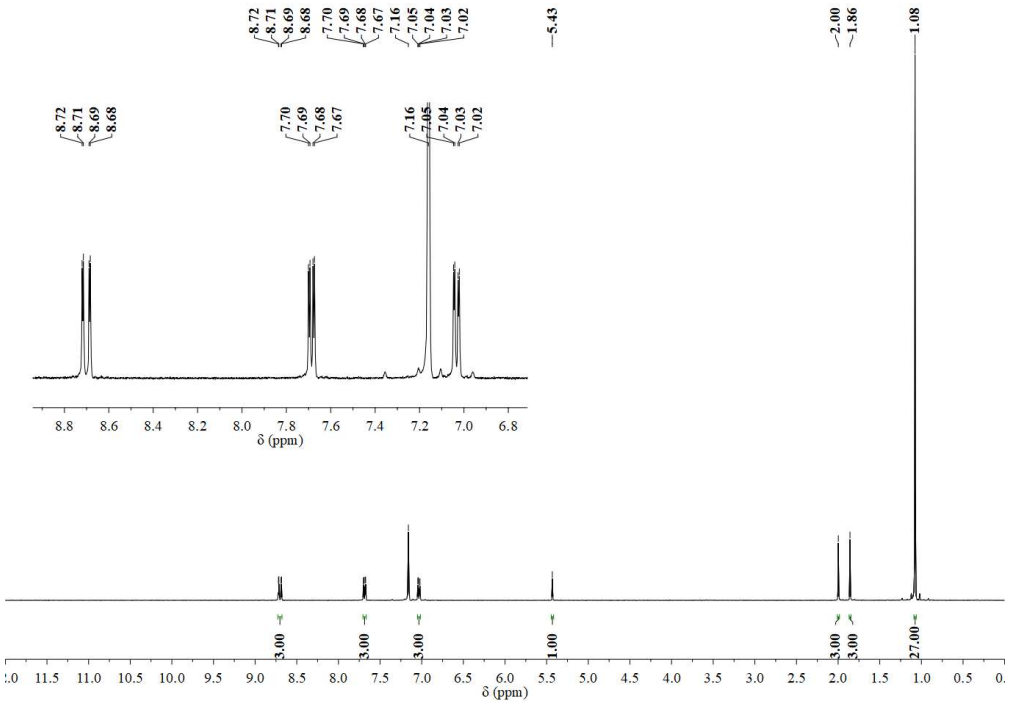

Figure 3.2. ^{1}H NMR (400 MHz, C_6D_6) spectrum of **12**.

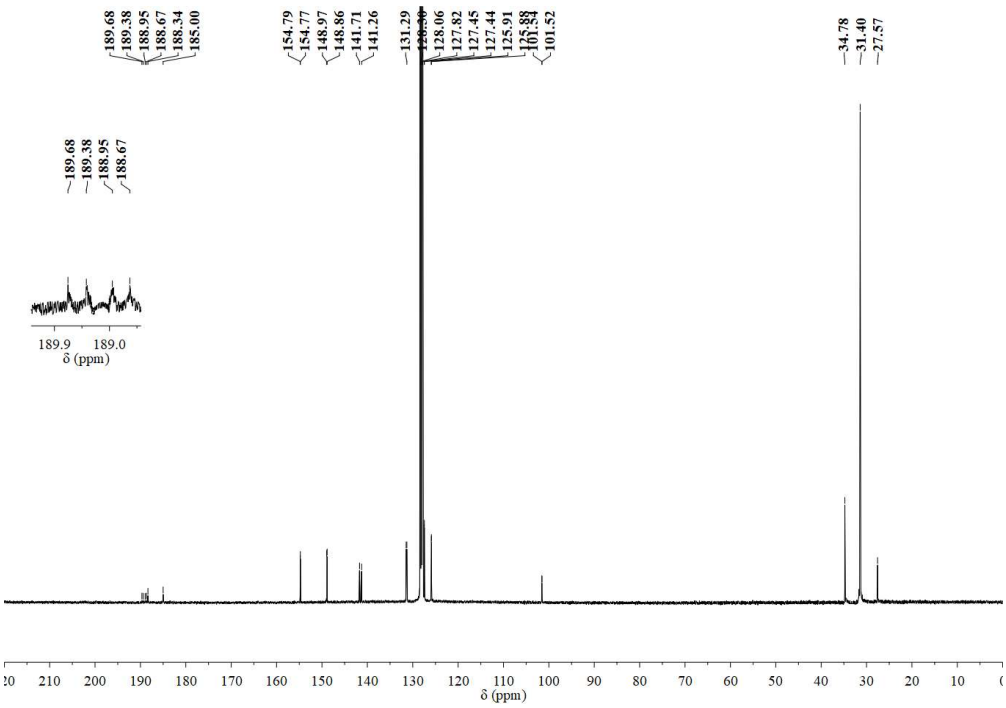

Figure 3.3. $^{13}C\{^{1}H\}$ NMR (101 MHz, C_6D_6) spectrum of **12**.

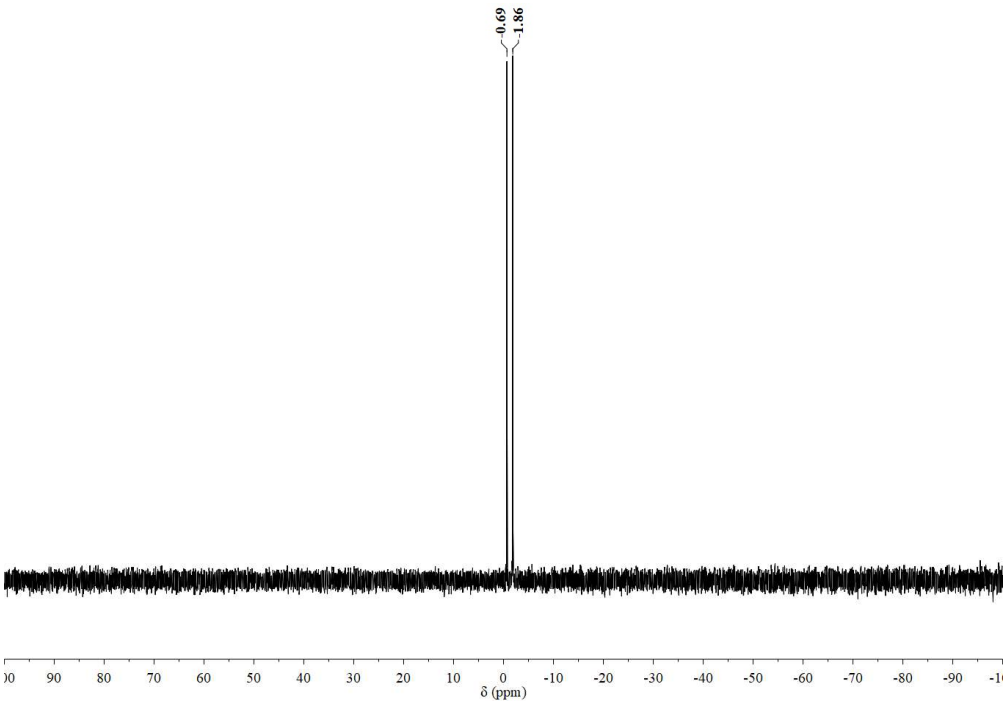

Figure 3.4. $^{31}P\{^{1}H\}$ NMR (162 MHz, C_6D_6) spectrum of **12**.

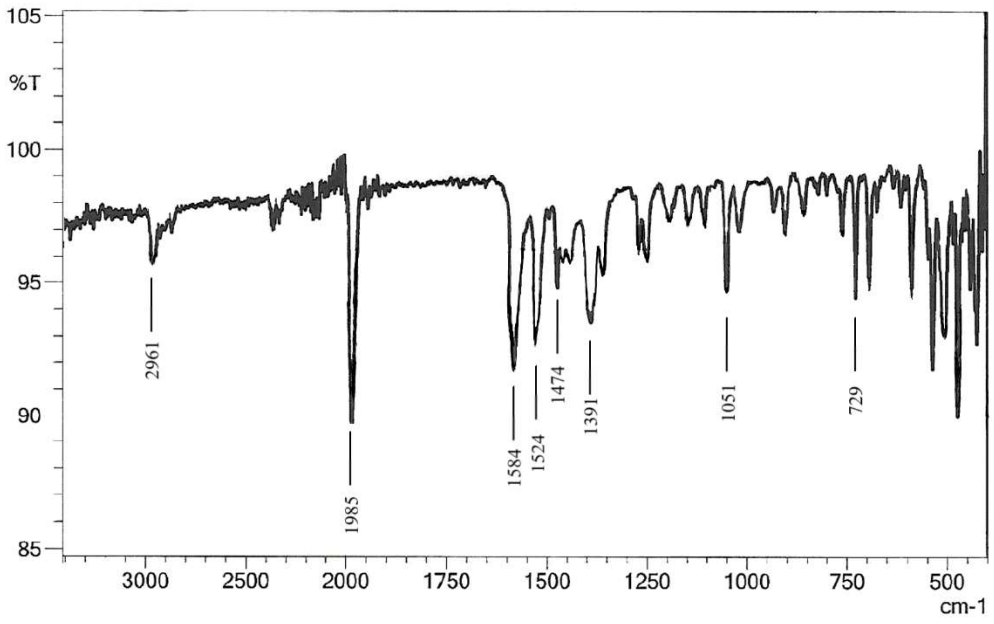

Figure 3.5. IR spectrum of **12**. ν_{CO} = 1985 cm^{-1}.

3.4.3 General procedure for hydroformylation studies

Ligand **7**, [Rh(acac)$(CO)_2$] and toluene were mixed in a glovebox and transferred via gastight syringe into a previously dried 300-mL stainless steel Parr reactor. The reactor was purged twice with N_2 (7 bar), then three times with syngas (7 bar). Substrate (1-octene, cyclohexene, 2,3-dihydrofuran or 3,4-dihydro-2*H*-pyran) was added into the Parr reactor via another gastight syringe, then the reactor was purged twice more with syngas (7 bar), and released to 1 bar. The reactor was then brought to the desired reaction temperature, a continuous working pressure of syngas was established, and stirring was initiated. The reaction mixture was stirred for the desired reaction time, then agitation was stopped and the reactor was cooled to room temperature in an ice bath. The gas inside the Parr reactor was slowly vented in the hood to a 4.0 mL cold bath of toluene (0 °C). The reactor was

opened and the organic phase was diluted to a defined volume. Aliquots taken from the organic phase and from cold toluene were analyzed by GC-FID. Amounts of starting substrates and products were determined by analysis of both the organic phase and the toluene solution for gas venting, based on pre-determined calibration curves. Aldehyde TOF was calculated from the molar quantity of aldehyde formed per mole of $Rh(acac)(CO)_2$ precatalyst per hour of reaction time.

Hydroformylation experiments of 1-octene[15] (Table 3.1 Entry 1) were conducted by dissolving catalyst precursors in toluene in the autoclave, then pressurizing with syngas and heating up to the desired pressure and temperature over 40 min. 1-Octene was added under pressure, and the reactions run for 1 h. To compare results in our laboratory (Table 3.1 Entry 2) to those of experiments reported using the same reaction conditions, catalyst precursor and 1-octene were dissolved in toluene in the autoclave, then the desired pressure of syngas was added and the mixture was heated over 20 min to the desired temperature, followed by a reaction time of 1 h. Hydroformylation experiments of cyclohexene was reproduced (Table 3.2 Entry 2) from literature reports (Table 3.2 Entry 1) under their reported conditions with modifications (listed in Table 3.2).[4b] Hydroformylation experiments of 2,3-dihydrofuran[4c] and 3,4-dihydro-2*H*-pyran[16] were reproduced from literature reports under their reported conditions with modifications (listed in Table 3.3). The hydroformylation products were determined by GC-MS and GC-FID and isomer aldehydes were identified by different retention times on GC based on boiling points. None of the experiments produced hydrogenation products.

3.4.4 X-ray diffraction studies

Single crystals of **12** was grown by the diffusion of pentane vapor into a solution of **12** in THF at room temperature. A suitable crystal was selected and mounted on a loop with Paratone oil a Bruker D8 Venture diffractometer. The crystal was kept at 100(2) K during data collection. Using Olex2[19], the structure was solved with the ShelXT[20] structure solution program using Intrinsic Phasing, and refined with the ShelXL[21] refinement package using Least Squares minimization.

Crystal Data for $C_{72}H_{86}N_2O_6P_2Rh_2$ (M_r = 1343.19 g/mol): triclinic, space group *P*-1 (no. 2), a = 10.6289(5) Å, b = 10.8230(5) Å, c = 17.8290(8) Å, α = 84.254(2)°, β = 78.440(2)°, γ = 63.6990(10)°, V = 1801.22(15) Å^3, Z = 1, T = 100(2) K, μ(MoK_α) = 0.551 mm^{-1}, D_{calc} = 1.238 g/cm^3, 16475 reflections measured (4.342° ≤ 2Θ ≤ 56.564°), 8804 unique (R_{int} = 0.0260, R_{sigma} = 0.0454) which were used in all calculations. The final R_1 was 0.0461 (I > 2σ(I)) and wR_2 was 0.1130 (all data).

3.5 References

[1] a) O. Roelen, (Chemische Verwertungsgesellschaft Oberhausen m.b.H.), German Patent, DE 849548, 841938/841952; O. Roelen, U.S. Patent, 2327066, 2321943; Chem. Abstr., 2321944, 2327038, 2323631; b) J. Falbe, *Carbon Monoxide in Organic Synthesis*, Springer-Verlag, Berlin, **1970**; c) J. Falbe, *New Syntheses with Carbon Monoxide*, Springer-Verlag, Berlin, **1980**; d) B. Cornils, W. A. Herrmann, M. Rasch, *Angew. Chem.* **1994**, *106*, 2219-2238; e) M. Beller, B. Cornils, C. D. Frohning, C. W. Kohlpaintner, *J. Mol. Catal. A: Chem.* **1995**, *104*, 17-85; f) A. M. Trzeciak, J. J. Ziółkowski, *Coord. Chem. Rev.* **1999**, *190-192*, 883-900; g) B. Breit, W. Seiche, *Synthesis* **2001**, 1-36.

[2] a) D. Evans, J. A. Osborn, G. Wilkinson, *J. Chem. Soc. A* **1968**, 3133-3142; b) C. K. Brown, G. Wilkinson, *J. Chem. Soc.* **1970**, 2753-2764.

[3] a) F. Agbossou, J.-F. Carpentier, A. Mortreux, *Chem. Rev.* **1995**, *95*, 2485-2506; b) R. Franke, D. Selent, A. Börner, *Chem. Rev.* **2012**, *112*, 5675-5732.

[4] a) R. L. Pruett, J. A. Smith, *J. Org. Chem.* **1969**, *34*, 327-330; b) P. W. N. M. van Leeuwen, C. F. Roobeek, *J. Organomet. Chem.* **1983**, *258*, 343-350; c) A. Polo, J. Real, C. Claver, S. Castillón, J. C. Bayón, *J. Chem. Soc., Chem. Commun.* **1990**, 600-601; d) A. van Rooy, E. N. Orij, P. C. J. Kamer, F. van den Aardweg, P. W. N. M. van Leeuwen, *J. Chem. Soc., Chem. Commun.* **1991**, 1096-1097; e) T. Jongsma, G. Challa, P. W. N. M. van Leeuwen, *J. Organomet. Chem.* **1991**, *421*, 121-128; f) A. van Rooy, E. N. Orij, P. C. J. Kamer, P. W. N. M. van Leeuwen, *Organometallics* **1995**, *14*, 34-43; g) E. Fernández, A. Ruiz, C. Claver, S. Castillón, A. Polo, J. F. Piniella, A. Alvarez-Larena, *Organometallics* **1998**, *17*, 2857-2864.

[5] D. Selent, K.-D. Wiese, D. Röttger, A. Börner, *Angew. Chem. Int. Ed.* **2000**, *39*, 1639-1641.

[6] a) S. C. van der Slot, P. C. J. Kamer, P. W. N. M. van Leeuwen, J. Fraanje, K. Goubitz, M. Lutz, A. L. Spek, *Organometallics* **2000**, *19*, 2504-2515; b) S. C. van der Slot, J. Duran, J. Luten, P. C. J. Kamer, P. W. N. M. van Leeuwen, *Organometallics* **2002**, *21*, 3873-3883.

[7] R. Jackstell, H. Klein, M. Beller, K.-D. Wiese, D. Röttger, *Eur. J. Org. Chem.* **2001**, 3871-3877.

[8] a) B. Breit, *Chem. Commun.* **1996**, 2071-2072; b) B. Breit, R. Winde, K. Harms, *J. Chem. Soc., Perkin Trans. 1* **1997**, 2681-2682; c) B. Breit, R. Winde, T. Mackewitz, R. Paciello, K. Harms, *Chem. Eur. J.* **2001**, *7*, 3106-3121; d) M. Rigo, J. A. W. Sklorz, N. Hatje, F. Noack, M. Weber, J. Wiecko, C. Müller, *Dalton Trans.* **2016**, *45*, 2218-2226.

[9] a) B. Breit, E. Fuchs, *Chem. Commun.* **2004**, 694-695; b) E. Fuchs, M. Keller, B. Breit, *Chem. Eur. J.* **2006**, *12*, 6930-6939; c) G. Märkl, F. Lieb, C. Martin, *Tetrahedron Lett.* **1971**, *12*, 1249-1252.

[10] D. de Montauzon, R. Poilblanc, *J. Organomet. Chem.* **1975**, *93*, 397-404.

[11] A. M. Trzeciak, J. J. Ziółkowski, *Inorg. Chim. Acta* **1985**, *96*, 15-20.

[12] J. G. Leipoldt, S. S. Basson, L. D. C. Bok, T. I. A. Gerber, *Inorg. Chim. Acta* **1978**, *26*, L35-L37.

[13] C. A. Tolman, *J. Am. Chem. Soc.* **1970**, *92*, 2956-2965.

[14] The numbering scheme is different from the organic numbering system for triptycenes. These numbers are used for consistency with the CIF.

[15] A. Buhling, P. C. J. Kamer, P. W. N. M. van Leeuwen, *J. Mol. Catal. A: Chem.* **1995**, *98*, 69-80.

[16] A. Polo, C. Claver, S. Castillón, A. Ruiz, J. C. Bayón, J. Real, C. Mealli, D. Masi, *Organometallics* **1992**, *11*, 3525-3533.

[17] T. Michinobu, E. Tsuchida, H. Nishide, *Bull. Chem. Soc. Jpn.* **2000**, *73*, 1021-1027.

[18] M. R. Talipov, M. M. Hossain, A. Boddeda, K. Thakur, R. Rathore, *Org. Biomol. Chem.* **2016**, *14*, 2961-2968.

[19] O. V. Dolomanov, L. J. Bourhis, R. J. Gildea, J. A. K. Howard, H. Puschmann, *J. Appl. Cryst.* **2009**, *42*, 339-341.

[20] G. M. Sheldrick, *Acta Cryst.* **2015**, *A71*, 3-8.

[21] G. Sheldrick, *Acta Cryst.* **2015**, *C71*, 3-8.

CHAPTER 4. NHC-SUPPORTED DINUCLEAR NICKEL COMPLEXES

4.1 Background

The organometallic chemistry of nickel is rich and diverse.[1] Organonickel complexes find applications in industrial homogenous catalytic processes,[2] and are key intermediates in the action of several enzymes.[3] Among different oxidation states of nickel, nickel(I) has been established as a central immediate state in bioinorganic chemistry[4] and small molecule activation[5] in stoichiometric transformations. One example in bioinorganic chemistry is the nickel(I) cofactor F430 enzyme in methyl-coenzyme M reductase (MCR), which catalyzes the reduction of methyl-coenzyme M (methyl−S−CoM) by coenzyme B (CoB−SH) to form methane and the corresponding heterodisulfide CoB−S−S−CoM during the metabolism of methanogenic archaea.[4d-h]

The interest of synthesis and characterization of nickel hydride complexes has arisen in the study of active sites of nickel-containing enzymes such as MCR,[4g] in developing nickel-catalyzed processes,[6] and in utilizing hydrogen as an energy carrier.[7] In contrast to the well-developed coordination chemistry of Ni(0) and Ni(II), the Ni(I) oxidation state still invites extensive exploration.[8] Reports of well synthesized and characterized nickel(I) hydride complexes were scant until recent years.[9] One of the few examples is phosphine-supported nickel(I) hydride-bridged dimers $[(dippe)NiH]_2$ (dippe = 1,2-bis(diisopropylphosphino)ethane),[9b] which readily undergoes H_2 reductive elimination to

two Ni(0) centers, and shows reactivity with organonitriles by formation of an η^2−(RCN) (R = alkyl and aryl) nitrile complexes before the C−CN bond cleavage.[10]

Electronic-rich and sterically bulky N-heterocyclic carbenes (NHCs) have shown an ability to the support of low-coordinate nickel(I) complexes.[11] As analogs of the widespread existence of multinuclear nickel sites in natural enzymes,[4] several NHC-supported nickel(I) complexes have been isolated as dimeric structures. For example, nickel(I) halide-bridged dimers $[(NHC)Ni(\mu\text{-}X)]_2$ (X= Cl,[11b] Br,[11o] and I[11m]) have been synthesized through comproportionation of Ni(II) halide and Ni(0) in the presence of free NHC. The μ-chloro dinickel cation complex $\{[(NHC)Ni(CO)]_2(\mu\text{-}Cl)]\}[BAr^F{}_4]$ ($BAr^F{}_4$ = tetrakis[3,5-bis(trifluoromethyl)phenyl]borate)[11p] has been synthesized via diphenylcarbene transfer from the dinickel carbene-bridged complex $\{[(NHC)Ni](\mu\text{-}Cl)(\mu\text{-}CPh_2)]\}[BAr^F{}_4]$ to carbon monoxide, while the μ-bromo dinickel cation complex $\{[(NHC)Ni(PPh_3)]_2(\mu\text{-}Br)]\}[BAr^F{}_4]$[11q] has been synthesized via halide abstraction from $[(NHC)Ni(PPh_3)Br]$ monomer with $NaBAr^F{}_4$. In analogy to the synthesis of phosphine-supported nickel(I) hydride dimers,[9a, 9b] the synthesis of an NHC-supported nickel(I) hydride dimer was attempted through the reaction of lithium triethylborohydride with $[(IDipp)Ni(\mu\text{-}Cl)]_2$,[11b] but led instead to the isolation of a dimeric Ni(0) complex, $[(IDipp)Ni^0]_2$, presumably through the fast reductive elimination of H_2 from an unobserved nickel(I) hydride dimer.[12] The $[(IDipp)Ni^0]_2$ could also be isolated through reaction of $[(IDipp)Ni(\mu\text{-}Cl)]_2$ with sodium *tert*-butoxide followed by triethoxysilane. In the solid-state structure, each nickel center interacts in η^6-fashion with an *N*-aryl group of the neighboring nickel's NHC, with a Ni•••Ni distance of 3.568(2) Å.

In this chapter, we initially attempted isolation of a stable (NHC)Ni(I) hydride-bridged complex, and succeeded in synthesis and characterization of the NHC-supported μ-hydrido dinickel(I) complexes {[(IDipp)Ni]$_2$(μ-H)}[X] (**13**[X], X = OTf or NTf$_2$, IDipp = 1,3-bis(2,6-diisopropylphenyl)imidazol-2-ylidene) with symmetric linear structure and a Ni•••Ni distance of 3.0076(5) Å. Whereas a (phosphine)nickel(I) hydride dimer [(dippe)NiH]$_2$[9b, 10] reductively eliminates dihydrogen to form Ni(0) centers, which then oxidatively add C–CN bonds, the salts of μ-hydrido dinickel(I) cation **13**[X] cleave C–CN bonds with concomitant formation of alkane, accompanied by a nickel(II) cyanide molecular square complex [(IDipp)Ni(CN)$_2$]$_4$ (**14**), the Ni(I)/Ni(0) mixed-valence radical complexes [(IDipp)Ni]$_2$[X] (**15**[X]), and the homoleptic nickel(I) complexes [(IDipp)$_2$Ni][X] (**16**[X]).

4.2 Results and Discussion

4.2.1 Synthesis of μ-hydrido dinickel(I) monocation complexes

4.2.1.1 Synthesis and characterization of {[(IDipp)Ni]$_2$(μ-H)}[OTf] (**13**[OTf])

The reaction of [(IDipp)Ni(μ-Cl)]$_2$[11b] with sodium *tert*-butoxide in a 1:2 ratio, followed by the addition of trimethylsilyl trifluoromethanesulfonate and pinacolborane, resulted in the isolation of the reddish-brown product {[(IDipp)Ni]$_2$(μ-H)}[OTf] (**13**[OTf]) in 46% yield (Scheme 4.1). The hydride resonance is observed at δ –25.4 ppm in the ^{1}H NMR spectrum. The *para*-H on one of the two sets of *N*-aryl in each IDipp shifts upfield to δ 4.79 ppm (t, J = 7.2 Hz) from normal aromatic resonances, due to the shielding from diatropic ring current as they poise over the centroid of *N*-aryl in IDipp on neighbor nickel.

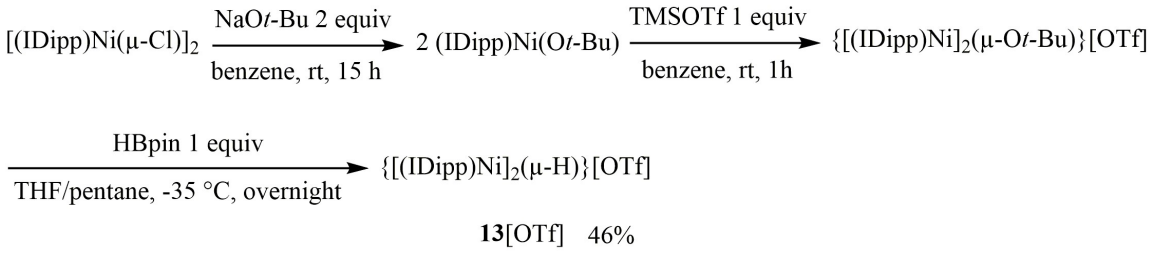

Scheme 4.1. Synthesis of {[(IDipp)Ni]$_2$(μ-H)}[OTf] (**13**[OTf]).

Neutron diffraction studies suggest that most dinuclear metal complexes with a single M−H−M linkage are bent at the hydride.[13] One of the rare examples of a linear M−H−M linkage in transition metal hydride complexes is a μ-hydrido Ni(I)/Ni(II) complex [(dippm)NiBr]$_2$(μ-H) (dippm = 1,2-bis(diisopropylphosphino)methane), with a Ni−H−Ni angle of 177.9(10)°.[14]

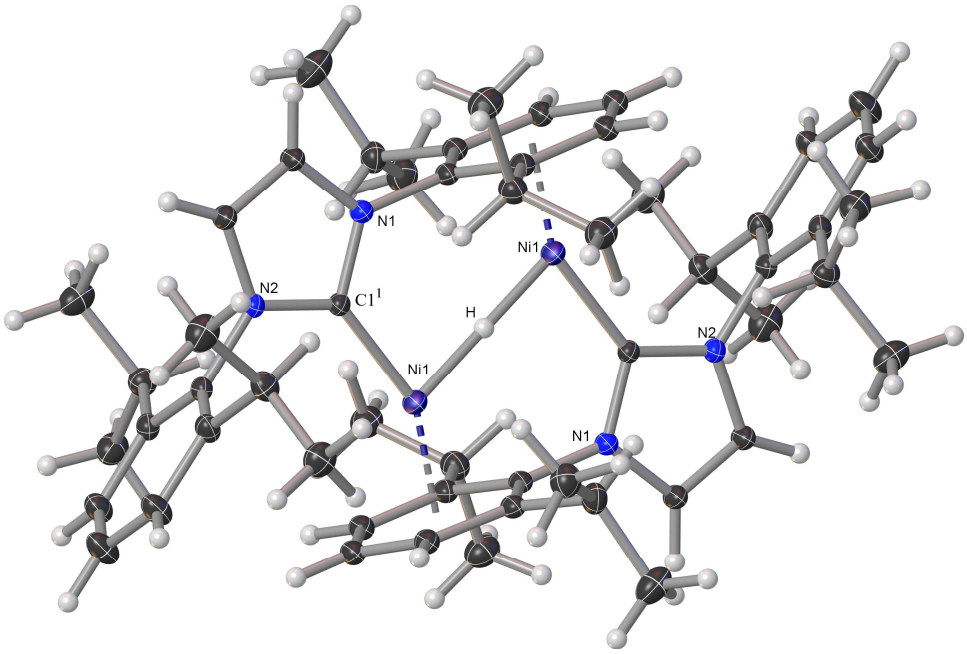

Figure 4.1. Solid-state structure of {[(IDipp)Ni]$_2$(μ-H)}[OTf] (**13**[OTf]), 50% probability ellipsoids. Anion omitted for clarity. Selected interatomic distances (Å) and angles (°): Ni(1)–H 1.5038(3), Ni(1)–C(1^1) 1.8880(18); Ni(1)–H–Ni(1) 180, C(1^1)–Ni(1)–H 84.85(5).

The solid-state structure of **13**[OTf] (Figure 4.1) features a symmetric linear hydride-bridged geometry with two identical Ni−H bond distances of 1.5038(3) Å and a Ni−H−Ni bond angle of exactly 180°. The presence of the hydride was indicated by a charge density maximum located at the midpoint of the nickel−nickel vector. The Ni−H−Ni bond in **13**[OTf] can be considered as an analog of the linear 3-center, 4-electrons $[F-H-F]^-$ bonding model.[13a] The η^6 interaction of the nickel to the *N*-aryl group of IDipp ligand on its neighbor nickel stabilizes the linear geometry.

4.2.1.2 Synthesis and characterization of $\{[(IDipp)Ni]_2(\mu\text{-}H)\}[NTf_2]$ (**13**[NTf_2])

The μ-hydrido dinickel(I) cation salt $\{[(IDipp)Ni]_2(\mu\text{-}H)\}[NTf_2]$ (**13**[NTf_2]) was synthesized by reaction of [(IDipp)Ni^0(benzene)][15] with trifluoromethanesulfonimide in a 2:1 ratio, with an isolated yield of 82%, or of $[(IDipp)Ni^0]_2$[12] with trifluoromethanesulfonimide in a 1:1 ratio, with an isolated yield of 85% (Scheme 4.2). Reaction of [(IDipp)Ni^0(benzene)][15] with trifluoromethanesulfonimide in a 1:1 stoichiometry ratio resulted in some protonation of ligand to form the imidazolium salt (IDipp)H[NTf_2] instead of **13**[NTf_2].

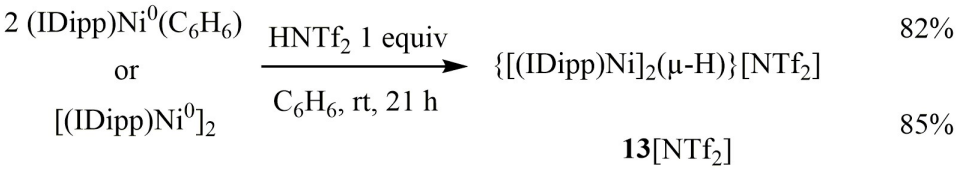

Scheme 4.2. Synthesis of $\{[(IDipp)Ni]_2(\mu\text{-}H)\}[OTf]$ (**13**[NTf_2]).

4.2.2 Reactivity of μ-hydrido dinickel(I) monocation complexes

4.2.2.1 Reactivity of {[(IDipp)Ni]$_2$(μ-H)}[OTf] (**13**[OTf]) with acetonitrile

The reaction of **13**[OTf] in THF-d_8 solution with acetonitrile in a J. Young tube changed the solution color from reddish-brown to brownish-yellow in one day at room temperature. ^{1}H NMR spectroscopy indicated the formation of methane as a singlet at δ 0.19 ppm in THF-d_8.[16] Alkane generation from the nitrile by (μ-hydrido)dinickel(I) implied the formation of a cyanide-bridged dinickel(I) cation, which was not observed. Disproportionation of this species, which would afford both Ni(II) and Ni(0), led to the isolation of a diamagnetic NHC-supported Ni(II) dicyanide complex [(IDipp)Ni(CN)$_2$]$_4$ (**14**) (Figure 4.2) (Scheme 4.3a). The solid-state structure of **14** exhibited a molecular square with disordered bridging cyanide groups. Reaction of **13**[OTf] with acetonitrile-d_3 in THF-d_8 solution at room temperature led to formation of methane-d_3, observed as a septet at δ 0.14 ppm ($^2J_{H\text{-}D}$ = 2.1 Hz) (Scheme 4.3b).[17]

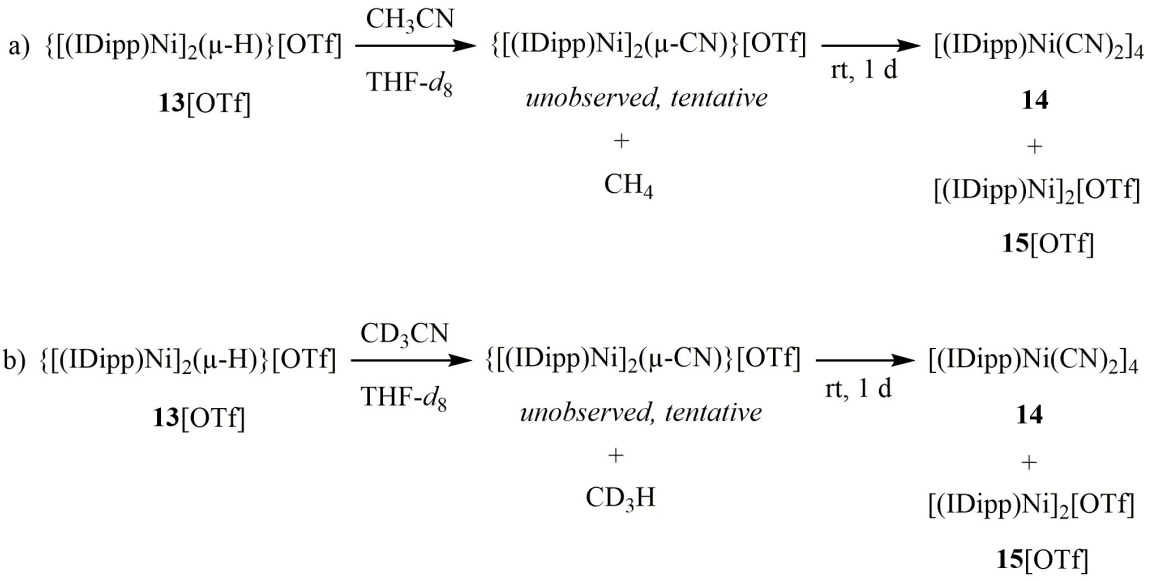

Scheme 4.3. Reaction of {[(IDipp)Ni]$_2$(μ-H)}[OTf] (**13**[OTf]) with acetonitrile.

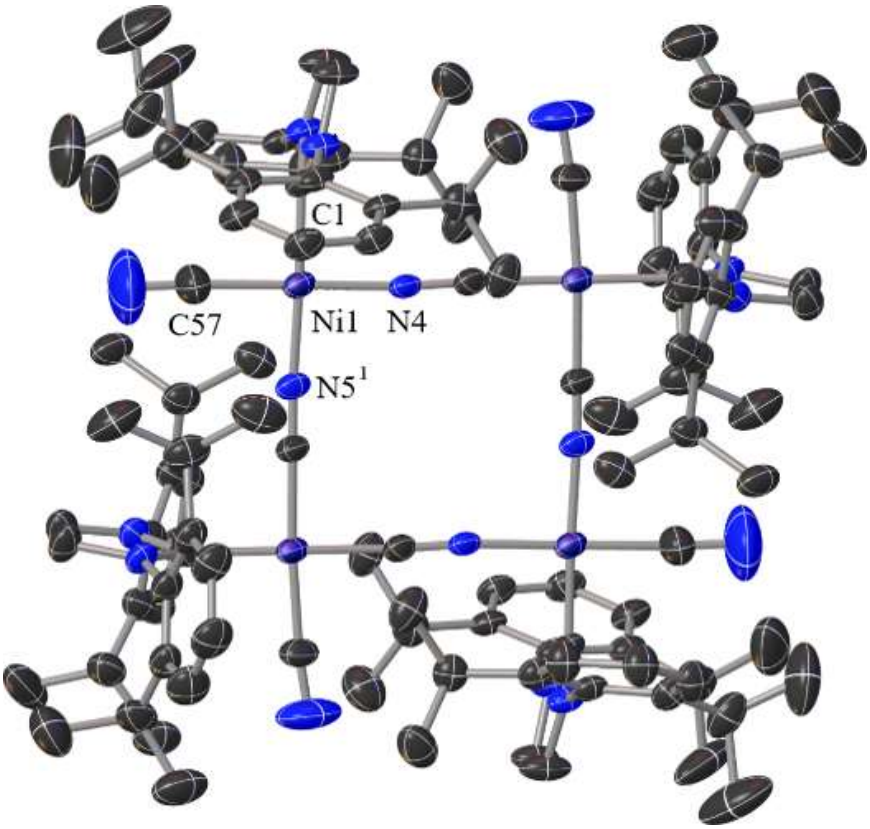

Figure 4.2. Solid-state structure of $[(IDipp)Ni(CN)_2]_4$ (**14**), 50% probability ellipsoids. Calculated hydrogen atoms are omitted for clarity. Selected interatomic distances (Å) and angles (°): Ni(1)–N(4) 1.886(7), Ni(1)–N(5^1) 1.868(6), Ni(1)–C(57) 1.877(9), Ni(1)–C(1) 1.871(6); N(5^1)–Ni(1)–N(4) 91.5(2), N(5^1)–Ni(1)–C(57) 87.7(3), C(1)–Ni(1)–C(57) 90.3(3), C(1)–Ni(1)–N(4) 90.4(3).

4.2.2.2 Reactions of $\{[(IDipp)Ni]_2(\mu\text{-}H)\}[NTf_2]$ (**13**$[NTf_2]$) with longer-chain nitriles

The reactions of **13**$[NTf_2]$ with longer-chain alkyl nitriles were more complicated than those with acetonitrile. Dealkylation occurred for the reaction of **13**$[NTf_2]$ with primary and secondary nitriles to form the corresponding alkanes, accompanied by competitive β-hydride elimination from nickel alkyl intermediates, and isomerization of nitriles (Scheme 4.4a). The results are summarized in Table 4.1.

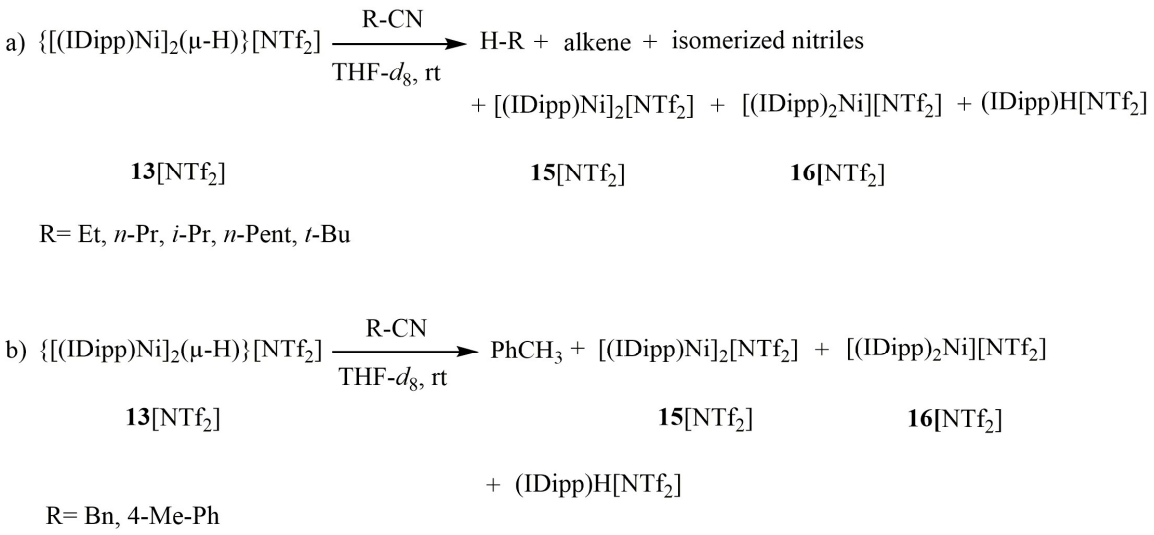

Scheme 4.4. Reaction of {[(IDipp)Ni]$_2$(μ-H)}[NTf$_2$] (**13**[NTf$_2$]) with longer nitriles.

The reaction mixture changed from reddish-brown to brownish-yellow in color when **13**[NTf$_2$] was fully converted. The longer the alkyl chain of the nitrile, the longer the time for complete consumption of **13**[NTf$_2$] as judged by ^{1}H NMR spectroscopy (Table 4.1 Entries 1-4). No reaction occurred between **13**[NTf$_2$] and the tertiary nitrile pivalonitrile, even after 1 week (Table 4.1 Entry 5). Instead of forming the diamagnetic complex [(IDipp)Ni(CN)$_2$]$_4$ (**14**) observed in the reaction with acetonitrile, reactions with longer-chain alkyl nitriles led to the isolation of two paramagnetic complexes, a Ni(I)/Ni(0) radical complex [(IDipp)Ni]$_2$[NTf$_2$] (**15**[NTf$_2$]) and a homoleptic bis-NHC nickel(I) complex [(IDipp)$_2$Ni][NTf$_2$] (**16**[NTf$_2$]), which were identified and characterized in Section *4.2.3* and *4.2.4*, respectively. Decomposed products such as imidazolium salt and other unidentified species were also found during the reactions with longer-chain alkyl nitriles. Reaction of **13**[NTf$_2$] with phenylacetonitrile at room temperature formed toluene, together with **15**[NTf$_2$], **16**[NTf$_2$], imidazolium salt and other unidentified species (Scheme 4.4b, Table 4.1 Entry 6). In contrast to the reaction of **13**[NTf$_2$] with alkyl nitriles, reaction of

13[NTf_2] with *p*-tolunitrile proceeded quickly at room temperature, leading after 30 minutes to the formation of only 2% toluene and an unidentified species, possibly an η^2–(RCN) (R = 4-methylphenyl) complex (Scheme 4.4b, Table 4.1 Entry 7).

Table 4.1. Reaction of {[(IDipp)Ni]$_2$(μ-H)}[NTf_2] (**13**[NTf_2]) with longer nitriles R–CN.[a]

Entry	R (Conv %)	*t*	H–R (%)	Alkene (%)	Nitrile (%)
1	Et (89)	2 d	ethane (12)[b]	ethylene (2)[b]	-
2	*n*-Pr (80)	4 d	propane (15)[b]	propene (10)[b]	*i*-Pr-CN (6)
3	*i*-Pr (72)	4 d	propane (12)[b]	propene (17)[b]	*n*-Pr-CN (7)
4	*n*-Pent (98)	7 d	pentane (11)	1-pentene (0.1), *trans*-2-pentene (19)	*sec*-Pent-CN (6)
5	*t*-Bu (0)	N. R.	-	-	-
6	Bn (100)	3 d	toluene (4)	-	-
7	4-MePh (100)	0.5 h	toluene (2)	-	-

[a] Reactions were conducted in THF-d_8 solution at room temperature. Conversion and yield (%) were calculated using 1,4-dimethoxybenzene as standard. [b] Yield (%) refers to the proton resonance integration of that portion of gaseous product present in THF-d_8 solution.

4.2.2.3 Hydrogen abstraction from {[(IDipp)Ni]$_2$(μ-H)}[NTf_2] (**13**[NTf_2])

Hydrogen atom transfer reactions are important in both chemistry and biology.[18] The abstraction of hydrogen from **13**[NTf_2] was attempted through the reaction with the

stable aryloxy radical 2,4,6-tri-*tert*-butylphenoxyl in a 1:1 ratio, which led to the formation of 2,4,6-tri-*tert*-butylphenol and $[(IDipp)Ni]_2[NTf_2]$ (**15**$[NTf_2]$), accompanied by $[(IDipp)_2Ni][NTf_2]$ (**16**$[NTf_2]$) and imidazolium salt (Scheme 4.5).

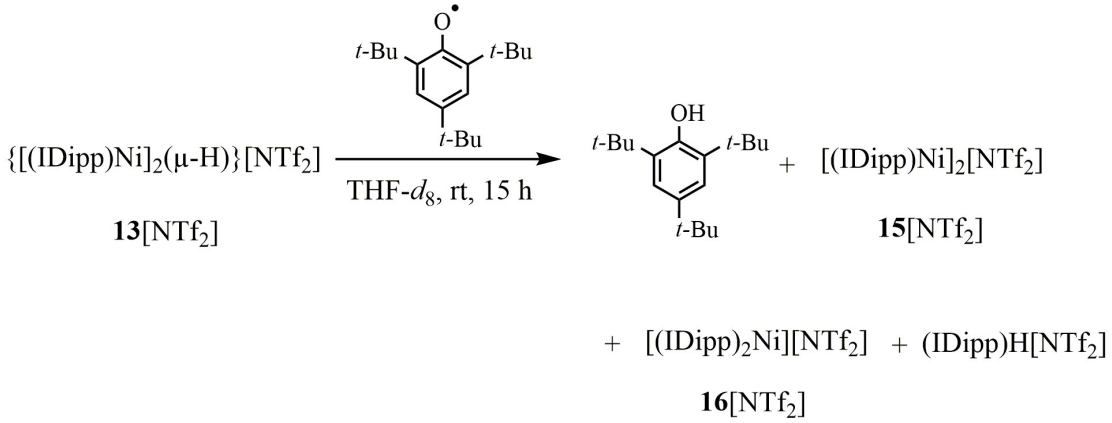

Scheme 4.5. Hydrogen abstraction from $\{[(IDipp)Ni]_2(\mu\text{-}H)\}[NTf_2]$ (**13**$[NTf_2]$).

4.2.2.4 Reactivity of $\{[(IDipp)Ni]_2(\mu\text{-}H)\}[OTf]$ (**13**[OTf]) with carbon monoxide

The μ-hydrido dinickel cation complex **13**[OTf] reacted with 1 atm carbon monoxide at room temperature, with rapid formation of $(IDipp)Ni(CO)_3$, nickel tetracarbonyl (the resonance at δ 192.40 ppm observed in the ^{13}C NMR spectrum matched the reported value[19]) and imidazolium salt (Scheme 4.6).

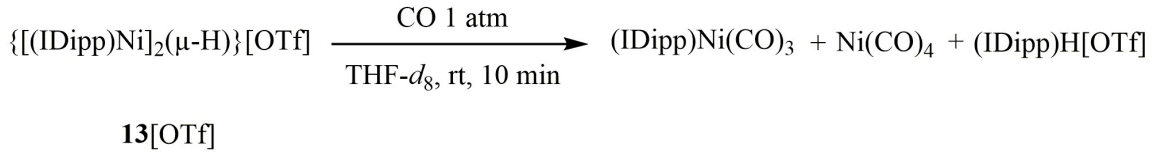

Scheme 4.6. Reaction of $\{[(IDipp)Ni]_2(\mu\text{-}H)\}[OTf]$ (**13**[OTf]) with carbon monoxide.

4.2.3 Synthesis of dinuclear nickel(I)/(0) complexes

Inspired by the formation of the paramagnetic NHC-supported dinuclear Ni(I)/Ni(0) complex [(IDipp)Ni]$_2$[X] (**15**[X], X = OTf and NTf$_2$) during the reaction of μ-hydrido dinickel cation complexes {[(IDipp)Ni]$_2$(μ-H)}[X] (**13**[X], X = OTf and NTf$_2$) with nitriles, we undertook the preparative-scale synthesis of the radical complex salts **15**[X], through either the comproportionation of Ni(II) and Ni(0) or the one-electron oxidation of two Ni(0) centers.

4.2.3.1 Comproportionation of Ni(II) and Ni(0)

Comproportionation reactions of Ni(II) and Ni(0) were conducted using different molar ratios of nickel(II) trifluoromethanesulfonate, [(IDipp)Ni^0(C$_6$H$_6$)] and IDipp. A summary is listed in Table 4.2.

Table 4.2. Comproportionation reactions of Ni(II) and Ni(0).[a]

Entry	Ni^{II}/Ni^0/IDipp	**15**[OTf] (Conv %)	**16**[OTf]	(IDipp)H[OTf]
1	1:4:0	product (18)[b]	-	-
2	1:3:1	product (13)[b]	-	-
3	1:1:1	product	product	product
4	3:1:3	-	product	product

[a] Ni^{II}(OTf)$_2$, [(IDipp)Ni^0(C$_6$H$_6$)] and IDipp were stirred in THF for 16 h. [b] isolated yield.

When the ratio of Ni(II)/Ni(0) was 1:3 (Scheme 4.7, Table 4.2 Entry 2) or even 1:4 (Table 4.2 Entry 1), the only isolated salt was the mono-cationic, dinuclear Ni(I)/Ni(0) complex $[(IDipp)Ni]_2[OTf]$ (**15**[OTf]).

$$Ni^{II}(OTf)_2 + 3\ (IDipp)Ni^0(C_6H_6) + IDipp \xrightarrow[rt,\ 16\ h]{THF} 2\ [(IDipp)Ni]_2[OTf]$$

15[OTf] 13%

Scheme 4.7. Synthesis of dinuclear Ni(I)/Ni(0) complex $[(IDipp)Ni]_2[OTf]$ (**15**[OTf]).

The ^1H NMR spectrum of **15**[OTf] displayed a series of broad resonances, suggesting paramagnetism, and EPR spectroscopy verified the presence of an unpaired electron in the complex. The solid-state structure of **15**[OTf], shown in Figure 4.3, matches closely that of the dinuclear Ni(I)/Ni(0) radical complex isolated from reactions of μ-hydrido dinickel cation complexes with longer-chain alkyl nitriles. In the solid-state structure, **15**[OTf] is inferred to have a nickel–nickel half-bond with the distance of 2.6356(6) Å, in analogy to the reported cobalt dimer radical cations $[(L)Co(CO)_2]_2^+$ (L = fulvalenediyl, cyclopentadienyl and pentamethylcyclopentadiene).[20] The isolated yields were low due to the competitive reaction of homoleptic bis-NHC nickel(0) $[(IDipp)_2Ni^0]$ formation. When the ratio of Ni(II)/Ni(0) increased, formation of **15**[OTf] decreased; however, formation of homoleptic bis-NHC nickel(I) complex $[(IDipp)_2Ni][OTf]$ (**16**[OTf]) and imidazolium salt increased (Table 4.2, Entries 3 and 4).

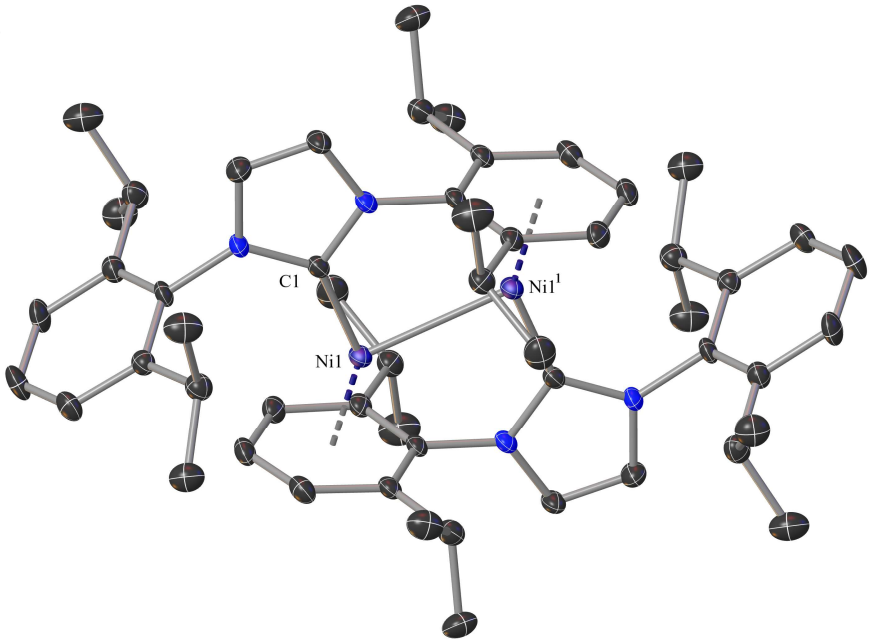

Figure 4.3. Solid-state structure of [(IDipp)Ni]$_2$[OTf] (**15**[OTf]), 50% probability ellipsoids. Calculated hydrogen atoms and anion omitted for clarity. Selected interatomic distances (Å) and angles (°): Ni(1)–Ni(1^1), 2.6356(6), Ni(1)–C(1) 1.889(3); C(1)–Ni(1)–Ni(1^1) 89.41(8).

4.2.3.2 One-electron oxidation of two Ni(0) centers

Oxidation of [(IDipp)Ni^0(C_6H_6)] was conducted using 0.5 equivalent of oxidant at room temperature. The results are given in Table 4.3. Decreasing the strength of the oxidant led to cleaner formation of dinuclear Ni(I)/Ni(0) monocation complex [(IDipp)Ni]$_2$[X] (**15**[X], X = OTf, BF_4 or PF_6), with less homoleptic byproduct [(IDipp)$_2$Ni] [X] (**16**[X], X = OTf, BF_4 or PF_6). The reaction of [(IDipp)Ni^0(C_6H_6)] with triphenylcarbenium tetrafluoroborate afforded [(IDipp)Ni]$_2$[BF_4] (**15**[BF_4]) in 57% isolated yield.

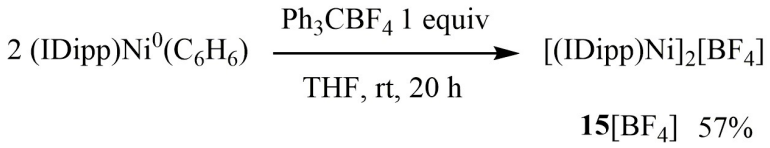

Scheme 4.8. Synthesis of dinuclear Ni(I)/Ni(0) complex [(IDipp)Ni]$_2$[BF$_4$] (**15**[BF$_4$]).

Table 4.3. One-electron oxidation of two Ni(0) centers.[a]

Entry	Oxidant	**15**[X][b]	**16**[X][b]
1	AgOTf	minor product	major product
2	Cp$_2$FeX[c]	major product	minor product
3	Ph$_3$CBF$_4$	sole product	-

[a] Reactions were conducted using [(IDipp)Ni^0(C$_6$H$_6$)] and oxidants in 2:1 ratio in THF solution for 20 h. [b] [X] according to the corresponding anions. [c] X = BF$_4$ and PF$_6$.

4.2.4 Synthesis of homoleptic nickel(I) complex

One example of a homoleptic bis-NHC nickel(I) complex with an outer-sphere anion in literature was [(6Mes)$_2$Ni][Br] (6Mes = 1,3-bis(2,4,6-trimethylphenyl)-3,4,5,6-tetrahydropyrimidin-2-ylidene), synthesized via addition of one equivalent of 6Mes to the three-coordinate Ni(I) precursor [Ni(6Mes)(PPh$_3$)(Br)].[21] I synthesized the homoleptic bis-NHC nickel(I) complex [(IDipp)$_2$Ni][BF$_4$] (**16**[BF$_4$]) through oxidation of [(IDipp)Ni^0(C$_6$H$_6$)] by ferrocenium tetrafluoroborate in the presence of one equivalent of free IDipp (Scheme 4.9). The white product **16**[BF$_4$] was isolated as an air-stable complex. Its broad ^{1}H NMR resonances were consistent with its paramagnetism. The solid-state

structure of **16**[BF_4] (Figure 4.4) shows the near-linear geometry at nickel, which matches that of the homoleptic nickel(I) complex isolated from reactions of μ-hydrido dinickel cation complex with longer-chain alkyl nitriles.

$$(IDipp)Ni^0(C_6H_6) + IDipp \xrightarrow[rt,\ 2\ h]{THF} Ni(IDipp)_2 \xrightarrow[THF,\ rt,\ 4\ h]{Cp_2FeBF_4} [(IDipp)_2Ni][BF_4]$$

16[BF_4] 97%

Scheme 4.9. Synthesis of homoleptic nickel(I) complex [$(IDipp)_2Ni$][BF_4] (**16**[BF_4]).

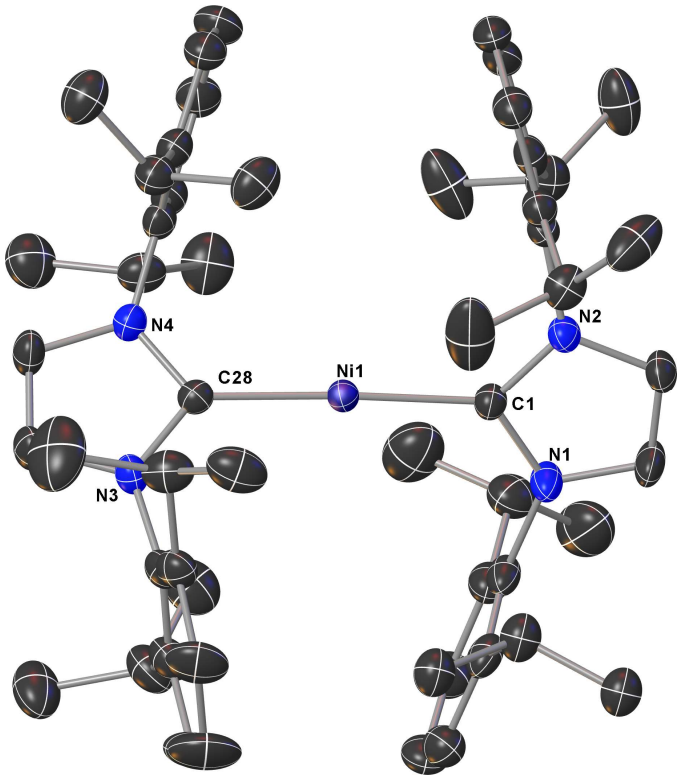

Figure 4.4. Solid-state structure of [$(IDipp)_2Ni$][BF_4] (**16**[BF_4]). 50% probability ellipsoids. Calculated hydrogen atoms and anion omitted for clarity. Selected interatomic distances (Å) and angles (°): Ni(1)–C(1), 1.936(4), Ni(1)–C(28), 1.933(4); C(1)–Ni–C(28), 176.85(14).

4.2.5 Reactivity of [(IDipp)Ni^0(C$_6$H$_6$)]

4.2.5.1 Reactivity of [(IDipp)Ni^0(C$_6$H$_6$)] with acetonitrile

To compare the reactivity of {[(IDipp)Ni]$_2$(μ-H)}[OTf] (**13**[OTf]) with acetonitrile, I conducted the reaction of [(IDipp)Ni^0(C$_6$H$_6$)] with acetonitrile in THF-d_8 (Scheme 4.10a). The red product was determined to be a η^2−(MeCN) complex as the observed ^{1}H and ^{13}C NMR resonances matched the reported value for that isolated through the reaction of bis(1,5-cyclooctadiene)nickel(0), IDipp and acetonitrile in 1:1:1 stoichiometry ratio in C$_6$D$_6$ solution (Scheme 4.10b).[22]

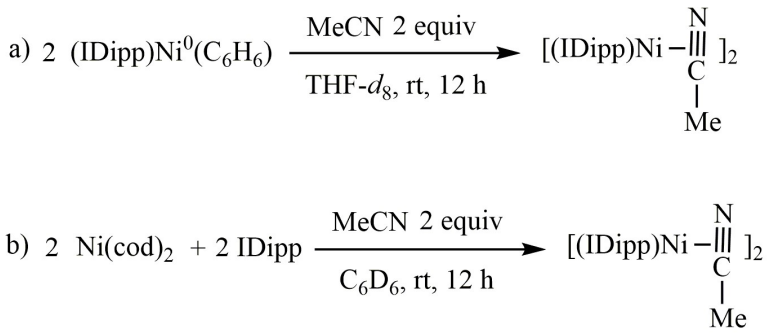

Scheme 4.10. Reaction of [(IDipp)Ni^0(C$_6$H$_6$)] with acetonitrile.

4.2.5.2 Reactivity of [(IDipp)Ni^0(C$_6$H$_6$)] with hexafluorobenzene

NHC-supported nickel(0) complexes have been studied in the C−F bond activation of hexafluorobenzene to form Ni(II) oxidative addition products (Scheme 4.11a).[23] The homoleptic nickel(0) complex [(IDipp)$_2$Ni^0] has been reported to react with aryl chloride to form the one-electron oxidation product [(IDipp)$_2$Ni^{I}(Cl)] instead of the oxidative addition product [(IDipp)$_2$Ni^{II}(Ph)(Cl)], possibly due to the steric bulk of IDipp ligand around nickel center.[11c] Interestingly, the reaction of [(IDipp)Ni^0(C$_6$H$_6$)] with

hexafluorobenzene in THF-d_8 led to the unexpected formation of a yellow [(IDipp)Ni(μ-C_6F_5)]$_2$ (**17**) complex in 50% yield (Scheme 4.11b) instead of the direct oxidative addition product nickel(II)(aryl) fluoride, possibly accompanied by an unobserved [(IDipp)Ni^{I}(F)] formation.

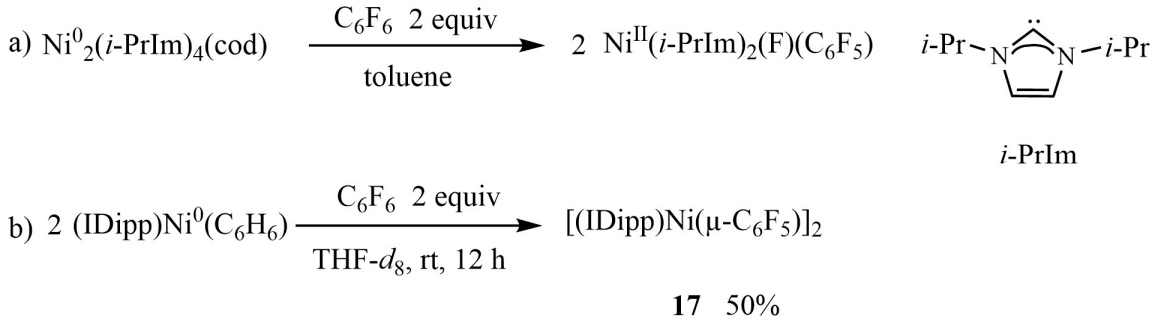

Scheme 4.11. Reaction of [(IDipp)Ni^0(C_6H_6)]with hexafluorobenzene.

The C−F bond activation in C_6F_6 at the [(IDipp)Ni^0] moiety is proposed to proceed through a pre-coordination of C_6F_6 ligand in η^2-fasion at the nickel center, as the ^{19}F NMR spectrum of the in-situ reaction in Scheme 4.11b shows one broad resonance at –173.60 ppm, consistent with those of the reported fluxional η^2-coordinated C_6F_6 at [(*i*-PrIm)$_2$Ni^0] moiety (δ_F –169.2 ppm)[23a] or phosphine-supported nickel [(dtbpe)Ni^0] moiety (δ_F –166.9 ppm).[24]

The solid-state structure of **17** is shown in Figure 4.5. The diamagnetic aryl-bridged Ni(I) dimer has a Ni•••Ni distance of 2.4701(8) Å. Each 16-electron nickel center is asymmetrically bridged by two aryls, with Ni(1)–C(28)–C(31) angles of 165.24(13)° and Ni(1)–C(28^1)–C(31^1) angles of 117.34(13)°.

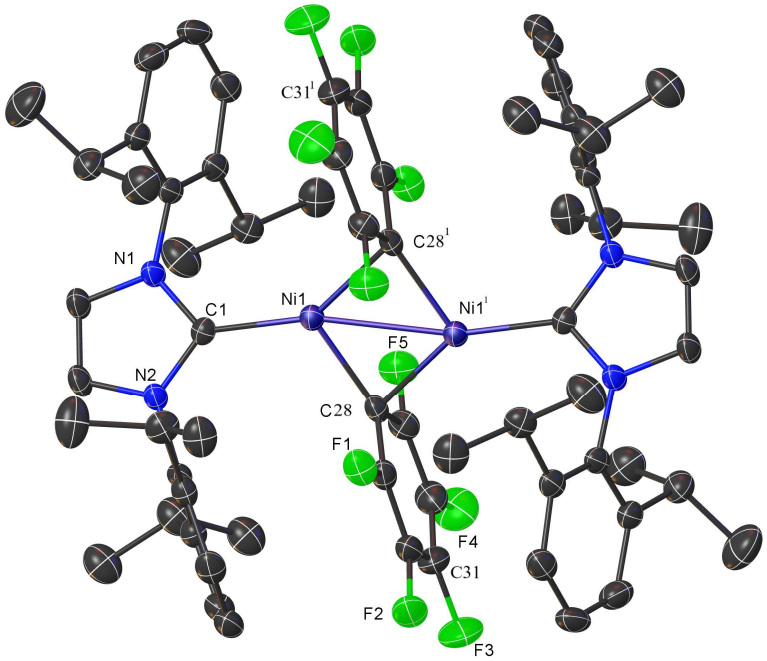

Figure 4.5. Solid-state structure of [(IDipp)Ni(μ-C_6F_5)]$_2$ (**17**), 50% probability ellipsoids. Calculated hydrogen atoms are omitted. Selected interatomic distances (Å) and angles (°): Ni(1)–Ni(1^1) 2.4701(8), C(1)–Ni(1) 1.929(3), C(28)–Ni(1) 1.937(3), C(28)–Ni(1^1) 2.012(3); Ni(1)–C(28)–Ni(1^1) 77.40(12), Ni(1)–C(28^1)–Ni(1^1) 77.40(12), C(1)–Ni(1)–C(28) 112.29(13), C(1)–Ni(1)–C(28^1) 145.05(12), Ni(1)–C(28)–C(31) 165.24(13), Ni(1)–C(28^1)–C(31^1) 117.34(13).

4.3 Conclusion

Unusual linear μ-hydrido dinickel complexes have been synthesized using NHC supporting ligands. These complexes transformed nitriles to the corresponding alkanes via hydrodecyanation. This process was accompanied by the formation of a nickel(II) cyanide complex in reactions of acetonitrile, and of novel dinuclear Ni(I)/Ni(0) complexes in reactions of longer-chain alkyl nitriles. The dinuclear Ni(I)/Ni(0) complexes could be synthesized independently through the comproportionation of Ni(II) and Ni(0), or by one-electron oxidation of two Ni(0) centers.

4.4 Experimental

4.4.1 General considerations

Unless otherwise indicated, manipulations were carried out in an MBraun glovebox under an inert atmosphere of nitrogen, or in sealable glassware on a Schlenk line under an atmosphere of argon. Glassware and magnetic stir bars were dried in a ventilated oven at 160 °C and allowed to cool under vacuum.

Tetrahydrofuran (THF, EMD Millipore Omnisolv) and toluene (EMD Millipore Omnisolv) were sparged with ultra-high purity argon (NexAir) for 45 minutes prior to first use and dried using an MBraun solvent purification system, transferred to Schlenk flasks, degassed using three freeze-pump-thaw cycles, and stored under nitrogen or argon. Anhydrous benzene (EMD Millipore Drisolv) and anhydrous pentane (EMD Millipore Drisolv), both sealed under a nitrogen atmosphere, were used as received and stored in a glovebox. Tetrahydrofuran (THF, EMD Millipore Omnisolv) and toluene (EMD Millipore Omnisolv) anhydrous benzene (EMD Millipore Drisolv) were further dried over sodium benzophenone ketyl, degassed by successive freeze-pump-thaw cycles and transferred under vacuum to an oven-dried resealable flask. Tap water was purified in a Barnstead International automated still prior to use. Acetonitrile (EMD Millipore OmniSolv) and acetonitrile-d_3 (Cambridge Isotope Labs) were dried by stirring overnight with calcium hydride (Alfa-Aesar, coarse powder), degassed by successive freeze-pump-thaw cycles, and vacuum-transferred into oven-dried resealable Schlenk flasks. Benzene-d_6 (Cambridge Isotope Laboratories) and tetrahydrofuran-d_8 (Cambridge Isotope Laboratories) was dried over sodium benzophenone ketyl, degassed by successive freeze-pump-thaw cycles and

vacuum-transferred into oven-dried resealable flasks. Potassium *tert*-butoxide (Alfa Aesar), sodium *tert*-butoxide (TCI America), trimethylsilyl trifluoromethanesulfonate (Sigma-Aldrich), 4,4,5,5-tetramethyl-1,3,2-dioxaborolane(Sigma-Aldrich), bis(1,5-cyclooctadiene)nickel(0) (Strem Chemicals), nickel(II) chloride ethylene glycol dimethyl ether complex (Strem Chemicals), nickel(II) trifluoromethanesulfonate (Sigma-Aldrich), ferrocenium tetrafluoroborate (Sigma-Aldrich), ferrocenium hexafluorophosphate (Sigma-Aldrich), silver trifluoromethanesulfonate (Alfa Aesar), triphenylcarbenium tetrafluoroborate (Alfa Aesar), and potassium ferricyanide (Sigma-Aldrich) were used as received and stored in a glove box. Propionitrile (Sigma-Aldrich), *n*-butyronitrile (Sigma-Aldrich), isobutyronitrile (TCI America), pivalonitrile (BeanTown Chemical), hexanenitrile (Sigma-Aldrich), phenylacetonitrile (Alfa Aesar), *p*-tolunitrile (Acros Organics), trifluoromethanesulfonimide (Matrix Scientific) and hexafluorobenzene (Sigma-Aldrich) were degassed by three freeze-pump-thaw cycles prior to use. 2,6-Diisopropylaniline (Sigma-Aldrich), acetic acid (Alfa Aesar), paraformaldehyde (Alfa Aesar), chlorotrimethylsilane (Sigma-Aldrich), glyoxal 40% w/w aqueous solution (Alfa Aesar), methanol (BDH), ethyl acetate (BDH), sodium hydroxide (EMD), sodium metal (Alfa Aesar), benzophenone (Alfa Aesar), calcium hydride (Alfa Aesar), nitrogen (NexAir), carbon monoxide (Sigma-Aldrich), hydrogen (both industrial and ultra-high purity grades, NexAir) and argon (both industrial and ultra- high purity grades, NexAir) were used as received.

IDipp·HCl,[25] IDipp,[26] $[(IDipp)Ni(\mu\text{-}Cl)]_2$[11b] and 2,4,6-tri-*tert*-butylphenoxyl radical[27] were prepared according to literature protocols and characterized by ^1H NMR spectroscopy. $[(IDipp)Ni^0(benzene)]$[15] was prepared according to literature protocols with

modifications, and was characterized by ^{1}H NMR spectroscopy (procedures in Section 4.4.2.2.). The stock solution of 1,4-dimethoxybenzene in THF-d_8 (0.100 g/mL) used in Section 4.2.2.2 was prepared by dissolving 0.100 g 1,4-dimethoxybenzene in 1000 μL THF-d_8.

^{1}H and ^{19}F NMR spectra were obtained using a Varian Vx 300 and Vx 400 MHz spectrometer, and ^{13}C NMR was obtained using a Bruker Avance IIIHD 700 MHz spectrometer. ^{1}H and ^{13}C NMR chemical shifts were referenced with respect to solvent signals[16] and reported relative to tetramethylsilane. Chemical shifts δ are reported in ppm.

Fourier-transform infrared spectra were collected using microcrystalline samples on a Bruker Alpha-P infrared spectrometer equipped with an attenuated total reflection (ATR) platinum diamond reflector accessory in a glovebox. UV-vis absorption spectra were acquired using a Varian Cary 50 spectrophotometer. Unless otherwise noted, all electronic absorption spectra were recorded at ambient temperatures in 1-cm sealed quartz cells. Samples for UV-vis absorption spectra were prepared under N_2 atmosphere in a glovebox with concentration of 5 x 10^{-5} M substrate in THF solution.

Samples for EPR measurements were prepared under N_2 atmosphere in a glovebox. The liquid sample was prepared by dissolving 0.004 g solid in 200 μL of dry THF and transferring to an EPR tube sealed in a glovebox. The solid sample was prepared by adding 0.004 g crystals into the EPR tube under N_2 atmosphere. The X-band continuous wave (CW) EPR measurement were performed on a Bruker EMX spectrometer with 9.854 GHz at 298 K for liquid sample and 9.873 GHz for solid-state sample.

4.4.2 Synthetic procedures

4.4.2.1 {[(IDipp)Ni]$_2$(μ-H)}[OTf] (**13**[OTf])

In the glovebox, [(IDipp)Ni(μ-Cl)]$_2$ (0.090 g, 0.093 mmol) and sodium *tert*-butoxide (0.018 g, 0.19 mmol) were dissolved in benzene (5 mL), and the solution was stirred at room temperature for 15 h. The color changed from orange to brownish-yellow, then brownish-green over the reaction period. The solution was filtered through Celite and trimethylsilyl trifluoromethanesulfonate (0.0209 g, 17.0 μL, 0.0939 mmol) was added. The resulting mixture was stirred at room temperature for 1 h. The color changed to brownish yellow immediately after trimethylsilyl trifluoromethanesulfonate addition. The solution was filtered through Celite again and the solvent was evaporated in vacuo to afford a brownish-yellow semisolid, tentatively assigned as {[(IDipp)Ni]$_2$(μ-O*t*-Bu)}[OTf], 0.069 g, 0.062 mmol. The crude product was dissolved in THF (1 mL) and cooled to –35 °C, and pinacolborane (0.0079 g, 9.0 μL, 0.062 mmol) was added. The solution was mixed well and kept at –35 °C for another 1 h and the color changed to reddish-brown. Pentane (5 mL) was carefully added over the THF solution, and the layers were allowed to mix by diffusion at –35 °C overnight, resulting in the formation of reddish-brown crystals. The mother liquor was decanted, and the crystals were collected on a fritted glass filter. The crystals were triturated, and then washed with pentane (3 x 1 mL) and dried in vacuo at room temperature for 16 h, affording **13**[OTf] as a reddish-brown powder, 0.045 g (46%). ^{1}H NMR (400 MHz, THF-d_8): δ (ppm) 7.78 (d, J = 2.0 Hz, 2H, NC*H*), 7.58 (t, J = 7.8 Hz, 2H, *para*-C*H*), 7.45 (d, J = 7.6 Hz, 4H, *meta*-C*H*), 7.40 (d, J = 2.0 Hz, 2H, NC*H*), 6.53 (d, J = 7.2 Hz, 4H, *meta*-C*H*), 4.79 (t, J = 7.2 Hz, 2H, *para*-C*H*), 2.74 (sept, J = 6.8 Hz, 4H, C*H*(CH$_3$)$_2$), 2.29 (sept, J = 6.8 Hz, 4H, C*H*(CH$_3$)$_2$), 1.49 (d, J = 6.8 Hz, 12H, CH(C*H*$_3$)$_2$), 1.41 (d, J = 6.8

Hz, 12H, CH(CH_3)$_2$), 1.11 (d, J = 6.8 Hz, 24H, CH(CH_3)$_2$), –25.43 (s, 1H, NiHNi); ^{13}C{^{1}H} NMR (176 MHz, THF-d_8): δ (ppm) 193.48 (NCNi), 146.65, 137.52, 130.67, 128.73, 126.39, 124.65, 124.07, 120.12, 113.40, 108.91, 104.77, 29.31 (CH(CH$_3$)$_2$), 28.79 (CH(CH$_3$)$_2$), 24.54 (CH(CH$_3$)$_2$), 23.21 (CH(CH$_3$)$_2$), 23.11 (CH(CH$_3$)$_2$); ^{19}F NMR (376 MHz, THF-d_8): δ (ppm) –76.89 (s). IR: ν (cm^{-1}) 2962 (s), 2927 (s), 2868 (s), 2366 (w), 2035 (w), 1452 (s), 1387 (s), 1362 (s), 1304 (s), 1267 (s), 1222 (s), 1185 (s), 1142 (s), 1059 (s), 1033 (s), 961 (w), 938 (w), 872 (s), 792 (s), 788 (s), 724 (w), 683 (w), 636 (s), 570 (s), 516 (s), 465 (s).

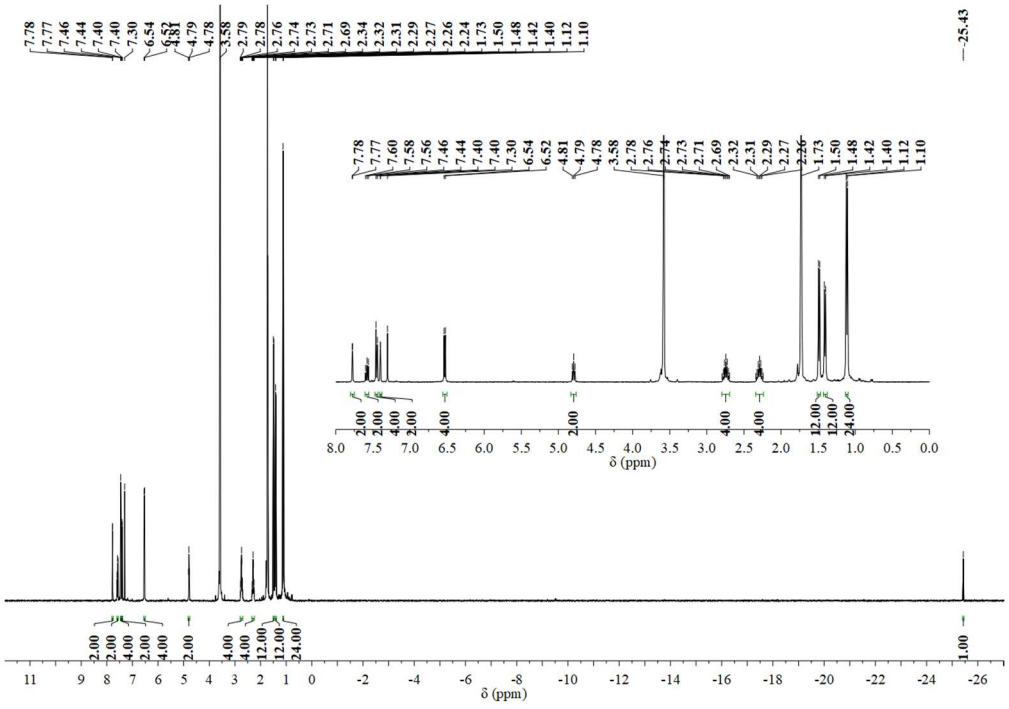

Figure 4.6. ^{1}H NMR (400 MHz, THF-d_8) spectrum of **13**[OTf]. A trace of benzene (δ 7.30 ppm)[16] is present as the result of benzophenone ketyl decomposition.

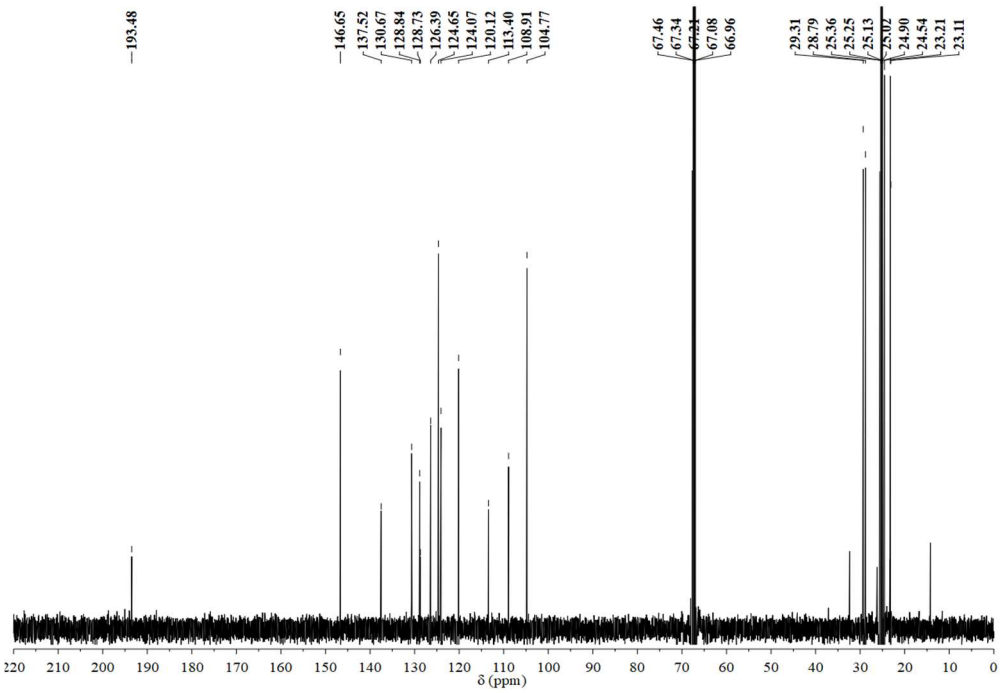

Figure 4.7. $^{13}C\{^{1}H\}$ NMR (176 MHz, THF-d_8) spectrum of **13**[OTf]. A trace of benzene (δ 128.84 ppm)[16] is present as the result of benzophenone ketyl decomposition.

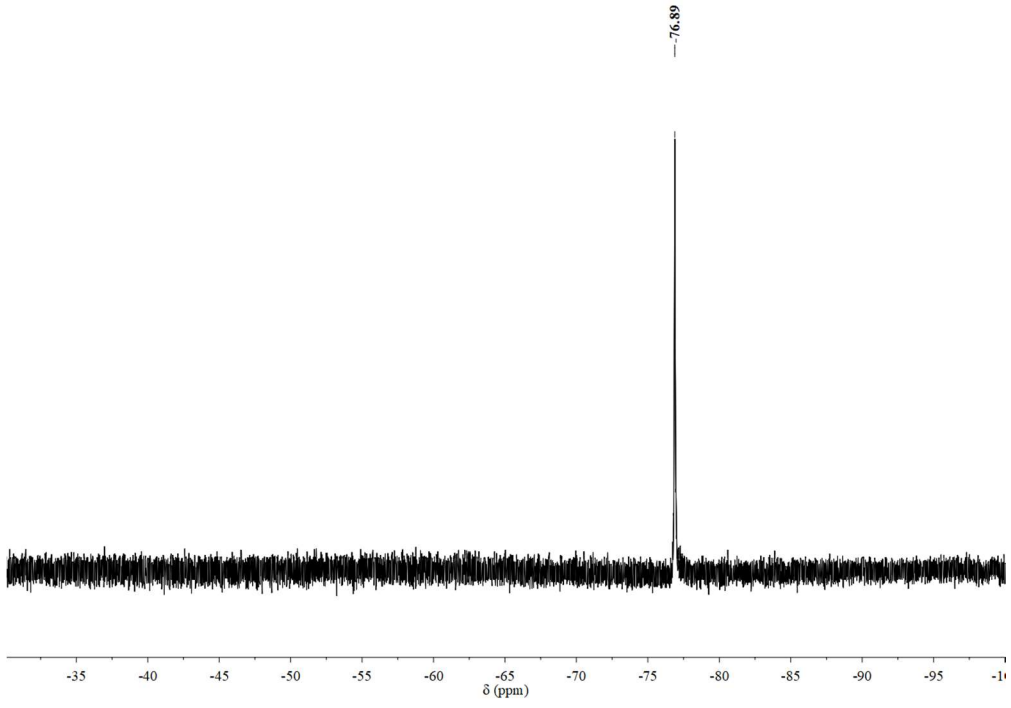

Figure 4.8. ^{19}F NMR (376 MHz, THF-d_8) spectrum of **13**[OTf].

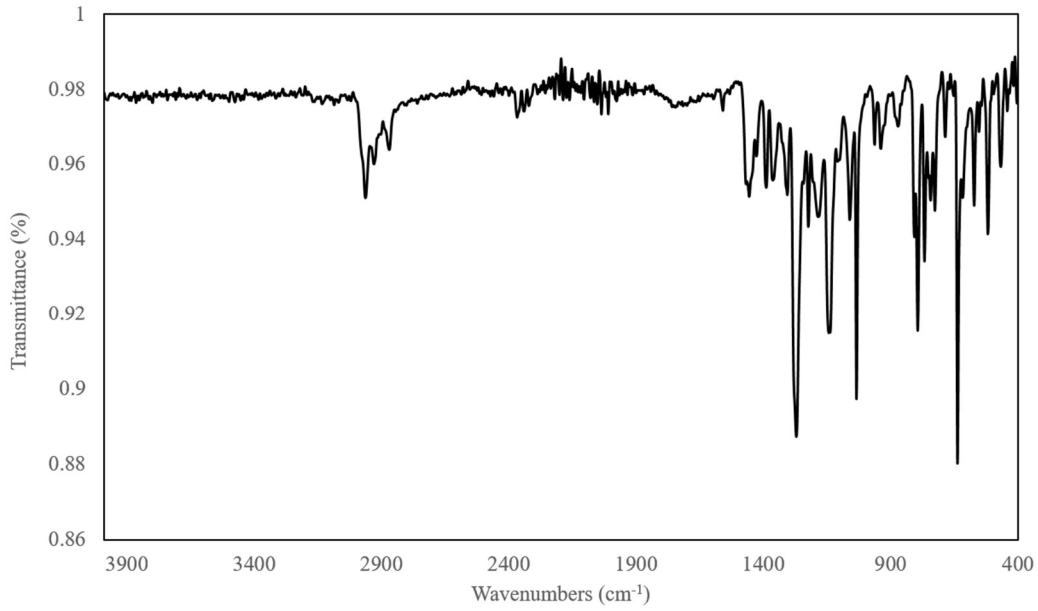

Figure 4.9. IR spectrum of **13**[OTf].

4.4.2.2 (IDipp)Ni^0(benzene)

[(IDipp)Ni^0(benzene)] was prepared via modification from literature procedure.[15] Ni(cod)$_2$ (0.283 g, 1.03 mmol) and IDipp (0.400 g, 1.03 mmol) were dissolved in benzene (15 mL) in a 50-mL Schlenk flask. The solution was degassed 3 times via freeze-pump-thaw and H_2 (3 atm) was added. The solution was stirred at room temperature for 6 d then evaporated in vacuo to dryness. The residue was dissolved in benzene (15 mL) and the solution was filtered through Celite. Solvent was evaporated in vacuo overnight to afford [(IDipp)Ni^0(benzene)] as a brown solid, 0.520 g (96%). ^{1}H NMR (400 MHz, C_6D_6): δ (ppm) 7.30 (t, J = 7.8 Hz, 2H, *para*-CH), 7.19 (d, J = 7.6 Hz, 4H, *meta*-CH), 7.16 (s, 6H, C_6H_6), 6.37 (s, 2H, NC*H*), 2.91 (sept, J = 6.8 Hz, 4H, C*H*(CH_3)$_2$), 1.40 (d, J = 6.8 Hz, 12H, CH(C*H*$_3$)$_2$), 1.13 (d, J = 6.8 Hz, 12H, CH(C*H*$_3$)$_2$).

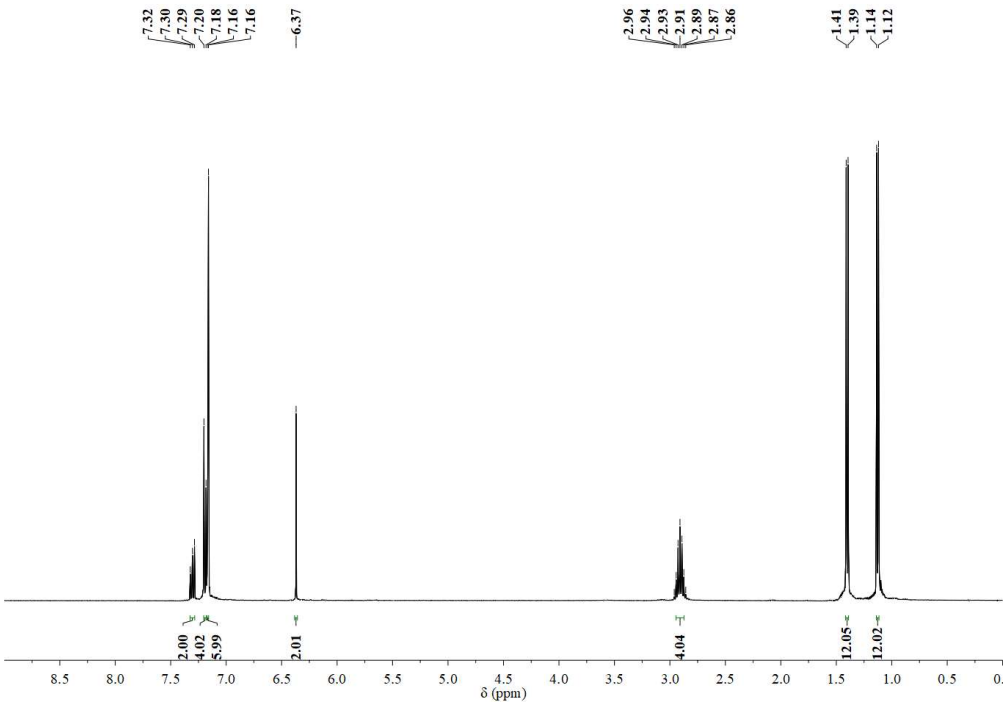

Figure 4.10. ^{1}H NMR (400 MHz, C_6D_6) spectrum of [(IDipp)Ni^{0}(benzene)].

4.4.2.3 {[(IDipp)Ni]$_2$(μ-H)}[NTf$_2$] (**13**[NTf$_2$])

In the glovebox, [(IDipp)Ni^{0}(benzene)] (0.090 g, 0.17 mmol) and trifluoromethanesulfonimide (0.024 g, 0.085 mmol) were dissolved in benzene (10 mL) in a 20-mL glass scintillation vial. The solution was mixed by swirling and kept at room temperature for 21 h, resulting in the formation of reddish-brown precipitate. The mother liquor was decanted, and the solid was collected on a fritted glass filter, and then washed with pentane (3 x 1 mL) and dried in vacuo at room temperature for 16 h, affording **13**[NTf$_2$] as a reddish-brown powder, 0.082 g (82%). ^{1}H NMR (400 MHz, THF-d_8): δ (ppm) 7.72 (d, J = 1.6 Hz, 2H, NC*H*), 7.58 (t, J = 7.8 Hz, 2H, *para*-C*H*), 7.45 (d, J = 7.6 Hz, 4H, *meta*-C*H*), 7.40 (d, J = 1.2 Hz, 2H, NC*H*), 6.53 (d, J = 7.2 Hz, 4H, *meta*-C*H*), 4.79 (t, J = 7.2 Hz, 2H, *para*-C*H*), 2.73 (sept, J = 7.0 Hz, 4H, C*H*(CH$_3$)$_2$), 2.29 (sept, J = 6.8

Hz, 4H, C*H*(CH_3)$_2$), 1.49 (d, *J* = 6.8 Hz, 12H, CH(C*H*$_3$)$_2$), 1.41 (d, *J* = 6.8 Hz, 12H, CH(C*H*$_3$)$_2$), 1.11 (d, *J* = 6.8 Hz, 24H, CH(C*H*$_3$)$_2$), –25.31 (s, 1H, Ni*H*Ni); ^{13}C{^{1}H} NMR (176 MHz, THF-d_8): δ (ppm) 193.56 (N*C*Ni), 146.63, 137.45, 130.71, 128.72, 126.33, 124.66, 123.83, 120.13, 113.39, 108.90, 104.76, 29.31 (*C*H(CH_3)$_2$), 28.79 (*C*H(CH_3)$_2$), 24.50 (CH(*C*H_3)$_2$), 23.18 (CH(*C*H_3)$_2$), 23.07 (CH(*C*H_3)$_2$); ^{19}F NMR (376 MHz, THF-d_8): δ (ppm) –79.79 (s). IR: ν (cm^{-1}) 2962 (s), 2931 (s), 2869 (s), 2164 (s), 1961 (w), 1465 (s), 1387 (s), 1354 (s), 1267 (s), 1228 (s), 1187 (s), 1140 (s), 1057 (s), 963 (s), 940 (s), 872 (s), 794 (s), 763 (s), 739 (s), 687 (w), 650 (w), 617 (s), 570 (s), 512 (s), 463 (s).

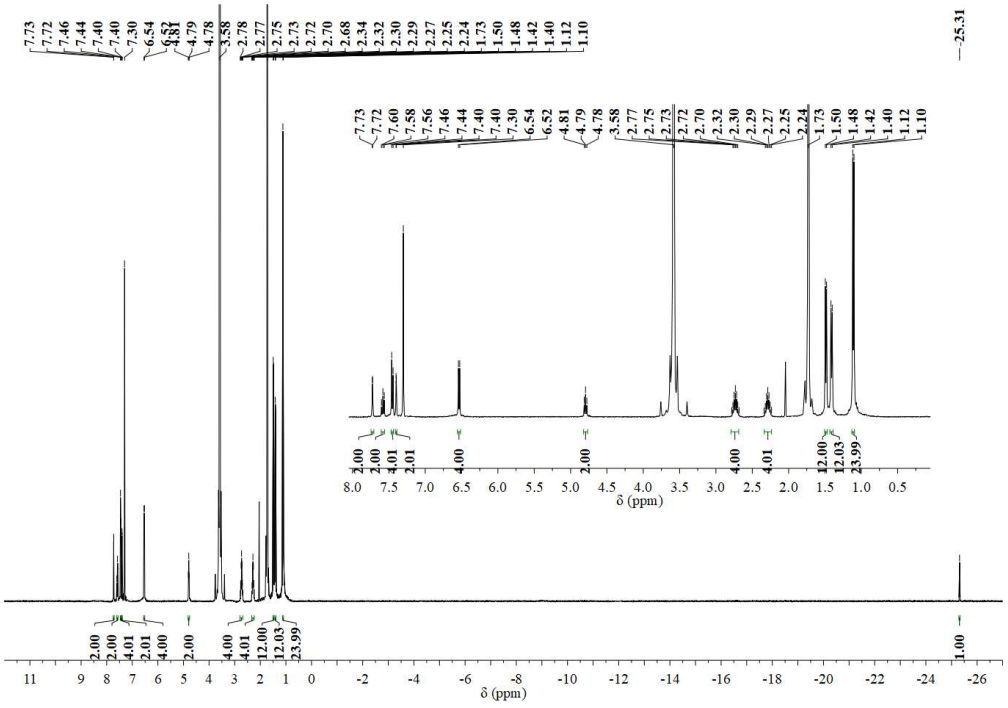

Figure 4.11. ^{1}H NMR (400 MHz, THF-d_8) spectrum of **13**[NTf_2]. A trace of benzene (δ 7.30 ppm)[16] is present as the result of benzophenone ketyl decomposition.

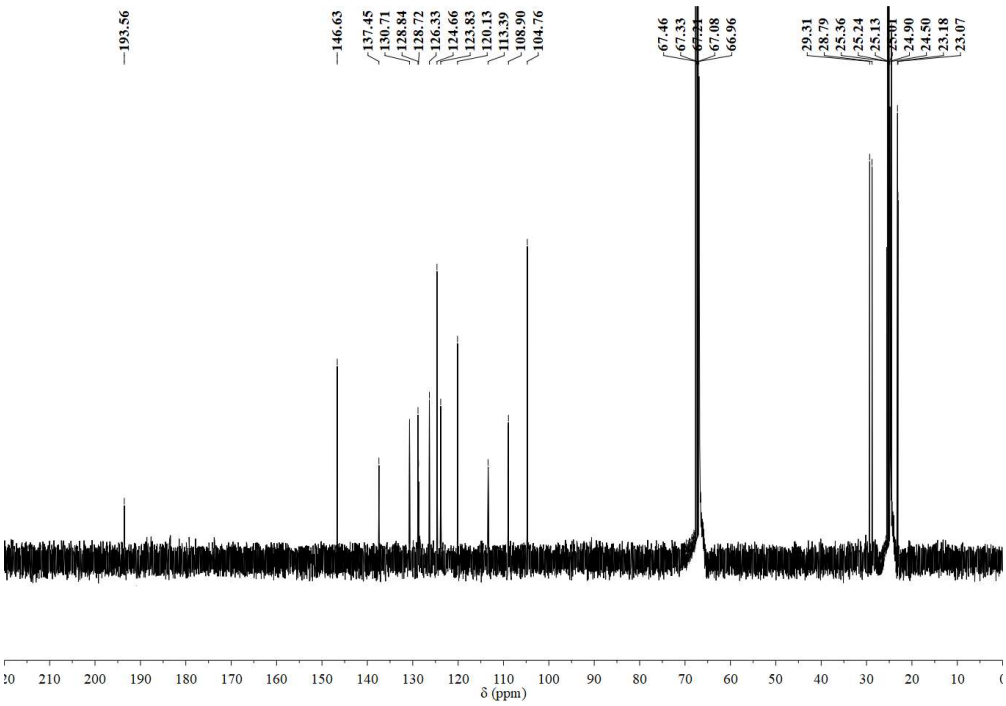

Figure 4.12. $^{13}C\{^{1}H\}$ NMR (176 MHz, THF-d_8) spectrum of **13**[NTf_2]. A trace of benzene (δ 128.84 ppm)[16] is present as the result of benzophenone ketyl decomposition.

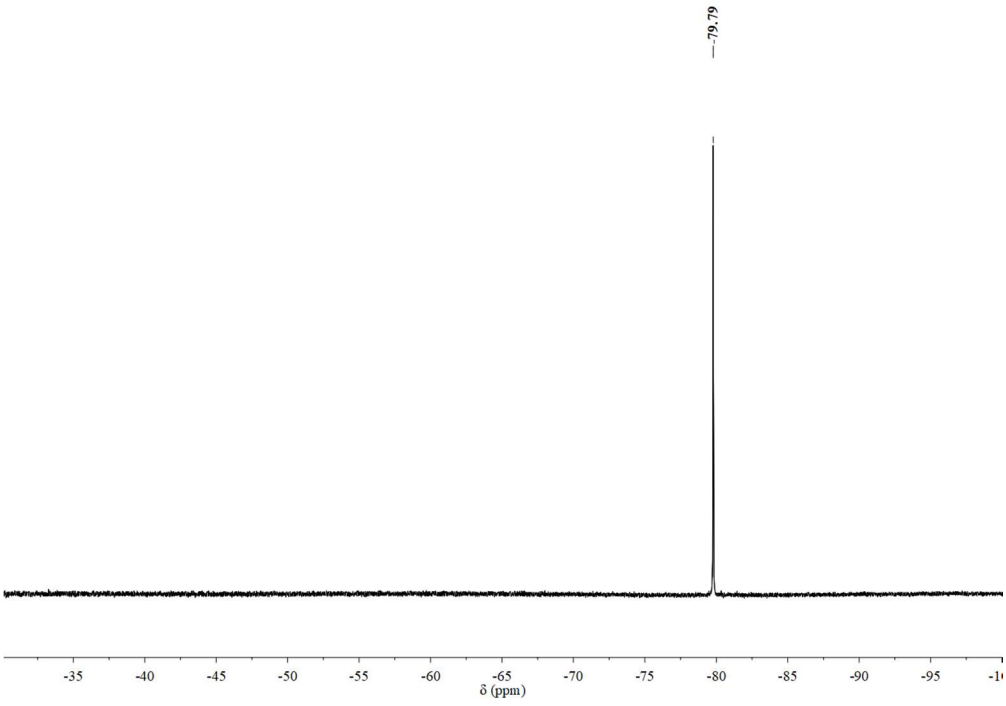

Figure 4.13. ^{19}F NMR (376 MHz, THF-d_8) spectrum of **13**[NTf_2].

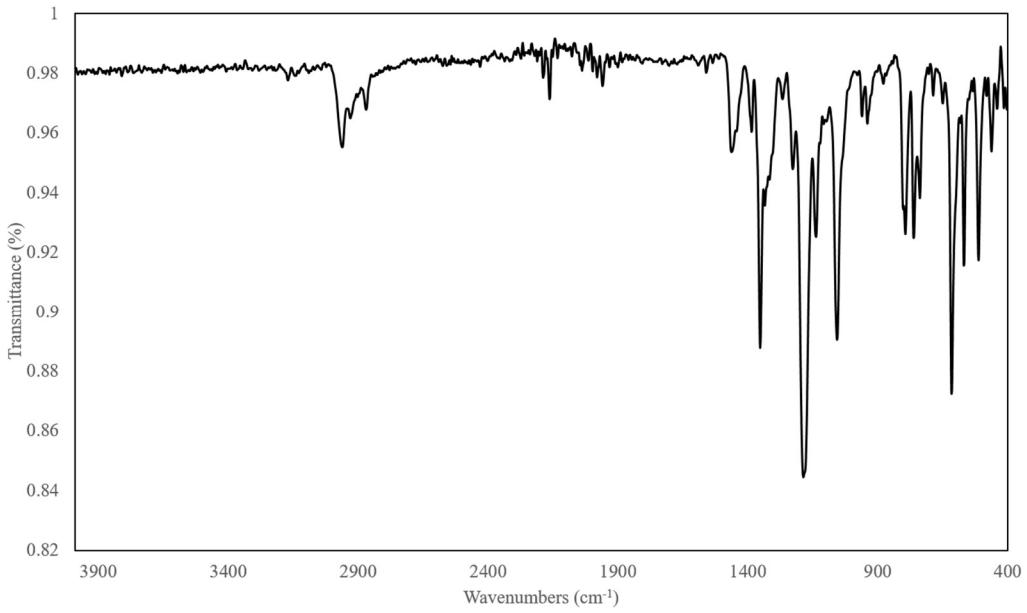

Figure 4.14. IR spectrum of **13**[NTf_2].

4.4.2.4 [(IDipp)Ni]$_2$[OTf] (**15**[OTf])

In the glovebox, nickel(II) trifluoromethanesulfonate (0.007 g, 0.02 mmol), [(IDipp)$Ni^0(C_6H_6)$] (0.028 g, 0.053 mmol) and IDipp (0.007 g, 0.02 mmol) were added in THF (5 mL) in a 20-mL scintillation vial. The solution were stirred at room temperature for 16 h and the color changed from reddish-brown to dark bluish green over the time. The solution was filtered through Celite and evaporated in vacuo to around 1 mL. Pentane (5 mL) was carefully added over the THF solution, the layers were allowed to mix by diffusion at –35 °C overnight, resulting in the formation of reddish-brown precipitate. The mother liquor was decanted, and the solid was collected on a fritted glass filter. The solid was triturated, and then washed with pentane (3 x 1 mL) and dried in vacuo at room temperature for 2 h, affording **15**[OTf] as a reddish-brown powder, 0.005 g (13%). ^{1}H NMR (400 MHz, THF-d_8): δ (ppm) 7.19 (br), 6.63 (br), 3.17 (br), 1.09 (br); ^{19}F NMR (376

MHz, THF-d_8): δ (ppm) –76.30 (s). IR: ν (cm^{-1}) 2967 (s), 2867 (w), 2356 (s), 2187 (s), 2107 (w), 2005 (w), 1946 (w), 1869 (w), 1552 (w), 1457 (s), 1410 (w), 1368 (s), 1267 (s), 1154 (s), 1031 (s), 804 (s), 760 (s), 639 (s). Brownish-red crystals were grown through THF/pentane vapor diffusion, and determined via X-ray crystallography to consist of **15**[OTf]. The mother liquor was collected and dried in vacuo for 2 h. ^{1}H NMR (400 MHz, THF-d_8): [$(IDipp)_2Ni^0$] δ (ppm) 7.21 (t, J = 7.2 Hz, 4H, *para*-C*H*), 6.98 (d, J = 7.6 Hz, 8H, *meta*-C*H*), 6.47 (s, 4H, NC*H*), 2.89 (sept, J = 6.8 Hz, 8H, C*H*$(CH_3)_2$), 1.03 (d, J = 6.8 Hz, 24H, CH(C*H*$_3)_2$), 0.96 (d, J = 6.8 Hz, 24H, CH(C*H*$_3)_2$).

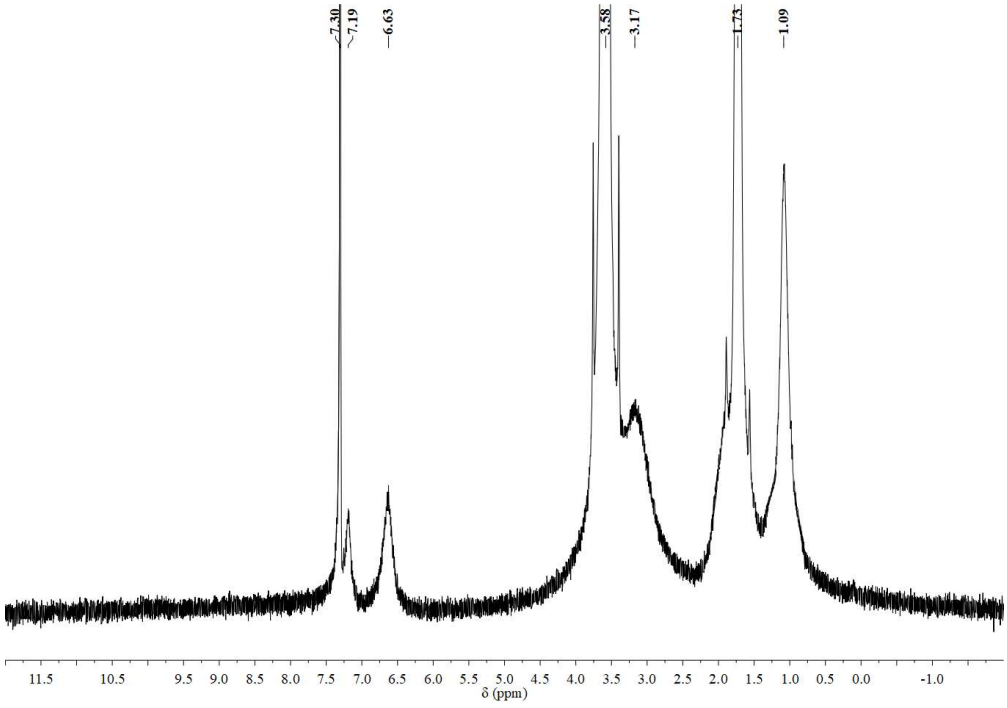

Figure 4.15. ^{1}H NMR (400 MHz, THF-d_8) spectrum of **15**[OTf]. A trace of benzene (δ 7.30 ppm)[16] is present as the result of benzophenone ketyl decomposition.

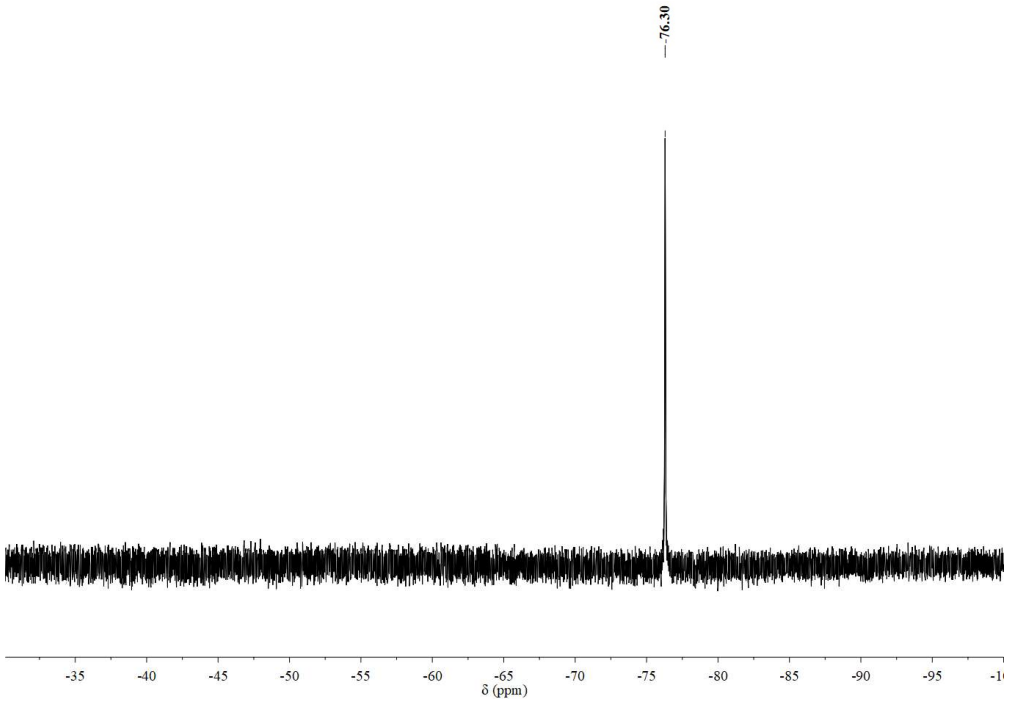

Figure 4.16. ^{19}F NMR (376 MHz, THF-d_8) spectrum of **15**[OTf].

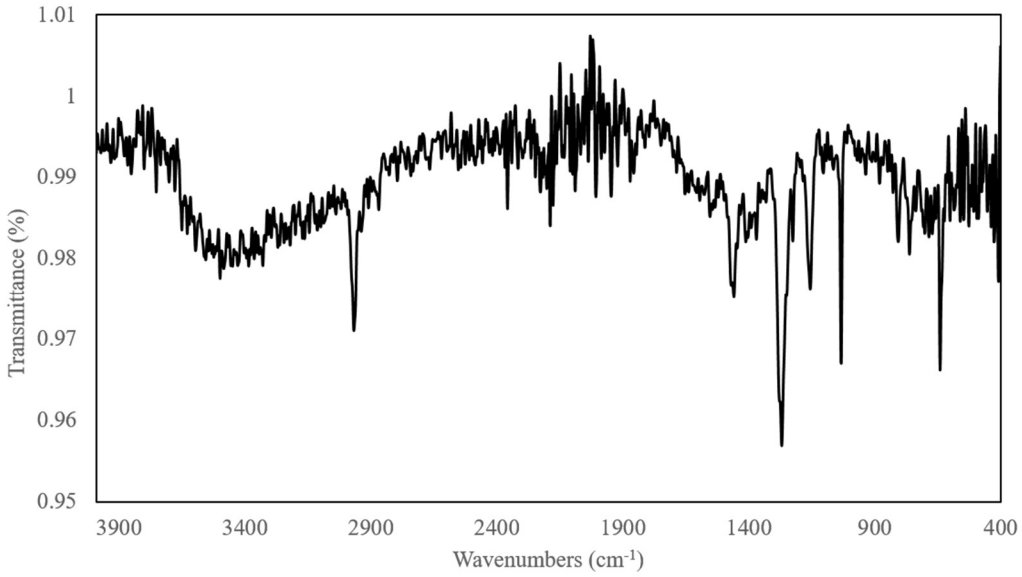

Figure 4.17. IR spectrum of **15**[OTf].

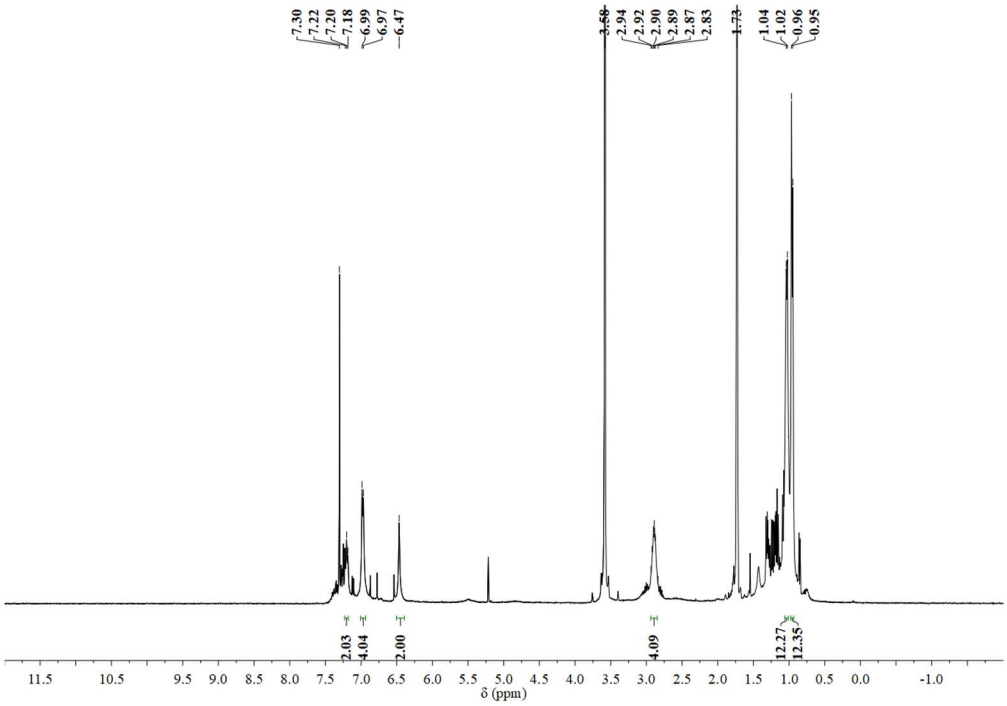

Figure 4.18. ^{1}H NMR (400 MHz, THF-d_8) spectrum of the product in mother liquor in comproportionation of Ni(II) and Ni(0) in ratio of 1:3. A trace of benzene (δ 7.30 ppm)[16] is present as the result of benzophenone ketyl decomposition.

4.4.2.5 [(IDipp)Ni]$_2$[BF$_4$] (**15**[BF$_4$])

In the glovebox, [(IDipp)Ni^0(C$_6$H$_6$)] (0.060 g, 0.11 mmol) and triphenylcarbenium tetrafluoroborate (0.018 g, 0.055 mmol) were added in THF (5 mL) in a 20-mL scintillation vial. The solution was stirred at room temperature for 20 h, during which time the color changed from brownish-yellow to brownish green, then filtered through Celite and concentrated in vacuo to around 1 mL. Pentane (5 mL) was carefully added over the THF solution, and the layers were allowed to mix by diffusion at –35 °C overnight, resulting in the formation of reddish-brown precipitate. The mother liquor was decanted, and the solid was collected on a fritted glass filter. The solid was triturated, and then washed with pentane (3 x 1 mL) and dried in vacuo at room temperature for 12 h, affording **15**[BF$_4$] as

reddish-brown crystals, 0.031 g (57%). ^{1}H NMR (300 MHz, THF-d_8): δ (ppm) 7.20 (br), 6.64 (br), 3.17 (br), 1.09 (br); ^{19}F NMR (376 MHz, THF-d_8): δ (ppm) –151.89 (s).

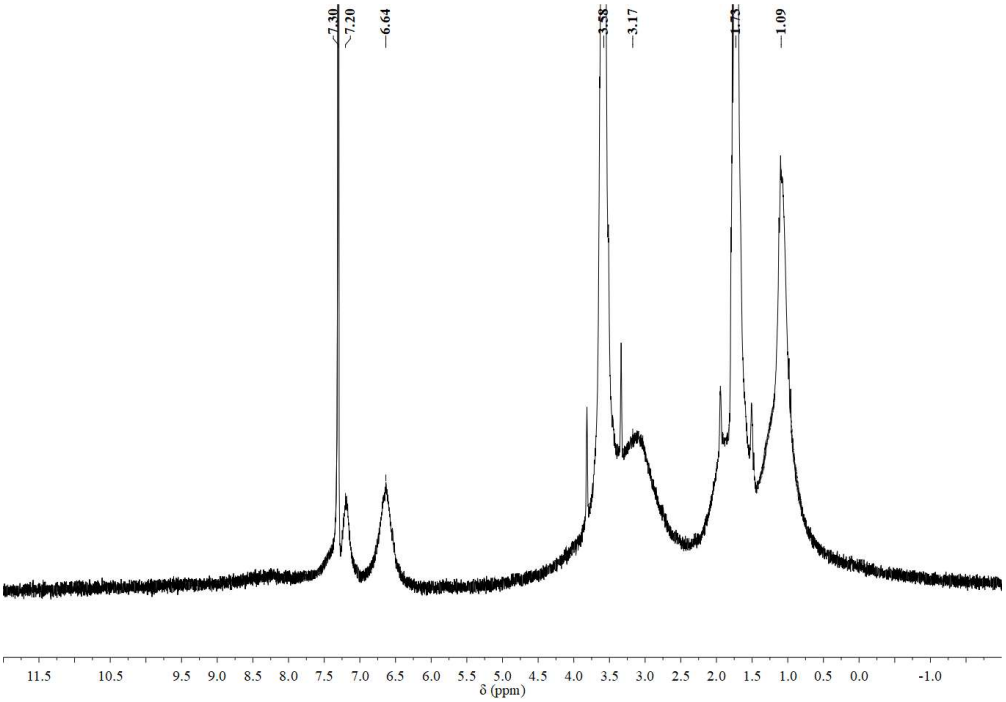

Figure 4.19. ^{1}H NMR (300 MHz, THF-d_8) spectrum of **15**[BF_4]. A trace of benzene (δ 7.30 ppm)[16] is present as the result of benzophenone ketyl decomposition.

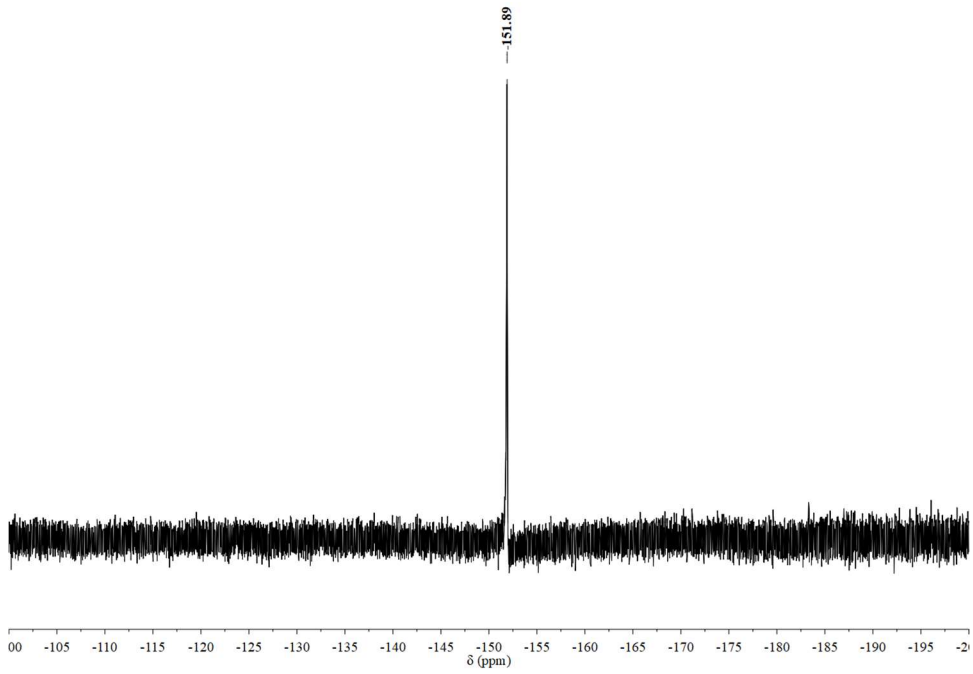

Figure 4.20. ^{19}F NMR (376 MHz, THF-d_8) spectrum of **15**[BF_4].

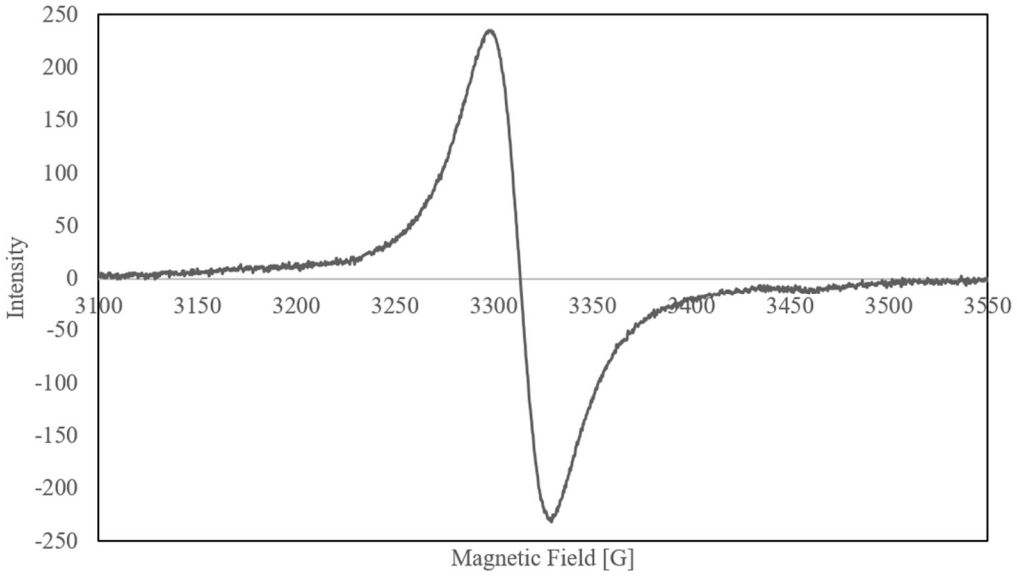

Figure 4.21. EPR spectrum of **15**[BF_4] in THF solution at room temperature. The calculated *g*-value was 2.117, indicating the presence of a single free electron.

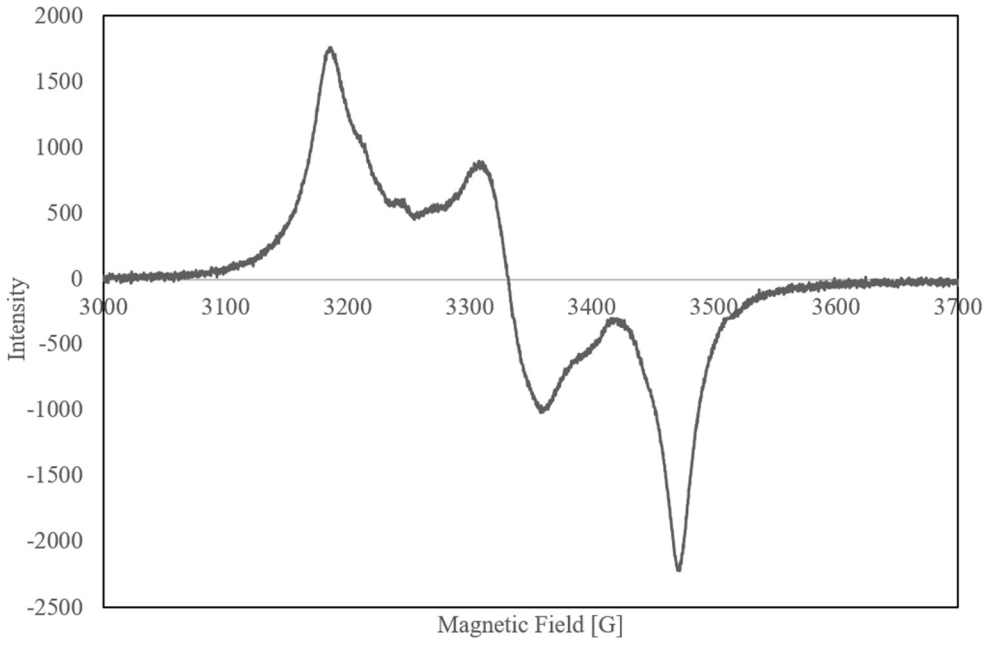

Figure 4.22. EPR spectrum of **15**[BF_4] solid at room temperature. The calculated *g*-values for the solid state sample are 2.032, 2.117 and 2.213. The symmetry of **15**[BF_4] is responsible for the rhombic *g*-tensor. In the solid state, the *g*-value depends on the x, y, z directions of crystals.[28]

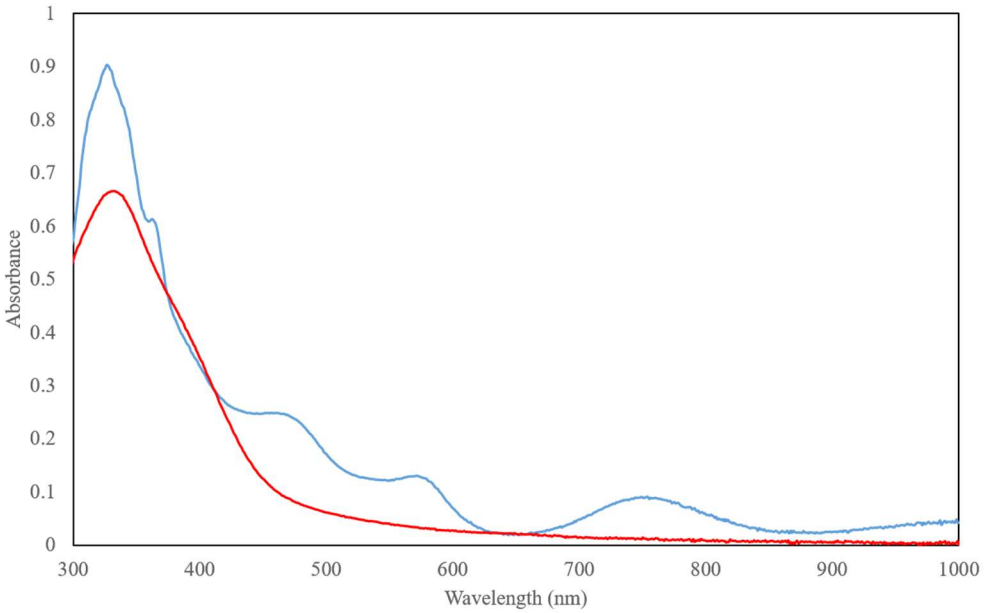

Figure 4.23. UV-vis spectra of **15**[NTf_2] (blue) and [(IDipp)$Ni^0(C_6H_6)$] (red). UV-vis absorption (nm): 15[NTf_2]: 326, 362, 456, 572, 754; [(IDipp)$Ni^0(C_6H_6)$]: 331.

4.4.2.6 [(IDipp)$_2$Ni][BF_4] (**16**[BF_4])

In the glovebox, [(IDipp)Ni^0(benzene)] (0.010 g, 0.019 mmol) and IDipp (0.008 g, 0.02 mmol) were added in THF (5 mL) in a 20-mL scintillation vial. The solution was stirred at room temperature for 2 h and the color changed from brownish-yellow to dark blue. Ferrocenium tetrafluoroborate (0.005 g, 0.02 mmol) was added and the solution was stirred at room temperature for another 4 h. During this time the color changed to yellowish-green. The solution was filtered through Celite and concentrated in vacuo to around 1 mL. Pentane (5 mL) was carefully added over the THF solution, and the layers were allowed to mix by diffusion at –35 °C overnight, resulting in the formation of white solid. The mother liquor was decanted, and the solid was collected on a fritted glass filter. The solid was triturated, and then washed with pentane (3 x 1 mL) and dried in vacuo at room temperature for 2 h, affording **16**[BF4] as a white powder 0.017 g (97%). ^{1}H NMR

(400 MHz, THF-d_8): δ (ppm) 8.35 (br), –9.01 (br), –11.98 (br); ^{19}F NMR (376 MHz, THF-d_8): δ (ppm) –151.56 (s).

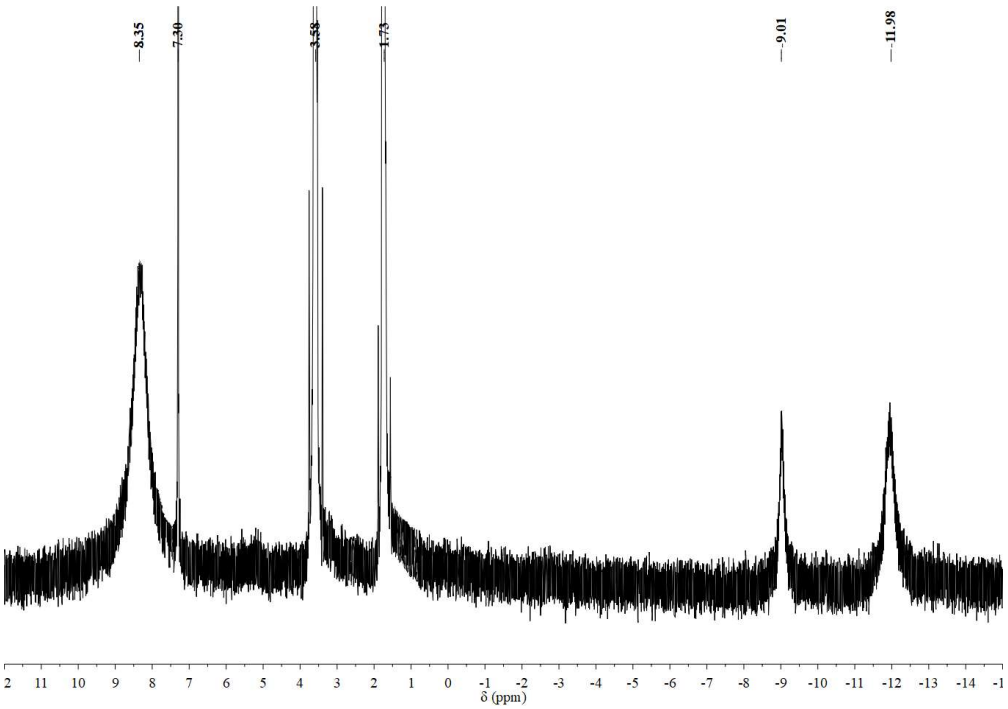

Figure 4.24. ^{1}H NMR (300 MHz, THF-d_8) spectrum of **16**[BF_4]. A trace of benzene (δ 7.30 ppm)[16] is present as the result of benzophenone ketyl decomposition.

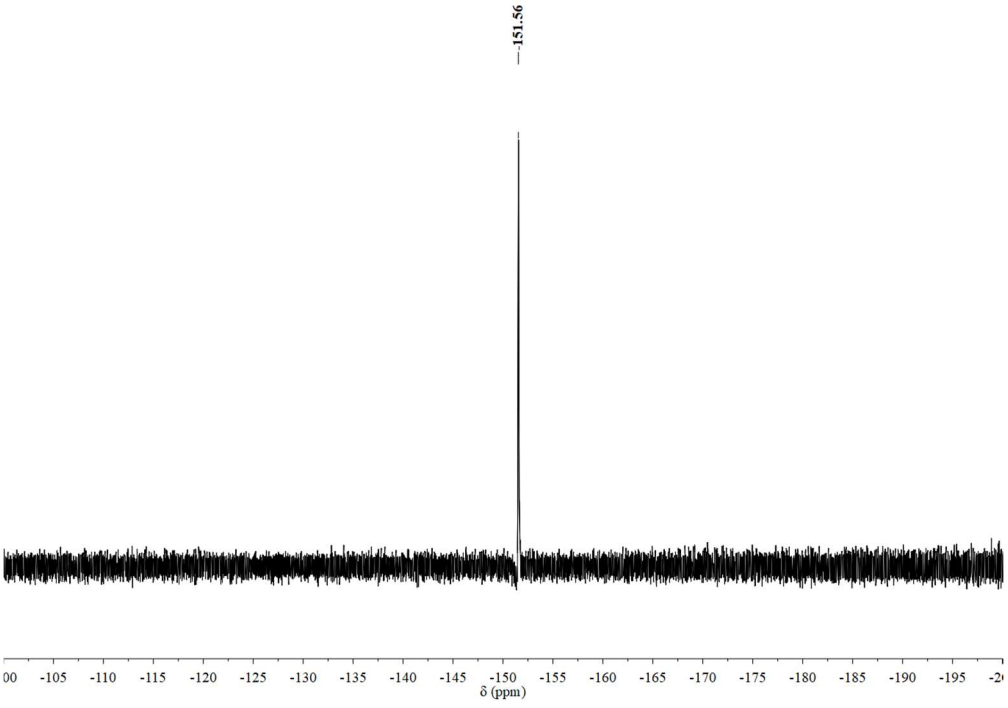

Figure 4.25. ^{19}F NMR (376 MHz, THF-d_8) spectrum of **16**[BF_4].

4.4.3 Reactivity studies

4.4.3.1 Reaction of {[(IDipp)Ni]$_2$(μ-H)}[OTf] (**13**[OTf]) with acetonitrile

In the glovebox, **13**[OTf] (0.008 g, 0.008 mmol) was dissolved in THF-d_8 (0.5 mL) and transferred into a J. Young tube, and acetonitrile (0.00063 g, 0.80 μL, 0.015 mmol) was added. The solution was mixed and the tube was sealed and kept at room emperature. The reddish-brown color changed to brownish-yellow over one day. ^{1}H NMR (400 MHz, THF-d_8): δ (ppm) 8.30 (s, 2H, NC*H*), 7.66 (t, *J* = 7.8 Hz, 2H, *para*-CH), 7.51 (d, *J* = 8.0 Hz, 4H, *meta*-CH), 2.43 (sept, *J* = 6.8 Hz, 4H, C*H*(CH$_3$)$_2$), 1.28 (d, *J* = 6.8 Hz, 12H, CH(C*H*$_3$)$_2$), 1.25 (d, *J* = 6.8 Hz, 12H, CH(C*H*$_3$)$_2$), 0.19 (s, C*H*$_4$); ^{13}C{^{1}H} NMR (176 MHz, THF-d_8): δ (ppm) 149.28 (N*C*Ni), 146.08 (*ortho*-*C*), 132.82 (*ipso*-C), 130.51 (*para*-*C*), 128.86 (N*C*H), 128.75 (*C*N), 126.88 (*meta*-*C*), 125.88 (*C*N), 29.83 (*C*H(CH$_3$)$_2$), 24.41 (CH(*C*H$_3$)$_2$), 23.33 (CH(*C*H$_3$)$_2$); ^{19}F NMR (376 MHz, THF-d_8): δ (ppm) –77.03 (s). Crystals were grown via THF/pentane vapor diffusion in the glovebox. The colorless crystals picked for X-ray crystallography study were found to be [(IDipp)Ni(CN)$_2$]$_4$ (**14**). IR for **14**: ν (cm^{-1}) 2965 (s), 2931 (s), 2871 (s), 2148 (w), 2032 (w), 1963 (w), 1622 (w), 1588 (w), 1537 (s), 1501 (s), 1460 (s), 1389 (s), 1367 (s), 1333 (s), 1256 (s), 1208 (s), 1183 (s), 1106 (s), 1061 (s), 936 (s), 901 (s), 810 (s), 760 (s), 684 (w), 632 (w), 540 (w), 517 (w), 442 (s).

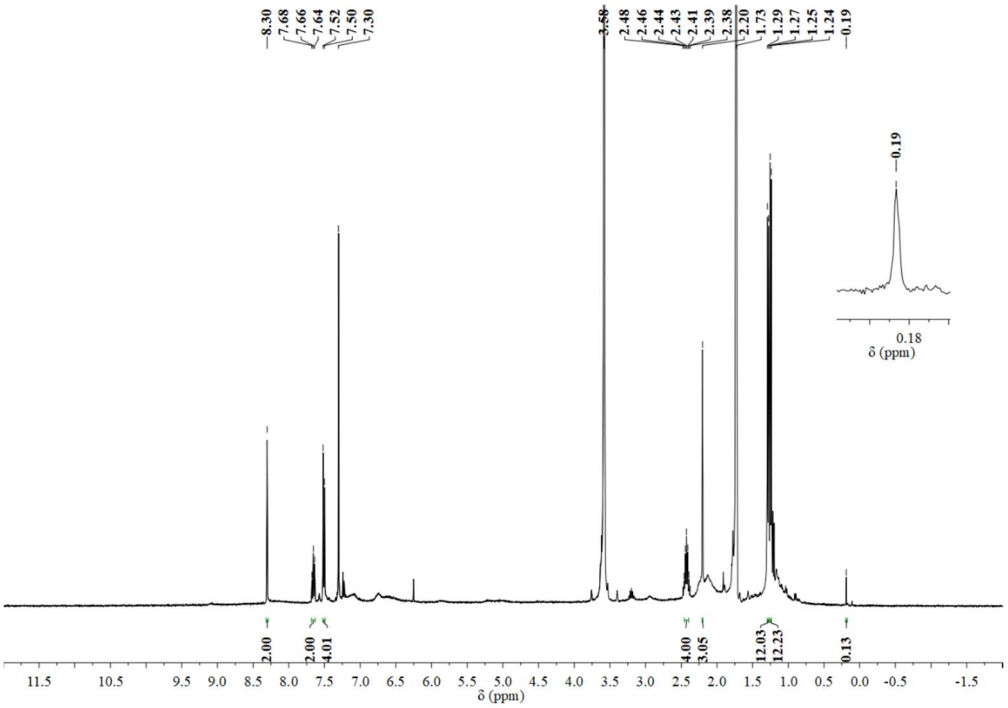

Figure 4.26. ^{1}H NMR (400 MHz, THF-d_8) spectrum of reaction of **13**[OTf] with acetonitrile. A trace of benzene (δ 7.30 ppm)[16] is present as the result of benzophenone ketyl decomposition.

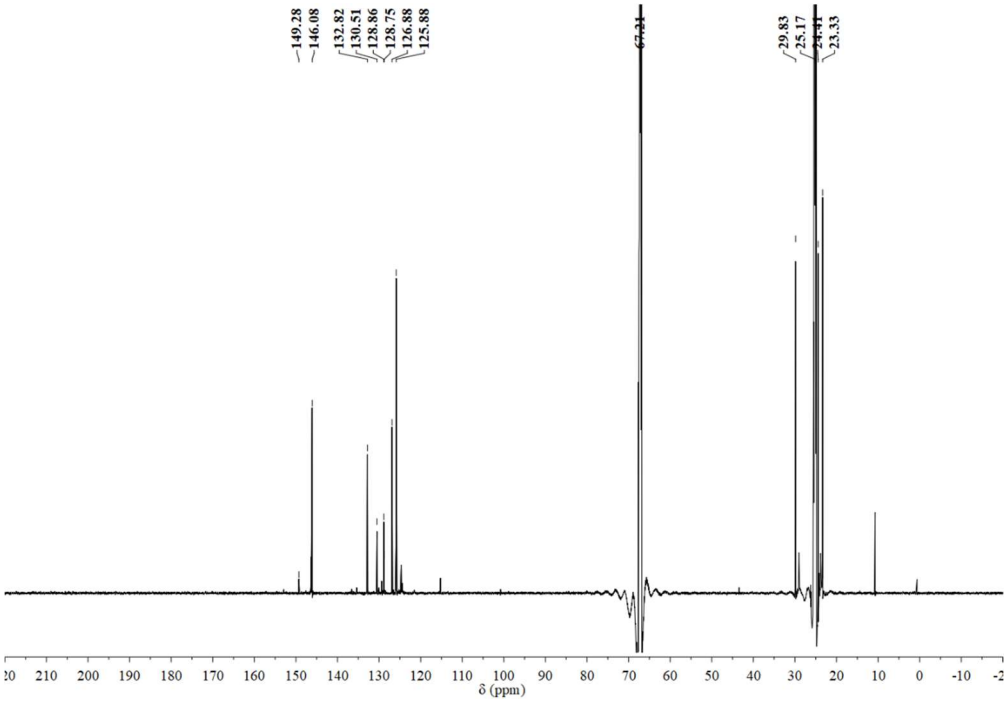

Figure 4.27. ^{13}C{^{1}H} NMR (176 MHz, THF-d_8) spectrum of reaction of **13**[OTf] with acetonitrile.

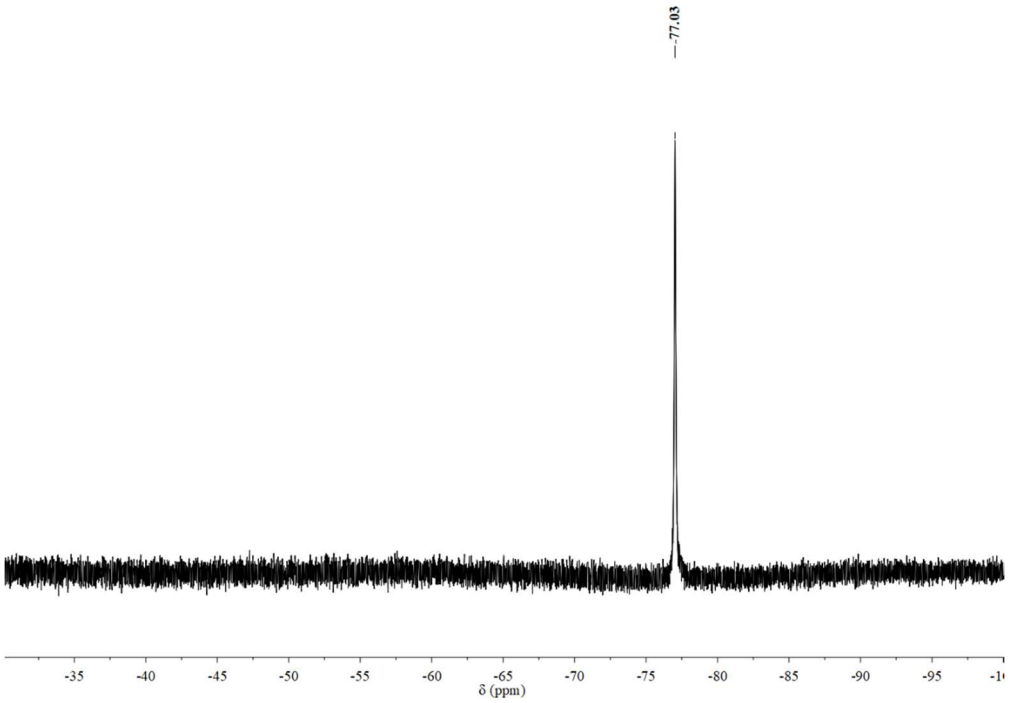

Figure 4.28. ^{19}F NMR (376 MHz, THF-d_8) spectrum of reaction of **13**[OTf] with acetonitrile.

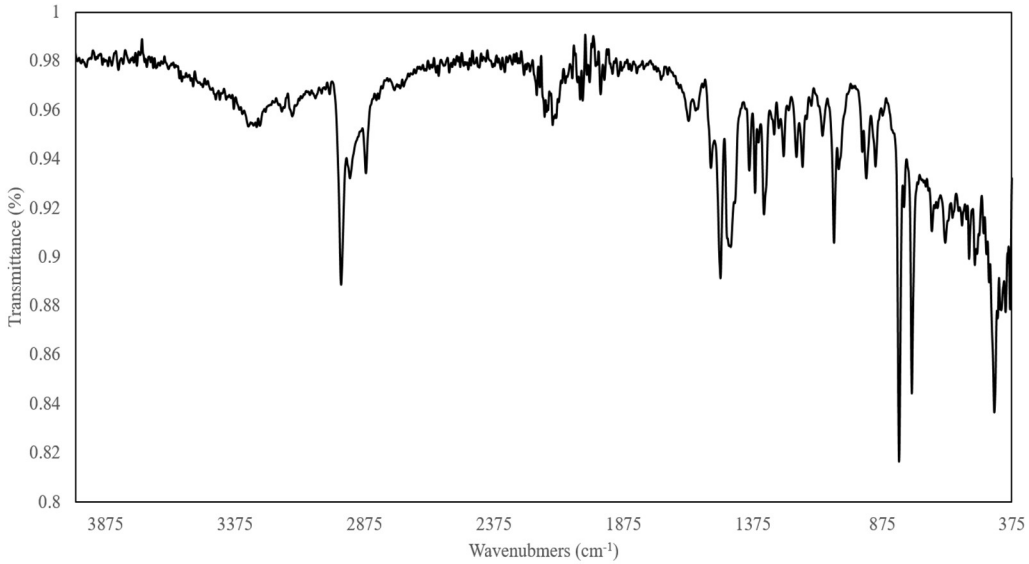

Figure 4.29. IR spectrum of **14**.

4.4.3.2 Reaction of {[(IDipp)Ni]$_2$(μ-H)}[OTf] (**13**[OTf]) with acetonitrile-d_3

In the glovebox, **13**[OTf] (0.010 g, 0.010 mmol) was dissolved in THF-d_8 (0.5 mL) and transferred into a J. Young tube, and acetonitrile-d_3 (0.000844 g, 1.00 μL, 0.0192 mmol) was added. The solution was mixed and the tube was sealed and kept at room temperature. The reddish-brown color of the solution changed to brownish-yellow over one day. ^{1}H NMR (700 MHz, THF-d_8): δ (ppm) 8.30 (s, 2H, NC*H*), 7.65 (t, J = 7.8 Hz, 2H, *para*-CH), 7.51 (d, J = 8.0 Hz, 4H, *meta*-CH), 2.43 (sept, J = 6.8 Hz, 4H, C*H*(CH$_3$)$_2$), 1.28 (d, J = 6.8 Hz, 12H, CH(C*H*$_3$)$_2$), 1.25 (d, J = 6.8 Hz, 12H, CH(C*H*$_3$)$_2$), 0.14 (sept, C*H*D$_3$, $^2J_{H\text{-}D}$ = 2.1 Hz); ^{13}C{^{1}H} NMR (176 MHz, THF-d_8): δ (ppm) 149.31 (N*C*Ni), 146.12 (*ortho-C*), 132.83 (*ipso*-C), 130.53 (*para-C*), 128.86 (N*C*H), 128.75 (*C*N), 126.95 (*meta-C*), 125.88 (*C*N), 29.84 (*C*H(CH$_3$)$_2$), 24.42 (CH(*C*H$_3$)$_2$), 23.34 (CH(*C*H$_3$)$_2$); ^{19}F NMR (376 MHz, THF-d_8): δ (ppm) –78.94 (s).

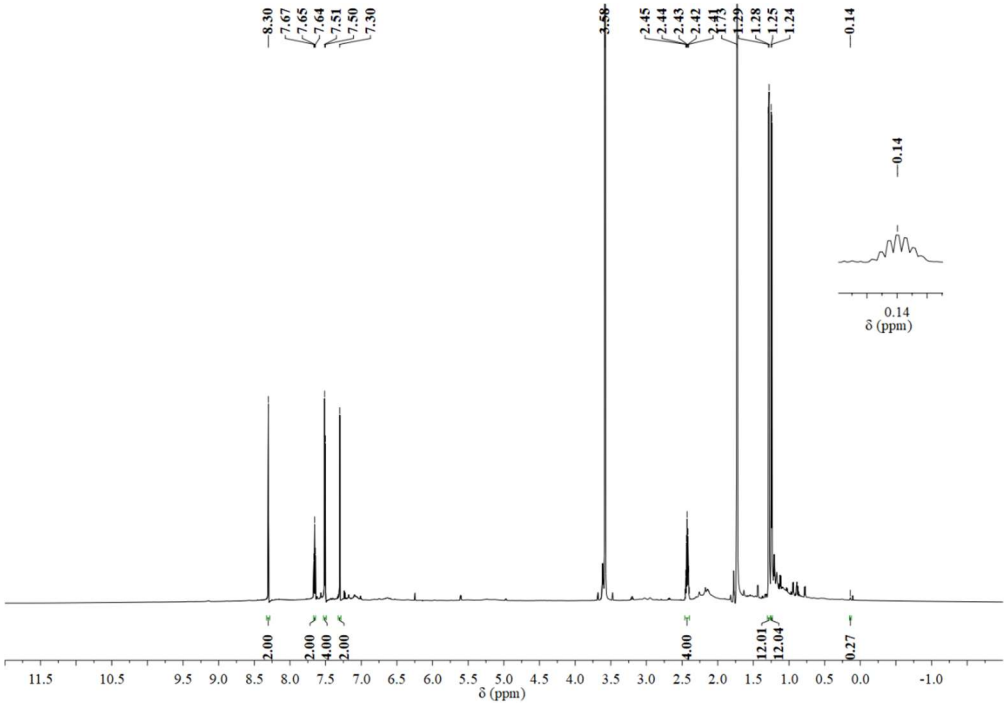

Figure 4.30. ^{1}H NMR (700 MHz, THF-d_8) spectrum of reaction of **13**[OTf] with acetonitrile-d_3. A trace of benzene (δ 7.30 ppm)[16] is present as the result of benzophenone ketyl decomposition.

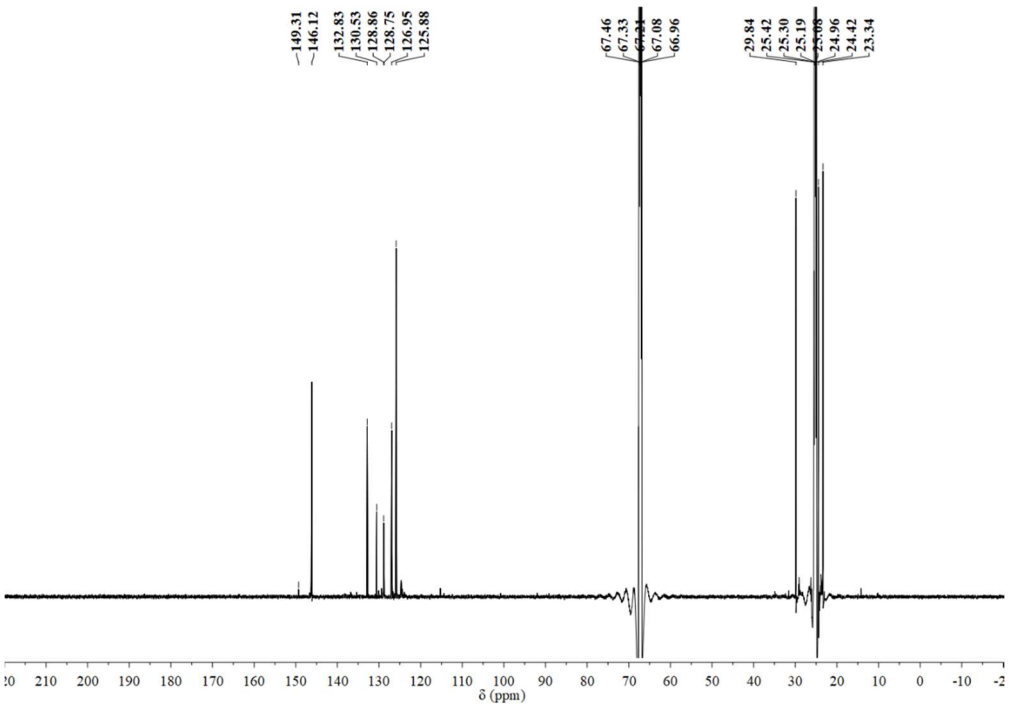

Figure 4.31. $^{13}C\{^{1}H\}$ NMR (176 MHz, THF-d_8) spectrum of reaction of **13**[OTf] with acetonitrile-d_3.

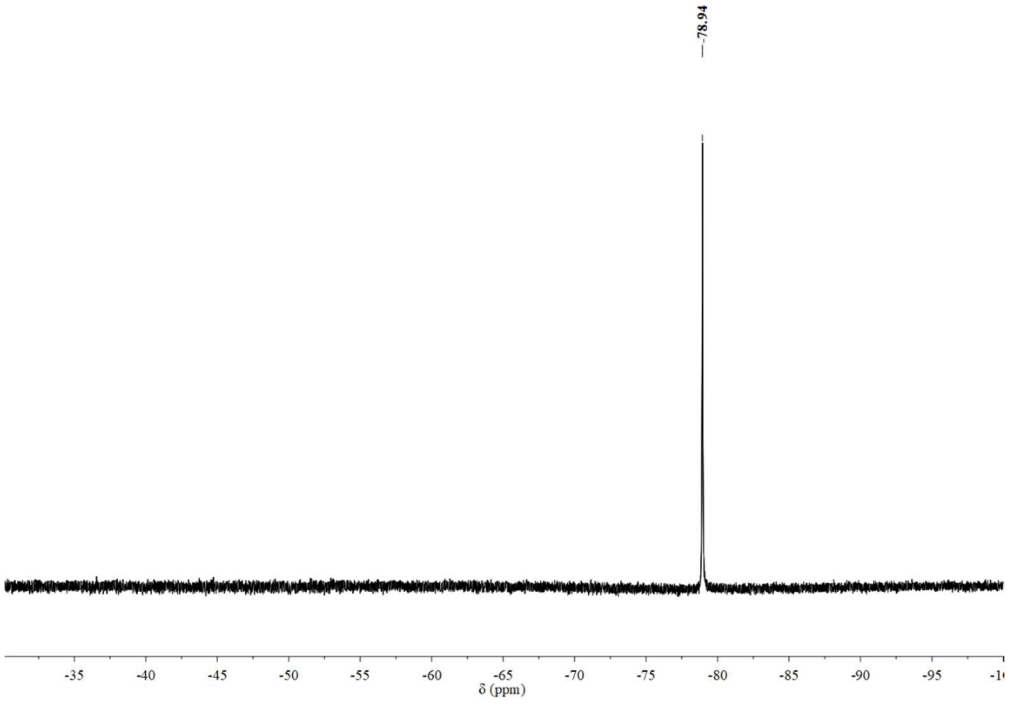

Figure 4.32. ^{19}F NMR (376 MHz, THF-d_8) spectrum of reaction of **13**[OTf] with acetonitrile-d_3.

4.4.3.3 Reaction of {[(IDipp)Ni]$_2$(μ-H)}[NTf$_2$] (**13**[NTf$_2$]) with propionitrile

In the glovebox, **13**[NTf$_2$] (0.008 g, 0.007 mmol) was dissolved in THF-d_8 (0.5 mL) and transferred into a J. Young tube, and propionitrile (0.00039 g, 0.50 μL, 0.0070 mmol) was added. The solution was mixed and the tube was sealed and kept at room temperature. The reddish-brown color of the solution changed to brownish-yellow over two days. ^{1}H NMR (400 MHz, THF-d_8): ethane δ (ppm) 0.85 (CH_3); ^{19}F NMR (376 MHz, THF-d_8): δ (ppm) –77.78 (s). The reaction was repeated in a 25-mL Schlenk flask and the solution was distilled to a J. Young tube after one freeze-pump-thaw cycle and 1,4-dimethoxybenzene (10 μL 1,4-dimethoxybenzene in THF-d_8 (0.100 g/mL) stock solution, 0.0072 mmol) was added as internal standard. ^{1}H NMR (400 MHz, THF-d_8): ethane δ (ppm) 0.85 (CH_3); ethylene δ (ppm) 5.36 (s); propionitrile δ (ppm) 2.35 (q, J = 7.6 Hz, 2H, CH_2CN), 1.20 (t, J = 7.6 Hz, 3H, CH_3CH$_2$); 1,4-dimethoxybenzene δ (ppm) 6.79 (s, 4H, aryl CH), 3.69 (s, 6H, OCH_3).

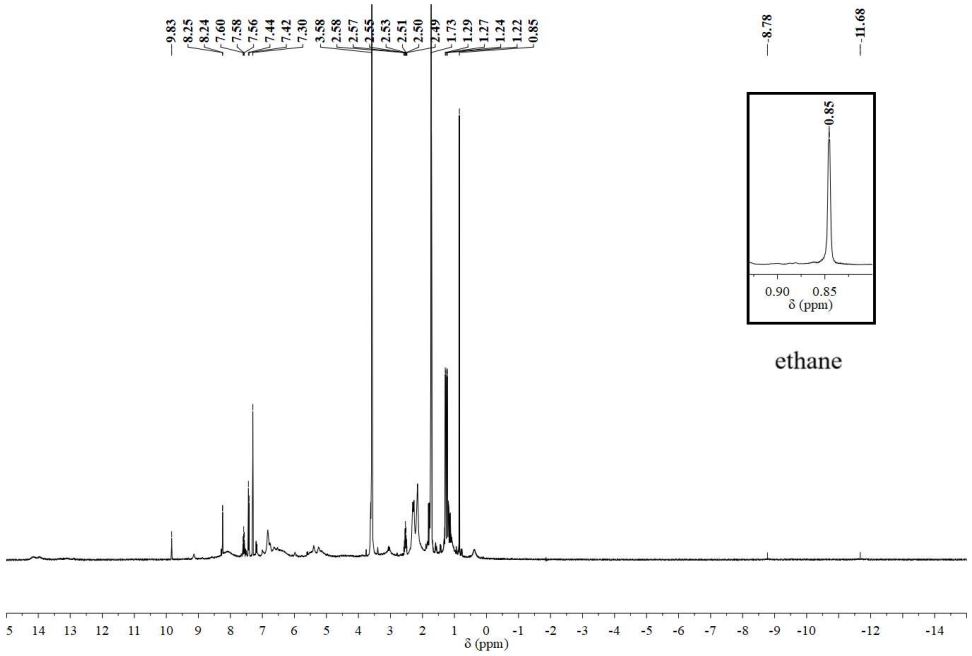

Figure 4.33. ^{1}H NMR (400 MHz, THF-d_8) spectrum of reaction of **13**[NTf$_2$] with propionitrile. A trace of benzene (δ 7.30 ppm)[16] is present as the result of benzophenone ketyl decomposition.

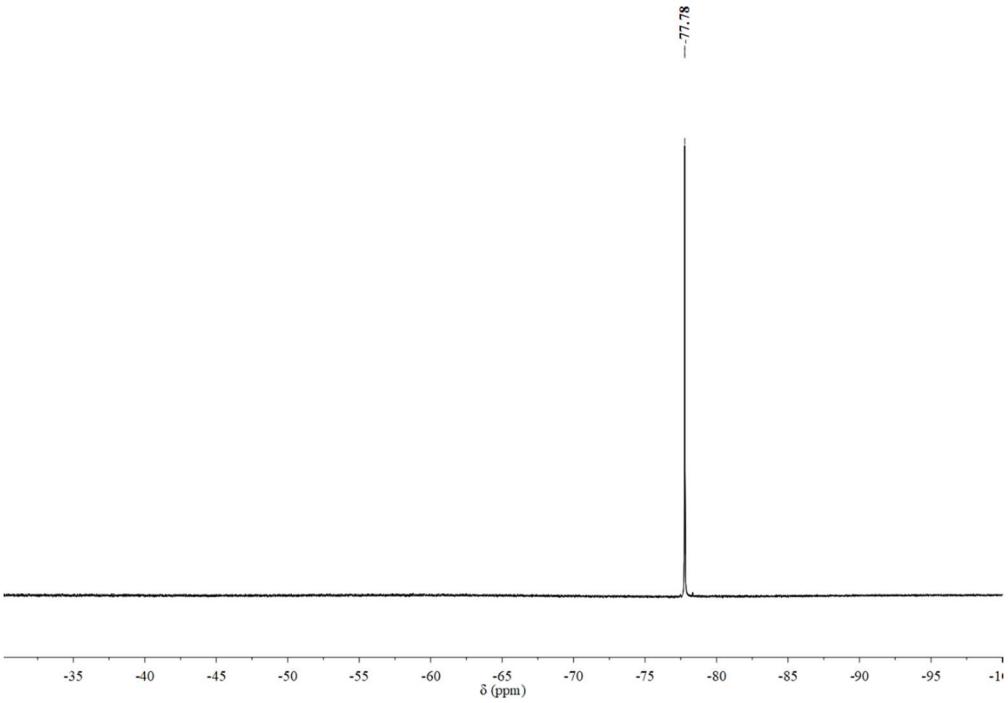

Figure 4.34. ^{19}F NMR (376 MHz, THF-d_8) spectrum of reaction of **13**[NTf_2] with propionitrile.

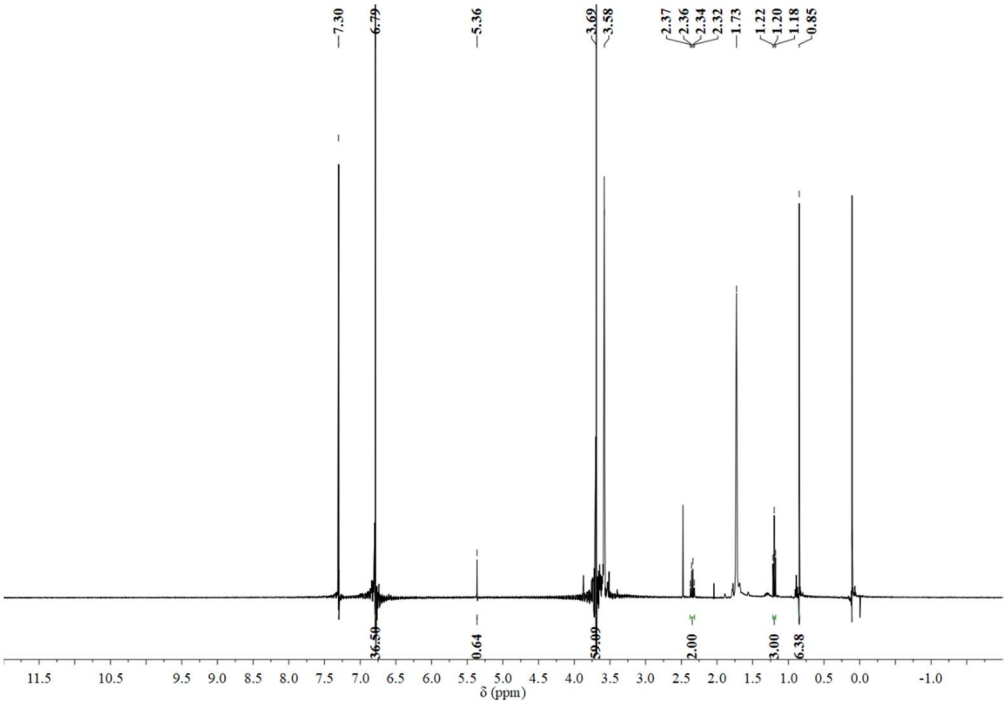

Figure 4.35. ^{1}H NMR (400 MHz, THF-d_8) spectrum of reaction of **13**[NTf_2] with propionitrile after distillation. A trace of benzene (δ 7.30 ppm) [16] is present as the result

of benzophenone ketyl decomposition. 1,4-dimethoxybenzene (0.0010 g, 0.0072 mmol) was added as proton integration standard.

4.4.3.4 Reaction of {[(IDipp)Ni]$_2$(μ-H)}[NTf$_2$] (**13**[NTf$_2$]) with *n*-butyronitrile

In the glovebox, **13**[NTf$_2$] (0.008 g, 0.007 mmol) was dissolved in THF-d_8 (0.5 mL) and transferred into a J. Young tube, and *n*-butyronitrile (0.00048 g, 0.60 μL, 0.0069 mmol) was added. The solution was mixed and the tube was sealed and kept at room temperature. The reddish-brown color changed to brownish-yellow over four days. ^{1}H NMR (400 MHz, THF-d_8): propane δ (ppm) 1.32 (sept, 2H, C*H*$_2$), 0.90 (t, 6H, C*H*$_3$); propene δ (ppm) 5.78 (m, 1H, C*H*), 5.00 (d, *J* = 16.0 Hz, 1H, C*H*$_2$(1)), 4.88 (d, *J* = 9.6 Hz, 1H, C*H*$_2$(2)), 1.69 (br, 3H, C*H*$_3$); ^{19}F NMR (376 MHz, THF-d_8): δ (ppm) –79.63 (s). The reaction was repeated in a 25-mL Schlenk flask and the solution was distilled to a J. Young tube after one freeze-pump-thaw cycle and 1,4-dimethoxybenzene (10 μL 1,4-dimethoxybenzene in THF-d_8 (0.100 g/mL) stock solution, 0.0072 mmol) was added as internal standard. ^{1}H NMR (400 MHz, THF-d_8): *n*-butyronitrile δ (ppm) 2.33 (t, *J* = 7.2 Hz, 2H, C*H*$_2$CN), 1.62 (sext, *J* = 7.2 Hz, 2H, CH$_3$C*H*$_2$), 1.03 (t, *J* = 7.2 Hz, 3H, C*H*$_3$); isobutyronitrile δ (ppm) 2.73 (sept, *J* = 6.8 Hz, 1H, C*H*), 1.25 (d, *J* = 6.8 Hz, 6H, C*H*$_3$); propane δ (ppm) 1.33 (sept, 2H, C*H*$_2$), 0.90 (t, 6H, C*H*$_3$); propene δ (ppm) 5.79 (m, 1H, C*H*), 4.99 (dm, *J* = 16.0 Hz, 1H, C*H*$_2$(1)), 4.89 (dm, *J* = 9.6 Hz, 1H, C*H*$_2$(2)), 1.69 (dt, *J* = 6.4 Hz, 1.6 Hz, 3H, C*H*$_3$); 1,4-dimethoxybenzene δ (ppm) 6.79 (s, 4H, aryl C*H*), 3.69 (s, 6H, OC*H*$_3$).

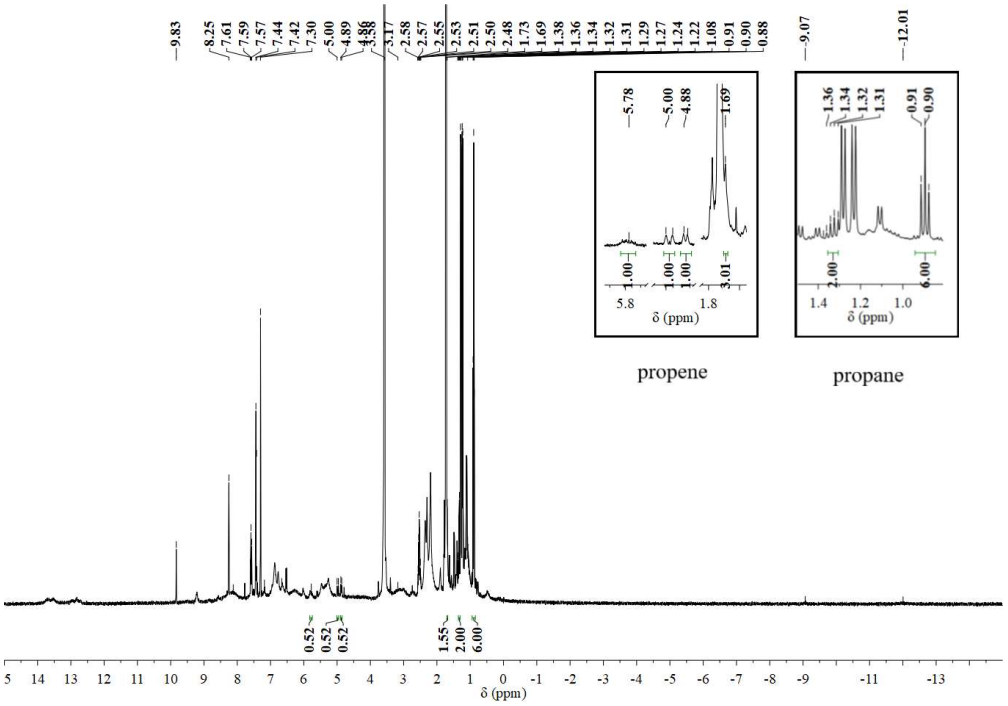

Figure 4.36. ^{1}H NMR (400 MHz, THF-d_8) spectrum of reaction of **13**[NTf_2] with *n*-butyronitrile. A trace of benzene (δ 7.30 ppm)[16] is present as the result of benzophenone ketyl decomposition.

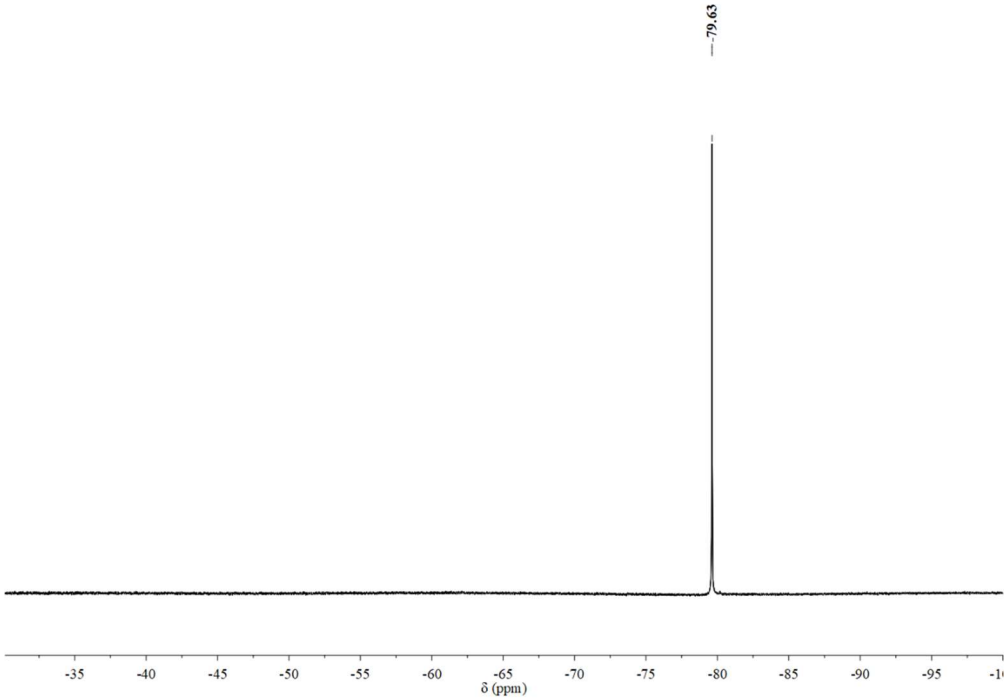

Figure 4.37. ^{19}F NMR (400 MHz, THF-d_8) spectrum of reaction of **13**[NTf_2] with *n*-butyronitrile.

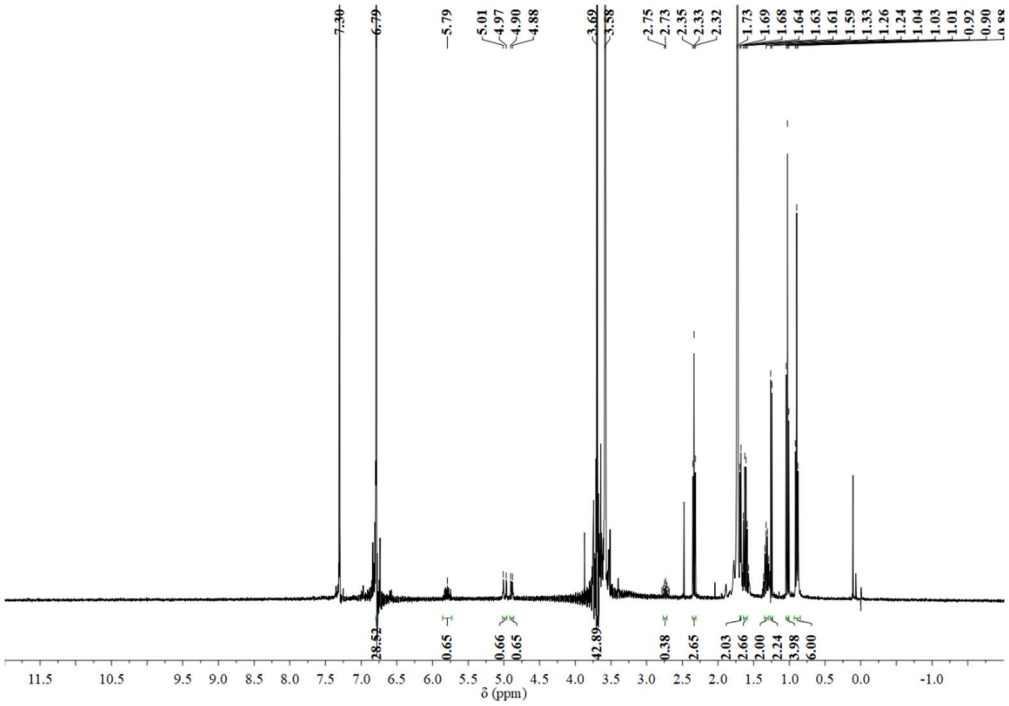

Figure 4.38. ^{1}H NMR (400 MHz, THF-d_8) spectrum of reaction of **13**[NTf_2] with *n*-butyronitrile after distillation. A trace of benzene (δ 7.30 ppm)[16] is present as the result of benzophenone ketyl decomposition. 1,4-dimethoxybenzene (0.0010 g, 0.0072 mmol) was added as proton integration standard.

4.4.3.5 Reaction of {[(IDipp)Ni]$_2$(μ-H)}[NTf_2] (**13**[NTf_2]) with isobutyronitrile

In the glovebox, **13**[NTf_2] (0.008 g, 0.007 mmol) was dissolved in THF-d_8 (0.5 mL) and transferred into a J. Young tube, and isobutyronitrile (0.00046 g, 0.60 μL, 0.0067 mmol) was added. The solution was mixed and the tube was sealed and kept at room temperature. The reddish-brown color changed to brownish-yellow over four days. ^{1}H NMR (400 MHz, THF-d_8): propane δ (ppm) 1.32 (sept, 2H, CH_2, overlap with paramagnetic species), 0.89 (t, 6H, CH_3); propene δ (ppm) 5.78 (m, 1H, CH), 5.00 (d, J = 16.0 Hz, 1H, CH_2(1)), 4.88 (d, J = 9.6 Hz, 1H, CH_2(2)), 1.69 (br, 3H, CH_3); ^{19}F NMR (376 MHz, THF-d_8): δ (ppm) –77.75 (s). The reaction was repeated in a 25-mL Schlenk flask and the solution was distilled to a J. Young tube after one freeze-pump-thaw cycle and 1,4-

dimethoxybenzene (10 μL 1,4-dimethoxybenzene in THF-d_8 (0.100 g/mL) stock solution, 0.0072 mmol) was added as internal standard. ^{1}H NMR (400 MHz, THF-d_8): propane δ (ppm) 1.31 (sept, 2H, CH_2), 0.90 (t, 6H, CH_3); propene δ (ppm) 5.79 (m, 1H, C*H*), 4.99 (d, J = 16.0 Hz, 1H, CH_2(1)), 4.89 (d, J = 9.6 Hz, 1H, CH_2(2)), 1.68 (d, J = 6.4 Hz, 3H, CH_3); *n*-butyronitrile δ (ppm) 2.33 (t, J = 7.2 Hz, 2H, CH_2CN), 1.62 (sext, J = 7.2 Hz, 2H, CH_3CH_2), 1.03 (t, J = 7.2 Hz, 3H, CH_3); isobutyronitrile δ (ppm) 2.73 (sept, J = 6.8 Hz, 1H, C*H*), 1.25 (d, J = 6.8 Hz, 6H, CH_3); 1,4-dimethoxybenzene δ (ppm) 6.79 (s, 4H, aryl C*H*), 3.69 (s, 6H, OCH_3).

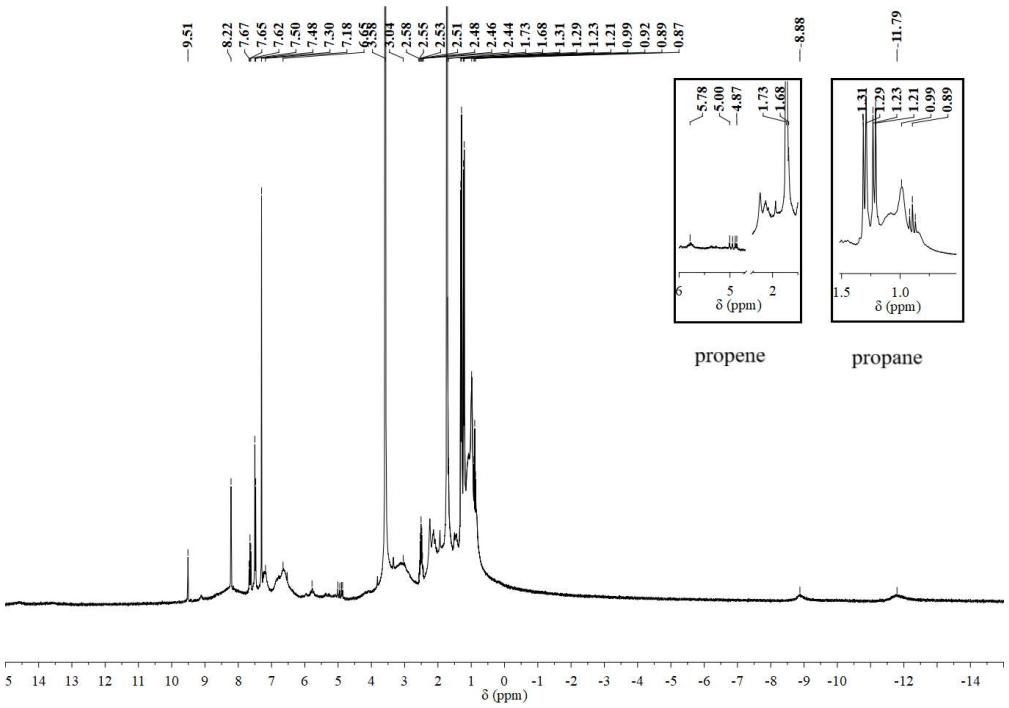

Figure 4.39. ^{1}H NMR (400 MHz, THF-d_8) spectrum of reaction of **13**[NTf_2] with isobutyronitrile. A trace of benzene (δ 7.30 ppm)[16] is present as the result of benzophenone ketyl decomposition.

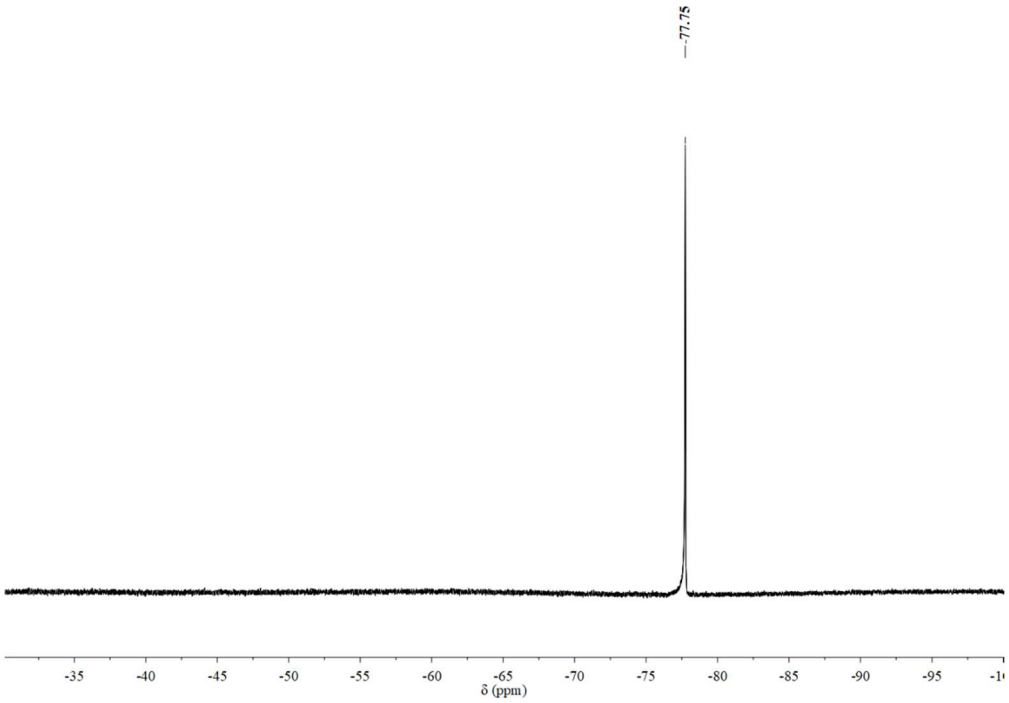

Figure 4.40. ^{19}F NMR (400 MHz, THF-d_8) spectrum of reaction of **13**[NTf_2] with isobutyronitrile.

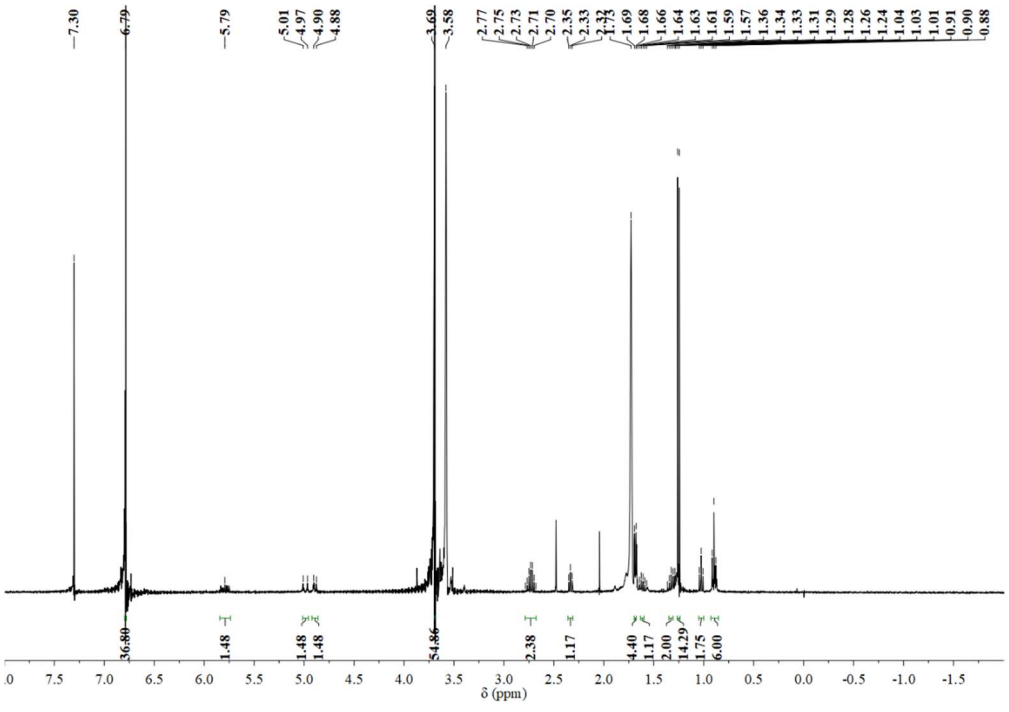

Figure 4.41. ^{1}H NMR (400 MHz, THF-d_8) spectrum of reaction of **13**[NTf_2] with isobutyronitrile after distillation. A trace of benzene (δ 7.30 ppm)[16] is present as the result

of benzophenone ketyl decomposition. 1,4-dimethoxybenzene (0.0010 g, 0.0072 mmol) was added as proton integration standard.

4.4.3.6 Reaction of {[(IDipp)Ni]$_2$(μ-H)}[NTf$_2$] (**13**[NTf$_2$]) with hexanenitrile

In the glovebox, **13**[NTf$_2$] (0.008 g, 0.007 mmol) was dissolved in THF-d_8 (0.5 mL) and transferred into a J. Young tube, and hexanenitrile (0.00065 g, 0.80 μL, 0.0067 mmol) was added. The solution was mixed and the tube was sealed and kept at room temperature. The reddish-brown color changed to brownish-yellow over seven days. ^{1}H NMR (400 MHz, THF-d_8): *n*-pentane δ (ppm) 1.32 (m, 6H, CH_2), 0.88 (t, 6H, CH_3); ^{19}F NMR (376 MHz, THF-d_8): δ (ppm) –79.54 (s). The reaction was repeated in a 25-mL Schlenk flask and the solution was distilled to a J. Young tube after one freeze-pump-thaw cycle and 1,4-dimethoxybenzene (10 μL 1,4-dimethoxybenzene in THF-d_8 (0.100 g/mL) stock solution, 0.0072 mmol) was added as internal standard. ^{1}H NMR (700 MHz, THF-d_8): *n*-pentane δ (ppm) 1.31 (m, 6H, CH_2), 0.89 (t, 6H, CH_3); hexanenitrile δ (ppm) 2.35 (t, J = 7.0 Hz, 2H, CH_2CN), 1.60 (m, 2H, CH$_3$CH_2, overlap), 1.39 (m, 4H, CH$_2$CH_2CH_2CH$_2$CN), 0.92 (t, J = 7.0 Hz, 3H, CH_3); *sec*-pentylnitrile δ (ppm) 1.58 (d, J = 5.6 Hz, 3H, CH_3CHCN), 1.26 (m, 4H, CH$_3$ CH_2CH_2), 0.94 (t, 3H, CH_3CH$_2$, overlap); *trans*-2-pentene δ (ppm) 5.40 (m, 2H, CH=CH), 1.96 (quin of quartets, J = 7.7 Hz, 1.4 Hz, 2H, CH$_3$CH_2), 1.61 (dq, J = 5.6 Hz, 1.4 Hz, 3H, CHCH_3), 0.94 (t, J = 7.7 Hz, 3H, CH_3CH); 1-pentene δ (ppm) 5.79 (m, 1H, CH), 4.97 (dm, J = 17.5 Hz, 1H, CH_2(1)), 4.91 (dm, J = 10.5 Hz, 1H, CH_2(2)), (CH_2)$_2$CH_3 overlap; 1,4-dimethoxybenzene δ (ppm) 6.79 (s, 4H, aryl CH), 3.69 (s, 6H, OCH_3).

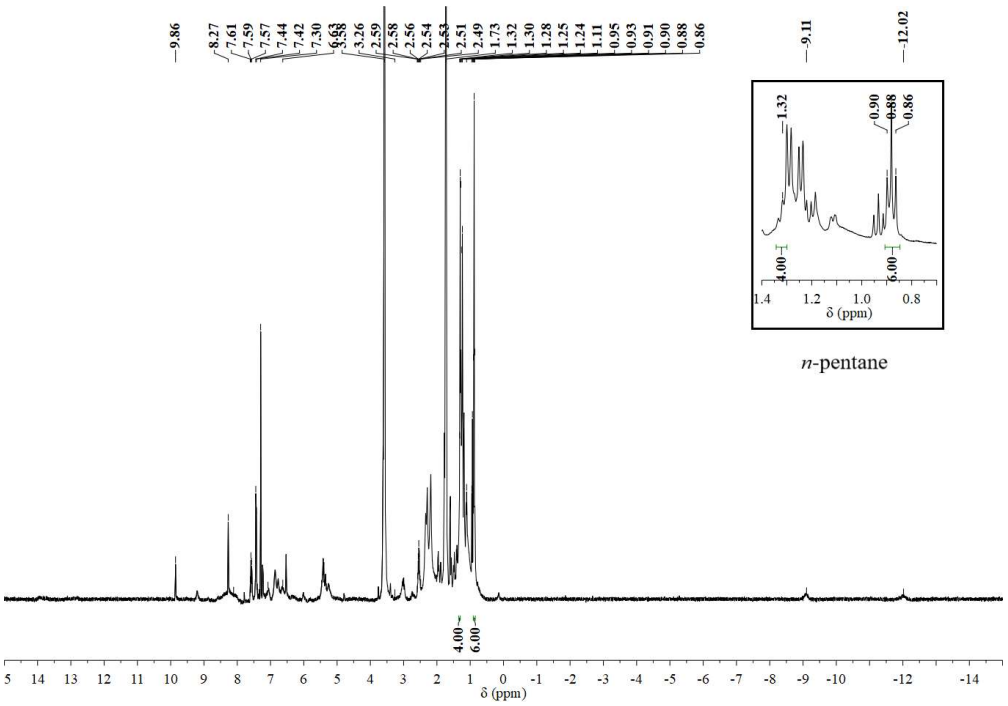

Figure 4.42. ^{1}H NMR (400 MHz, THF-d_8) spectrum of reaction of **13**[NTf_2] with hexanenitrile. A trace of benzene (δ 7.30 ppm)[16] is present as the result of benzophenone ketyl decomposition.

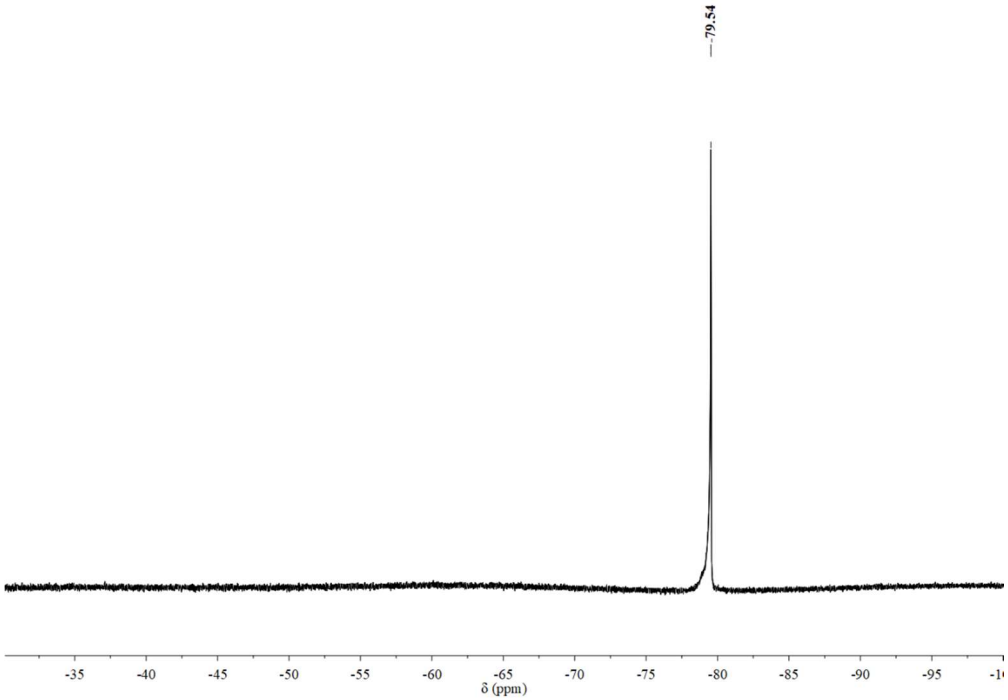

Figure 4.43. ^{19}F NMR (376 MHz, THF-d_8) spectrum of reaction of **13**[NTf_2] with hexanenitrile.

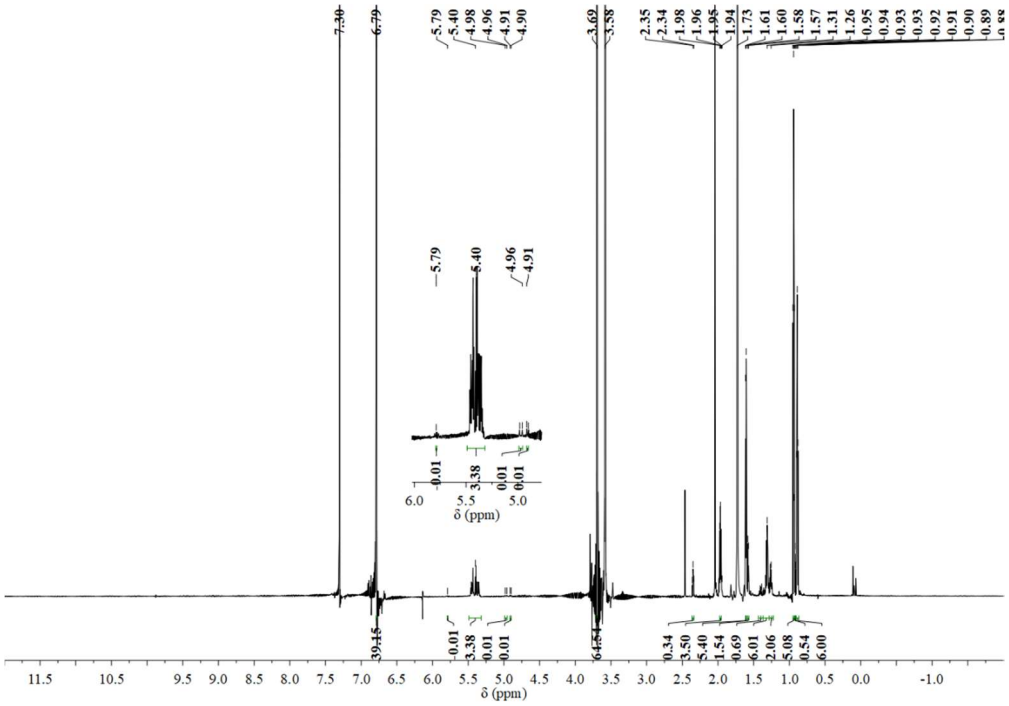

Figure 4.44. ^{1}H NMR (700 MHz, THF-d_8) spectrum of reaction of **13**[NTf$_2$] with hexanenitrile after distillation. A trace of benzene (δ 7.30 ppm) [16] is present as the result of benzophenone ketyl decomposition. 1,4-dimethoxybenzene (0.0010 g, 0.0072 mmol) was added as proton integration standard.

4.4.3.7 Reaction of {[(IDipp)Ni]$_2$(μ-H)}[NTf$_2$] (**13**[NTf$_2$]) with phenylacetonitrile

In the glovebox, **13**[NTf$_2$] (0.008 g, 0.007 mmol) was dissolved in THF-d_8 (0.5 mL) and transferred into a J. Young tube, and phenylacetonitrile (0.00081 g, 0.80 μL, 0.0069 mmol) was added. The solution was mixed and the tube was sealed and kept at room temperature. The reddish-brown color changed to brownish-yellow over three days. ^{1}H NMR (400 MHz, THF-d_8): toluene δ (ppm) 7.18 (m, 2H, C$_6H_5$, overlap with paramagnetic species), 7.11 (m, 3H, C$_6H_5$, overlap with paramagnetic species), 2.30 (s, 3H, CH_3); ^{19}F NMR (376 MHz, THF-d_8): δ (ppm) –79.60 (s). The reaction was repeated in a 25-mL Schlenk flask and the solution was distilled to a J. Young tube after one freeze-pump-thaw

cycle and 1,4-dimethoxybenzene (10 µL 1,4-dimethoxybenzene in THF-d_8 (0.100 g/mL) stock solution, 0.0072 mmol) was added as internal standard. ^{1}H NMR (400 MHz, THF-d_8): toluene δ (ppm) 7.18 (m, 2H, C_6H_5, overlap with paramagnetic species), 7.11 (m, 3H, C_6H_5, overlap with paramagnetic species), 2.30 (s, 3H, CH_3); 1,4-dimethoxybenzene δ (ppm) 6.79 (s, 4H, aryl C*H*), 3.69 (s, 6H, OCH_3).

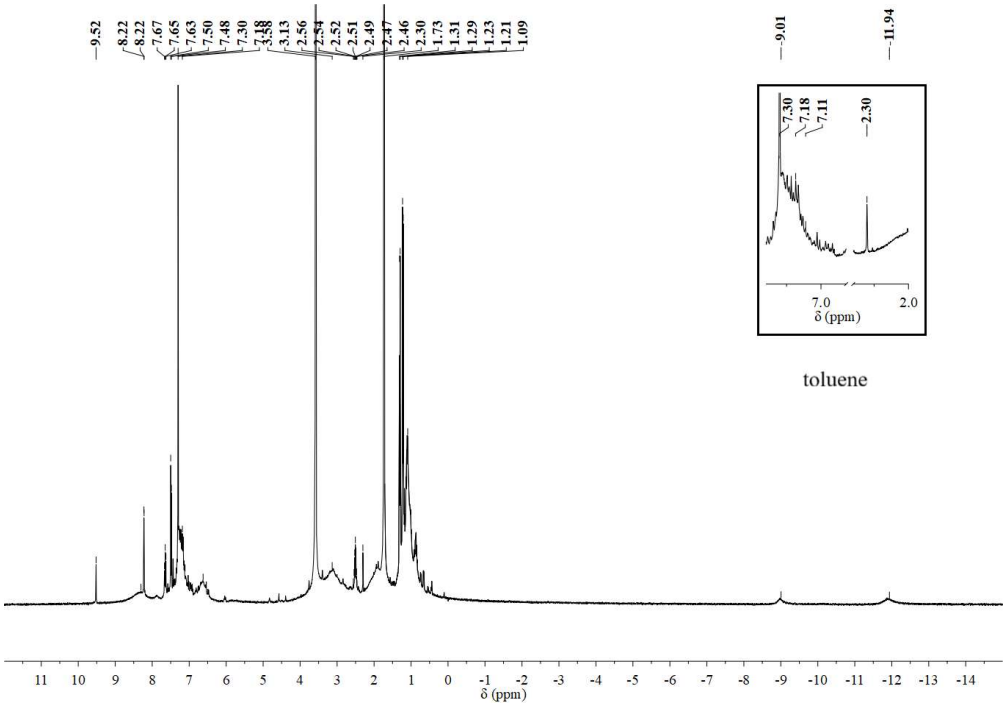

Figure 4.45. ^{1}H NMR (400 MHz, THF-d_8) spectrum of reaction of **13**[NTf_2] with phenylacetonitrile. A trace of benzene (δ 7.30 ppm)[16] is present as the result of benzophenone ketyl decomposition.

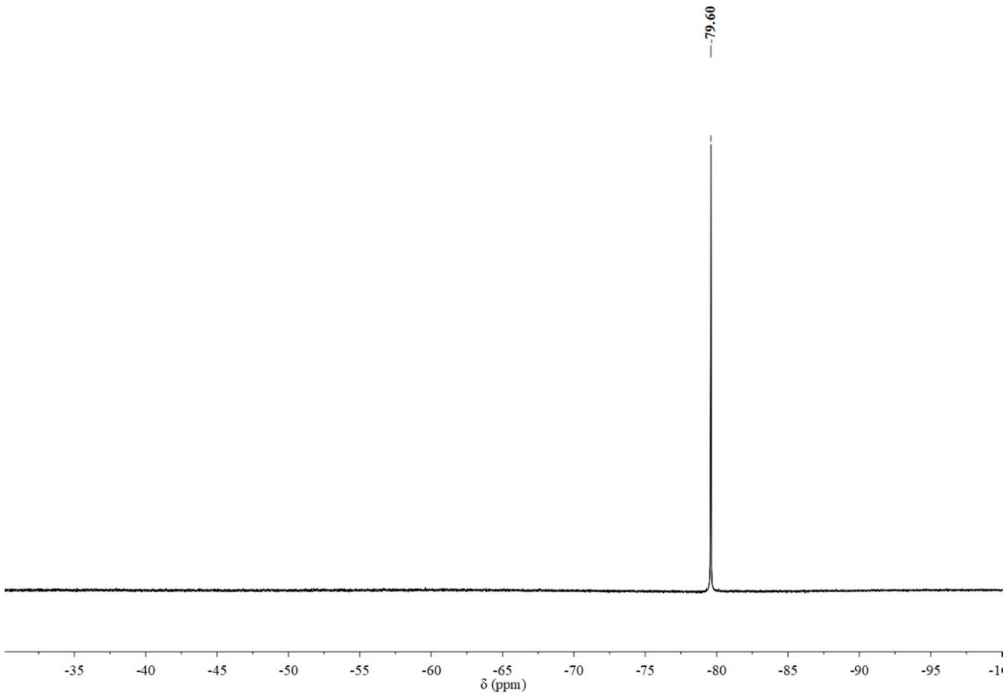

Figure 4.46. ^{19}F NMR (376 MHz, THF-d_8) spectrum of reaction of **13**[NTf_2] with phenylacetonitrile.

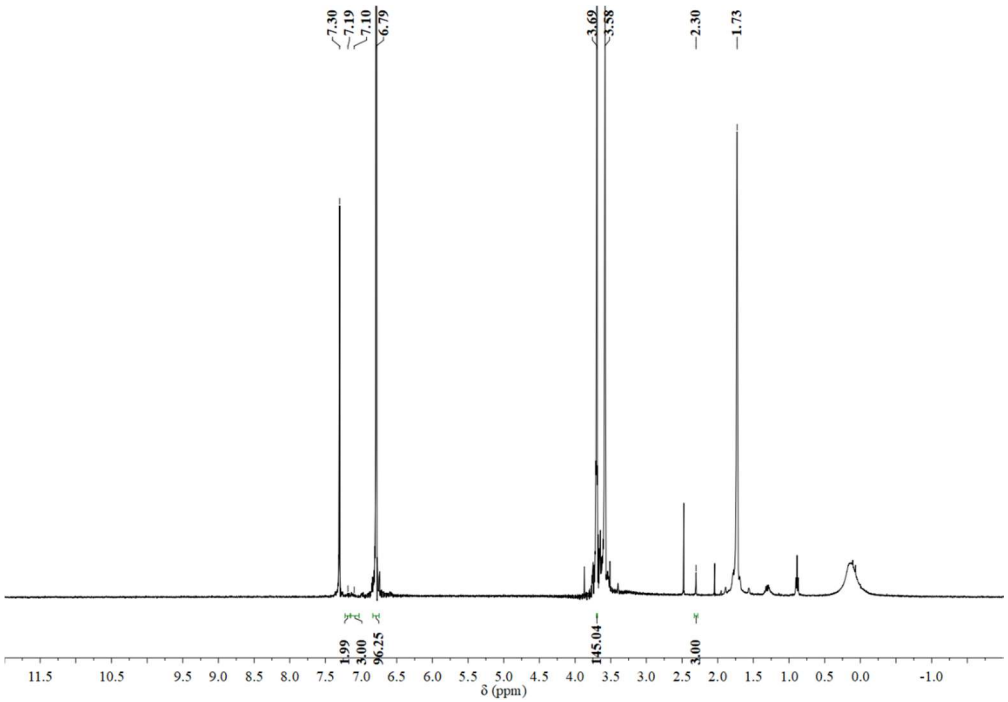

Figure 4.47. ^{1}H NMR (400 MHz, THF-d_8) spectrum of reaction of **13**[NTf_2] with phenylacetonitrile. A trace of benzene (δ 7.30 ppm)[16] is present as the result of benzophenone ketyl decomposition. 1,4-dimethoxybenzene (0.0010 g, 0.0072 mmol) was added as proton integration standard.

4.4.3.8 Reaction of {[(IDipp)Ni]$_2$(μ-H)}[NTf$_2$] (**13**[NTf$_2$]) with *p*-tolunitrile

In the glovebox, **13**[NTf$_2$] (0.008 g, 0.007 mmol) was dissolved in THF-d_8 (0.5 mL) and transferred into a J. Young tube, and *p*-tolunitrile (0.00078 g, 0.80 μL, 0.0067 mmol) was added. The solution was mixed and the tube was sealed and kept at room temperature. The reddish-brown color changed to brownish-yellow over 30 minutes. ^{1}H NMR (400 MHz, THF-d_8): toluene δ (ppm) 7.20-7.06 (m, 5H, C$_6H_5$), 2.31 (t, 3H, CH_3); ^{19}F NMR (376 MHz, THF-d_8): δ (ppm) –79.56 (s). The reaction was repeated in a 25-mL Schlenk flask and the solution was distilled to a J. Young tube after one freeze-pump-thaw cycle and 1,4-dimethoxybenzene (1.0 μL 1,4-dimethoxybenzene in THF-d_8 (0.100 g/mL) stock solution, 0.00072 mmol) was added as internal standard. ^{1}H NMR (400 MHz, THF-d_8): toluene δ (ppm) 7.19-7.08 (m, 5H, C$_6H_5$), 2.31 (t, 3H, CH_3); 1,4-dimethoxybenzene δ (ppm) 6.79 (s, 4H, aryl C*H*), 3.70 (s, 6H, OCH_3).

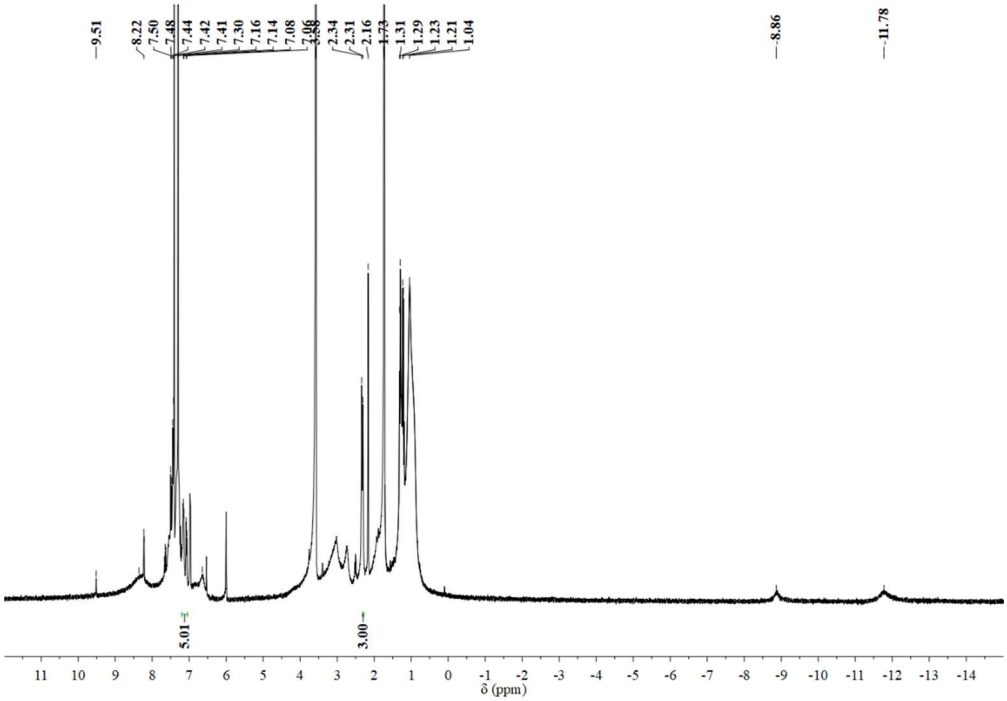

Figure 4.48. ^{1}H NMR (400 MHz, THF-d_8) spectrum of reaction of **13**[NTf$_2$] with *p*-tolunitrile. A trace of benzene (δ 7.30 ppm)[16] is present as the result of benzophenone ketyl decomposition.

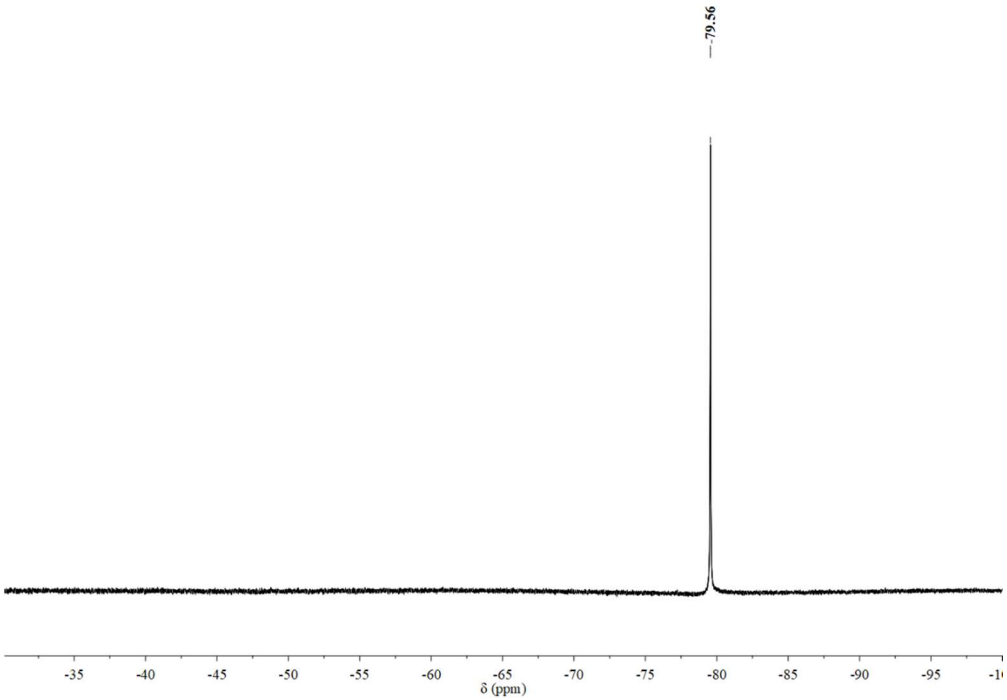

Figure 4.49. ^{19}F NMR (376 MHz, THF-d_8) spectrum of reaction of **13**[NTf_2] with *p*-tolunitrile.

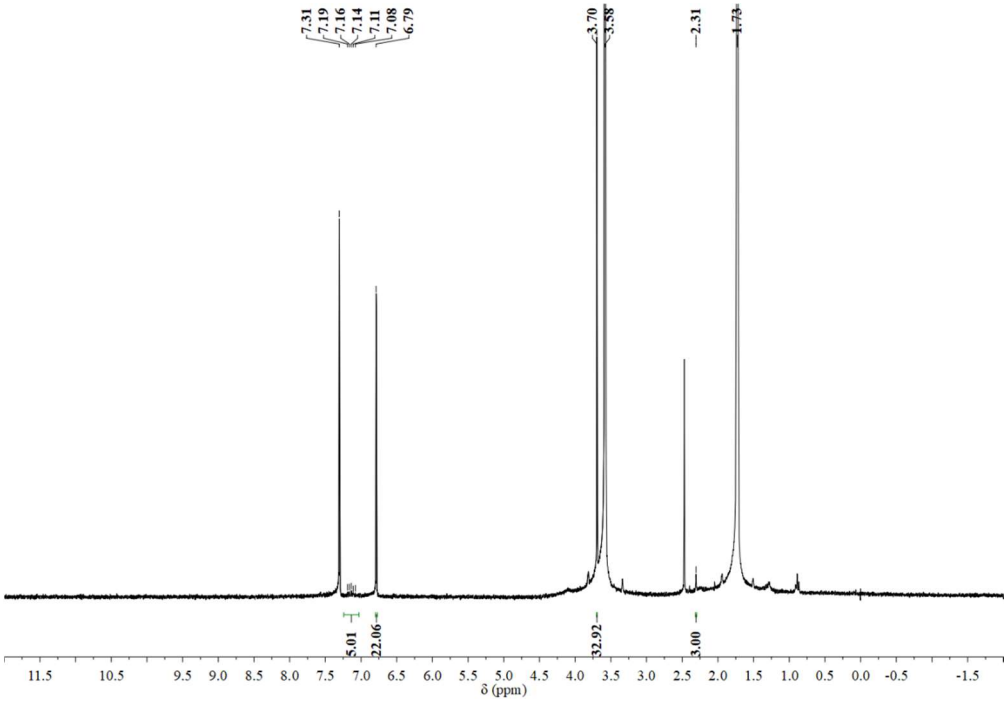

Figure 4.50. ^{1}H NMR (400 MHz, THF-d_8) spectrum of reaction of **13**[NTf_2] with *p*-tolunitrile after distillation. A trace of benzene (δ 7.30 ppm) [16] is present as the result of benzophenone ketyl decomposition. 1,4-dimethoxybenzene (0.00010 g, 0.00072 mmol) was added as proton integration standard.

4.4.3.9 Hydrogen abstraction from {[(IDipp)Ni]$_2$(μ-H)}[NTf$_2$] (**13**[NTf$_2$])

In the glovebox, **13**[NTf$_2$] (0.010 g, 0.0085 mmol) was dissolved in THF-d_8 (0.5 mL) and transferred into a J. Young tube. 2,4,6-Tri-*tert*-butylphenoxyl radical (0.002 g, 0.008 mmol) was added into the solution. The solution was mixed and kept at room temperature for 18 h. ^{1}H NMR (300 MHz, THF-d_8): 2,4,6-tri-*tert*-butylphenol δ (ppm) 7.16 (s, 2H, aryl *H*), 5.89 (s, 1H, O*H*), 1.42 (s, 18H, C(C*H*$_3$)$_3$), 1.27 (s, 9H, C(C*H*$_3$)$_3$); [(IDipp)Ni]$_2$[NTf$_2$] (**15**[NTf$_2$]) δ (ppm) 7.18 (br), 6.63 (br), 3.11 (br), 1.10 (br); [(IDipp)$_2$Ni][NTf$_2$] (**16**[NTf$_2$]) δ (ppm) 8.30 (br), –8.85 (br), –11.77 (br); ^{19}F NMR (376 MHz, THF-d_8): δ (ppm) –79.66 (s).

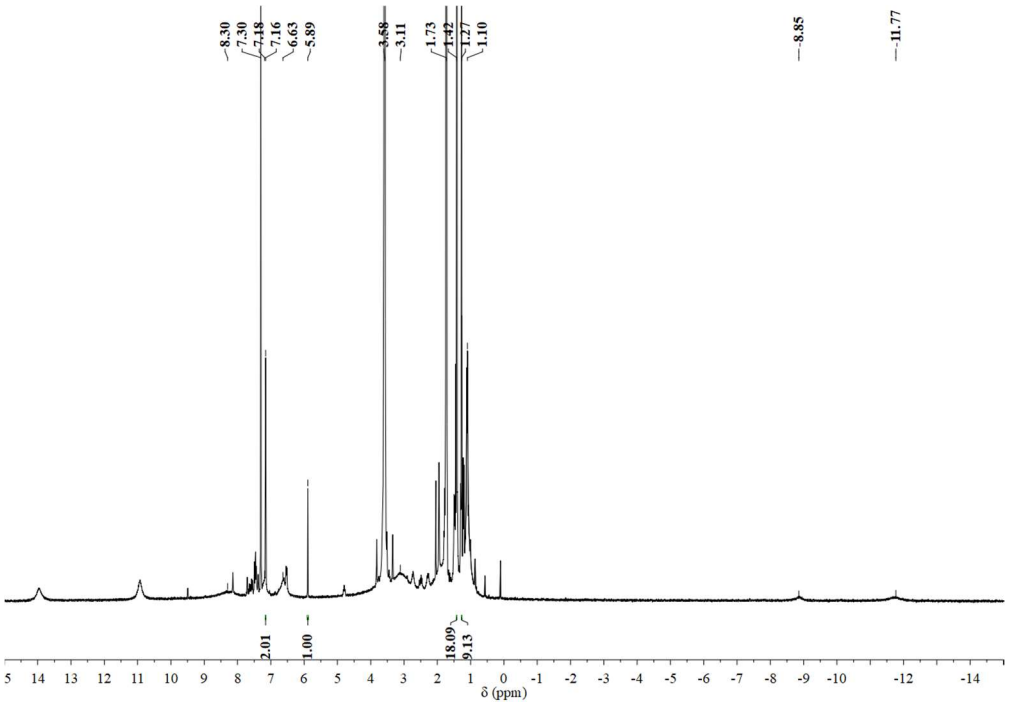

Figure 4.51. ^{1}H NMR (300 MHz, THF-d_8) spectrum of reaction of **13**[NTf$_2$] with 2,4,6-tri-*tert*-butylphenoxyl radical. A trace of benzene (δ 7.30 ppm)[16] is present as the result of benzophenone ketyl decomposition.

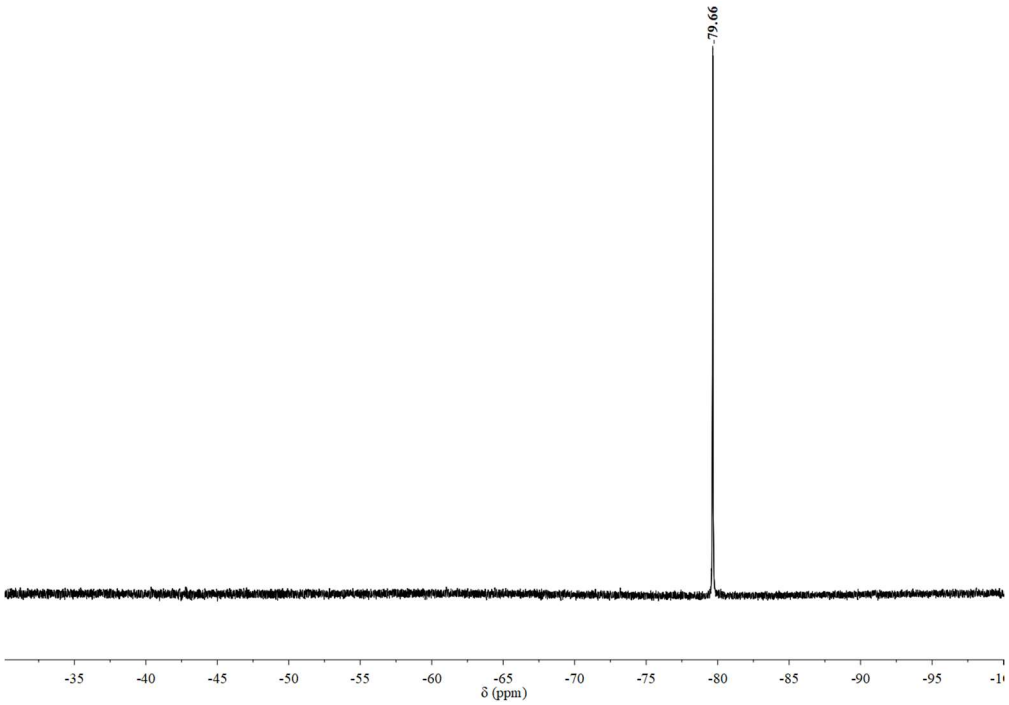

Figure 4.52. ^{19}F NMR (376 MHz, THF-d_8) spectrum of reaction of **13**[NTf_2] with 2,4,6-tri-*tert*-butylphenoxyl radical.

4.4.3.10 Reaction of {[(IDipp)Ni]$_2$(μ-H)}[OTf] (**13**[OTf]) with carbon monoxide

In the glovebox, **13**[OTf] (0.012 g, 0.011 mmol) was dissolved in THF-d_8 (0.5 mL) and transferred into a J. Young tube. The solution was degassed three times via freeze-pump-thaw and 1 atm CO was added. The reddish-brown color disappeared over 10 mins at room temperature. ^{1}H NMR (300 MHz, THF-d_8): (IDipp)H[OTf] δ (ppm) 9.77 (m, 1H, NC*H*N), 8.26 (d, *J* = 1.8 Hz, 2H, NC*H*), 7.61 (dd, *J* = 8.4 Hz, 7.2 Hz, 2H, *para*-CH), 7.42 (d, *J* = 7.2 Hz, 4H, *meta*-CH), 2.53 (sept, *J* = 6.8 Hz, 4H, C*H*(CH_3)$_2$), 1.29 (d, *J* = 6.8 Hz, 12H, CH(C*H*$_3$)$_2$), 1.23 (d, *J* = 6.8 Hz, 12H, CH(C*H*$_3$)$_2$); [(IDipp)Ni(CO)$_3$] δ (ppm) 7.46 (s, *6*H, *para*-CH and *meta*-CH), 7.32 (s, 2H, NC*H*), 2.71 (sept, *J* = 6.8 Hz, 4H, C*H*(CH_3)$_2$), 1.28 (d, *J* = 6.9 Hz, 12H, CH(C*H*$_3$)$_2$), 1.15 (d, *J* = 6.9 Hz, 12H, CH(C*H*$_3$)$_2$); ^{13}C{^{1}H} NMR

(176 MHz, THF-d_8): [$Ni(CO)_4$] δ (ppm) 192.40 (*C*O); (IDipp)H[OTf] δ (ppm) 146.06 (*ortho-C*), 132.46 (*ipso-C*), 128.83 (*para-C*), 127.54 (N*C*H), 125.19 (*meta-C*), 29.74 (*C*H(CH_3)$_2$), 24.47 (CH(*C*H_3)$_2$), 23.68 (CH(*C*H_3)$_2$); [(IDipp)$Ni(CO)_3$] δ (ppm) 198.00 (N*C*Ni), 196.24 (*C*O), 146.51 (*ortho-C*), 138.44 (*ipso*-C), 130.24 (*para-C*), 128.72 (N*C*H), 124.35 (*meta-C*), 29.11 (*C*H(CH_3)$_2$), 26.20 (CH(*C*H_3)$_2$), 22.74 (CH(*C*H_3)$_2$); ^{19}F NMR (376 MHz, THF-d_8): δ (ppm) –77.47 (s). The solution was evaporated in vacuo and C_6D_6 (0.5 mL) was added into the J. Young tube. The ^{1}H NMR resonances of the product matched the reported values for [(IDipp)$Ni(CO)_3$].[29]

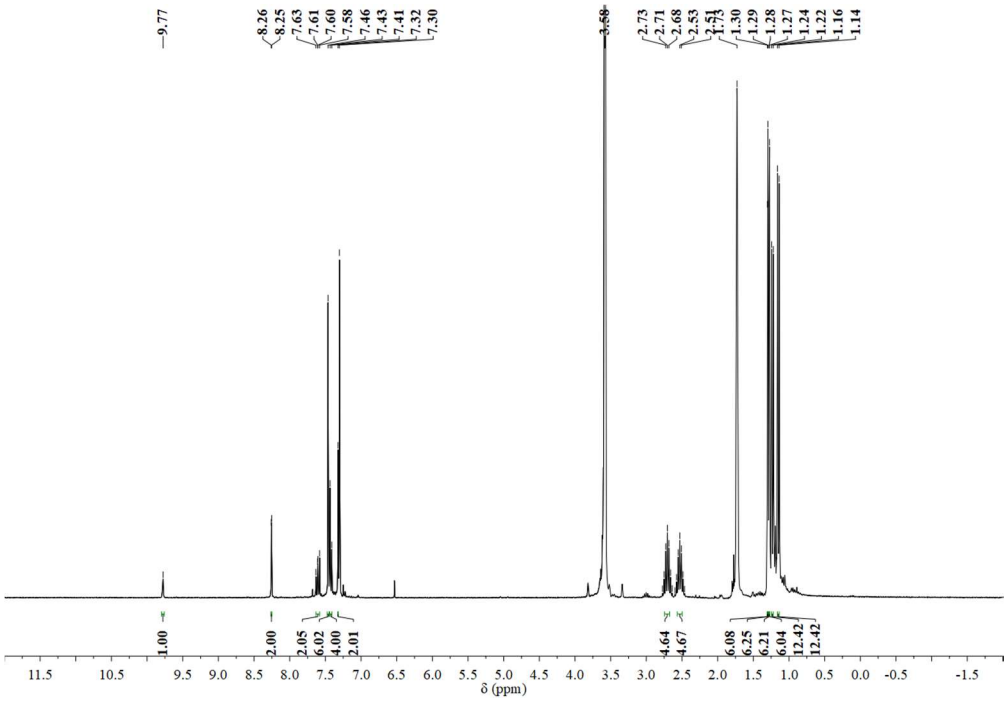

Figure 4.53. ^{1}H NMR (300 MHz, THF-d_8) spectrum of reaction of **13**[OTf] with CO. A trace of benzene (δ 7.30 ppm)[16] is present as the result of benzophenone ketyl decomposition.

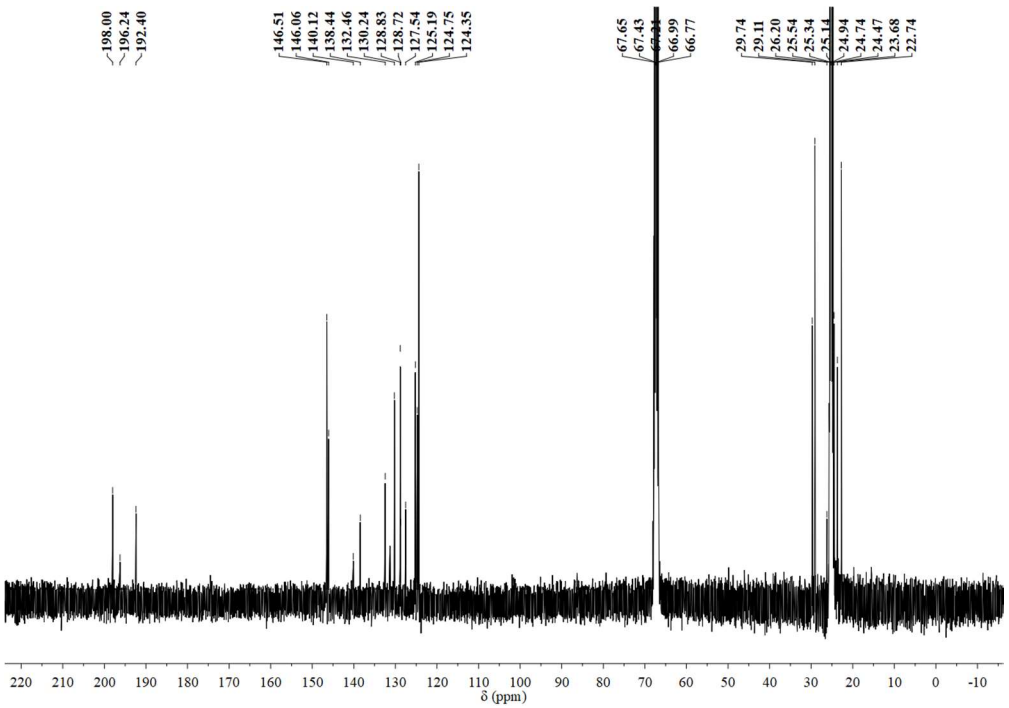

Figure 4.54. $^{13}C\{^{1}H\}$ NMR (176 MHz, THF-d_8) spectrum of reaction of **13**[OTf] with CO. The resonance assigned to $Ni(CO)_4$ (δ 192.40 ppm) matches the reported value.[19]

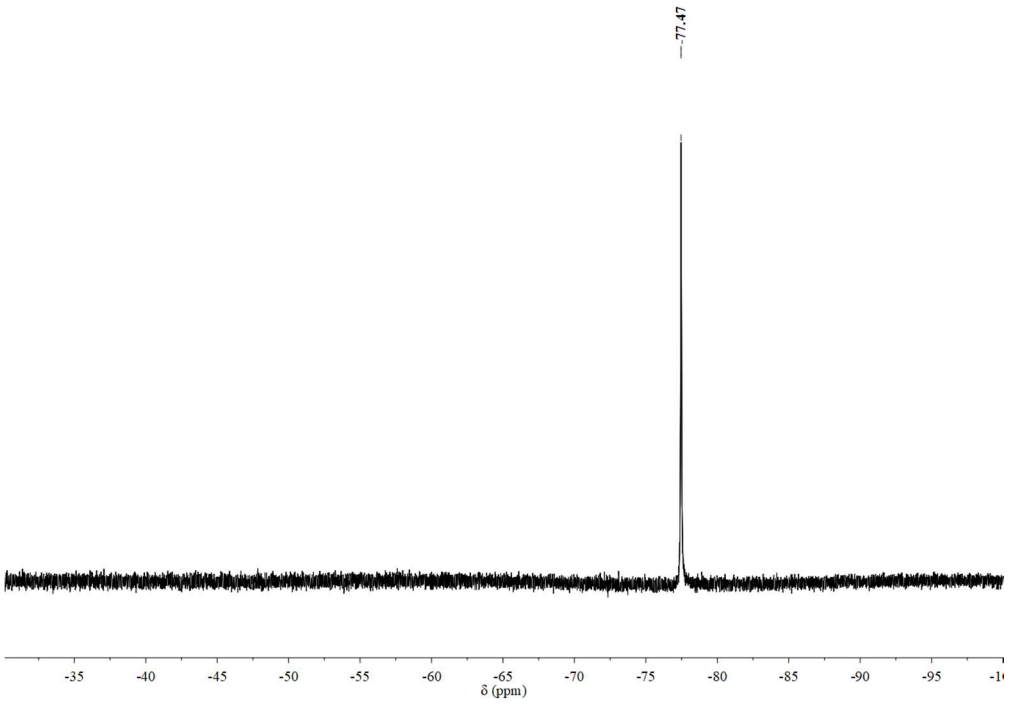

Figure 4.55. ^{19}F NMR (376 MHz, THF-d_8) spectrum of reaction of **13**[OTf] with CO.

4.4.3.11 General procedure for comproportionation of Ni(II) and Ni(0)

In the glovebox, nickel(II) trifluoromethanesulfonate, [(IDipp)$Ni^0(C_6H_6)$] and IDipp were added into THF (5 mL) in a 20-mL scintillation vial. The solution were stirred at room temperature for 16 h, followed by filtered through Celite and evaporated in vacuo to around 1 mL. Pentane (5 mL) was carefully added over the THF solution, the layers were allowed to mix by diffusion at –35 °C overnight, resulting in the formation of a reddish-brown precipitate. The mother liquor was decanted, and the solid was collected on a fritted glass filter. The solid was triturated, then washed with pentane (3 x 1 mL) and dried in vacuo at room temperature for 2 h to afford the product. ^{1}H NMR (400 MHz, THF-d_8): [(IDipp)Ni]$_2$[OTf] (**15**[OTf]) δ (ppm) 7.19 (br), 6.63 (br), 3.17 (br), 1.09 (br); [(IDipp)$_2$Ni][OTf] (**16**[OTf]) δ (ppm) 8.36 (br), –9.12 (br), –12.05 (br); (IDipp)H[OTf] δ (ppm) 9.87 (br, 1H, NC*H*N), 8.31 (s, 2H, NC*H*), 7.61 (t, *J* = 7.6 Hz, 2H, *para*-C*H*), 7.46 (d, *J* = 7.2 Hz, 4H, *meta*-C*H*), 2.57 (sept, *J* = 6.8 Hz, 4H, C*H*(CH_3)$_2$), 1.32 (d, *J* = 6.8 Hz, 12H, CH(C*H*$_3$)$_2$), 1.27 (d, *J* = 6.8 Hz, 12H, CH(C*H*$_3$)$_2$); ^{19}F NMR (376 MHz, THF-d_8): δ (ppm) –76.30 (s).

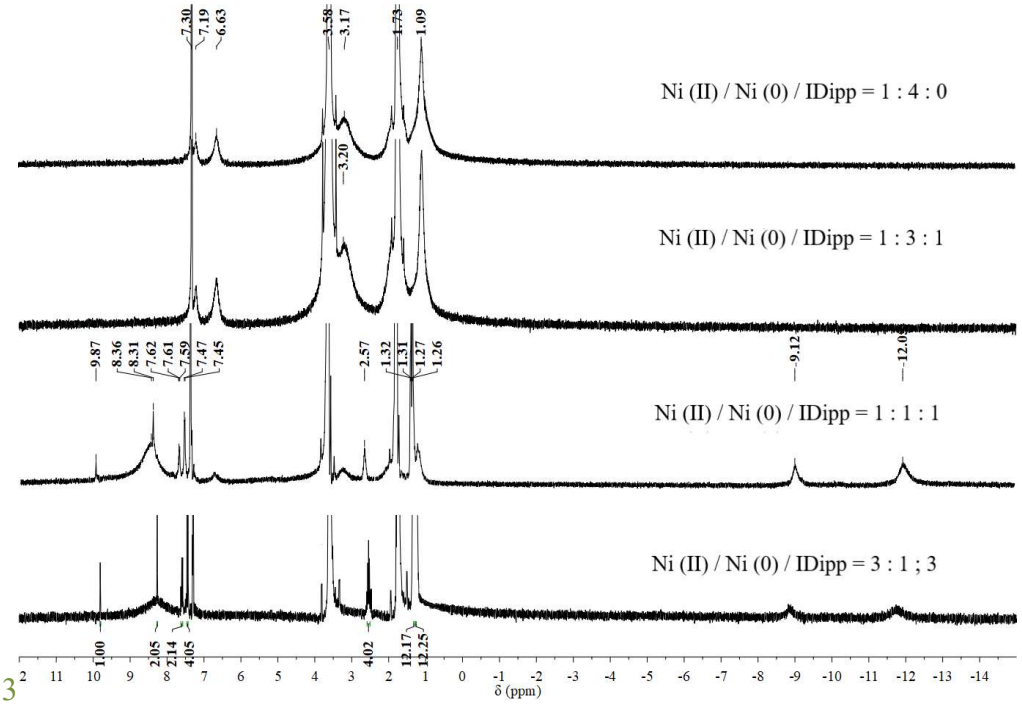

Figure 4.56. ^{1}H NMR (400 MHz, THF-d_8) spectra of comproportionation of Ni(II) and Ni(0) in different ratios. A trace of benzene (δ 7.30 ppm)[16] is present as the result of benzophenone ketyl decomposition.

4.4.3.12 General procedure for one-electron oxidation of two Ni(0) centers

In the glovebox, (IDipp)Ni^{0}(C_6H_6) and oxidant (silver trifluoromethanesulfonate, ferrocenium tetrafluoroborate, ferrocenium hexafluorophosphate or triphenylcarbenium tetrafluoroborate) in a 2:1 ratio were dissolved in THF (5 mL) in a 20-mL scintillation vial. The solutions were stirred at room temperature for 20 h, followed by filtering through Celite and evaporating in vacuo to around 1 mL. Pentane (5 mL) was carefully added over the THF solution, and the layers were allowed to mix by diffusion at –35 °C overnight, resulting in the formation of a brown solid. The mother liquor was decanted, and the solid was collected on a fritted glass filter. The solid was triturated, then washed with pentane (3 x 1 mL) and dried in vacuo at room temperature for 2 h to afford the product. ^{1}H NMR

(300 MHz, THF-d_8): [(IDipp)Ni]$_2$[X] (**15**[X], X = OTf, BF_4 or PF_6) δ (ppm) 7.22 (br), 6.67 (br), 3.17 (br), 1.09 (br); [(IDipp)$_2$Ni][X] (**16**[X], X= OTf, BF_4 or PF_6) δ (ppm) 8.36 (br), –8.87 (br), –11.77 (br); (IDipp)H[X] (X = OTf, BF_4 or PF_6) δ (ppm) 9.87 (br, 1H, NC*H*N), 8.31 (s, 2H, NC*H*), 7.61 (t, *J* = 7.6 Hz, 2H, *para*-C*H*), 7.46 (d, *J* = 7.2 Hz, 4H, *meta*-C*H*), 2.57 (sept, *J* = 6.8 Hz, 4H, C*H*$(CH_3)_2$), 1.32 (d, *J* = 6.8 Hz, 12H, CH(C*H*$_3)_2$), 1.27 (d, *J* = 6.8 Hz, 12H, CH(C*H*$_3)_2$).

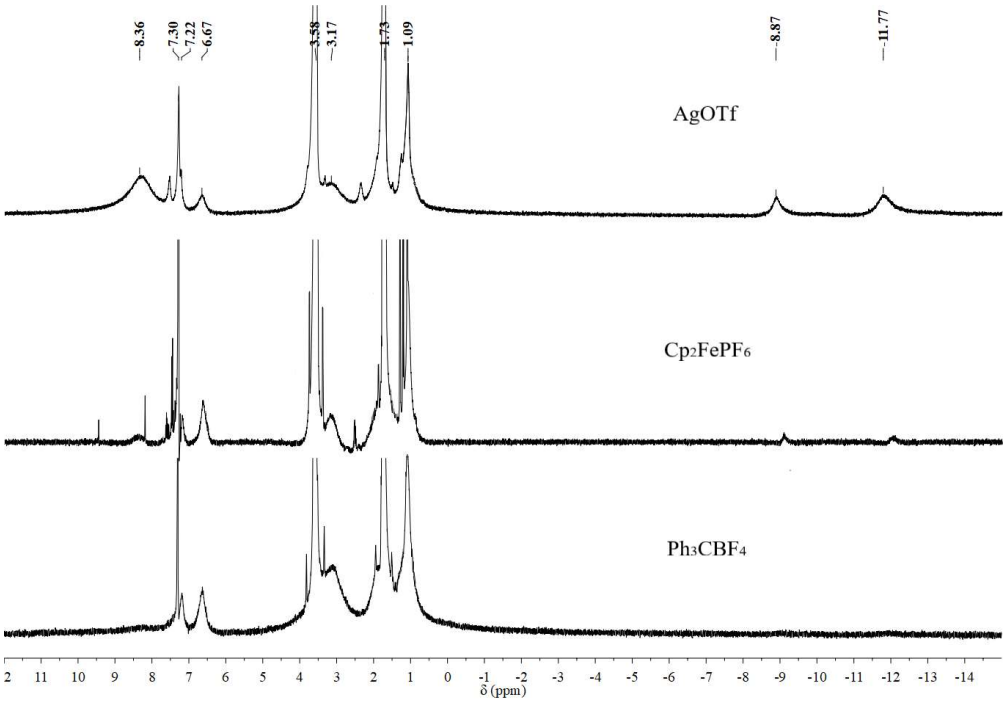

Figure 4.57. ^{1}H NMR (300 MHz, THF-d_8) spectra of oxidation of [(IDipp)Ni^0(C_6H_6)] with oxidants AgOTf, Cp_2FePF_6 and Ph_3CBF_4 in 2:1 ratio. A trace of benzene (δ 7.30 ppm)[16] is present as the result of benzophenone ketyl decomposition.

4.4.3.13 Reactivity of [(IDipp)Ni^0(C_6H_6)] with acetonitrile

In the glovebox, [(IDipp)Ni^0(benzene)] (0.012 g, 0.023 mmol) was dissolved in THF-d_8 (0.5 mL) and transferred into a J. Young tube, and acetonitrile (0.00094 g, 1.2 µL, 0.023 mmol) was added. The solution was mixed and the tube was sealed and kept at room temperature. The brownish-yellow color changed to red over 12 h. The ^{1}H NMR and ^{13}C NMR resonances those reported for [(IDipp)Ni(η^2-MeCN)]$_2$.[22] ^{1}H NMR (400 MHz, THF-d_8): δ (ppm) 7.24 (t, J = 8.0 Hz, 4H, *para*-C*H*), 7.12 (d, J = 8.0 Hz, 8H, *meta*-C*H*), 6.80 (s, 4H, NC*H*), 3.02 (sept, J = 6.8 Hz, 8H, C*H*(CH$_3$)$_2$), 1.23 (d, J = 6.8 Hz, 24H, CH(C*H*$_3$)$_2$), 1.04 (d, J = 6.8 Hz, 24H, CH(C*H*$_3$)$_2$), 0.60 (s, 6H, C*H*$_3$CN); ^{13}C{^{1}H} NMR (176 MHz, THF-d_8): δ (ppm) 199.43 (N*C*Ni), 154.13 (CH$_3$*C*N), 146.54 (*ortho*-*C*), 139.52 (*ipso*-C), 128.76 (*para*-*C*), 123.81 (N*C*H), 123.07 (*meta*-*C*), 28.78 (*C*H(CH$_3$)$_2$), 24.52 (CH(*C*H$_3$)$_2$), 23.85 (CH(*C*H$_3$)$_2$), 8.63 (*C*H$_3$CN).

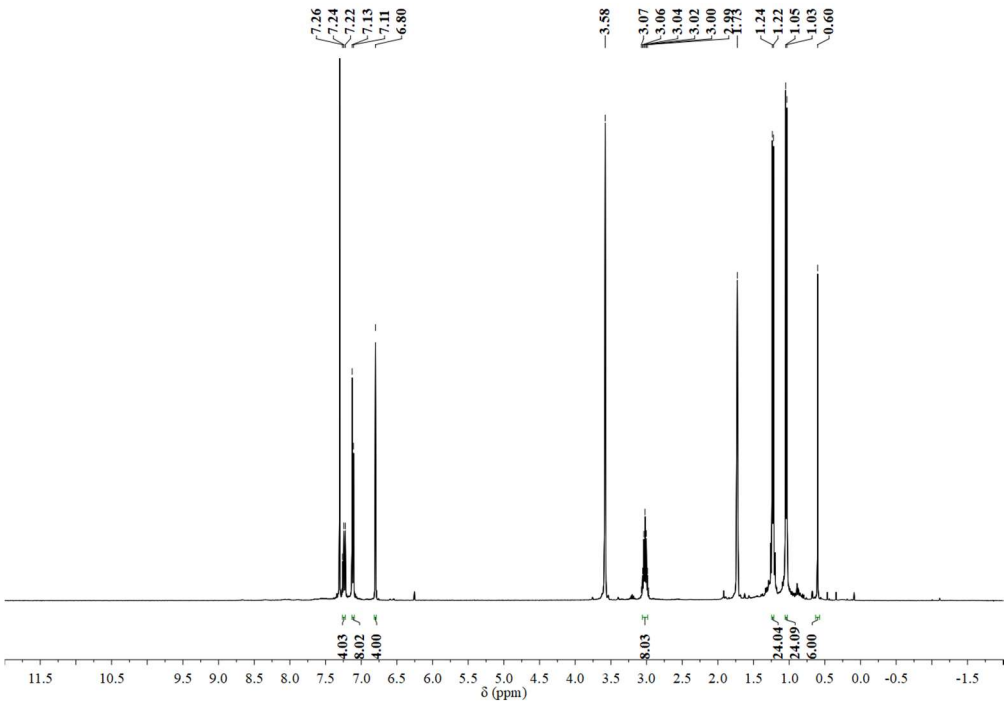

Figure 4.58. ^{1}H NMR (400 MHz, THF-d_8) spectrum of [(IDipp)Ni(η^2-MeCN)]$_2$.

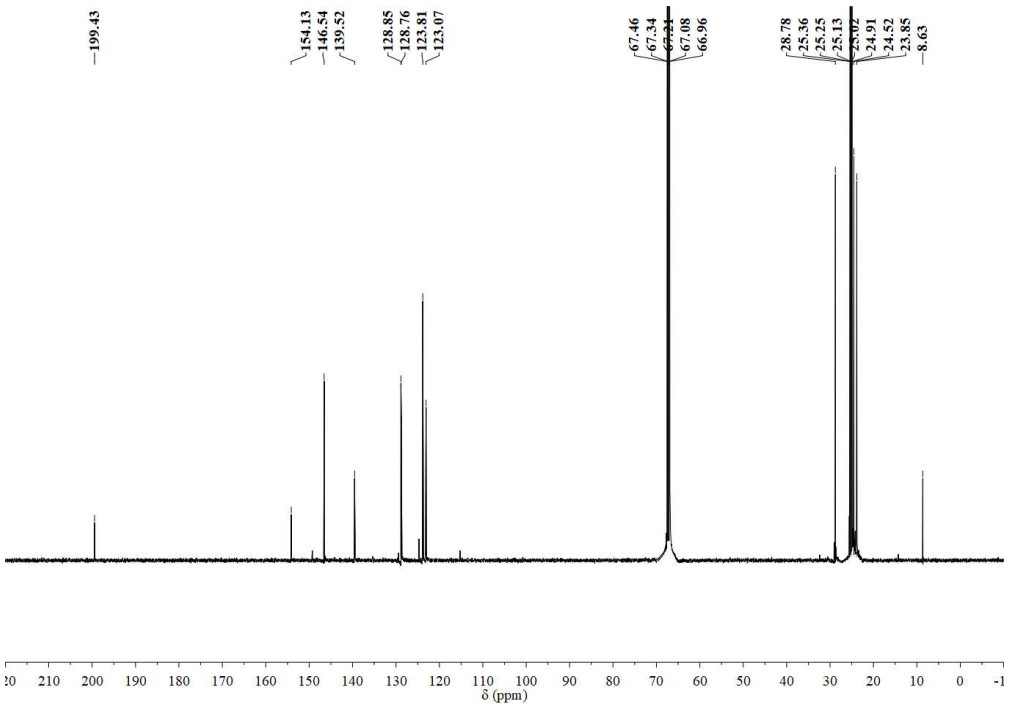

Figure 4.59. $^{13}C\{^{1}H\}$ NMR (176 MHz, THF-d_8) spectrum of [(IDipp)Ni(η^2-MeCN)]$_2$.

4.4.3.14 Reaction of [(IDipp)Ni^0(C_6H_6)] with hexafluorobenzene

In the glovebox, [(IDipp)Ni^0(benzene)] (0.007 g, 0.01 mmol) and hexafluorobenzene (0.0024 g, 1.5 µL, 0.013 mmol) was dissolved in THF (1 mL) in a 20-mL scintillation vial. The solution was stirred at room temperature for 12 h. Pentane (5 mL) was carefully added over the THF solution, and the layers were allowed to mix by diffusion at –35 °C for 1 week, resulting in the formation of yellow crystals. The mother liquor was decanted, and the crystals were collected on a fritted glass filter. The crystals were dried in vacuo at room temperature for 1 h, affording [(IDipp)Ni(µ-C_6F_5)]$_2$ (**17**) as a yellow powder, 0.004 g (50%). ^{1}H NMR (400 MHz, THF-d_8): δ (ppm) 7.20 (t, J = 7.8 Hz, 4H, *para*-CH), 7.04 (d, J = 8.0 Hz, 8H, *meta*-CH), 6.93 (s, 4H, NC*H*) , 3.42 (sept, J = 6.8 Hz, 8H, C*H*(CH_3)$_2$), 1.33 (d, J = 6.8 Hz, 24H, CH(C*H*$_3$)$_2$), 0.91 (d, J = 6.8 Hz, 24H,

$CH(CH_3)_2$); ^{19}F NMR (376 MHz, THF-d_8): δ (ppm) –93.83 (d, J = 33.1 Hz, 4F, *ortho*-F), –153.17 (t, J = 22.2 Hz, 2F, *para*-F), –162.63 (dd, J = 30.1 Hz, 22.6 Hz, 4F, *meta*-F).

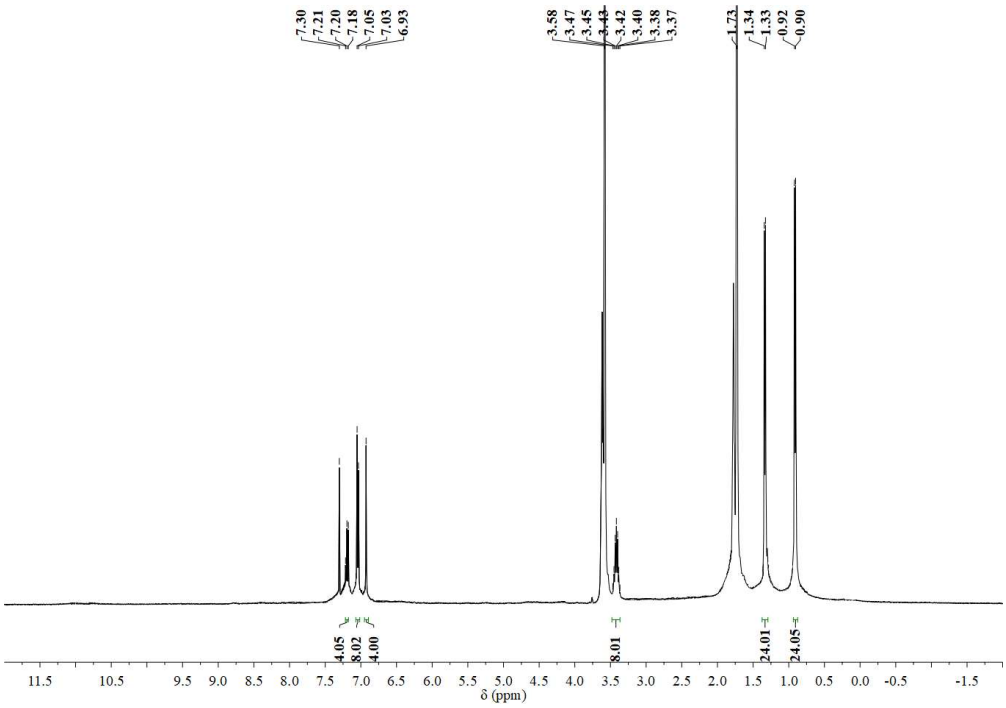

Figure 4.60. ^{1}H NMR (400 MHz, THF-d_8) spectrum of **17**.

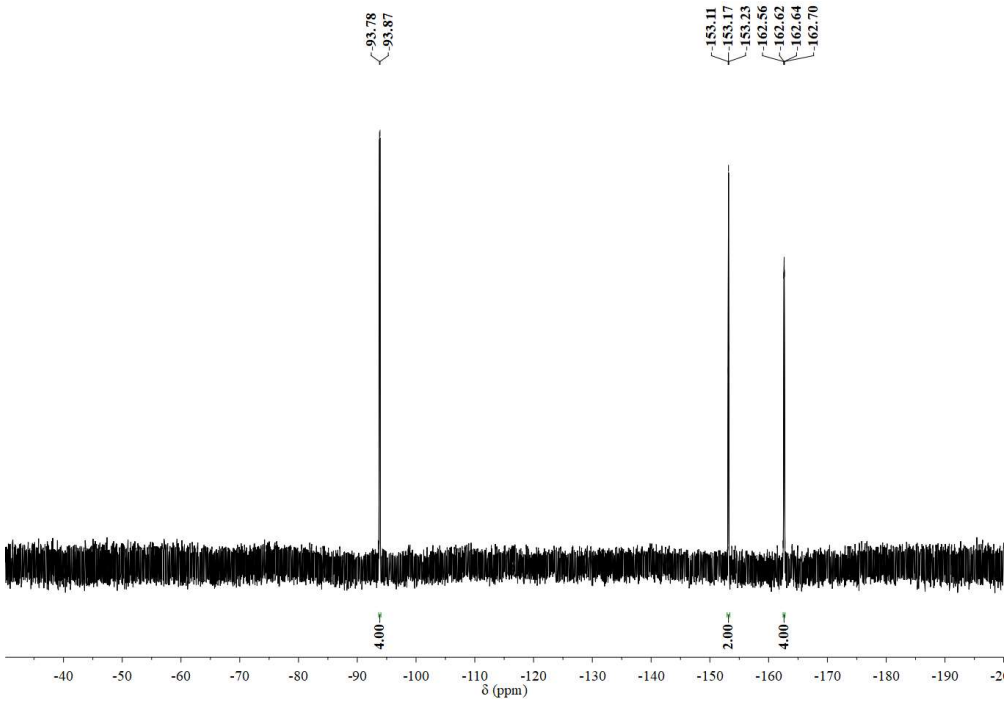

Figure 4.61. ^{19}F NMR (376 MHz, THF-d_8) spectrum of **17**.

4.4.4 X-ray diffraction studies

4.4.4.1 {[(IDipp)Ni]$_2$(μ-H)}[OTf] (**13**[OTf])

Experimental. Diffraction-quality crystals were grown by the diffusion of pentane vapor into a solution of **13**[OTf] in THF at room temperature. A single red needle-shaped crystal (0.32 mm x 0.14 mm x 0.12 mm) was selected and mounted on a loop with Paratone oil on a Bruker D8 VENTURE diffractometer. The crystal was cooled to T = 100(2) K during data collection. The structure was solved with the ShelXT[30] structure solution program using the Intrinsic Phasing solution method and by using Olex2[31] as the graphical interface. The model was refined with version 2014/7 of ShelXL[32] using Least Squares minimization.

Crystal Data for $C_{55}H_{73}F_3N_4Ni_2O_3S$ (M_r = 1044.65 g/mol): monoclinic, $P2_1/c$ (no. 14), a = 12.2859(8) Å, b = 11.0064(7) Å, c = 19.2375(11) Å, β = 99.771(2)°, $\alpha = \gamma$ = 90°, V = 2563.6(3) Å^3, T = 100(2) K, Z = 2, Z' = 0.5, μ(MoK$_\alpha$) = 0.833 mm^{-1}, 51694 reflections measured, 7506 unique (R_{int} = 0.0571) which were used in all calculations. The final wR_2 was 0.1239 (all data) and R_1 was 0.0474 (I > 2σ(I)).

4.4.4.2 [(IDipp)Ni(CN)$_2$]$_4$ (**14**)

Experimental. Diffraction-quality crystals were grown by diffusion of pentane vapor into a solution of reaction of **14**[OTf] with acetonitrile in THF at room temperature. A suitable crystal was selected and mounted on a loop with paratone oil on a Bruker APEX-II CCD diffractometer. The crystal was kept at 100(2) K during data collection. Using Olex2[31], the structure was solved with the ShelXT[30] structure solution program using

Intrinsic Phasing and refined with the ShelXL[32] refinement package using Least Squares minimization.

Crystal Data for $C_{116}H_{144}N_{16}Ni_4$ (M_r = 1997.22 g/mol): monoclinic, $P2_1/n$ (no. 14), a = 19.5394(9) Å, b = 15.8369(8) Å, c = 20.4489(9) Å, β = 104.868(4)°, V = 6115.9(5) Å^3, Z = 2, T = 100(2) K, μ(CuK$_\alpha$) = 1.057 mm^{-1}, D_{calc} = 1.085 g/cm^3, 40799 reflections measured (5.582° ≤ 2Θ ≤ 117.858°), 8589 unique (R_{int} = 0.1227, R_{sigma} = 0.1134) which were used in all calculations. The final R_1 was 0.0855 (I > 2σ(I)) and wR_2 was 0.2410 (all data).

4.4.4.3 [(IDipp)Ni]$_2$[OTf] (**15**[OTf])

Experimental. Diffraction-quality crystals were grown by the diffusion of pentane vapor into a solution of **15**[OTf] in THF at room temperature. A single red prism-shaped crystal (0.21 mm x 0.12 mm x 0.06 mm) was selected and mounted on a loop with Paratone oil on an XtaLAB Synergy, Dualflex, HyPix diffractometer. The crystal was kept at a steady T = 102(3) K during data collection. The structure was solved with the ShelXT[30] structure solution program using the Intrinsic Phasing solution method and by using Olex2[31] as the graphical interface. The model was refined with version 2018/3 of ShelXL-2014[32] using Least Squares minimization.

Crystal Data for $C_{55}H_{72}F_3N_4Ni_2O_3S$ (M_r = 1043.64 g/mol): monoclinic, $P2_1/c$ (no. 14), a = 12.2961(5) Å, b = 10.9882(4) Å, c = 19.2078(8) Å, β = 99.892(4)°, $\alpha = \gamma$ = 90°, V = 2556.62(18) Å^3, T = 102(3) K, Z = 2, Z' = 0.5, μ(MoK$_\alpha$) = 0.835 mm^{-1}, 28318 reflections measured, 5858 unique (R_{int} = 0.0655) which were used in all calculations. The final wR_2 was 0.1350 (all data) and R_1 was 0.0482 (I > 2σ(I)).

4.4.4.4 [(IDipp)$_2$Ni][BF$_4$] (**16**[BF$_4$])

Experimental. Diffraction-quality crystals were grown by the diffusion of pentane vapor into a solution of **16**[BF$_4$] in THF at room temperature. A light yellow needle-shaped crystal (0.51 mm x 0.20 mm x 0.16 mm) was selected and mounted on a loop with paratone oil on a Bruker D8 VENTURE diffractometer. The crystal was kept at a steady T = 100(2) K during data collection. The structure was solved with the ShelXT[30] structure solution program using the Intrinsic Phasing solution method and by using Olex2[31] as the graphical interface. The model was refined with version 2018/3 of ShelXL[32] using Least Squares minimization.

Crystal Data for $C_{58}H_{80}BF_4N_4NiO$ (M_r = 994.76 g/mol): tetragonal, $I4_1cd$ (no. 110), a = 25.9564(12) Å, b = 25.9564(12) Å, c = 32.6252(18) Å, $\alpha = \beta = \gamma = 90^\circ$, V = 21981(2) Å^3, T = 100(2) K, Z = 16, Z' = 1, μ(MoK$_\alpha$) = 0.408 mm^{-1}, 116221 reflections measured, 12604 unique (R_{int} = 0.0776) which were used in all calculations. The final wR_2 was 0.0944 (all data) and R_1 was 0.0418 (I > 2σ(I)).

4.4.4.5 [(IDipp)Ni(μ-C$_6$F$_5$)]$_2$ (**17**)

Experimental. Diffraction-quality crystals were grown by the diffusion of pentane vapor into a solution of **17** in THF at room temperature. A suitable crystal was selected and mounted on a loop with Paratone oil on a Bruker D8 VENTURE diffractometer. The crystal was kept at 100(2) K during data collection. Using Olex2[31], the structure was solved with the ShelXT[30] structure solution program using Intrinsic Phasing and refined with the ShelXL[32] refinement package using Least Squares minimization.

Crystal Data for $C_{66}H_{72}F_{10}N_4Ni_2$ (M_r = 1228.69 g/mol): monoclinic, $P2_1/n$ (no. 14), a = 13.9266(14) Å, b = 11.9612(11) Å, c = 18.8990(16) Å, β = 95.163(3)°, V = 3135.4(5) Å^3, Z = 2, T = 100(2) K, μ(MoK$_\alpha$) = 0.672 mm^{-1}, D_{calc} = 1.301 g/cm^3, 41989 reflections measured (4.328° ≤ 2Θ ≤ 55.01°), 7184 unique (R_{int} = 0.1435, R_{sigma} = 0.1101) used in all calculations. The final R_1 was 0.0554 (I > 2σ(I)) and wR_2 was 0.1175 (all data).

4.5 References

[1] a) P. W. Jolly, *The Organic Chemistry of Nickel*, New York, Academic Press, New York, **1974**; b) L. S. Hegedus, *Coord. Chem. Rev.* **2000**, *204*, 199-307.

[2] a) C. A. Tolman, R. J. McKinney, W. C. Seidel, J. D. Druliner, W. R. Stevens, in *Advances in Catalysis, Vol. 33*, Elsevier, **1985**, pp. 1-46; b) B. Cornils, W. A. Herrmann, *Aqueous-Phase Organometallic Catalysis: Concepts and Applications*, Wiley-VCH, **2004**; c) W. Keim, *Angew. Chem. Int. Ed.* **1990**, *29*, 235-244; d) G. Wilke, *Angew. Chem. Int. Ed.* **1988**, *27*, 185-206; e) W. C. Seidel, C. A. Tolman, *Ann. N.Y. Acad. Sci.* **1983**, *415*, 201; f) M. L. Green, H. Munakata, *J. Chem. Soc., Dalton Trans.* **1974**, 269-272.

[3] a) C. E. Webster, M. Y. Darensbourg, P. A. Lindahl, M. B. Hall, *J. Am. Chem. Soc.* **2004**, *126*, 3410-3411; b) V. Svetlitchnyi, H. Dobbek, W. Meyer-Klaucke, T. Meins, B. Thiele, P. Römer, R. Huber, O. Meyer, *Proc. Natl. Acad. Sci. U. S. A.* **2004**, *101*, 446-451; c) J. L. Craft, Y.-C. Horng, S. W. Ragsdale, T. C. Brunold, *J. Am. Chem. Soc.* **2004**, *126*, 4068-4069; d) A. Volbeda, J. C. Fontecilla-Camps, *Dalton Trans.* **2003**, 4030-4038; e) S. B. Mulrooney, R. P. Hausinger, *FEMS Microbiol. Rev.* **2003**, *27*, 239-261; f) R. P. Hausinger, *Nat. Struct. Biol.* **2003**, *10*, 234-236; g) C. L. Drennan, J. Heo, M. D. Sintchak, E. Schreiter, P. W. Ludden, *Proc. Natl. Acad. Sci. U. S. A.* **2001**, *98*, 11973-11978; h) H. Dobbek, V. Svetlitchnyi, L. Gremer, R. Huber, O. Meyer, *Science* **2001**, *293*, 1281-1285; i) U. Ermler, W. Grabarse, S. Shima, M. Goubeaud, R. K. Thauer, *Science* **1997**, *278*, 1457-1462.

[4] a) S. W. Ragsdale, M. Kumar, *Chem. Rev.* **1996**, *96*, 2515-2540; b) T. Wongnate, D. Sliwa, B. Ginovska, D. Smith, M. W. Wolf, N. Lehnert, S. Raugei, S. W. Ragsdale, *Science* **2016**, *352*, 953-958; c) M. Can, F. A. Armstrong, S. W. Ragsdale, *Chem. Rev.* **2014**, *114*, 4149-4174; d) S. Scheller, M. Goenrich, S. Mayr, R. K. Thauer, B. Jaun, *Angew. Chem. Int. Ed.* **2010**, *49*, 8112-8115; e) S. Scheller, M. Goenrich, R. Boecher, R. K. Thauer, B. Jaun, *Nature* **2010**, *465*, 606-608; f) X. Li, J. Telser, R. C. Kunz, B. M. Hoffman, G. Gerfen, S. W. Ragsdale, *Biochemistry* **2010**, *49*, 6866-6876; g) J. Harmer, C. Finazzo, R. Piskorski, S. Ebner, E. C. Duin, M. Goenrich, R. K. Thauer, M. Reiher, A. Schweiger, D. Hinderberger, B. Jaun, *J.*

Am. Chem. Soc. **2008**, *130*, 10907-10920; h) N. Yang, M. Reiher, M. Wang, J. Harmer, E. C. Duin, *J. Am. Chem. Soc.* **2007**, *129*, 11028-11029; i) S. W. Ragsdale, *Chem. Rev.* **2006**, *106*, 3317-3337; j) D. J. Evans, *Coord. Chem. Rev.* **2005**, *249*, 1582-1595; k) C. Finazzo, J. Harmer, C. Bauer, B. Jaun, E. C. Duin, F. Mahlert, M. Goenrich, R. K. Thauer, S. Van Doorslaer, A. Schweiger, *J. Am. Chem. Soc.* **2003**, *125*, 4988-4989; l) J.-i. Nishigaki, T. Matsumoto, K. Tatsumi, *Inorg. Chem.* **2012**, *51*, 5173-5187.

[5] a) M. Ito, T. Matsumoto, K. Tatsumi, *Inorg. Chem.* **2009**, *48*, 2215-2223; b) C. Jones, C. Schulten, L. Fohlmeister, A. Stasch, K. S. Murray, B. Moubaraki, S. Kohl, M. Z. Ertem, L. Gagliardi, C. J. Cramer, *Chem. Eur. J.* **2011**, *17*, 1294-1303; c) M. T. Kieber‐Emmons, R. Schenker, G. P. A. Yap, T. C. Brunold, C. G. Riordan, *Angew. Chem. Int. Ed.* **2004**, *43*, 6716-6718; d) M. T. Kieber-Emmons, C. G. Riordan, *Acc. Chem. Res.* **2007**, *40*, 618-625; e) D. Adhikari, S. Mossin, F. Basuli, B. R. Dible, M. Chipara, H. Fan, J. C. Huffman, K. Meyer, D. J. Mindiola, *Inorg. Chem.* **2008**, *47*, 10479-10490; f) B. C. Fullmer, H. Fan, M. Pink, K. G. Caulton, *Inorg. Chem.* **2008**, *47*, 1865-1867; g) S. Yao, Y. Xiong, C. Milsmann, E. Bill, S. Pfirrmann, C. Limberg, M. Driess, *Chem. Eur. J.* **2010**, *16*, 436-439; h) B. Horn, S. Pfirrmann, C. Limberg, C. Herwig, B. Braun, S. Mebs, R. Metzinger, *Z. Anorg. Allg. Chem.* **2011**, *637*, 1169-1174; i) V. M. Iluc, G. L. Hillhouse, *J. Am. Chem. Soc.* **2010**, *132*, 11890-11892; j) V. M. Iluc, G. L. Hillhouse, *J. Am. Chem. Soc.* **2010**, *132*, 15148-15150; k) S. Yao, M. Driess, *Acc. Chem. Res.* **2011**, *45*, 276-287; l) R. Beck, M. Shoshani, J. Krasinkiewicz, J. A. Hatnean, S. A. Johnson, *Dalton Trans.* **2013**, *42*, 1461-1475; m) B. Horn, C. Limberg, C. Herwig, B. Braun, *Chem. Commun.* **2013**, *49*, 10923-10925; n) M. I. Lipschutz, X. Yang, R. Chatterjee, T. D. Tilley, *J. Am. Chem. Soc.* **2013**, *135*, 15298-15301; o) M. M. Schwab, D. Himmel, S. Kacprzak, D. Kratzert, V. Radtke, P. Weis, K. Ray, E. W. Scheidt, W. Scherer, B. de Bruin, S. Weber, I. Krossing, *Angew. Chem. Int. Ed.* **2015**, *54*, 14706-14709.

[6] a) S. Chakraborty, H. Guan, *Dalton Trans.* **2010**, *39*, 7427-7436; b) X. Hu, *Chem. Sci.* **2011**, *2*, 1867-1886; c) S. A. Johnson, *Dalton Trans.* **2015**, *44*, 10905-10913; d) S. Chakraborty, P. Bhattacharya, H. Dai, H. Guan, *Acc. Chem. Res.* **2015**, *48*, 1995-2003.

[7] M. R. DuBois, D. L. DuBois, *Chem. Soc. Rev.* **2009**, *38*, 62-72.

[8] a) C.-Y. Lin, P. P. Power, *Chem. Soc. Rev.* **2017**, *46*, 5347-5399; b) P. Zimmermann, C. Limberg, *J. Am. Chem. Soc.* **2017**, *139*, 4233-4242.

[9] a) K. Jonas, G. Wilke, *Angew. Chem. Int. Ed.* **1970**, *9*, 312-313; b) D. A. Vicic, W. D. Jones, *J. Am. Chem. Soc.* **1997**, *119*, 10855-10856; c) I. Bach, R. Goddard, C. Kopiske, K. Seevogel, K.-R. Pörschke, *Organometallics* **1999**, *18*, 10-20; d) M. D. Fryzuk, G. K. B. Clentsmith, D. B. Leznoff, S. J. Rettig, S. J. Geib, *Inorg. Chim. Acta* **1997**, *265*, 169-177; e) B. L. Barnett, C. Krüger, Y.-H. Tsay, R. H. Summerville, R. Hoffmann, *Chem. Ber.* **1977**, *110*, 3900-3909.

[10] a) T. A. Ateşin, T. Li, S. Lachaize, W. W. Brennessel, J. J. García, W. D. Jones, *J. Am. Chem. Soc.* **2007**, *129*, 7562-7569; b) T. Li, J. J. García, W. W. Brennessel, W. D. Jones, *Organometallics* **2010**, *29*, 2430-2445; c) J. J. García, A. Arévalo, N. M. Brunkan, W. D. Jones, *Organometallics* **2004**, *23*, 3997-4002; d) J. J. Garcia, W. D. Jones, *Organometallics* **2000**, *19*, 5544-5545; e) J. J. Garcia, N. M. Brunkan, W. D. Jones, *J. Am. Chem. Soc.* **2002**, *124*, 9547-9555.

[11] a) X. Hu, I. Castro-Rodriguez, K. Meyer, *Chem. Commun.* **2004**, 2164-2165; b) B. R. Dible, M. S. Sigman, A. M. Arif, *Inorg. Chem.* **2005**, *44*, 3774-3776; c) S. Miyazaki, Y. Koga, T. Matsumoto, K. Matsubara, *Chem. Commun.* **2010**, *46*, 1932-1934; d) M. S. Varonka, T. H. Warren, *Organometallics* **2010**, *29*, 717-720; e) S. Nagao, T. Matsumoto, Y. Koga, K. Matsubara, *Chem. Lett.* **2011**, *40*, 1036-1038; f) K. Zhang, M. Conda-Sheridan, S. Cooke, J. Louie, *Organometallics* **2011**, *30*, 2546-2552; g) C. A. Laskowski, G. R. Morello, C. T. Saouma, T. R. Cundari, G. L. Hillhouse, *Chem. Sci.* **2013**, *4*, 170-174; h) J. Wu, A. Nova, D. Balcells, G. W. Brudvig, W. Dai, L. M. Guard, N. Hazari, P. H. Lin, R. Pokhrel, M. K. Takase, *Chem. Eur. J.* **2014**, *20*, 5327-5337; i) S. Pelties, E. Carter, A. Folli, M. F. Mahon, D. M. Murphy, M. K. Whittlesey, R. Wolf, *Inorg. Chem.* **2016**, *55*, 11006-11017; j) D. D. Beattie, E. G. Bowes, M. W. Drover, J. A. Love, L. L. Schafer, *Angew. Chem. Int. Ed.* **2016**, *55*, 13290 –13295; k) K. Matsubara, Y. Fukahori, T. Inatomi, S. Tazaki, Y. Yamada, Y. Koga, S. Kanegawa, T. Nakamura, *Organometallics* **2016**, *35*, 3281-3287; l) K. Matsubara, H. Yamamoto, S. Miyazaki, T. Inatomi, K. Nonaka, Y. Koga, Y. Yamada, L. F. Veiros, K. Kirchner, *Organometallics* **2017**, *36*, 255-265; m) A. B. Dürr, H. C. Fisher, I. Kalvet, K.-N. Truong, F. Schoenebeck, *Angew. Chem. Int. Ed.* **2017**, *56*, 13431-13435; n) C. A. Laskowski, G. L. Hillhouse, *J. Am. Chem. Soc.* **2008**, *130*, 13846-13847; o) C. A. Laskowski, D. J. Bungum, S. M. Baldwin, S. A. Del Ciello, V. M. Iluc, G. L. Hillhouse, *J. Am. Chem. Soc.* **2013**, *135*, 18272-18275; p) C. A. Laskowski, G. L. Hillhouse, *Chem. Sci.* **2011**, *2*, 321-325; q) W. J. M. Blackaby, S. Sabater, R. C. Poulten, M. J. Page, A. Folli, V. Krewald, M. F. Mahon, D. M. Murphy, E. Richards, M. K. Whittlesey, *Dalton Trans.* **2018**, *47*, 769-782.

[12] C. H. Lee, D. S. Laitar, P. Mueller, J. P. Sadighi, *J. Am. Chem. Soc.* **2007**, *129*, 13802-13803.

[13] a) R. Bau, R. G. Teller, S. W. Kirtley, T. F. Koetzle, *Acc. Chem. Res.* **1979**, *12*, 176-183; b) R. Bau, M. H. Drabnis, *Inorg. Chim. Acta* **1997**, *259*, 27-50.

[14] D. A. Vicic, T. J. Anderson, J. A. Cowan, A. J. Schultz, *J. Am. Chem. Soc.* **2004**, *126*, 8132-8133.

[15] Y. Hoshimoto, Y. Hayashi, H. Suzuki, M. Ohashi, S. Ogoshi, *Organometallics* **2014**, *33*, 1276-1282.

[16] G. R. Fulmer, A. J. M. Miller, N. H. Sherden, H. E. Gottlieb, A. Nudelman, B. M. Stoltz, J. E. Bercaw, K. I. Goldberg, *Organometallics* **2010**, *29*, 2176-2179.

[17] F. A. L. Anet, D. J. O'Leary, *Tetrahedron Lett.* **1989**, *30*, 2755-2758.

[18] a) P. Renaud, M. P. Sibi, *Radicals in Organic Synthesis*, WILEY‐VCH Verlag GmbH, Weinheim, **2008**; b) D. C. Eisenberg, C. J. C. Lawrie, A. E. Moody, J. R. Norton, *J. Am. Chem. Soc.* **1991**, *113*, 4888-4895.

[19] J. L. Simunic, A. R. Pinhas, *Organometallics* **1987**, *6*, 1358-1360.

[20] a) A. Nafady, P. J. Costa, M. J. Calhorda, W. E. Geiger, *J. Am. Chem. Soc.* **2006**, *128*, 16587-16599; b) X. Zheng, X. Wang, Z. Zhang, Y. Sui, X. Wang, P. P. Power, *Angew. Chem. Int. Ed.* **2015**, *54*, 9084-9087.

[21] R. C. Poulten, M. J. Page, A. G. Algarra, J. J. Le Roy, I. López, E. Carter, A. Llobet, S. A. Macgregor, M. F. Mahon, D. M. Murphy, M. Murugesu, M. K. Whittlesey, *J. Am. Chem. Soc.* **2013**, *135*, 13640-13643.

[22] R. M. Stolley, H. A. Duong, D. R. Thomas, J. Louie, *J. Am. Chem. Soc.* **2012**, *134*, 15154-15162.

[23] a) T. Schaub, P. Fischer, A. Steffen, T. Braun, U. Radius, A. Mix, *J. Am. Chem. Soc.* **2008**, *130*, 9304-9317; b) T. Schaub, U. Radius, *Chem. Eur. J.* **2005**, *11*, 5024-5030.

[24] I. Bach, K.-R. Pörschke, R. Goddard, C. Kopiske, C. Krüger, A. Rufińska, K. Seevogel, *Organometallics* **1996**, *15*, 4959-4966.

[25] L. Hintermann, *Beilstein J. Org. Chem.* **2007**, *3*, 22.

[26] A. J. Arduengo, R. Krafczyk, R. Schmutzler, H. A. Craig, J. R. Goerlich, W. J. Marshall, M. Unverzagt, *Tetrahedron* **1999**, *55*, 14523-14534.

[27] V. W. Manner, T. F. Markle, J. H. Freudenthal, J. P. Roth, J. M. Mayer, *Chem. Commun.* **2008**, 256-258.

[28] J. A. Weil, J. R. Bolton, in *Electron Paramagnetic Resonance*, 2nd ed., John Wiley & Sons, Inc., Hoboken, New Jersey, **2006**.

[29] R. Dorta, E. D. Stevens, N. M. Scott, C. Costabile, L. Cavallo, C. D. Hoff, S. P. Nolan, *J. Am. Chem. Soc.* **2005**, *127*, 2485-2495.

[30] G. M. Sheldrick, *Acta Cryst.* **2015**, *A71*, 3-8.

[31] O. V. Dolomanov, L. J. Bourhis, R. J. Gildea, J. A. K. Howard, H. Puschmann, *J. Appl. Cryst.* **2009**, *42*, 339-341.

[32] G. Sheldrick, *Acta Cryst.* **2015**, *C71*, 3-8.

CHAPTER 5. CONCLUSIONS

This thesis describes synthesis and characterization of novel late transition metal complexes with phosphatriptycene and NHC ligands, which have shown reactivity toward small molecules in catalytic systems or stoichiometry transformations.

Most functionalized phosphatriptycenes in literature, which have been studied as useful ligands in several homogeneous reactions, are those with functionalized groups *ortho* or *meta* to the opposite site of the bridgehead phosphorus for synthetic convenience.[1] We have designed the new target of 10-aza-9-phosphatriptycene with *tert*-butyl substituents on the *meta* postion to phosphorus, available in three laboratory steps from commercially available precursors. This study has suggested potential on synthesizing more derivatives of *meta*-substituted 10-aza-9-phosphatriptycene, with the possibility of effective electronic and steric properties control when used as ligands in designed catalysis systems.

The catalytic properties of the 9-phopshatriptycene class had not been assessed in hydroformylation so far. A rhodium complex of the new 10-aza-9-phosphatriptycene has been applied as a precursor to highly efficient catalyst systems for the hydroformylation of less reactive alkenes, notably cyclic alkenes. These results were consistent with the fact that strong π-acceptor phosphines increase the activity of rhodium in hydroformylation catalysis.[2] The study has provided new perspectives in the use of constrained phosphatriptycene ligands in more unexplored homogeneous catalysis systems that require supporting ligand to possess good π-accepting electronic ability and steric bulky property.

Small molecule activation at nickel(I) center is an emerging field, because nickel(I) can act as a one-electron reducing agent or transfer electron density to the substrate.[3] There have been a number of reported nickel(I) complexes supported by electron-rich and sterically bulky NHC ligands.[4] As transition metal hydrides can serve as intermediates in a variety of homogeneous and heterogeneous catalytic cycles, structure and reactivity studies of nickel(I) hydride complexes might provide insights into the action of nickel-containing enzymes,[5] the development of new nickel-catalyzed synthetic processes,[6] and the use of hydrogen as an energy carrier.[7] This thesis has involved the first synthesis of NHC-supported μ-hydrido dinickel(I) cation salts {[(IDipp)Ni]$_2$(μ-H)}[X] (X = OTf or NTf_2) and their reactivity study on nitrile activation. The unusual linear geometry of the μ-hydrido dinickel(I) complexes suggests a 3-center, 4-electron bonding model, leading to diamagnetic ^{1}H NMR resonances. A long-lived Ni(I)/Ni(0) monocation radical can be accessed by the action of suitable oxidants on nickel(0) precursors. A transient monomeric Ni(I) radical cation is proposed to react quickly with Ni(0) to give a Ni−Ni bonded dimer monocation through a radical-substrate coupling reaction.[8]

The interest in study of transition metal mediated activation of C−F bonds has grown in recent years, especially on understanding of the mechanisms.[9] The most common reaction pathway invoked for the cleavage of C−F bonds in fluoroaromatics by nickel(0) is the η^2-precoordination of fluoroaromatics at the nickel center prior to concerted oxidative addition.[10] The NHC-supported nickel system exhibits much faster oxidative addition rate to hexafluorobenzene substrate than the corresponding phosphine-supported nickel system, which has been proposed through a contribution of charge separation from the nickel fragment at the C−F bond, considering the nucleophilicity of nickel(0)

moiety.[10c] The reaction of [(IDipp)Ni^0(benzene)] with hexafluorobenzene has suggested that C−F bond activation at the nickel center supported by one NHC ligand leads to the generation of new product [(IDipp)Ni(μ-C_6F_5)]$_2$, which guides us to consider a distinctly different reaction pathway from the better-established systems. Activation of C−F bond at the [(IDipp)Ni^0] moiety is proposed to proceed through a pre-coordination of C_6F_6 ligand in η^2-fasion at the nickel center, followed by the nucleophilic attack of the metal at the electrophilic site of the aromatic system. This process also suggests the possible formation of a nickel(I) fluoride complex. Complexes containing the hard and largely ionic fluoride anion bound to the soft and strongly reducing nickel(I) center have not been described, and could display interesting reactivity for carbon–fluorine bond formation.[9b, 11]

5.1 References

[1] a) D. Hellwinkel, W. Schenk, *Angew. Chem. Int. Ed.* **1969**, *8*, 987-988; b) D. Hellwinkel, W. Schenk, W. Blaicher, *Chem. Ber.* **1978**, *111*, 1798-1814; c) C. Jongsma, J. P. de Kleijn, F. Bickelhaupt, *Tetrahedron* **1974**, *30*, 3465-3469; d) T. Agou, J. Kobayashi, T. Kawashima, *Chem. Lett.* **2004**, *33*, 1028-1029; e) H. Tsuji, T. Inoue, Y. Kaneta, S. Sase, A. Kawachi, K. Tamao, *Organometallics* **2006**, *25*, 6142-6148; f) T. Iwai, S. Konishi, T. Miyazaki, S. Kawamorita, N. Yokokawa, H. Ohmiya, M. Sawamura, *ACS Catal.* **2015**, *5*, 7254-7264; g) H. Ube, Y. Yasuda, H. Sato, M. Shionoya, *Nat. Commun.* **2017**, *8*, 14296; h) S. Konishi, T. Iwai, M. Sawamura, *Organometallics* **2018**, *37*, 1876-1883; i) M. W. Drover, K. Nagata, J. C. Peters, *Chem. Commun.* **2018**, *54*, 7916-7919; j) J. Kobayashi, T. Agou, T. Kawashima, *Chem. Lett.* **2003**, *32*, 1144-1145; k) T. Agou, J. Kobayashi, T. Kawashim, *Heteroat. Chem* **2004**, *15*, 437-446.

[2] a) R. L. Pruett, J. A. Smith, *J. Org. Chem.* **1969**, *34*, 327-330; b) P. W. N. M. van Leeuwen, C. F. Roobeek, *J. Organomet. Chem.* **1983**, *258*, 343-350; c) A. Polo, J. Real, C. Claver, S. Castillón, J. C. Bayón, *J. Chem. Soc., Chem. Commun.* **1990**, 600-601; d) A. van Rooy, E. N. Orij, P. C. J. Kamer, F. van den Aardweg, P. W. N. M. van Leeuwen, *J. Chem. Soc., Chem. Commun.* **1991**, 1096-1097; e) T. Jongsma, G. Challa, P. W. N. M. van Leeuwen, *J. Organomet. Chem.* **1991**, *421*, 121-128; f) A. van Rooy, E. N. Orij, P. C. J. Kamer, P. W. N. M. van Leeuwen, *Organometallics* **1995**, *14*, 34-43; g) E. Fernández, A. Ruiz, C. Claver, S. Castillón, A. Polo, J. F. Piniella, A. Alvarez-Larena, *Organometallics* **1998**, *17*, 2857-2864; h) D. Selent, K.-D. Wiese, D. Röttger, A. Börner, *Angew. Chem. Int. Ed.* **2000**, *39*,

1639-1641; i) S. C. van der Slot, P. C. J. Kamer, P. W. N. M. van Leeuwen, J. Fraanje, K. Goubitz, M. Lutz, A. L. Spek, *Organometallics* **2000**, *19*, 2504-2515; j) S. C. van der Slot, J. Duran, J. Luten, P. C. J. Kamer, P. W. N. M. van Leeuwen, *Organometallics* **2002**, *21*, 3873-3883; k) R. Jackstell, H. Klein, M. Beller, K.-D. Wiese, D. Röttger, *Eur. J. Org. Chem.* **2001**, 3871-3877; l) B. Breit, *Chem. Commun.* **1996**, 2071-2072; m) B. Breit, R. Winde, K. Harms, *J. Chem. Soc., Perkin Trans. 1* **1997**, 2681-2682; n) B. Breit, R. Winde, T. Mackewitz, R. Paciello, K. Harms, *Chem. Eur. J.* **2001**, *7*, 3106-3121; o) M. Rigo, J. A. W. Sklorz, N. Hatje, F. Noack, M. Weber, J. Wiecko, C. Müller, *Dalton Trans.* **2016**, *45*, 2218-2226; p) B. Breit, E. Fuchs, *Chem. Commun.* **2004**, 694-695; q) E. Fuchs, M. Keller, B. Breit, *Chem. Eur. J.* **2006**, *12*, 6930-6939; r) G. Märkl, F. Lieb, C. Martin, *Tetrahedron Lett.* **1971**, *12*, 1249-1252; s) A. Lee, S. Ahn, K. Kang, M.-S. Seo, Y. Kim, W. Y. Kim, H. Kim, *Org. Lett.* **2014**, *16*, 5490-5493.

[3] a) M. Ito, T. Matsumoto, K. Tatsumi, *Inorg. Chem.* **2009**, *48*, 2215-2223; b) C. Jones, C. Schulten, L. Fohlmeister, A. Stasch, K. S. Murray, B. Moubaraki, S. Kohl, M. Z. Ertem, L. Gagliardi, C. J. Cramer, *Chem. Eur. J.* **2011**, *17*, 1294-1303; c) M. T. Kieber‐Emmons, R. Schenker, G. P. A. Yap, T. C. Brunold, C. G. Riordan, *Angew. Chem. Int. Ed.* **2004**, *43*, 6716-6718; d) M. T. Kieber-Emmons, C. G. Riordan, *Acc. Chem. Res.* **2007**, *40*, 618-625; e) D. Adhikari, S. Mossin, F. Basuli, B. R. Dible, M. Chipara, H. Fan, J. C. Huffman, K. Meyer, D. J. Mindiola, *Inorg. Chem.* **2008**, *47*, 10479-10490; f) B. C. Fullmer, H. Fan, M. Pink, K. G. Caulton, *Inorg. Chem.* **2008**, *47*, 1865-1867; g) S. Yao, Y. Xiong, C. Milsmann, E. Bill, S. Pfirrmann, C. Limberg, M. Driess, *Chem. Eur. J.* **2010**, *16*, 436-439; h) B. Horn, S. Pfirrmann, C. Limberg, C. Herwig, B. Braun, S. Mebs, R. Metzinger, *Z. Anorg. Allg. Chem.* **2011**, *637*, 1169-1174; i) V. M. Iluc, G. L. Hillhouse, *J. Am. Chem. Soc.* **2010**, *132*, 11890-11892; j) V. M. Iluc, G. L. Hillhouse, *J. Am. Chem. Soc.* **2010**, *132*, 15148-15150; k) S. Yao, M. Driess, *Acc. Chem. Res.* **2011**, *45*, 276-287; l) R. Beck, M. Shoshani, J. Krasinkiewicz, J. A. Hatnean, S. A. Johnson, *Dalton Trans.* **2013**, *42*, 1461-1475; m) B. Horn, C. Limberg, C. Herwig, B. Braun, *Chem. Commun.* **2013**, *49*, 10923-10925; n) M. I. Lipschutz, X. Yang, R. Chatterjee, T. D. Tilley, *J. Am. Chem. Soc.* **2013**, *135*, 15298-15301; o) M. M. Schwab, D. Himmel, S. Kacprzak, D. Kratzert, V. Radtke, P. Weis, K. Ray, E. W. Scheidt, W. Scherer, B. de Bruin, S. Weber, I. Krossing, *Angew. Chem. Int. Ed.* **2015**, *54*, 14706-14709; p) P. Zimmermann, C. Limberg, *J. Am. Chem. Soc.* **2017**, *139*, 4233-4242; q) C.-Y. Lin, P. P. Power, *Chem. Soc. Rev.* **2017**, *46*, 5347-5399.

[4] a) X. Hu, I. Castro-Rodriguez, K. Meyer, *Chem. Commun.* **2004**, 2164-2165; b) B. R. Dible, M. S. Sigman, A. M. Arif, *Inorg. Chem.* **2005**, *44*, 3774-3776; c) S. Miyazaki, Y. Koga, T. Matsumoto, K. Matsubara, *Chem. Commun.* **2010**, *46*, 1932-1934; d) M. S. Varonka, T. H. Warren, *Organometallics* **2010**, *29*, 717-720; e) S. Nagao, T. Matsumoto, Y. Koga, K. Matsubara, *Chem. Lett.* **2011**, *40*, 1036-1038; f) K. Zhang, M. Conda-Sheridan, S. Cooke, J. Louie, *Organometallics* **2011**, *30*, 2546-2552; g) C. A. Laskowski, G. R. Morello, C. T. Saouma, T. R. Cundari, G. L. Hillhouse, *Chem. Sci.* **2013**, *4*, 170-174; h) J. Wu, A. Nova, D. Balcells, G. W. Brudvig, W. Dai, L. M. Guard, N. Hazari, P. H. Lin, R. Pokhrel, M. K. Takase, *Chem. Eur. J.* **2014**, *20*, 5327-5337; i) S. Pelties, E. Carter, A. Folli, M. F. Mahon,

D. M. Murphy, M. K. Whittlesey, R. Wolf, *Inorg. Chem.* **2016**, *55*, 11006-11017; j) D. D. Beattie, E. G. Bowes, M. W. Drover, J. A. Love, L. L. Schafer, *Angew. Chem. Int. Ed.* **2016**, *55*, 13290 –13295; k) K. Matsubara, Y. Fukahori, T. Inatomi, S. Tazaki, Y. Yamada, Y. Koga, S. Kanegawa, T. Nakamura, *Organometallics* **2016**, *35*, 3281-3287; l) K. Matsubara, H. Yamamoto, S. Miyazaki, T. Inatomi, K. Nonaka, Y. Koga, Y. Yamada, L. F. Veiros, K. Kirchner, *Organometallics* **2017**, *36*, 255-265; m) A. B. Dürr, H. C. Fisher, I. Kalvet, K.-N. Truong, F. Schoenebeck, *Angew. Chem. Int. Ed.* **2017**, *56*, 13431-13435; n) C. A. Laskowski, G. L. Hillhouse, *J. Am. Chem. Soc.* **2008**, *130*, 13846-13847; o) C. A. Laskowski, D. J. Bungum, S. M. Baldwin, S. A. Del Ciello, V. M. Iluc, G. L. Hillhouse, *J. Am. Chem. Soc.* **2013**, *135*, 18272-18275; p) C. A. Laskowski, G. L. Hillhouse, *Chem. Sci.* **2011**, *2*, 321-325; q) W. J. M. Blackaby, S. Sabater, R. C. Poulten, M. J. Page, A. Folli, V. Krewald, M. F. Mahon, D. M. Murphy, E. Richards, M. K. Whittlesey, *Dalton Trans.* **2018**, *47*, 769-782.

[5] a) S. W. Ragsdale, M. Kumar, *Chem. Rev.* **1996**, *96*, 2515-2540; b) T. Wongnate, D. Sliwa, B. Ginovska, D. Smith, M. W. Wolf, N. Lehnert, S. Raugei, S. W. Ragsdale, *Science* **2016**, *352*, 953-958; c) M. Can, F. A. Armstrong, S. W. Ragsdale, *Chem. Rev.* **2014**, *114*, 4149-4174; d) S. Scheller, M. Goenrich, S. Mayr, R. K. Thauer, B. Jaun, *Angew. Chem. Int. Ed.* **2010**, *49*, 8112-8115; e) S. Scheller, M. Goenrich, R. Boecher, R. K. Thauer, B. Jaun, *Nature* **2010**, *465*, 606-608; f) X. Li, J. Telser, R. C. Kunz, B. M. Hoffman, G. Gerfen, S. W. Ragsdale, *Biochemistry* **2010**, *49*, 6866-6876; g) J. Harmer, C. Finazzo, R. Piskorski, S. Ebner, E. C. Duin, M. Goenrich, R. K. Thauer, M. Reiher, A. Schweiger, D. Hinderberger, B. Jaun, *J. Am. Chem. Soc.* **2008**, *130*, 10907-10920; h) N. Yang, M. Reiher, M. Wang, J. Harmer, E. C. Duin, *J. Am. Chem. Soc.* **2007**, *129*, 11028-11029; i) S. W. Ragsdale, *Chem. Rev.* **2006**, *106*, 3317-3337; j) D. J. Evans, *Coord. Chem. Rev.* **2005**, *249*, 1582-1595; k) C. Finazzo, J. Harmer, C. Bauer, B. Jaun, E. C. Duin, F. Mahlert, M. Goenrich, R. K. Thauer, S. Van Doorslaer, A. Schweiger, *J. Am. Chem. Soc.* **2003**, *125*, 4988-4989; l) J.-i. Nishigaki, T. Matsumoto, K. Tatsumi, *Inorg. Chem.* **2012**, *51*, 5173-5187.

[6] a) S. Chakraborty, H. Guan, *Dalton Trans.* **2010**, *39*, 7427-7436; b) X. Hu, *Chem. Sci.* **2011**, *2*, 1867-1886; c) S. A. Johnson, *Dalton Trans.* **2015**, *44*, 10905-10913; d) S. Chakraborty, P. Bhattacharya, H. Dai, H. Guan, *Acc. Chem. Res.* **2015**, *48*, 1995-2003.

[7] M. R. DuBois, D. L. DuBois, *Chem. Soc. Rev.* **2009**, *38*, 62-72.

[8] A. Nafady, P. J. Costa, M. J. Calhorda, W. E. Geiger, *J. Am. Chem. Soc.* **2006**, *128*, 16587-16599.

[9] a) E. F. Murphy, R. Murugavel, H. W. Roesky, *Chem. Rev.* **1997**, *97*, 3425-3468; b) J. L. Kiplinger, T. G. Richmond, C. E. Osterberg, *Chem. Rev.* **1994**, *94*, 373-431; c) N. M. Doherty, N. W. Hoffmann, *Chem. Rev.* **1991**, *91*, 553-573; d) H. Torrens, *Coord. Chem. Rev.* **2005**, *249*, 1957-1985; e) U. Mazurek, H. Schwarz, *Chem.*

Commun. **2003**, 1321-1326; f) T. Braun, R. N. Perutz, *Chem. Commun.* **2002**, 2749-2757.

[10] a) L. Cronin, C. L. Higgitt, R. Karch, R. N. Perutz, *Organometallics* **1997**, *16*, 4920-4928; b) I. Bach, K.-R. Pörschke, R. Goddard, C. Kopiske, C. Krüger, A. Rufińska, K. Seevogel, *Organometallics* **1996**, *15*, 4959-4966; c) T. Schaub, P. Fischer, A. Steffen, T. Braun, U. Radius, A. Mix, *J. Am. Chem. Soc.* **2008**, *130*, 9304-9317.

[11] a) O. Eisenstein, J. Milani, R. N. Perutz, *Chem. Rev.* **2017**, *117*, 8710-8753; b) K. S. Pedersen, M. A. Sørensen, J. Bendix, *Coord. Chem. Rev.* **2015**, *299*, 1-21.

APPENDIX A. COLLABORATOR CONTRIBUTIONS

Much of this research presented in this thesis was a result of collaborative efforts. This appendix serves to credit collaborators and their respective contributions.

A.1 Synthesis, Characterization, Coordination Chemistry of Phosphatriptycene

Synthesis and NMR characterization of 2,7,14-tri-*tert*-butyl-10-aza-9-phosphatriptycene **7** and its copper complex were performed by Ms. Sabrine Cypher under the mentorship of Yu Cao. Dr. John Bacsa performed all of the X-ray diffraction studies and solved all solid-state structures within this chapter.

A.2 Azaphosphatriptycene in Rhodium-Catalyzed Hydroformylation

Dr. Jonathan W. Napoline obtained 2,7,14-tri-methyl-10-aza-9-phosphatriptycene and confirmed the reported difficulties in reproducibility, and provided insightful discussions on the hydroformylation studies, especially on the preliminary hydroformylation tests using the 10-hydroxy-9-phosphatriptycene and 2,7,14-tri-methyl-10-aza-9-phosphatriptycene. Dr. John Bacsa performed the X-ray diffraction study and solved the solid-state structure within this chapter.

A.3 NHC-Supported Dinuclear nickel complexes

Dr. John Bacsa performed all of the X-ray crystallography studies and solved the solid-state structure within this chapter.

VITA

Yu Cao

Yu (Jady) Cao was born and grew up in Dongying, Shandong, China. She attended Nankai University in Tianjin, China, where she participated in undergraduate research in the lab of Professor Yu Liu, and received a B.S. in chemistry in 2013. She attended graduate school at the Georgia Institute of Technology in Atlanta, Georgia, where she conducted graduate research under the advisement of Professor Joseph P. Sadighi, and obtained her Ph.D. in chemistry in 2018.